Analysis of Driving Parameters for Green Flight Trajectories

J. Grande Pardo

Delft University of Technology

TU Delft Delft University of Technology

Challenge the future

Analysis of Driving Parameters for Green Flight Trajectories

By

J. Grande Pardo

in partial fulfilment of the requirements for the degree of

Master of Science
in Aerospace Engineering

at the Delft University of Technology,
to be defended publicly on Friday October 28, 2016 at 11:00 AM.

Supervisor:	Prof. dr. V. Grewe	
Thesis committee:	Prof. dr. V. Grewe,	TU Delft
	Prof. dr. D. Simons,	TU Delft
	Dr. ir. M. Voskuijl,	TU Delft

Word count: 21183
Number of Figures: 44
Total: 29983

An electronic version of this thesis is available at http://repository.tudelft.nl/.

TU Delft Delft University of Technology

Summary

Climate change is an important problem nowadays. There are several industries causing this problem. One of them is the air transport industry. In order to reduce its induced climate impact there are different approaches: design of new aircrafts or engines, use of alternative fuels, more efficient air traffic management, or re-routing. All of them except re-routing aim on reducing carbon dioxide emissions. Re-routing, on the other hand, aims on reducing the climate impact of non-CO_2 emissions (that considerably alter their climate impact depending on the region of the atmosphere where they are released) by increasing slightly the carbon dioxide emissions. This study focuses on this last approach. It establishes an analysis of the results obtained within the REACT4C project (Reducing Emissions from Aviation by Changing Trajectories for the benefit of Climate). The project aims to reduce aircraft induced climate impact in the North Atlantic flight corridor by changes in flight trajectories and considers fleets of around 400 aircraft. Moreover, this project considers eight different weather patterns (three for summer and five for winter), two flight directions (westbound and eastbound), and three climate metrics. Therefore, a total of 48 configurations have to be studied. Moreover it considers six different climate parameters causing the total climate impact. The climate parameters are carbon dioxide, water vapor, contrails, and NO_x. The NO_x climate impact is obtained as the summation of ozone, methane, and primary mode ozone climate impacts. The results that are analyzed are the climate impact caused by each of the climate parameters and how this climate impact changes when applying gradual changes on the aircraft trajectories.

The analysis shows that water vapor has a negligible effect on climate impact. Carbon dioxide climate impact is more relevant when considering long term time horizons. Also, it increases when more trajectories are modified since the fuel consumption increases. Contrails are the main driver of the optimization for seven out of eight weather patterns. Their climate impact goes down during the optimization. Moreover, they are more important when considering short term time horizons and westbound flights. NO_x is driving the optimization for only one weather pattern. Its contribution to reduce the total climate impact during the optimization is higher in the long term due to the enhanced net-cooling effect caused by methane depletion. Moreover, it is more important for eastbound flights. However, for winter weather patterns, NO_x is controlled mainly by methane and primary mode ozone during most part of the optimization. Ozone is only important in the first and last segments. In addition, ozone presents the highest values of climate impact and has more contribution in the short term; while methane has always a negative climate impact or net-cooling effect due to its depletion, and is more important in the long term.

The climate impact reduction is caused in the first part of the optimization by a small number of flights that reduce considerably their climate impact. Their trajectories change to go through regions of the atmosphere where their climate impact is smaller. As the optimization progresses, there are more flights modifying their routes. However, their climate impact reduction is not as noticeable as in the first cases. This happens because the regions of the atmosphere where the emissions have a lower climate impact are busier with the prior flights. Therefore the latter flights changing their trajectories have less potential to reduce their climate impact. This leads to a small part of the fleet causing an important climate impact reduction while the vast majority of flights slightly reduce their climate impact.

List of figures

List of tables

Table of contents

1

Introduction

Climate change and global warming are important problems nowadays. Due to the high amount of anthropogenic emission of certain gases, the atmospheric composition and cloudiness are altered. This leads to a change in radiation exchange and therefore a change in climate. This alteration impacts relevant aspects of society, such as nature, agriculture and energy production. Furthermore, costs, as well as damages, emerge [1].

The air traffic industry is one of the responsible industries for climate change. Its relative importance of CO_2 emissions has increased from 2% to 2.5% from 1980 to 2007 [2]. However, CO_2 is not the only pollutant altering the climate. There are other emissions and effects such as NO_x emissions or contrail formation that are critical in this aspect. Considering them, the total climate impact from aviation represents 5% of the global anthropogenic climate change [3]. In order to reduce this effect some changes are necesary. Different solutions include new aircraft and engine designs, use of alternative fuels, more efficient traffic management or re-routing [1].

In order to understand how the atmosphere composition is altered via the air transport activity, it is important to define the aircraft emissions and their effect on the atmosphere. These emissions are mainly CO_2, H_2O, NO_x, soot, SO_2, CO and hydrocarbons. The main effects are contrail formation and aerosol effect [4]. These emissions and effects have different importance on climate change. In order to have a first overview of them, a climate metric is defined: radiative forcing (RF). It expresses the difference between the amount of energy trapped by the Earth and its atmosphere, and the energy expulsed out of the atmosphere. It is related with the mean surface temperature change (ΔT_s) as shown in equation (1) [5]. ΔT_s shows the average increment or drop in temperature of the Earth surface due to the emission or effect considered. The climate sensitivity parameter lambda (λ) changes depending on the species considered [1].

$$\Delta T_s \approx \lambda \, RF \tag{1}$$

To understand the climate effect of air transport, it is assumed that most comercial aircraft fly between 8 and 12 kilometers of altitude. This fact has an important effect on the way emissions affect the atmosphere and therefore modify climate. There are three main ways for the atmosphere composition to be altered: atmospheric transport of emitted species, perturbation in chemical composition due to chemical reactions, and microphysics that lead to changes in cloudiness [5].

In the first way, atmospheric transport, the emitted species are transported from the emission point to different parts of the atmosphere. To identify the different parts of this complex system the use of models is mandatory. However depending on the selected schema, models show a high variability [6]. The most important points to take into account when modelling are:

- High vertical model resolution is required for an accurate distribution of species [7].
- High horizontal resolution gives more precise results especially with cross-tropopause transport [8].
- The tendency of the atmospheric transport is downwards, therefore most species end up in the troposphere and are removed there [5].

The second way of altering the atmosphere is by chemical reactions. The main precursor of this effect is NO_x. NO_x emissions have two main effects. The first one is an increase in the production and therefore concentration of ozone. This occurs via the creation of O and O_2 forming ozone (O_3). The increment in ozone concentration has a warming effect. Furthermore, the NO_x reacts and forms OH. This OH radical reacts with methane leading to a depletion of this

gas. Therefore the atmospheric concentration of methane goes down and a reduced warming effect takes place [9]. The perturbation lifetime of ozone is around one year while for methane is twelve years [10] [11]. These are the durations these gases modify the atmosphere composition of equilibrium.

The last way of altering the atmospheric is by changing its cloudiness. Aircraft form contrails which are straight cirrus that appear when the aircraft exhaust plume (warm and humid) mixes with the surrounding local atmosphere under a specific temperature. This temperature is only determined by the Schmidt-Appleman criterion [12]. Contrails reflect solar radiation and capture departing earthly energy. Trapping this radiation emitted by the Earth is very important and therefore a positive radiative forcing occurs [13]. In order to precisely state the effect cloudiness has on climate, it is necessary to know the supersaturated regions of the atmosphere with respect to ice. However, this is a complicated task and has only been characterized where flights are common [14] [15].

Until this point the major emissions and effects caused by aircraft have been explained. However, there is not a direct way of measuring the impact they have on climate. In order to measure climate impact, the use of climate metrics is necessary [1]. The radiative forcing mentioned above is only valid as a first approximation, but it is not accurate enough for a detailed analysis. Therefore more specific climate metrics are required. Some of the most used ones are:

- *AGTP*: Absolute Global Temperature Potential.
- *AGWP*: Absolute Global Warming Potential.
- *ATR*: Average Temperature Response.

Depending on the objective of the optimization, one or another is chosen. This election can seem ambiguous, but specifying the final objective of the optimization, the ambiguity is notoriously reduced. From the final objective can be extracted a reference, as well as an emission scenario, a climate metric and a time horizon [16].

2

REACT4C project

After seeing how the climate is altered by air traffic, some solutions can be formulated to reduce this impact. The main possibilities are [1]:

- New engine and aircraft designs
- Alternative fuels
- More efficient traffic management
- Re-routing

In this analysis re-routing is the chosen option. The advantage of this approach over the others is that it can be applied right now without the need of doing big investments [1]. While all the other options aim to achieve a reduction in carbon dioxide emissions, the aim of re-routing is to achieve a strong drop in non-CO_2 emissions at a low expense of carbon dioxide. These non-CO_2 emissions, contrary to CO_2, not only contribute to climate depending on the amount of emitted pollutants, but the time and location where the emissions are released have a vital role on climate impact. Therefore, modifying the original flight route in order to avoid climate sensitive regions of the atmosphere will lead to a reduction in climate impact by non-CO_2 emissions. However, these route changes usually lead to longer trajectories and more fuel consumption, increasing the amount of CO_2 emissions [5].

From the different projects that have been performed regarding eco-friendly re-routing, the newest is the REACT4C (Reducing Emissions from Aviation by Changing Trajectories for the benefit of Climate) [17]. The project aims to reduce the aircraft induced climate impact by changes on aircraft trajectories depending on specific weather conditions in the North Atlantic flight corridor [17]. This idea has been analyzed before in other studies [18], but this is the first time that many different effects are addressed. The effects addressed (also known as climate parameters) in the REACT4C project are contrails, carbon dioxide, ozone from NO_x emission, methane from NO_x emission, ozone from variation on methane (or PMO[1]), and water vapor.

The approach followed makes use of CCF[2] for the first time. They give the climate impact (in climate metric units) for an emission in a point of the atmosphere at a certain time. This forms a 4-dimensional data set. After the CCF is obtained, the aircraft trajectories are calculated based on the minimization of the climate impact, the economic costs, or a combination of both [17].

In order to perform the optimization some models are required. These models simulate the behavior of the atmosphere, the air traffic management and the aircraft emissions.

- Atmosphere: The EMAC model is used. It simulates climate and also chemistry in a numerical way from the troposphere to the middle-atmosphere. It includes the effect that human activity, land and oceans have on climate [19]. The model uses a grid with a resolution of 2.8º of latitude, 2.8º of longitude and 41 vertical layers [17]. This is called the EMAC grid. In order to relate the individual processes, the second version of MESSy2 is used [20]. The main advantage of this second version is that apart from relating the chemical and physical processes, it also provides routines for remapping and data extraction. These routines reduce the time required in order to extract the results and analyze them.

[1] Primary Mode Ozone
[2] Climate Cost Functions

- Air traffic management: The SAAM system is used to simulate the aircraft routes [21]. It is able to simulate routes based on any demand (origin and destination, type of aircraft and time of departure) and also allows the application of restricions such as maximum flight level and avoidance of accidents.
- Aircraft emissions: To simulate the species emitted by aircraft the AEM model is used. It gives the mass of fuel used and also the emitted species for a given engine and aircraft, and a specific trajectory in space and time. The considered emissions are CO_2, H_2O, NO_x, SO_x, unburned hydrocarbons and CO [22].

The models used for the air traffic management (SAAM) and the aircraft emissions (AEM) are coupled. The coupling between both models is applied in the following way [17]:

1. Flights are chosen from a database. The information includes origin, destination, aircraft type and a reference trajectory. Each trajectory has the lowest economic cost for each flight.
2. Routes are generated in a random way by blocking air space areas and modifying cruise altitude. The grid used for this process is the same used by the SAAM model. In the end, for every flight there are 105 different possible trajectories. In this part the possible routes are known, but there is not information about the required time to complete each of them.
3. A calculation is carried out in order to obtain the 4-dimensional aircraft trajectories. Wind fields are included in the calculation. Therefore results for different weather patterns are obtained.
4. Using the AEM model, the emissions are calculated for each trajectory.
5. Depending on the target of the optimization, a combination of trajectories is selected. The possible targets are minimum economic costs, minimum climate impact, or a combination of both. This part also includes a procedure to avoid conflicts between the trajectories in order to avoid accidents.

The calculation of the CCF is based on a Lagrangian approach. This means that the air parcels containing emissions considered for its calculation are followed for the whole trajectory. The characteristics of this approach are [17]:

- It is numerically efficient because the different regions are calculated in parallel.
- It calculates the different contributions of the emitted species and separates them from possible compensating effects due to changes in contribution from other sectors.
- Contribution of time-region grid points is not very detailed due to interpolation. This time-region grid points will be explained in the following lines.

This approach is the most appropriate for the objective of the calculation because it does not consider non-linear compensation effects in the chemical processes [23] [24]. The complete methodology used to obtain the Climate Cost Functions, which makes use of the Lagrangian approach, is as follows [17]:

1. A new grid is defined. It is called time-region grid. It represents the points where the emissions will take place and also the time when this will happen. It has a resolution of 6 points in longitude, 7 in latitude, 4 in altitude and 3 in time.
2. Different emissions are considered from the time-region grid points. These emissions are shown in Table 1.

Parameter	Value	Comment
NO_x emissions [kg(NO)]	$5 \cdot 10^5$	Equals $2.33 \cdot 10^5$ kg and occurs during 15 minutes
H_2O emission [kg]	$1.25 \cdot 10^7$	Occurs during 15 minutes

Table 1. Emissions considered from the time-region grid points to obtain the CCF [17]

The engine characteristics are important to accurately obtain the Climate Cost Function. The values considered here are presented in Table 2 [25].

Parameter	Value
Overall propulsion efficiency	0.31
H_2O emission index [kg(H_2O)/(kg(fuel))]	1.25
Kerosene combustion heat [J/kg]	$43.2 \cdot 10^7$

Table 2. Engine general characteristics [25]

3. Emissions considered from each time-region grid point are divided into 50 different air parcel trajectories. These air parcel trajectories are distributed in the EMAC grid box where the time-region grid points are situated.
4. The climate impact of the emissions is calculated and associated with each time-region grid point.
5. The climate impact obtained for each time-region grid point is interpolated in the EMAC grid. The grid obtained with the data for the Climate Cost Functions is denominated final climate cost function grid.

A comparison between the interpolated results for the final climate cost function grid and the ones that would have been obtained by calculating them point by point was performed in the REACT4C project to see how critical the interpolation was [17]. The results are shown in Table 3. The horizontal interpolation is more critical than the temporal one. Nevertheless, the variation expected in NO_x (and therefore O_3) are of one order of magnitude larger than the interpolation error. Therefore this does not represent a problem.

Variation	NO_x	O_3
Temporal variation	±40%	±25%
Horizontal variation	±50%	±35%

Table 3. Temporal and horizontal variation of NO_x and ozone between interpolated and exact results in the REACT4C project [17]

The next step in the REACT4C project methodology was to obtain the changes in the atmospheric composition and cloudiness. Different procedures were followed. These were mainly related with the results of emitting NO_x, the changes in contrails, and the emissions of H_2O and CO_2.

First, the results of emitting NO_x are ozone production, methane depletion and reduction ozone production due to methane depletion [5]. The EMAC model [19] calculated the loss (L) and production (P) terms of several chemical species. The emissions are divided into two different groups: aircraft emissions (superscript *e*) and background emissions (superscript *b*). The process of production and loss of ozone is described in Reactions (R1) and (R2).

$$HO_2 + NO \rightarrow OH + NO_2 \quad \text{(R1)}$$
$$NO_2 + O_3 \rightarrow NO + 2O_2 \quad \text{(R2)}$$

Taking into account these reactions and following the procedure described in [23], the equation describing the changes in ozone from aviation is obtained, as shown in Equation 2.

$$\frac{d}{dt}O_3^e = \frac{P_{O_3}^b}{NO_x^b}NO_x^e - \frac{1}{2}D_{O_3,1}^b\left(\frac{NO_x^e}{NO_x^b} + \frac{O_3^e}{O_3^b}\right) - D_{O_3,2}^b\frac{O_3^e}{O_3^b} \quad (2)$$

The first term on the right hand side represents the ozone production. It is main dependent on NO_x. The second and last terms represent ozone destruction. The second one considered a chemical family based on NO_x, while the last one takes into account all other loss processes [17].

The same procedure is followed for the remaining species. Thirteen chemical reactions are considered in order to obtain all the effects caused by the NO_x pollutants [17].

Secondly, to obtain the induced contrails, the Schmidt-Appleman criterion [25] and the approaches describe in [26] and [27] are used for the REACT4C project. It relates the formation of additional cloudiness with two characteristics of the atmosphere: temperature and moisture. The additional cloudiness is usually due to contrails, which are straight cirrus forming from the engine exhaust. These contrails are formed when the exhaust gases (humid and hot) are mixed with the surrounding atmosphere which is cold. Droplets form in the engine exhaust and freeze, forming the contrails. Persistance is only possible if the surrounding atmosphere is supersaturated with ice. Otherwise contrail does not persist [5].

The approach followed to obtain the contrail behavior makes use of two different parameters: the contrail coverage and the contrail ice mass mixing ratio [26] [27]. These parameters are calculated for the different time steps. Their main characteristics and the way they are obtained are [17]:

- Contrail coverage: It is the fraction of the considered atmospheric region which is covered by contrails. It is obtained for each grid box of the EMAC grid. It basically depends on the relative humidity, the critical relative

humidity for formation of contrails, the relative humidity over ice to fulfill the Schmidt-Appleman criterion, and the humidity of saturation. In order to obtain the development of cloudiness, both newly created contrails and dispersion of prevailing ones are considered.
- Contrail ice mass mixing ratio: is obtained taking into account the creation of new contrails, deposition and sublimation processes involving the water contained in the contrail, and the precipitation of ice from the contrail due to its weight. The most important values to calculate these parameters are the rate of condensation for natural cirrus [28], the relative humidity, the density of air and the ice-particle falling speed [29].

The next emission considered is water vapor. From the emission time, only loss processes are considered. It has been shown that if the emission occurs in the troposphere, the water vapor disappears in a short period of time and does not have any impact on higher levels of the atmosphere [30]. The most important parameter to see the way water vapor concentration evolves in time is the precipitation rate due to snow and rain fall.

Finally, carbon dioxide is considered. This emission has a long impact in time and therefore it is assumed that it mixes globally [5]. The approach to model it takes into account the amount of fuel consumed, the type of fuel used (kerosene) and the way the concentration decreases with time [31].

The next step to be taken is to calculate the climate impact of the different emissions and induced cloudiness. In order to calculate the climate impact of the different parameters first the induced radiative forcing (*RF*) of each of them is obtained. Its general expression is shown in equation 1. The way the radiative forcing is calculated in each case is:

- Carbon dioxide: Linearization relating RF with the carbon dioxide mass in the atmosphere with a factor of $1.82 \cdot 10^{-12}$ mW/(m^2 kg(CO_2)) [31].
- Contrails: Obtained from the changes in the global mean radiation flux at the tropopause in one year.
- Ozone: Obtained in the same way as the contrails´ radiative forcing but adjusting it based on season and altitude.
- Methane: The formula presented in [32] is used, which takes into account the concentration of CH_4 and N_2O.
- Primary Mode Ozone: A factor of 0.29 is applied to methane radiative forcing in order to obtain the value for PMO [33].
- Water vapor: Obtained following a similar procedure as the one used for carbon dioxide, but with a factor of $4.38 \cdot 10^{-13}$ W/(m^2 kg(H_2O)) [30].

The radiative forcing results are then used to obtain more accurate climate metrics such as AGWP[3] or ATR[4] [1]. These new climate metrics consider different emission types and also can be used for different time horizons. The climate metrics are then used to measure the climate impact of the different emissions. The selection of the climate metrics aimed to answer three different question: *"what is the short-term climate impact of the REACT4C re-routing strategy?"* [17], *"what is the long-term climate impact of the REACT4C re-routing strategy?"* [17], and *"what is the medium-range climate impact of a present-day REACT4C re-routing decision?"* [17] The analysis performed in [17] suggested that the best climate metrics to use in the future for the purposes explained were:

- Pulse emission with AGWP in a 20 years time horizon.
- Pulse emission with AGWP in a 100 years time horizon.
- Future air traffic scenario with ATR in a 20 years time horizon.
- Future air traffic scenario with ATR in a 100 years time horizon.

The time horizons chosen represent the short term (20 years) and the long term (100 years) climate impact. For the former the most important climate parameters are contrails and ozone. For the latter, it is carbon dioxide. Contrails have a perturbation lifetime of the order of hours while ozone´s perturbation lifetime is of the order of one year. On the other hand, carbon dioxide affects the atmospheric composition for centuries.

Finally, as a first application of the REACT4C project, a first optimization was performed for a winter day type. It showed that a 15% of climate impact reduction could be achieved with only a 0.5% increase in economic cost for a specific climate metric (AGWP with a time horizon of 100 years) and one direction (westbound) [34]. The Pareto front obtained for that analysis can be seen in Figure 1. It relates the maximum climate impact reduction that can be

[3] Absolute Global Warming Potential
[4] Average Temperature Response

obtained with the minimum increase in economic costs. Each point on the Pareto front represents a combination of flights, all of them causing a climate impact and having an economic cost. The combination of all flights is called fleet. Each flight has a climate impact and a economic cost associated. The summation of climate impacts of each individual flight gives the total climate impact of the fleet. Same with the economic costs. These agregated values are presented in the Pareto front for the optimum situations. These situations are the maximum climate impact reduction that can be achieved with the minimum economic cost increase. The results from this case are really promising especially for the westbound flight direction and the long term climate metric. However, the analysis performed was only illustrative and therefore it did not show all the details. For this reason it is necessary to perform a deeper analysis.

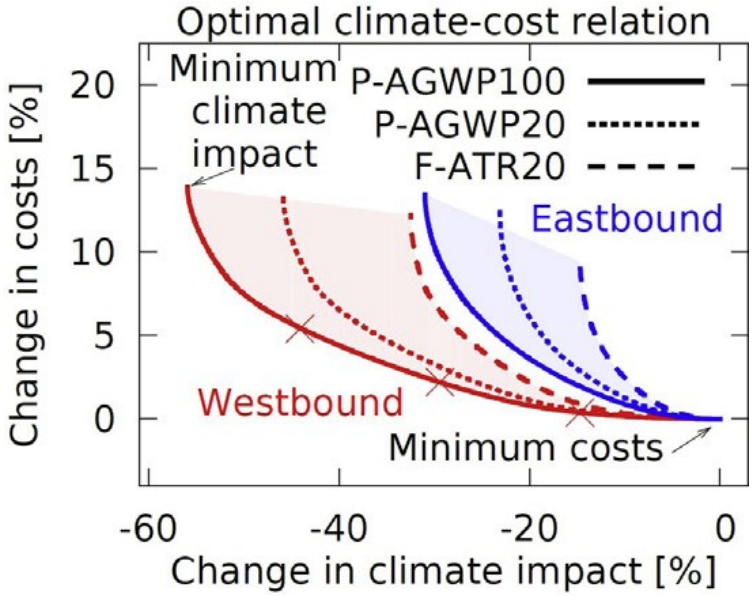

Figure 1. Illustration of the Pareto front obtained as the first study case from the REACT4C project [34].

The objective of this study is to analyse and show the importance of the different climate parameters (contrails, ozone, PMO (Primary Mode Ozone), methane, water vapor and carbon dioxide) during the optimization (for each of the points forming the Pareto front). Also similarities and differences will be described between the different weather patterns, flight directions and climate metrics. The main content will focus on analyzing data sets containing all the information regarding the climate impact and the economic costs. The aim is to assess the importance and tendency of the individual climate parameters during the optimization process for all the configurations. Furthermore, the project will create a comparison between the different results obtained in each individual case and find similarities and differences for several weather patterns, flight directions and climate metrics. Hence, the main findings will be a result of two aspects: firstly, the assessment of the importance of the different aircraft emissions and the effects they have on the climate when re-routing using the REACT4C project results; and secondly, the similarities between the different individual cases. Moreover, an analysis on the contribution that presents each individual flight to total climate impact reduction will be performed. This will lead to a better understanding of the reasons behind the modification of the original routes. With the eco-friendly re-routing, anthropogenic climate change can be reduced with a low increase in economic cost.

3

Methodology and Normalization

As a result of the REACT4C project, there is a large amount of data to be analized and compared. This includes climate impact caused by the different emissions, economic costs, flight times, flight distances, changes in latitude, changes in longitude, etc... This study will focus mainly on climate impact. The possible configurations are defined by a weather pattern, a flight direction and a climate metric. The number of each category is:

- Weather pattern: There are eight different weather patterns, three for summer and five for winter. They were obtained from observation and data analysis in the North Atlantic flight corridor for a period of 21 years from June 1989 to February 2010 making use of the European Centre for Medium-Range Weather Forecasts Re-Analysis Interim dataset [35].
- Flight direction: There are two different flight directions; from Europe to the East Coast of USA or westbound, and from the East Coast of USA to Europe or eastbound.
- Climate metrics: There are three different climate metrics; pulse emission with AGWP in a 20 years time horizon or P-AGWP20, pulse emission with AGWP in a 100 years time horizon or P-AGWP100, and future air traffic scenario with ATR in a 20 years time horizon or F-ATR20 [34]. For simplicity they will be called AGWP20, AGWP100, and ATR20 respectively.

The combination of the different possibilities gives a total amount of 48 configurations. In order to analize and compare them, a normalization of the climate impact induced by the different climate parameters is required. This is required because it is not possible to compare absolute values while the units of the different climate metrics are different. Moreover, the total climate impact is changing from case to case, hence the absolute value does not provide enough information in order to see the importance of the emission climate impact. Some important definitions are:

- *Absolute Climate Impact of climate parameter i:* is the climate impact caused by the individual climate parameter *i*, for example contrails. Depending on the climate metric, it has different units. For AGWP the units are [fw/m^2] (femtowatts divided by square meter) and for ATR they are [fK] (femto Kelvin).
- *Absolute Total Climate Impact:* is obtained as the summation of the individual climate impacts for each climate parameter. There are two points with special importance: the minimum economic cost point (min. ECO), and the minimum total climate impact point (min. CLIM).
- *Economic Cost:* is the operating cost including fuel and crew required to complete all flights.

With these three definitions some normalized values can be defined. For now only the results of the complete fleet are considered. First of all, in order to represent the Pareto Front for each case the *Relative Total Climate Impact Change (RTCIC)* and the *Relative Economic Cost Change (RECC)* are defined in Equation 3 and 4 respectively:

$$RTCIC(j) = \frac{Absolute\ Total\ Climate\ Impact\ (j) - Absolute\ Total\ Climate\ Impact\ (min.ECO)}{Absolute\ Total\ Climate\ Impact\ (min.ECO)} \cdot 100\ [\%] \quad (3)$$

$$RECC(j) = \frac{Economic\ Cost\ (j) - \ Economic\ Cost\ (min.ECO)}{Economic\ Cost\ (min.ECO)} \cdot 100\ [\%] \quad (4)$$

In this first normalization j represents the different points in the Pareto fronts. It goes from the minimum economic cost point to the minimum total climate impact point. The results are shown as a percentage. In Figure 2 the result of plotting the *RECC* versus the *RTCIC* is shown for a configuration of summer weather pattern 1 (SP1), westbound flight direction (W), and AGWP100 as climate metric. This configuration has been chosen in an arbitrary way just for

clarification purposes. With this representation (which is the same than in [34]), it is easy to see how costly it is to reduce the climate impact by re-routing and what is the maximum reduction that can be achieved. In this case a reduction in climate impact of 14% can be achieved with an increase in costs of 12%.

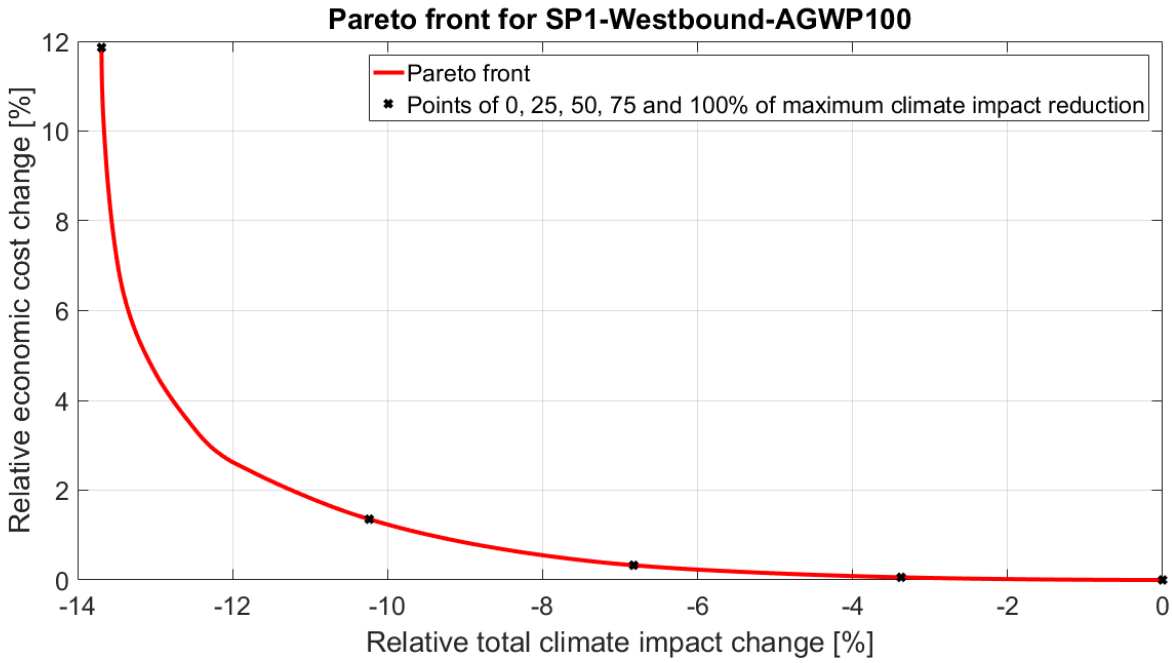

Figure 2. Pareto front for Summer Pattern 1, westbound flight direction and AGWP100 climate metric.

To be able to compare the different cases, a common scale has to be used. Plotting the *RTCIC* or the *RECC* on the horizontal axis will not be useful to compare the different configurations because these values vary from case to case. Therefore the *Normalized Total Climate Impact Change* (*NTCIC*) which also can be found as *Optimization criteria relative to maximum [%]* in [34] is defined. Its definition can be seen in Equation 5.

$$NTCIC(j) = \frac{Absolute\ Total\ Climate\ Impact\ (j) - Absolute\ Total\ Climate\ Impact\ (min.ECO)}{Absolute\ Total\ Climate\ Impact\ (min.CLIM) - Absolute\ Total\ Climate\ Impact\ (min.ECO)} \cdot 100\ [\%] \quad (5)$$

In this case, *j* has the same meaning than in Equations 3 and 4. The *NTCIC* value goes from 0% at the minimum economic cost point, to 100% at the mininum total climate impact point. With this normalization the different values can be compared using the same horizontal axis. However a normalization with the *Absolute Climate Impact of the individual species* is required in order to compare them due to the differences in magnitude and the different units used for AGWP and ATR. The question that this new parameter has to answer is: what is the relative importance of each climate parameter´s climate impact along the Pareto front? This new parameter will be called *Normalized Climate Impact of i* (*NCI*) where *i* is one of the climate parameters, such as ozone. Several possibilities appear here, however two of them are more interesting than the others. A good idea is to compare them and choose which one is better for more clarity. These two options are shown in Equation 6 and Equation 7.

$$NCI\ of\ i(j) option\ 1 = \frac{Absolute\ Climate\ Impact\ of\ i(j)}{Absolute\ Total\ Climate\ Impact(min.ECO)} \cdot 100\ [\%] \quad (6)$$

$$NCI\ of\ i(j) option\ 2 = \frac{Absolute\ Climate\ Impact\ of\ i(j)}{Absolute\ Total\ Climate\ Impact(j)} \cdot 100\ [\%] \quad (7)$$

The only difference between them is that the *Absolute Total Climate Impact* dividing remains constant in the first option and changes in the second one. A comparison of the two options can be seen in Figure 3. It shows the *NCI* of contrails for the same configuration than in Figure 2. *NCI* value of option 1 decays faster because the absolute climate impact of the contrails is divided by a constant factor, and therefore it maintains the same shape than the absolute climate impact graph. *NCI* value of option 2 goes down but in a slower pace because the number dividing the absolute climate impact of contrails goes down on each point. This second option is better only for checking the importance of the different climate parameters and its exact significance during the optimization.

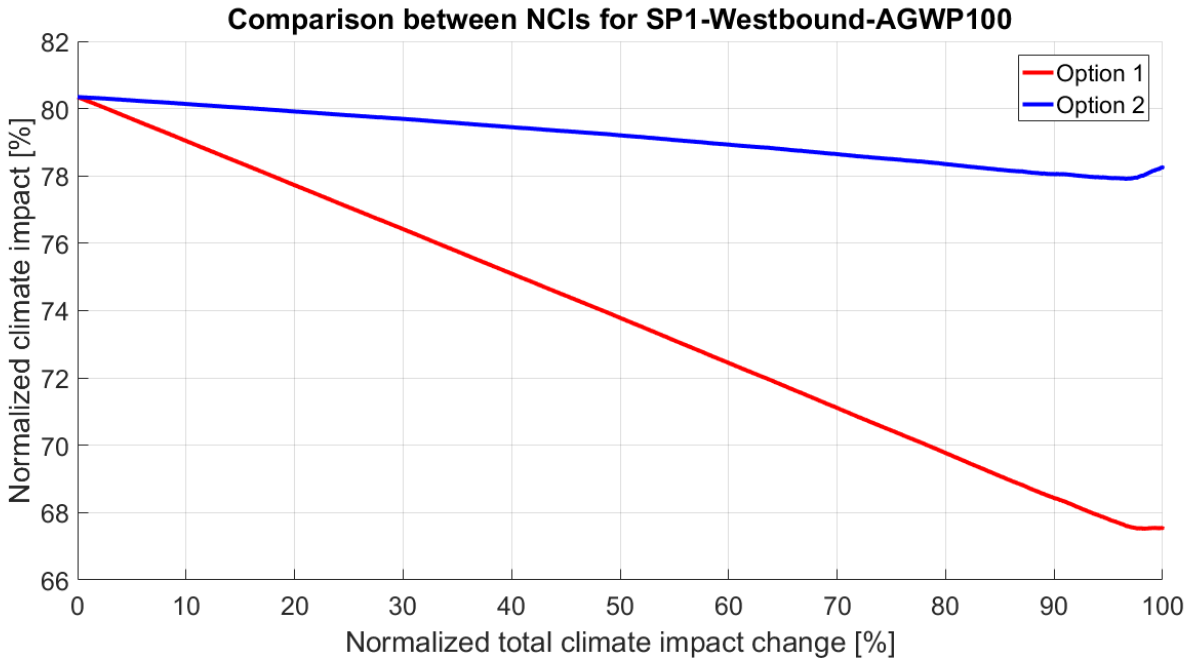

Figure 3. Comparison between the two options available to calculate the *NCI* of contrails for Summer Pattern 1, westbound flight direction and AGWP100 climate metric. Option 1 appears in red while Option 2 in blue.

For this study, it is better to choose the Option 1. The main advantages in comparison with the Option 2 are:

- Same shape when using absolute values.
- Easier to see if a climate parameter changes or remains constant during the optimization.
- Easier to obtain the absolute climate impact of each climate parameter on each point. Only requires to multiply the *NCI* by the *Absolute Total Climate Impact* at the minimum economic cost point.

With the normalization proposed, it is possible to see what are the driving parameters for each individual case. With the simplified following example it may be easier to understand this process. In the hipothetic case where there were only two climate parameters (contrails and NO_x) and that their respectives *NCIs* were straight lines when plotted versus the *NTCIC*:

- *RTCIC(min. ECO)* : 5%
- *Contrails NCI* : From 70% at min. ECO to 67% at min. CLIM
- *NO_x NCI* : From 30% at min. ECO to 28% at min. CLIM

The contrails *NCI* is reduced by 3% while the NO_x *NCI* drops by 2%. The summation of both *NCI* changes gives the total *RTCIC*. Also, it can be deduced from it that 60% of the reduction is caused by contrails and 40% by NO_x. This would be useful if there were only a few cases to study, less climate parameters, no comparison required betweeen the different cases and a clear behavior of the different climate parameters. However the study is way more complex than what was presented in the example. Hence, a new definition is required to be able to compare the different results. This will answer the question: How much is each climate parameter contributing to decrease the total climate impact? The new parameter is going to be called *Relative Contribution of i* (*RC*) and it is defined the same way as the *Contribution to the optimization of individual species at the optimisation target* in [34]. Its definition can be seen in Equation 8.

$$RC\ of\ i(j) = \frac{Absolute\ Climate\ Impact\ of\ i(j) - \ Absolute\ Climate\ Impact\ of\ i(min.ECO)}{Absolute\ Total\ Climate\ Impact(min.CLIM) - \ Absolute\ Total\ Climate\ Impact(min.ECO)} \cdot 100\ [\%] \qquad (8)$$

This *Relative Contribution* represents the contribution of each climate parameter to the *Normalized Total Climate Impact Change* for each point *j* in the Pareto front. If, for example, contrails have a *Relative Contribution* value of 50% when the *Normalized Total Climate Impact Change* is 60%, this means that the *RC* of the remaining climate parameters will be 10%. Hence, this parameter gives the information required to know the climate parameters

causing the total climate impact change. Moreover, *NCI* and *RC* in combination with *NTCIC* can be used to obtain the *RTCIC* at the min. CLIM point. The way to obtain this value is shown in Equation 9.

$$RTCIC(min.ECO) = \frac{NCI(j) - NCI(min.ECO)}{RC(j) - RC(min.ECO)} \cdot 100\ [\%] \tag{9}$$

In this equation, *j* represents any value of *NTCIC*. Therefore, there is a lot of information contained in the normalization explained above. It will be the basis for the analysis performed in Section 4: "Complete Fleet Analysis".

Section 5 will consist on a individual flight analysis. In order to see how is each individual flight contributing to the total climate impact reduction, another parameter is required. This parameter will answer the question: how much is each individual flight contributing to the climate impact change of each climate parameter? To answer this question the parameter *Relative Climate Impact Change* (*RCIC*) is defined. Its expression is shown in Equation 10.

$$RCIC(i,j,k) = \frac{Climate\ Impact\ (i,j,k) - Climate\ Impact(i,j,min.ECO)}{\frac{Absolute\ Total\ Climate\ Impact(min.ECO)}{Number\ of\ Flights}} \cdot 100 \tag{10}$$

Where *i* refers to the climate parameter considered, *j* to the flight considered, and *k* to the *Normalized Total Climate Impact Change* value, where *min. ECO* is 0%. Hence, *j* goes from 1 to 391 for eastbound flights, and from 1 to 394 for westbound flights. The *Number of Flights* is 391 for eastbound and 394 for westbound direction.

Table 4 presents a summary with the parameters that are going to be used during the analysis.

Scientific Question	Parameter	Abbreviation
What is the relative change with respect to min. ECO situation in total climate impact for each point of the Pareto front?	*Relative Total Climate Impact Change*	*RTCIC*
What is the relative change with respect to min. ECO situation in economic cost for each point of the Pareto front?	*Relative Economic Cost Change*	*RECC*
What point of the Pareto front is being analyzed?	*Normalized Total Climate Impact Change*	*NTCIC*
What is the relative importance of each climate parameter´s climate impact along the Pareto front?	*Normalized Climate Impact*	*NCI*
How much is each climate parameter contributing to decrease the total climate impact?	*Relative Contribution*	*RC*
How much is each individual flight contributing to the climate impact change of each climate parameter?	*Relative Climate Impact Change*	*RCIC*

Table 4. Summary with the scientific question and the parameter that is going to be used to answer it.

Before proceeding with the analysis, it is important to mention again the climate parameters considered. These are carbon dioxide, water vapor, contrails and NO_x. The NO_x effect is obtained as the summation of ozone, methane and PMO effects. The PMO climate impact is computed as the methane climate impact multiplied by a factor of 0.29 [33]. Therefore, studying the methane will give the results for the PMO. For this reason the PMO is not going to be considered any more.

With all the definitions clear, the next step to perform is the data analysis. This will be divided into two major analyses: the first one, performed in Section 4, will consider the aggregated values of the individual flights, obtaining therefore the effect of the complete fleet; and the second one, in Section 5, will take a look into the individual flights for each case and see how the changes on the climate parameters are caused.

4

Complete Fleet Analysis

This section deals with the analysis of the driving parameters taking into account the contribution of the whole fleet which is the summation of all flights contributions. For westbound direction the fleet is formed by 394 flights while for eastbound there are 391 aircraft involved [34]. First of all, it is important to know the absolute values for the different configurations. Figure 4 shows the economic cost at the min. ECO point for different weather patterns and flight directions. The horizontal axis indicates the combination of weather pattern and flight direction. The first letter shows the flight direction (E for eastbound and W for westbound). The second letter and the number show the weather pattern (S for summer and W for winter). All climate metrics are presented because in the min. ECO situation they have same economic cost for same weather pattern and flight direction.

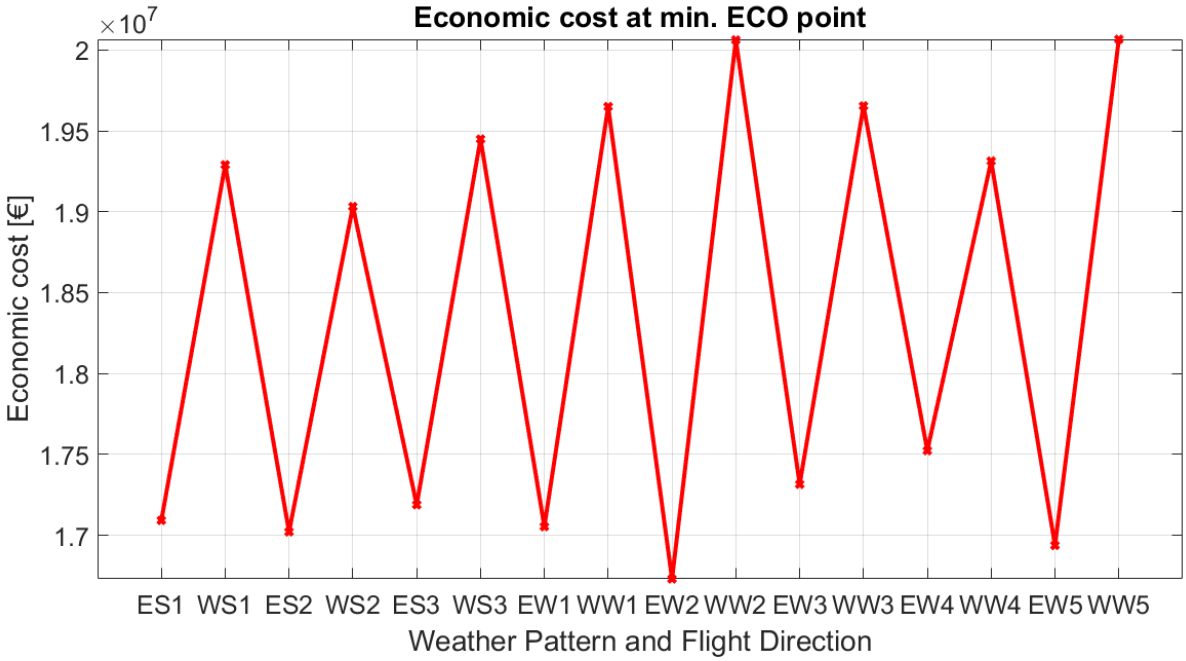

Figure 4. Comparison between the economic cost at min. ECO point for different weather pattern and flight direction.

The economic costs are quite similar for the different weather patterns when the direction of the flight is the same. For eastbound flights, the economic costs are around 17 million of euros and for westbound flights this amount increases to around 19 million of euros. The economic costs are the same for same weather pattern and flight direction, no matter the climate metric. This happens because the situation presented is the minimum economic cost point.

Figure 5 presents the absolute total climate impact in the min. ECO situation. All possible configurations are shown. The left vertical axis shows the values for AGWP climate metrics while the red vertical axis does the same for ATR20 climate metric. Looking at one climate metric (does not matter which one), it can be seen that the absolute total climate impact values are similar for the several weather patterns and flight directions. This value is around three times larger for Summer Pattern 1 when compared to other weather patterns. Moreover, the absolute total climate impact is always higher for westbound flights than for eastbound flights when the weather pattern is the same.

Finally, the value for the AGWP100 climate metric is always higher than the respective value of the AGWP20. This means that in this study, the total climate impact is bigger in the long term than in the short term.

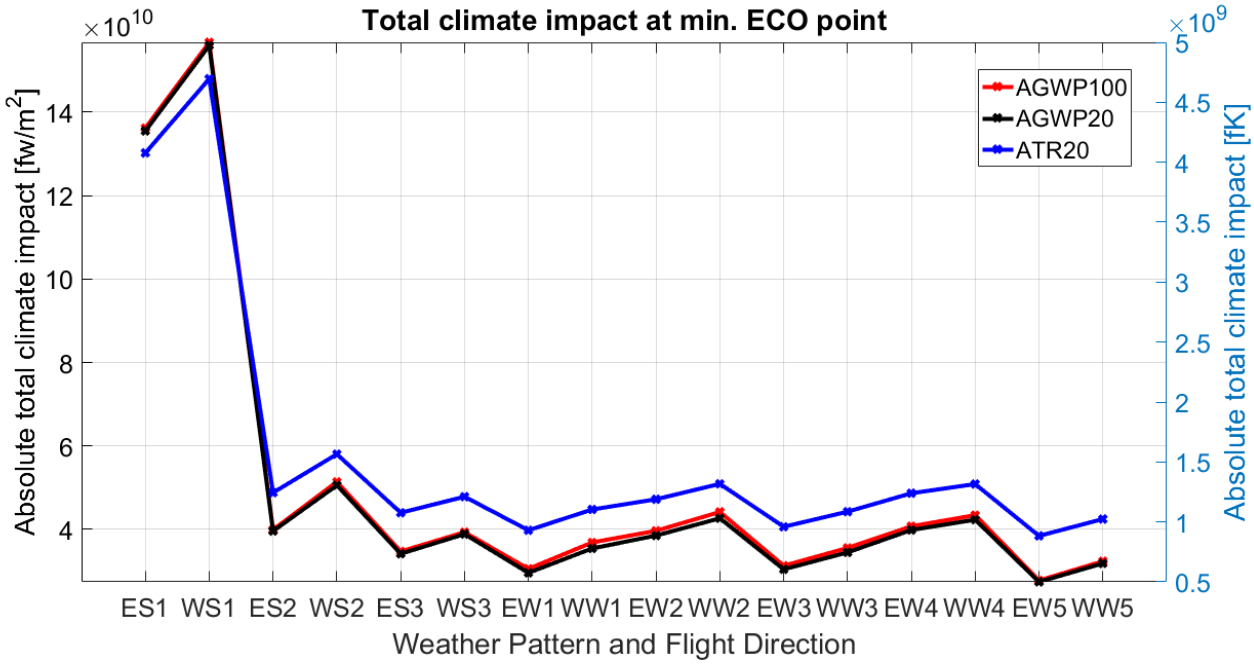

Figure 5. Comparison between the total climate impact at min. ECO point for different weather pattern, climate metrics and flight direction.

Knowing the absolute values at the minimum economic cost point and making use of the normalization presented in Section 3, it is possible to obtain the absolute results for each point during the optimization. With that in mind, the results can be presented. There are different ways to group the data results depending on what question has to be answered:

1. What is the importance of the different climate parameters for an individual case? The best option here would be showing the results of all climate parameters in two graphs (one for *NCI* and one for *RC*) for a combination of weather pattern, flight direction, and climate metric. For example Summer Pattern 1, westbound flight direction and AGWP100 climate metric.
2. How are the different flight directions and climate metrics affecting the results for a specific weather pattern? The best option to show the results is presenting only one climate parameter per graph. There should be two graphs containing the information of *NCI* and *RC*. These figures should show the values of the different flight direction and climate metric combinations for one weather pattern. For example contrails for Summer Pattern 1.
3. How are the different weather patterns and flight directions affecting the results for a specific climate metric? The best option here is showing only one climate parameter per figure. There should be also two graphs with *NCI* and *RC* results. The figures should show the values of the different weather patterns and flight directions combinations for one climate metric. For example carbon dioxide for AGWP100.

From the options presented, the second and the third one are going to be used. The first option is already contained within the other two and does not lead to an easy comparison of the different results. In addition, with the use of *NCI* and *RC*, it is not required to present all climate parameters in just one graph (as suggested in option 1). The reason is that *NCI* and *RC* values give enough information to know how much is contributing each climate parameter to the total climate impact and to the climate impact reduction. Moreover, option 2 was already use in [34], therefore, using it again will make easier to relate both studies.

In this first analysis the main climate parameters will be considered. This includes carbon dioxide, water vapor, contrails and NO_x. Also, the 2 most important contributions to NO_x climate impact will be studied to understand its behavior. This includes ozone and methane.

Due to the large amount of data to represent, not all the figures will appear in this section. If the reader is interested in further details, there is a complete list in Annex A and Annex B.

4.1. Summer Pattern 1

The first weather pattern to be analyzed is SP1. The Pareto front for this first case is shown in Figure 6. Westbound flights ("W") are presented in red color while eastbound flights ("E") appear in blue. AGWP100 is presented with a solid line, AGWP20 with a dotted line, and ATR20 with a dashed line. The black "X" and "O" show the values for 0%, 25%, 50%, 75%, and 100% of *NTCIC* for W-AGWP100 and E-AGWP100 respectively. This color and line format will be consistent for all the following representations. The Pareto fronts have almost the same shape when the flight direction is the same. The main difference occurs in the last segment of the optimization, from 75% to 100% of *NTCIC*. Also, the *RTCIC* achieved with AGWP20 is a bit higher than the one obtained with AGWP100 and ATR20, which represents the lowest change. The difference in the capability of reducing the *RTCIC* between eastbound and westbound flights is noticeable. While the reduction of the climate impact for westbound flights can be up to around 13%, the reduction of the climate impact for eastbound flights gives only a 5%. Considering that total climate impact at the minimum economic cost point is always higher in westbound flights than in eastbound flights as shown in Figure 5, more total climate impact reduction can be achieved with westbound flights. Finally, the relation between the *RTCIC* and *RECC* should be taken into account. From 0% to 25% of NTCIC the increase in costs is very low compared to the climate impact reduction. However, when proceeding with the optimization, this climate impact reduction becomes more costly, especially in the last segment. It goes from 0.2% of *RECC* in the first segment to 11% (from 1% to 12% approximately) in the last one to obtain the same *RTCIC*.

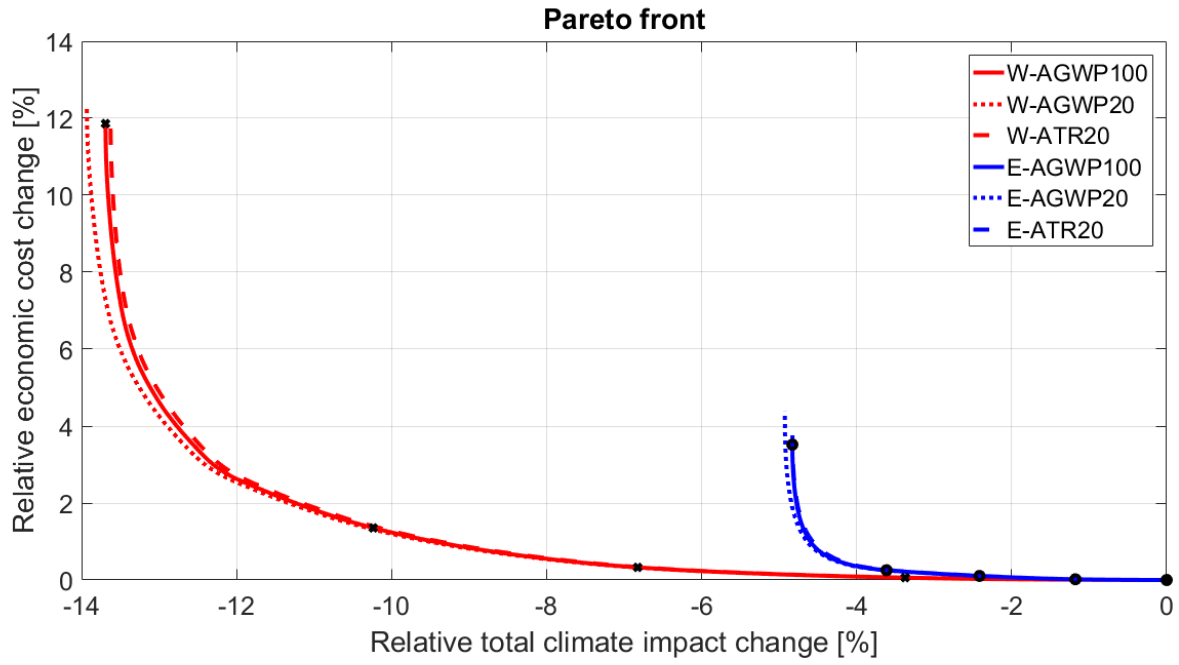

Figure 6. Comparison of Pareto fronts for Summer Pattern 1 and different flight directions and climate metrics.

In Figure 7 *NCI* and *RC* values of carbon dioxide are presented. The *NCI* is very similar for the same climate metric. In all cases, eastbound has a higher *NCI* than westbound except for the last 15% of *NTCIC*. There westbound *NCI* becomes a bit higher. It is important to realize the differences in *NCI* for the different climate metrics. AGWP100 is the highest with around a 3.5%, followed by AGWP20 with a 1% and finally ATR20 with a 0.7%. The difference may be explained by the long term impact that carbon dioxide has on climate, of the order of centuries [5]. Therefore it becomes more important when the time horizon is higher. The difference between AGWP20 and ATR20 can be explained due to the type of emission considered. Remember that AGWP was related to a pulse emission while ATR20 to a future air traffic scenario.

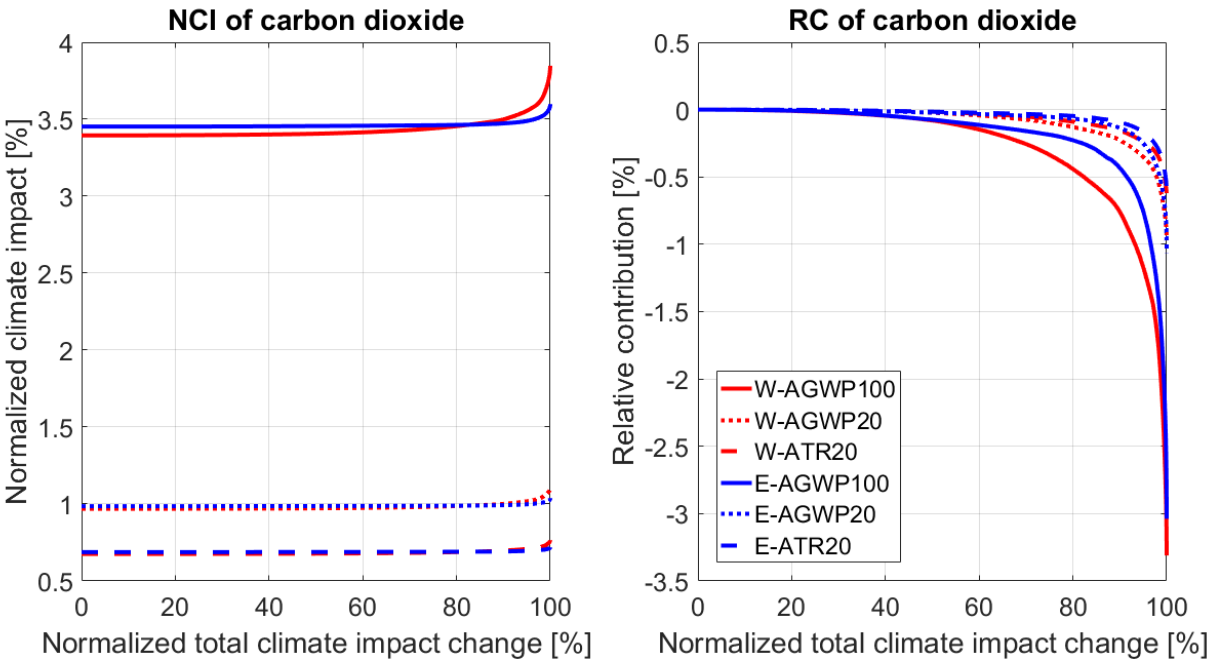

Figure 7. Comparison of carbon dioxide *NCI* and *RC* for Summer Pattern 1 and different flight directions and climate metrics.

Regarding the carbon dioxide *RC*, it is quite similar in all cases until a *NTCIC* of 60%. It drops during the whole optimization but especially from 80% to 100% of *NTCIC*. The minimum value it reaches is around -3.3% for W-AGWP100; therefore it is not very important. Also, *RC* is always negative, meaning that it is not helping in reducing the total climate impact, having a warming effect. This was expected because the re-routing approach aims on achieving a big reduction in non-CO_2 emissions at a low cost in CO_2 emissions increase [1]. Climate metrics follow the same order than in *NCI* case. The same explanation can be applied. Finally, the *RC* change in the last part can be related to higher fuel consumption and therefore higher carbon dioxide emission due to larger modifications on the routes. This increase can be also seen in the Pareto front of Figure 6 because the fuel consumption is directly related to the increase in economic costs.

The next climate parameter to be analyzed is water vapor. Its behavior is shown in Figure 6. Its *NCI* follows a similar behavior for same flight direction and it is higher for AGWP20 followed by AGWP100 and finally ATR20. *NCI* is higher for AGWP20 because water vapor has short term climate impact of the order of days [30]. The reason why *NCI* for AGWP100 is higher than for ATR20 while the time horizon is shorter for the latter one is the emission type considered. AGWP makes use of pulse emission type while ATR20 considers future air traffic scenario. The shape of the curve is characterized by a decreasing part due to the avoidance of climate sensitive regions followed by a sudden increase due to the larger amount of fuel consumption that leads to higher amount of water vapor emissions. However, its value is around 0.35% during the optimization, and therefore very small.

About water vapor *RC*, it follows almost the same tendency for the same flight direction. In all cases, it increases up to 0.15% when the *NTCIC* is around 80%, but then drops to a -0.3% for eastbound flights and -0.1% for westbound flights. This behavior is explained in the first part with the reduction in climate impact due to the avoidance of atmospheric regions where water vapor has a bigger effect. The regions where water vapor emission has a bigger effect are characterized by a low precipitation rate. This leads to higher water vapor concentration in the atmosphere and therefore higher climate impact. However, due to the high increase in fuel consumption in the last part of the optimization, the water vapor emission increases and completely cancels the re-routing effect. Nevertheless, its *Relative Contribution* is negligible.

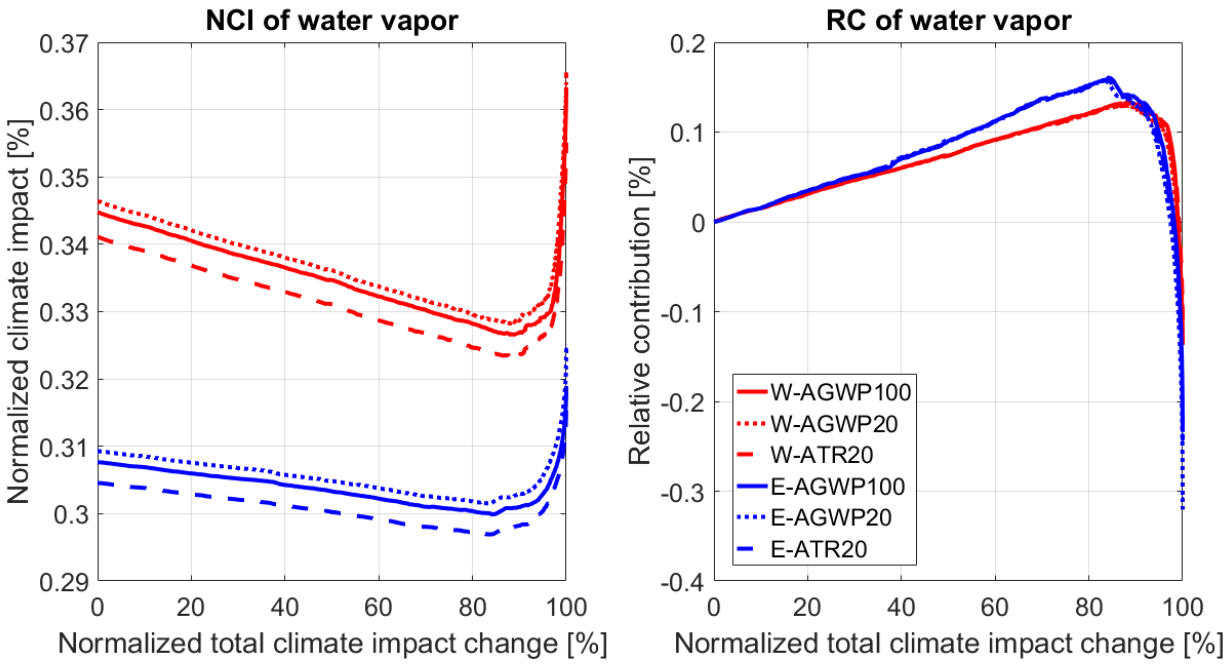

Figure 8. Comparison of water vapor *NCI* and *RC* for Summer Pattern 1 and different flight directions and climate metrics.

The following climate parameter to be study is contrails. Its *NCI* and *RC* are presented in Figure 9. The *NCI* is quite similar during the whole optimization for the same direction. Its value is also quite high, starting at 81% in all cases and finishing in 77% for eastbound flights and 67% for westbound. Because its perturbation lifetime is in the order of hours [5], the climate metrics are organized in the same order than in water vapor case. So AGWP20 is higher than AGWP100, which is also higher than ATR20.

The *RC* of contrails follows a linear behavior up to a *NTCIC* of 90% for eastbound and 95% for westbound. Linear behavior means that the curve is almost a straight line. Until *NTCIC*=90%, the *RC* is the same for all cases and increases considerably during the whole process. For example, its value is a bit higher than 80% for a *NTCIC* of 85%. After its maximum value, it remains almost constant and even goes down for a bit. Therefore there is not more reduction in aircraft induced cloudiness in the last part of the optimization.

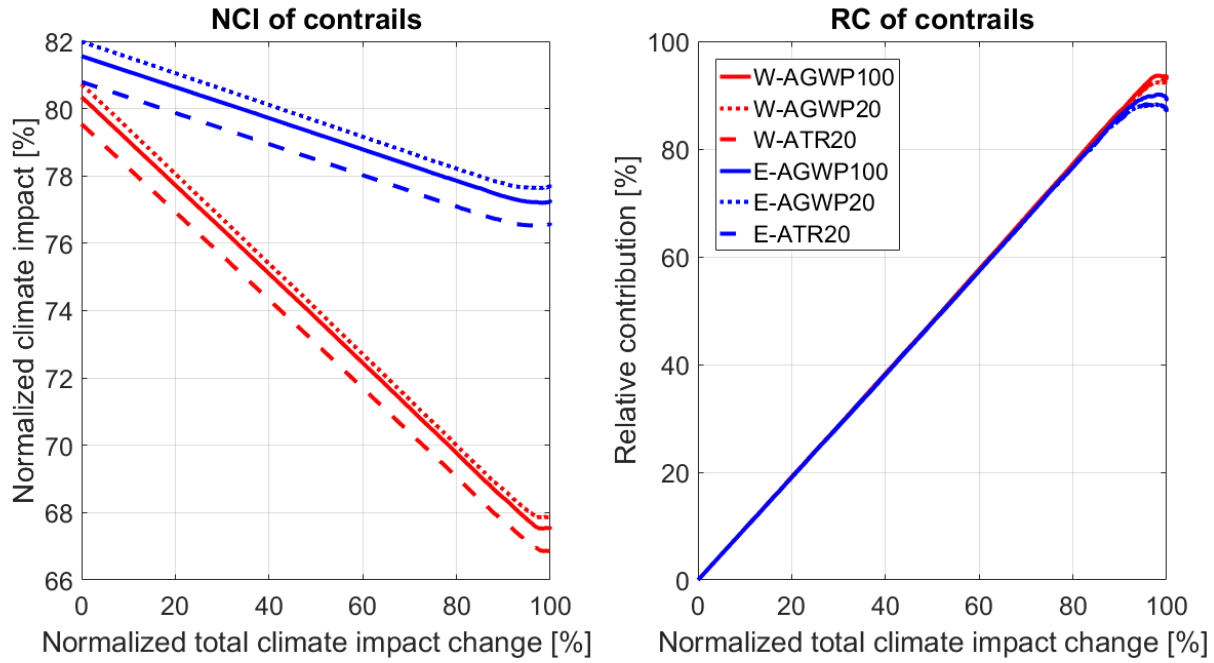

Figure 9. Comparison of contrails *NCI* and *RC* for Summer Pattern 1 and different flight directions and climate metrics.

The last of the four principal climate parameters is NO_x. Its *NCI* and *RC* are presented in Figure 10. The *NCI* varies for the different cases. However it is similar in value for the same climate metric, and similar in shape for the same flight direction. Its range of value goes from 19.5% to 14%, so it does not change considerably. It is important to realize that the maximum value corresponds to ATR20 followed by AGWP20. The last one is the AGWP100. This will be explained after seeing the behavior of ozone and methane. Also, the NCI is always positive.

The *RC* is very similar in the different cases for same flight direction. It is a bit higher for eastbound flights. Until *NTCIC* reaches a value of 80%, the behavior is mostly linear for all cases reaching a *RC* of around 3%. From that point, it increases rapidly up to around 9% for westbound flights and 14.5% for eastbound flights. Therefore in this last part the NO_x is compensating the increase in CO_2 emissions and the constant value of contrails *RC*.

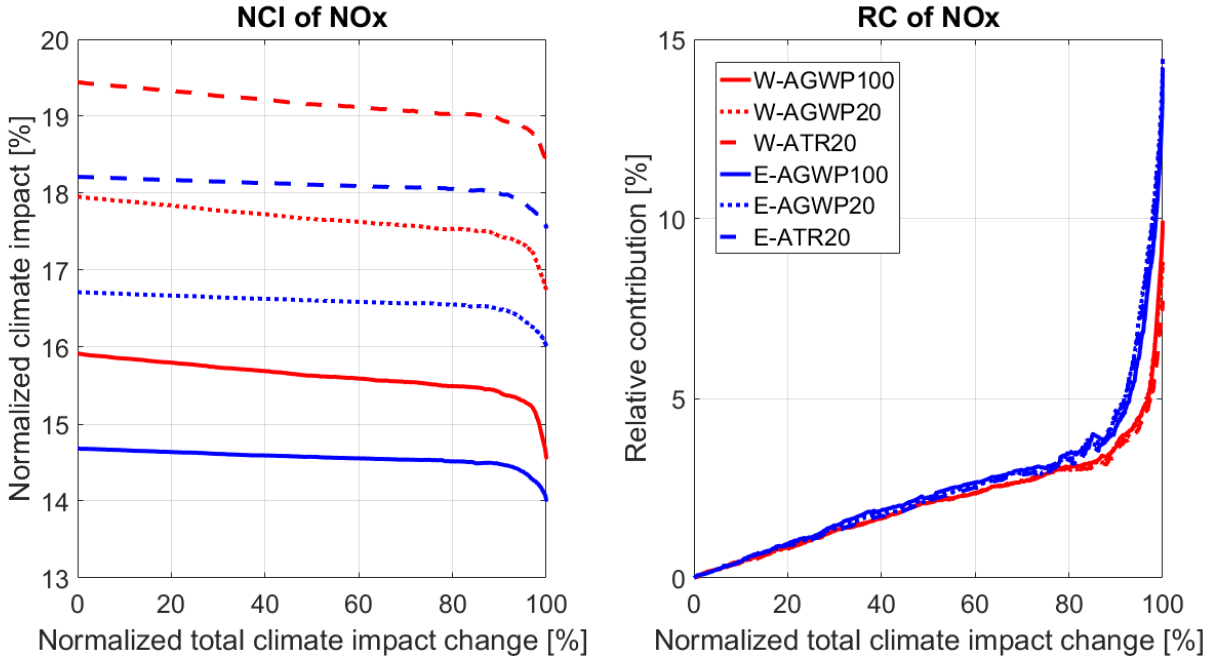

Figure 10. Comparison of NO_x *NCI* and *RC* for Summer Pattern 1 and different flight directions and climate metrics.

In order to see how the NO_x is driven, ozone and methane have to be analyzed. Figure 11 shows *RC* and *NCI* of ozone. The *NCI* is almost the same for the same direction. Also, there is not much difference between westbound and eastbound flights. However, in westbound flights, *NCI* is slightly larger. Its range of value remains between 26.5% and 24%. The way the values are ordered for the different climate metrics is the same than in water vapor and contrails. The reason behind that is the short-term climate impact of ozone, which is around one year [5].

The ozone *RC* is almost the same for same direction. In both cases it increases up to 2.8% when *NTCIC* is 80%. Then it increases rapidly, especially for eastbound flights reaching a value of 11.5% for ATR20 and 9.5% for AGWP100. For westbound flights it increases up to 5% when *NTCIC* is equal to 98% and then decreases to 4%. It is important to realize that the *RC* of the ATR20 climate metric is the highest followed by AGWP20 and finally AGWP100. This means that the effect that re-routing has on ozone climate impact is more important in the short term.

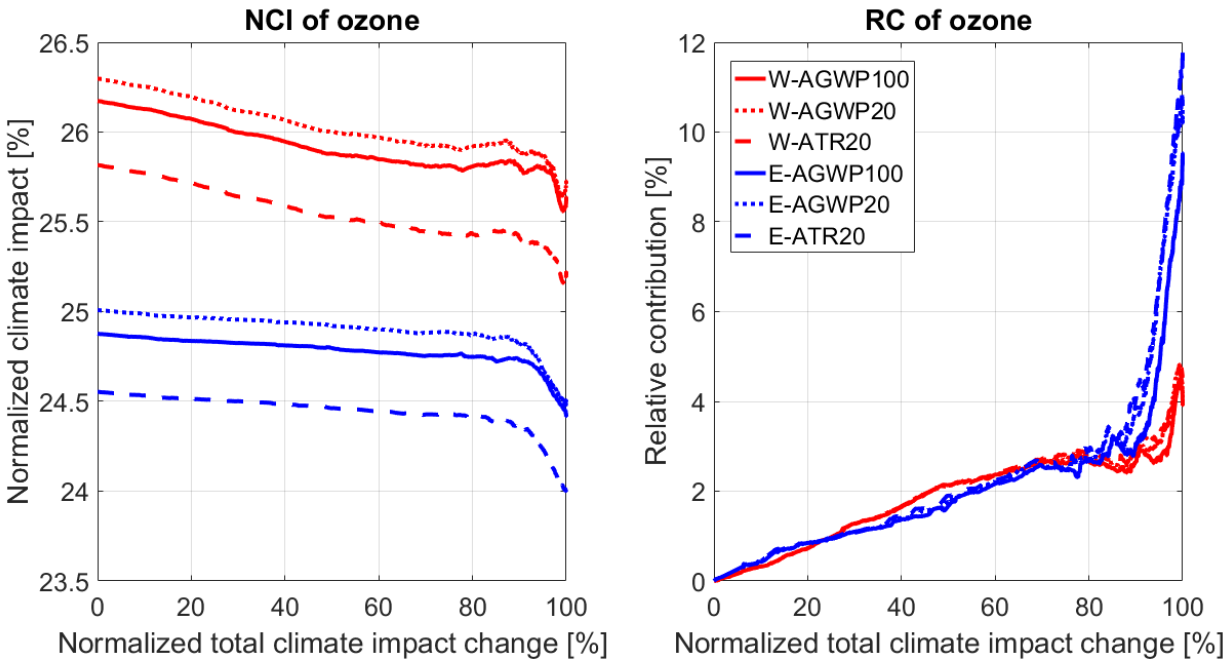

Figure 11. Comparison of ozone *NCI* and *RC* for Summer Pattern 1 and different flight directions and climate metrics.

The last climate parameter to be considered is methane. Its *NCI* and *RC* are shown in Figure 12. First of all, its *NCI* is always negative. This implies that it has a net-cooling effect. Remember that methane is depleted due to NO_x emission [5]. Also, the *NCI* is quite similar in value for the same climate metric and similar in shape for the same flight direction. Moreover the value remains between -5% and -8.5%, so there are not big differences. Considering absolute values, AGWP100 values are larger than AGWP20 values which are also bigger than ATR20 values. Since methane perturbation lifetime is around 12 years [5], it will be more important for long term climate metric when compared to contrails, ozone, or water vapor.

Methane *RC* is quite similar when the flight direction is the same. However, especially from 80% to 100% of *NTCIC*, it is obvious that the *RC* of AGWP100 is the highest followed by AGWP20 and then ATR20. The shape of the different curves when the flight direction is the same is almost constant and there is a difference between the climate metrics of less than 0.5% until *NTCIC* is 80%. From that point there is a difference of a 1% in *RC* between the different climate metrics. The maximum value is reached at 100% of *NTCIC* and for the AGWP100 climate metric is 4.6% (westbound) and 3.6% (eastbound). Methane *Relative Contribution* is more important in long term scenarios compared to contrails, ozone and water vapor.

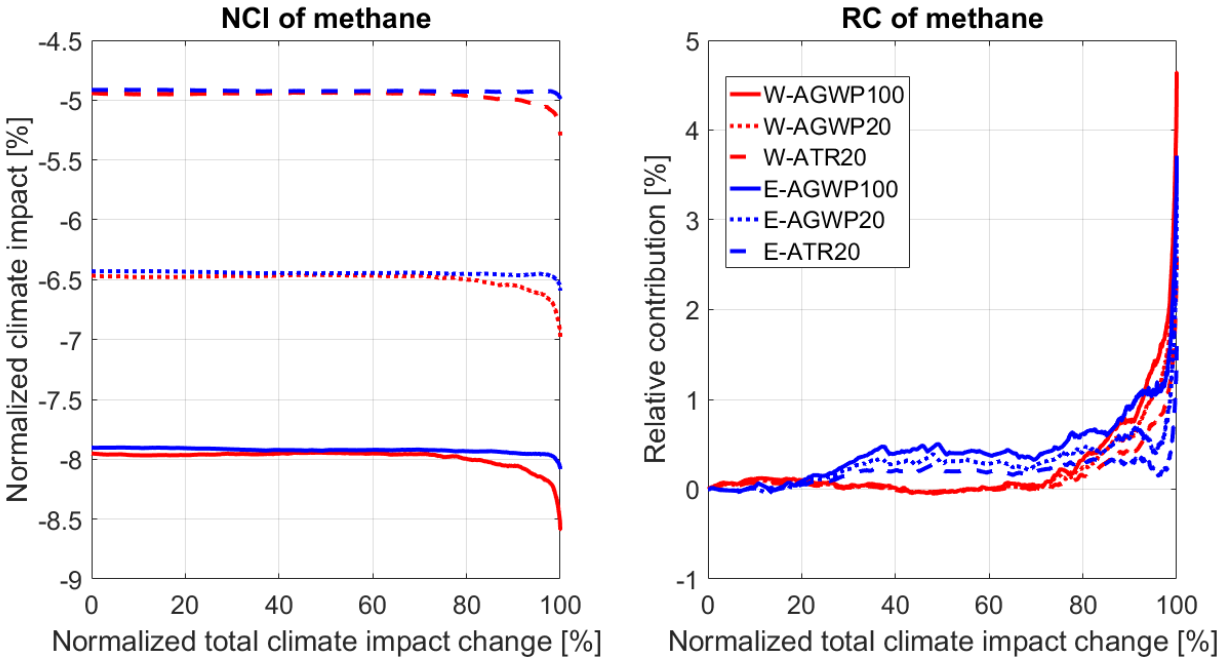

Figure 12. Comparison of methane *NCI* and *RC* for Summer Pattern 1 and different flight directions and climate metrics.

After analyzing ozone and methane, the shape of the *NCI* curves can be explained. For ozone the followed order is AGWP20 bigger than AGWP100 also bigger than ATR20. However all values are quite similar. For methane, the followed order in absolute value is AGWP100 bigger than AGWP20 which is also larger than ATR20. The effect of PMO (not presented here) is the same than methane´s but multiplied by 0.29 [33]. Therefore it is adding to methane. Finally, NO_x values are obtained by addition of ozone, methane and PMO. Taking into account that values for ozone are quite similar but larger in absolute value than the combination of methane of PMO, the NO_x *NCI* is always positive in SP1. Adding all the results it is clear that the order is going to be determined by methane and PMO because the gap between the different climate metrics values is higher. Therefore the climate metric with the lowest *NCI* in absolute value for methane will be the highest for NO_x.

Regarding the contribution of ozone and methane to NO_x, *RC* for NO_x is driven by ozone up to a *NTCIC* of 80%. After that point it varies depending on the flight direction. For eastbound flights ozone is dominant during the whole optimization and methane only helps a little bit. For westbound flights both climate parameters have a similar importance.

After analyzing this first weather pattern, some conclusions for SP1 can be drawn:

- Water vapor is negligible.
- Contrails *NCI* and *RC* curves follow a linear behavior and are driving the optimization until a *NTCIC* of 90% (eastbound flights) and 95% (westbound flights). Linear behavior means that *NCI* and *RC* curves are almost straight lines. After that point NO_x is responsible for the total climate impact reduction.
- Carbon dioxide becomes more important during the last part of the optimization due to the increase in fuel consumption. It is more important for AGWP100 followed by AGWP20 and then ATR20 due to its long-term climate impact. Its *RC* is always negative.
- NO_x *Relative Contribution* is driven by ozone up to a *NTCIC* of 80%. From that point, for eastbound flights, ozone remains more important. For westbound flights, methane and ozone have a similar contribution.

4.2. Summer Pattern 2

The second weather pattern to be analyzed has a high maximum *RTCIC*. This value is especially high for eastbound flights, where the reduction is larger than 55% for the different climate metrics accompanied with a RECC smaller than 8%. For westbound flights the maximum reduction achieved is around 45% with a *RECC* of 15%. The larger reductions are obtained for AGWP20 followed by AGWP100 and then ATR20. For more details see Annex A.

Moving to the first climate parameter, carbon dioxide, like in the prior case, its *NCI* is quite similar for same climate metric but a bit higher for eastbound flights. This value is around 11% for AGWP100, 3% for AGWP20 and 2% for ATR20. Again the long-term climate impact is noticeable for carbon dioxide. Regarding its *RC* of carbon dioxide, it follows a parabolic behavior most noticeable for the long-term climate metric and westbound flights. The reason is the increment of required fuel to perform the new routes of the last segments. The biggest *RC* in absolute terms corresponds to W-AGWP100 and is -4%. The next one is around -2% and corresponds to E-AGWP100. Therefore it is not very important. In addition, water vapor effect is negligible. Its *NCI* is ordered the same way than in SP1. For the graphs, see Annex A.

The next climate parameter to be analyzed is contrails. Its NCI and RC are presented in Figure 13. The values of *NCI* are almost the same during the whole optimization for the same direction. It changes considerably during the process and eastbound flights even reach values lower than -12%, meaning that they have a cooling effect.

Regarding its *Relative Contribution*, its value is almost the same for all cases. However for eastbound flights is a bit higher up to a *NTCIC* of 95%. After that, westbound flights values are a bit larger. All cases reach a value higher than 100%. Moreover, during the whole optimization, *RC* is almost the same than *NTCIC*. Considering this, contrails are the driving parameters of this optimization.

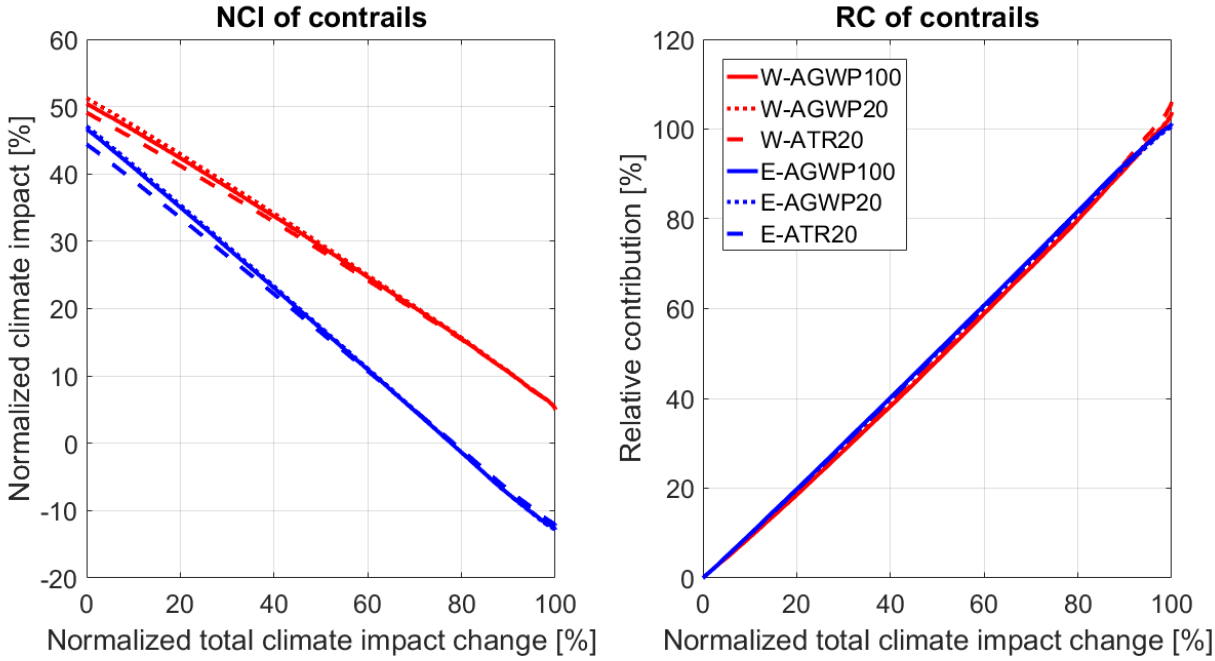

Figure 13. Comparison of contrails *NCI* and *RC* for Summer Pattern 2 and different flight directions and climate metrics.

The last of the four main climate parameters is NO_x. It is shown in Figure 14. Its *NCI* is different for each case, however all cases are between 37% and 53%. This value is higher for eastbound flights and the order followed by the climate metrics is ATR20 bigger than AGWP20 bigger than AGWP100. The explanation for this is the same than in the Summer Pattern 1 analysis. Moreover, the curve shapes are quite similar when the flight direction is the same.

About the *Relative Contribution*, for eastbound flights, it is quite similar. It is slightly positive up to a *NTCIC* of 50%, then it goes down to -1.5% and finally increases in the last 10% of the optimization reaching a value of 1% for AGWP100, 0% for AGWP20 and -0.5% for ATR20. The differences are quite small, and it is a negligible climate parameter in this optimization. For westbound flights there is a certain difference between the different climate metrics. In all three cases the value increases up to a *NTCIC* of 40%. Then the RC goes down ending in 1% for AGWP100, -2% for AGWP20 and almost -5% for ATR20. This is caused due to the different contributions to NO_x and their perturbation lifetimes in the atmosphere.

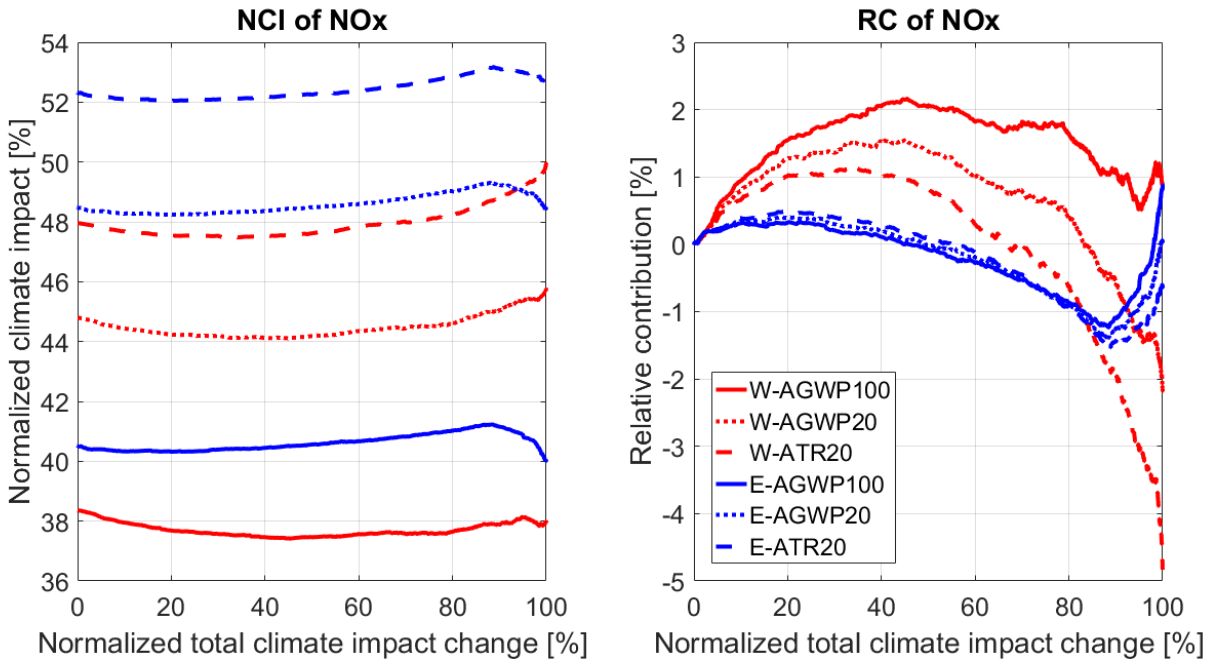

Figure 14. Comparison of NO_x *NCI* and *RC* for Summer Pattern 2 and different flight directions and climate metrics.

In order to explain the NO_x behavior both ozone and methane have to be analyzed. Figure 15 shows *NCI* and *RC* of ozone. *NCI* is quite high for all cases and values are similar for the same direction. There is a maximum difference of 5% for eastbound flights and 4 % for westbound flights between the different climate metrics. The order followed by the climate metrics is the same than in SP1 and is caused by the different time horizons. The RC is the same for the same flight direction. For eastbound flights, it is slightly positive up to a *NTCIC* of 60% and then decreases to -3.5%. Therefore it is not very important. For westbound flights, *RC* is a bit larger than 0% up to a *NTCIC* of 20%. Then it drops rapidly to -15%. This sudden change can be explained, especially in the last segment due to the increase in fuel consumption that also increases the NO_x production and emission. Due to the higher concentration of NO_x in the ambient, there is more ozone creation and therefore a warming effect. Hence, there are two effects related to the NO_x emission: the molecule effect that is highly controlled by the emission point and time, and the amount emitted NO_x that depends on the fuel consumption.

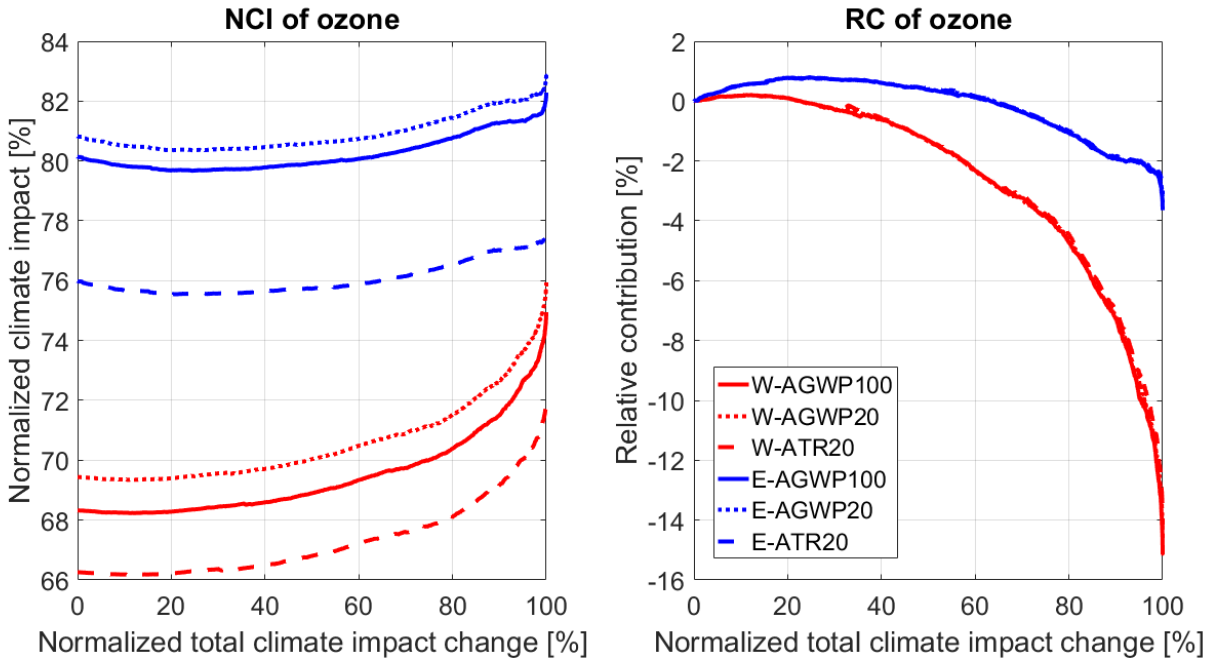

Figure 15. Comparison of ozone *NCI* and *RC* for Summer Pattern 2 and different flight directions and climate metrics.

Methane *NCI* and *RC* are presented in Figure 16. *NCI* values differ for each case. The values are between -33% and -14%. Also, in absolute sense, eastbound values are larger than westbound ones. The order followed by climate metrics is the same than in SP1 for the same reason. Moving to *RC*, it is almost the same for eastbound flights. It is slightly negative until a *NTCIC* of 75% and then it increases up to 3.5% for AGWP100 and 2% for ATR20. Westbound flights show some difference between the climate metrics. In all three cases it increases linearly up to a *NTCIC* of 75% and then in a parabolic way for the last segment of the optimization. The value is higher for AGWP100 followed by AGWP20 and then ATR20 due to a longer-term climate impact of methane in comparison with other climate parameters. This behavior can be explained, as in the case of ozone, with an increase in NO_x emissions due to fuel consumption, leading to a higher depletion of methane and therefore reducing its warming effect.

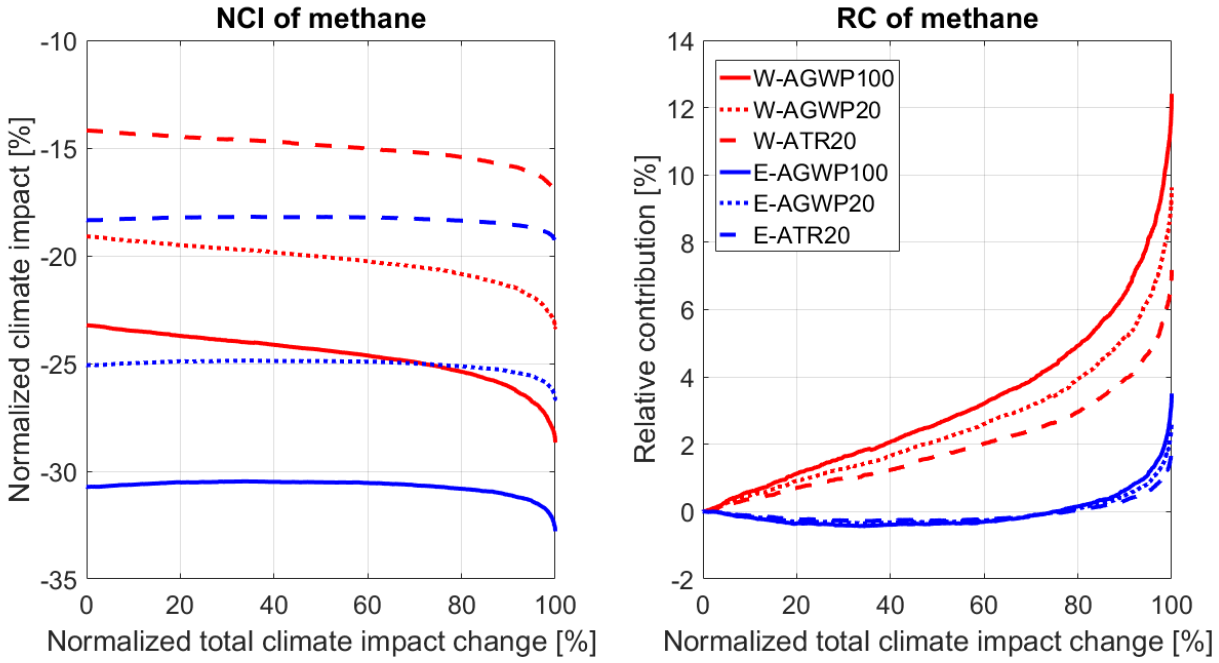

Figure 16. Comparison of methane *NCI* and *RC* for Summer Pattern 2 and different flight directions and climate metrics.

Some conclusions can be obtained from the SP2 analysis:

- Water vapor effect is negligible.
- Contrails, that have a linear behavior, are driving the optimization and reaching values of *RC* higher than 100%. This is compensated in the last part by carbon dioxide in the long term time horizon and NO_x in the short term.
- NO_x has two effects on climate impact, one related to emission region and the other related to the amount of pollutant emitted.
- NO_x *RC* for eastbound flights is driven by ozone and methane up to a *NTCIC* of 60%. After that ozone becomes more important up to a *NTCIC* of 90%, and the methane controls the rest of the optimization. *RC* is higher for AGWP100 followed by AGWP20 and then ATR20.
- NO_x *RC* for westbound flights is controlled by methane for AGWP100, by methane up to a *NTCIC* of 80% for AGWP20 and by methane up to a *NTCIC* of 70% for ATR20. After that point ozone is more important in the optimization.

4.3. Summer Pattern 3

The last summer pattern shows similar Pareto fronts for same flight direction. The *RTCIC* that can be achieved is around -14% for westbound flights with a *RECC* smaller than 8%. For eastbound flights these values are -11% and 10% respectively. In addition, the maximum climate impact reduction is achieved with AGWP as climate metric. ATR20 gives fewer possibilities.

Moving to carbon dioxide, its *NCI* is the same when looking at the same climate. Values are around 15% for AGWP100, 4% for AGWP20 and 3% for ATR20. The longer the time horizon, the larger the *NCI* because of the long-term climate impact of carbon dioxide. Carbon dioxide *Relative Contribution* has a parabolic shape in all six cases. It is important especially for E-AGWP100 with a -14% and W-AGWP100 with a -10%. The other cases do not reach a -5%. The shape of the curve is explained with the increase in fuel consumption especially in the last segment of the optimization. Water vapor has very low both *NCI* and *RC*. Its *NCI* is around 1.3% and the climate metrics follow the same order than in the prior cases. The *RC* reaches a value of -1.5% for westbound flights and -2.5% for eastbound. It can be considered negligible. For more details see Annex A.

Contrails, for first time, are not the driving parameters for most part of the optimization. *RC* and *NCI* are presented in Figure 17. The *NCI* is quite similar for the same direction. Values for all 6 cases are between 19% and 24.5%. The order of the climate metrics is the same than in the prior cases and the reasons are the same. AGWP20 values are higher than AGWP100 ones, which is bigger than ATR20 values.

The *RC* of contrails is lower than in the prior cases. It is almost the same for the same direction, but in the last part of the optimization depending on the climate metric, *RC* has different values. ATR20 is higher than AGWP20 which is bigger than AGWP100. This is explained taking into account the short-term climate impact of contrails, and therefore its higher *Relative Contribution* when considering short term climate metrics. For eastbound flights the *RC* increases up to 5% for a *NTCIC* of 20%. Then it keeps increasing but at a slower pace, reaching 15% in the end. For westbound flights, a 20% is reached when *NTCIC* is equal to 50%. After that it increases up to around 30%.

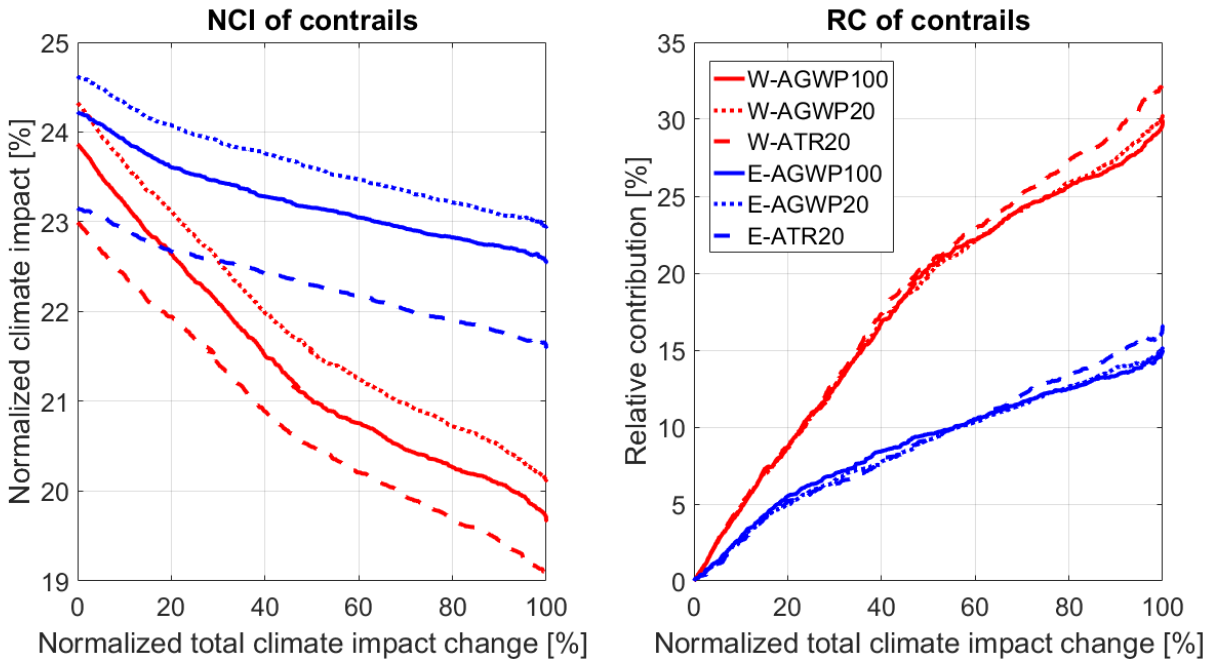

Figure 17. Comparison of contrails *NCI* and *RC* for Summer Pattern 3 and different flight directions and climate metrics.

The following climate parameter to study is NO_x. It is presented in Figure 18. Its NCI is almost equal for the same climate metric. It is quite important in this case with values between 73% and 50%. Also, the order of climate metrics is equal than in the prior cases due to its several impact terms as a combination of ozone, methane and PMO. Regarding the *RC*, it is quite similar for the same direction. In all cases from a *NTCIC* of 40% the growing rate for the AGWP100 climate metric is higher. The behavior of the curves is almost linear increasing more rapidly from a NTCIC of 20% for eastbound flights and 30% for westbound. The values that are reached are around 100% for E-AGWP100 and 80% for W-AGWP100. The other climate metrics reach approximately a 10% less than AGWP100 with the same flight direction. Therefore, especially for eastbound flights, NO_x is driving the optimization.

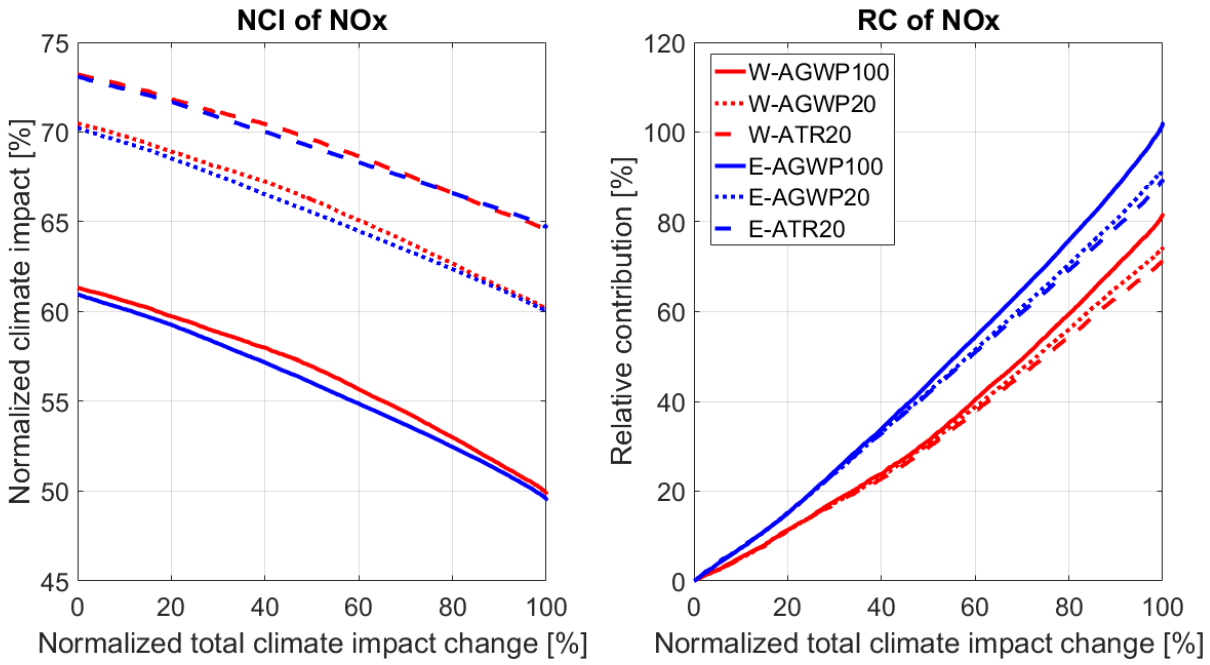

Figure 18. Comparison of NO_x *NCI* and *RC* for Summer Pattern 3 and different flight directions and climate metrics.

In order to see what are the climate parameters controlling the NO_x effect, ozone and methane have to be studied. *NCI* and *RC* of ozone are shown in Figure 19. In this case, *NCI* is quite similar for the same climate metric. Moreover, it reaches really high values, even over 100%. The order of these climate metrics is the same than in the prior cases. This is caused by the short-term climate impact of ozone.

The RC follows a similar tendency for same direction. For eastbound flights, it increases up to 55% for ATR20 while *NTCIC* is 95% and 45% for AGWP100 while *NTCIC* is 90%. For westbound flights, RC reaches 45% and 33% almost in the end of the optimization for ATR20 and AGWP100 climate metrics respectively. In all cases, after reaching the maximum, the *Relative Contribution* decreases rapidly. This last drop is most likely caused by the increment in NO_x emission due to the higher amount of burned fuel.

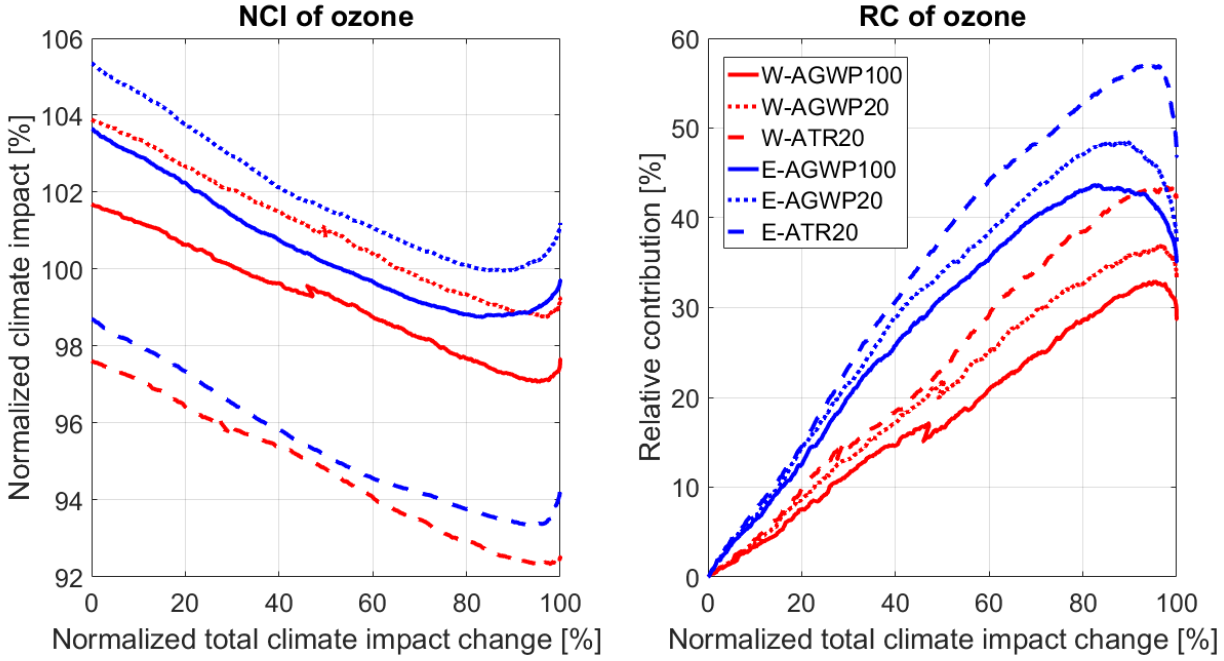

Figure 19. Comparison of ozone *NCI* and *RC* for Summer Pattern 3 and different flight directions and climate metrics.

The last climate parameter is methane. It is represented in Figure 20. The range of values of *NCI* remains between -18% and -38%, and it is quite similar for same climate metric. Also, the order followed by the climate metrics is the same than in the prior cases. The explanation is the mid-term climate impact of methane.

The *RC* curve has a similar tendency in all cases, but especially when the flight direction is the same. All curves are increasing during the whole optimization process, but the growth is always larger for AGWP100 and smaller for ATR20. They have a parabolic behavior, increasing the growing pace when the *NTCIC* increases. The maximum values reached by eastbound flights are between 50% and 30%, while for westbound flights the *RC* reaches between 40% and 25% at *NTCIC* equal to 100%.

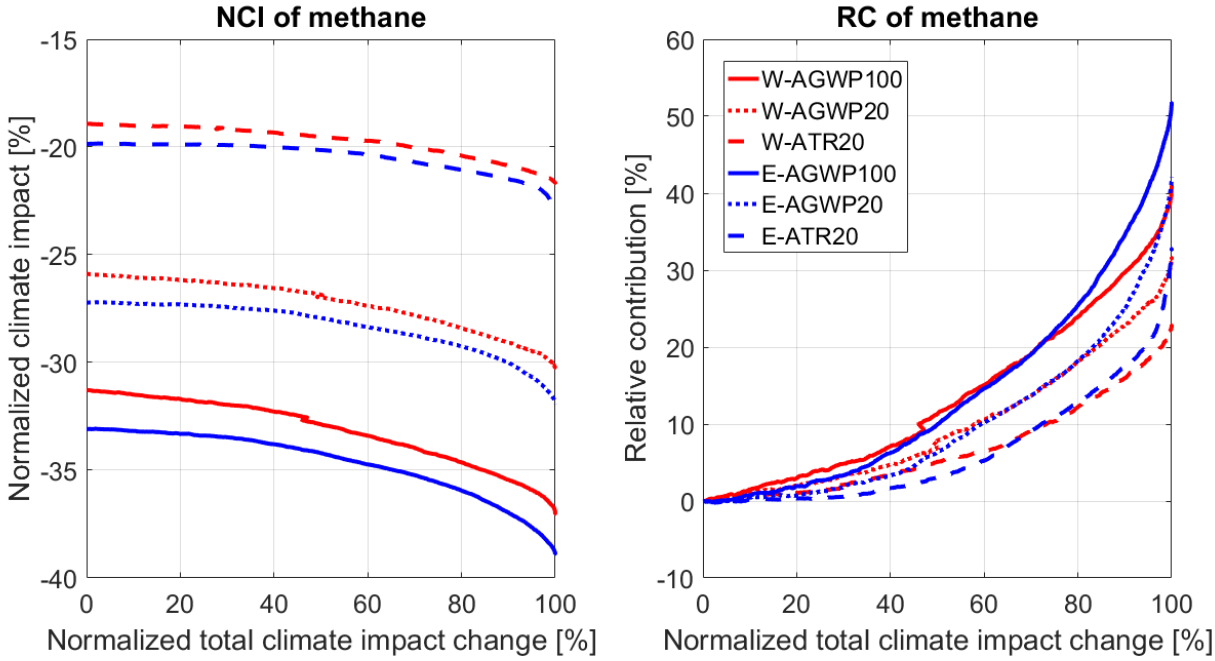

Figure 20. Comparison of methane *NCI* and *RC* for Summer Pattern 3 and different flight directions and climate metrics.

With the analysis performed, some conclusions can be extracted for Summer Pattern 3:

- Water vapor effects are negligible.
- NO_x is driving the optimization with a bit of help from contrails. However NO_x is more dominant.
- NO_x is driven by ozone during the whole process. However, the *Relative Contribution* of methane is also relevant during the whole process and especially from 75% to 100% of *NTCIC* because the increment in NO_x emissions at this point produces more warming effect from ozone and more net-cooling from methane. Methane relevance is higher when using climate metrics with long term time horizons.

4.4. Summary of summer patterns

Before continuing with the next weather pattern analysis, making a short summary of what has been observed until now may be helpful. Doing that, the most interesting similarities can be explained.

First of all, the behavior followed by carbon dioxide is very consistent through the three analyses. Its *NCI* is always higher for AGWP100 and then followed by AGWP20 and ATR20. This occurs due to its long-term climate impact, and therefore it reaches higher values when the time horizon considered is larger. Its value is low in comparison with contrails and NO_x even when looking at the AGWP100. Its *RC* is always negative and decreases more when the *NTCIC* goes up. It decreases faster in the last segment of the optimization because the fuel consumption goes up more rapidly. The Relative Contribution is always negative and higher in absolute sense for AGWP100 and then AGWP20 and ATR20. This happens for the same reason than for the *NCI*. However, it can be important for AGWP100. For the other climate metrics, *RC* does not even reach -5%.

The second climate parameter to be considered is water vapor. Its *NCI* is always very low and similar for the different directions and climate metrics. The climate metrics also follow an established order, being the AGWP20 the highest and ATR20 the lowest. This occurs because water vapor has a short-term climate impact and therefore it is more important with a time horizon of 20 years than with 100 years. The reason why ATR20 remains in the last position is the different type of emission used (future air traffic scenario instead of pulse emission). The *RC* is the same for same direction and it is really low. Therefore water vapor can be considered a negligible effect.

The third climate parameter is contrails. It is an important parameter in all cases. Its *NCI* varies in value from one case to another, but it is always quite high. Also, the values are quite similar when the direction is the same for the same weather pattern. Moreover, the *Normalized Climate Impact* has a slightly different value depending on the climate parameter, but it follows always the same order. AGWP20 is higher than AGWP100 which is higher than ATR20. The same explanation used for water vapor is applied in this case. The *RC* is very similar for the same flight direction. It increases almost during the whole optimization but it can also remain constant or go down in the end. Furthermore, it is higher for ATR20 followed by AGWP20, and finally by AGWP100. This happens because its importance is higher when the time horizon is smaller due to its short-term climate impact.

The next climate parameter is NO_x. It is the combination of ozone, methane and PMO. Its *NCI* has always a positive value, meaning that the warming effect of ozone is more important than the net-cooling effect caused by the depletion of methane and PMO. The value changes for each case but the order is always the same in relation with the climate metrics. ATR20 values are higher than AGWP20 values, which are also higher than AGWP100 ones. The reason for this order has been explained during the analysis and it is related with the different perturbation lifetime of ozone, methane and PMO in the atmosphere. The *Relative Contribution* shows some similarities when the direction is the same in the different cases. However, the most interesting result obtained is the order depending on the climate parameters. When moving to a *NTCIC* of 100%, the *RC* curves for same direction tend to split. The highest value corresponds to AGWP100 followed by AGWP20. The smallest value corresponds to ATR20. This happens also due to the different perturbation lifetimes of the climate parameters considered to obtain the NO_x effect.

Talking about climate parameters determining the climate impact of NO_x, ozone appears in first place. Its *NCI* is always positive and quite high. Also, the configurations with same weather pattern and direction are very similar in values and shape. Moreover, the climate metrics are ordered in all cases with AGWP20 as the biggest and ATR20 as the smallest. This is explained by the short-term climate impact of ozone, which is less than one year, and the different emission type used for AGWP and ATR calculations. The *Relative Contribution* is quite similar for same direction and weather pattern. Nevertheless, it changes a bit depending on the climate metric. In this case, again, an order is followed. ATR20 is always higher than AGWP20. AGWP100 is always the smallest. This happens because ozone has a higher importance in the short term. In addition, in some cases, the *RC* goes down in the last part of the optimization due to the larger emissions of NO_x caused by the increase in fuel consumption. This increase in NO_x emissions stimulates higher ozone production.

Finally, the other important climate parameter controlling NO_x is methane. Its *NCI* is always negative and varies considerably depending on the climate metric and direction considered. However, in absolute value, it is always way smaller than ozone *NCI*. Moreover, the order followed by the climate metrics is consistent. Considering absolute values, AGWP100 is higher than AGWP20, which is also higher than ATR20. The *Relative Contribution* is different for the different cases, but the tendency is quite similar for same weather pattern and flight direction. However, there is a clear order of the curves depending on the climate metric considered. AGWP100 has always the highest value while ATR20 has the lowest. Its value, when looking at the long term climate metric, is higher because methane´s perturbation lifetime is around twelve years, therefore one order of magnitude larger than ozone and a few orders of magnitude larger than contrails or water vapor. Also, in some cases, in the last segment of the optimization the *RC* increases rapidly due to the increase in NO_x emission and therefore the enhanced effect in methane depletion.

From these paragraphs some interesting conclusions can be obtained:

- The short term effects (water vapor, contrails and ozone) have similar values of *NCI* and *RC* when the weather pattern is the same. Moreover, from the highest to the lowest, the climate metrics are ordered as AGWP20, AGWP100 and ATR20 for *NCI*; and ATR20, AGWP20 and AGWP100 for *RC*. The reason why the values are so similar especially for contrails and water vapor (perturbation lifetimes of the order of one day) is explained looking at the considered time horizons. Both 20 years and 100 years are several orders of magnitude larger than one day; therefore the difference between them has to be small. In the case the time

horizons considered were for example one month and one year, the differences between *NCI* and *RC* for the different climate metrics would be way higher.
- The mid and long term effects (carbon dioxide and methane) have a wider range of *NCI* and *RC* values. However, in absolute value, the climate metrics follow the same order. From the biggest to the smallest, AGWP100, AGWP20 and ATR20. This can be applied for both *NCI* and *RC*. The wide range of values for *NCI* and *RC* occurs because the time horizons considered are of the same order than the perturbation lifetimes.
- The case of the NO_x is a bit different in terms of *NCI* but follows the same order than methane for *RC*. This happens because it is the combination of ozone, methane and PMO. Its *NCI* is always positive due to ozone and the order it follows is: ATR20 is the highest followed by AGWP20, and finally AGWP100.
- Water vapor effect is negligible.
- The optimization is driven by contrails and/or NO_x.
- Pareto fronts for the same weather pattern and flight direction are very similar in terms of *RTCIC* and *RECC*. Moreover, AGWP100 and AGWP20 are almost equal, while ATR20 shows a smaller climate impact reduction.

The summary made here will help clarifying the ideas. In the next weather pattern analyses, the results commented in this part are assumed unless something different is indicated. This will clarify the results and avoid repeating the same explanations.

4.5. Winter Patterns

It has been shown that depending on the weather pattern for summer patterns, some noticeable differences can be found especially regarding which are the driving parameters of the optimization. However, winter patterns show a similar behavior in almost every aspect. This includes *NCI* and *RC* values and the way they behave during the optimization process.

The Pareto fronts change from case to case. Both carbon dioxide and water vapor have the same behavior than in Summer Patterns. Contrails are the most important driver of the optimization especially for ATR20 and westbound flights. NO_x contributes to the optimization and it is also important but always smaller than contrails *Relative Contribution*. It is more noticeable for long term climate metrics and eastbound flights. NO_x *RC* is first controlled by the reduction in climate impact from ozone and methane due to the avoidance of climate sensitive regions. The last segment of the optimization is characterized by an increase in NO_x emissions. This leads to a higher *RC* of methane but a decrease in ozone *Relative Contribution*. Usually methane *RC* is higher in absolute sense than ozone´s. However ozone can be noticeable especially for short term climate metrics. For all the details see Annex A.

The most important highlights of each winter pattern are:

WINTER PATTERN 1

- Water vapor effect is negligible.
- Contrails are the primary drivers of the optimization and their *Relative Contribution* curve is a straight line. This happens especially for westbound flights, where their *RC* is higher. For eastbound flights, NO_x becomes more important and it is more noticeable with AGWP100.
- NO_x is mostly controlled by methane, but ozone becomes also important in the last segment of the optimization, been notorious in W-ATR20.
- Carbon dioxide becomes more important in the last segment of the optimization, especially for AGWP100. This is caused by the increase in fuel consumption.

WINTER PATTERN 2

- Water vapor effect is negligible.
- Contrails are the primary driving parameters of the optimization in all cases but especially for westbound flights.
- NO_x is controlled by methane in all cases except for the last 20% and 10% of the optimization for W-ATR20 and W-AGWP20. In those cases, ozone becomes more important.

WINTER PATTERN 3

- Water vapor effect is negligible.
- Contrails are the main drivers of the optimization for all configurations. However, NO_x is also important especially when considering the long term climate impact.
- NO_x is controlled by methane during the whole process. Ozone contributes with positive values at least during the first 90% of the optimization. However, when its *RC* becomes negative, this value is compensated by the combination of methane and PMO.

WINTER PATTERN 4

- Water vapor effect is negligible.
- Contrails are driving the optimization in all cases. NO_x becomes more important when considering the climate metric with long time horizon.
- NO_x is controlled primarily by methane and PMO. The last segment of the optimization, between 80% and 100% of *NTCIC*, is characterized for an increase in fuel consumption due to larger modifications on the routes. This increases NO_x emissions and enhances ozone formation and methane depletion.

WINTER PATTERN 5

- Water vapor effects are negligible.
- Contrails are driving the optimization in all cases. However NO_x is also important for eastbound flights and long-term climate metrics.
- NO_x is controlled by methane and PMO during the whole optimization. Ozone is also noticeable in the last 2% of the optimization.

4.6. Comparison between different weather patterns and flight directions for same climate metric

After analyzing the different weather patterns one by one, it is interesting to show some results so the different weather patterns can be compared easily. The different weather patterns and flight directions combinations are going to be presented to establish the new comparison. Only one climate metric is going to be used since it has been already studied the influence the climate metrics have on the different configurations. The chosen climate metric is AGWP100 since it is important to focus in the long term impact. Consider that carbon dioxide will remain in the atmosphere for centuries after the emission is released while the other emissions will vanish.

Figure 21 shows different values of *Normalized Climate Impact* for different combinations of weather pattern and flight direction. The horizontal axis indicates the weather pattern and flight direction combination. The first letter shows the flight direction (E for eastbound and W for westbound). The second letter and the number give the information regarding the weather patter (S for summer and W for winter). Each of the curves presented show different values of *NTCIC*. These values are 0% (red), 25% (magenta), 50% (blue), 75% (black), and 100% (green). This code of color is going to be used for the following figures.

Figure 21, in particular, shows the results for carbon dioxide *NCI*. Same weather patterns show almost the same values, not matter the flight direction. Comparing the different configurations, except for Summer Pattern 1 where the *NCI* is smaller than 4%, the *NCI* values are close to 14% for the major part of the optimization. When increasing the *NTCIC* there are not great changes in the *Normalized Climate Impact* values except from 75% to 100%. In this last segment there is a noticeable increase in all cases. However, it is never higher than 2%. It is caused by the higher increase in fuel consumption associated to the last part of the optimization.

The *Relative Contribution* of carbon dioxide is negligible in all cases for the first 75% of the optimization. When *NTCIC* is 100%, carbon dioxide *RC* reaches its minimum value in all cases. However, it is never lower than -15% (for Eastbound-SP3). This negative *RC* means that carbon dioxide is having a warming effect when carrying out the optimization. This is related with the increase in fuel consumption. Nevertheless, when considering the different climate metrics, *RC* is always higher since their time horizon is shorter. If the reader is more interested, there is a complete list with the different figures of *NCI* and *RC* comparisons for different weather patterns and flight directions.

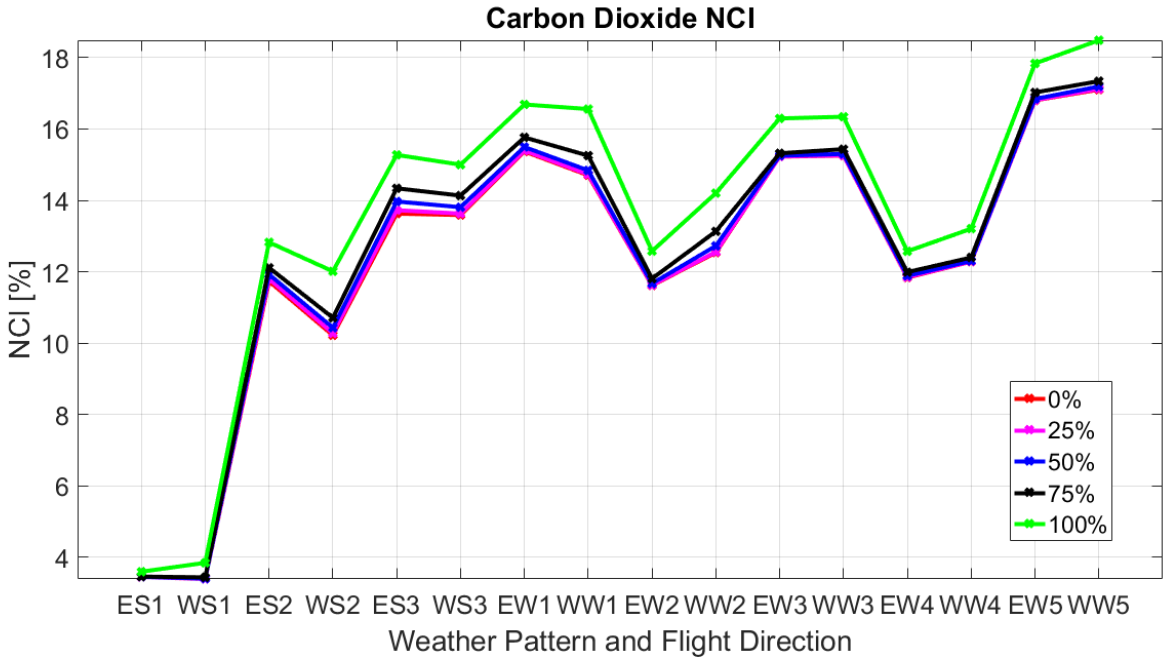

Figure 21. Comparison of carbon dioxide *NCI* for AGWP100 climate metric and different flight directions and weather patterns. The *NTCIC* values presented are 0%, 25%, 50%, 75%, and 100%.

In the case of water vapor, its *NCI* as well as *RC* are negligible in all cases. However, the way its *Relative Contribution* behaves during the optimization is interesting. In the first segment, up to a *NTCIC* equal to 25%, its value is almost 0%. From that point, depending on the case, it can increase or go down, but the change, in absolute sense, is never higher than 1% when *NTCIC* is equal to 75%. The cases where *RC* goes up when *NTCIC* increases are changing the trajectories avoiding climate sensitive areas of the atmosphere in relation with water vapor. In the final segment of the optimization the values are always negative and the lowest for each configuration. This effect is related with an increase in fuel consumption and therefore water vapor emission coming from the combustion process. To see this with more detail, refer to Annex B.

In Figure 22, the *NCI* values of contrails are presented. For summer patterns, the range of values is quite large as seen in the prior analyses. However, winter patterns show similar values for the different configurations of flight direction and weather pattern. This value is around 60% when *NTCIC* is equal to 0% and then decreases differently depending on each case, but never reaching values lower than 35% (for Westbound-WP2). Moreover, *NCI* goes down during the whole optimization. Looking at any given configuration, it is important to realize that the gaps between the curves with different *NTCIC* values are almost the same. This means that the changes in contrails *NCI* are almost the same on each segment of the optimization.

Figure 23 shows the results of contrails *Relative Contribution* for different configurations. The different values are presented following the same color code as in *NCI* figures. However values for *NTCIC* equal to 0% are not presented since the *Relative Contribution* is 0% in that case. For all configurations, except Summer Pattern 3, contrails show high *RC.* In all these cases, its value is at least 70% when *NTCIC* is equal to 100%. This means that for all those cases, contrails are driving the optimization. Moreover, here is only shown AGWP100 climate metric. With this climate metric, since it considers the largest time horizon, contrails have the smallest *RC* compared to the other climate metrics that consider shorter time horizons. Hence, contrails will be driving the optimization in each configuration except for Summer Pattern 3. Moreover, values for westbound flights are higher in most cases during the whole optimization, but always when *NTCIC* is equal to 100%.

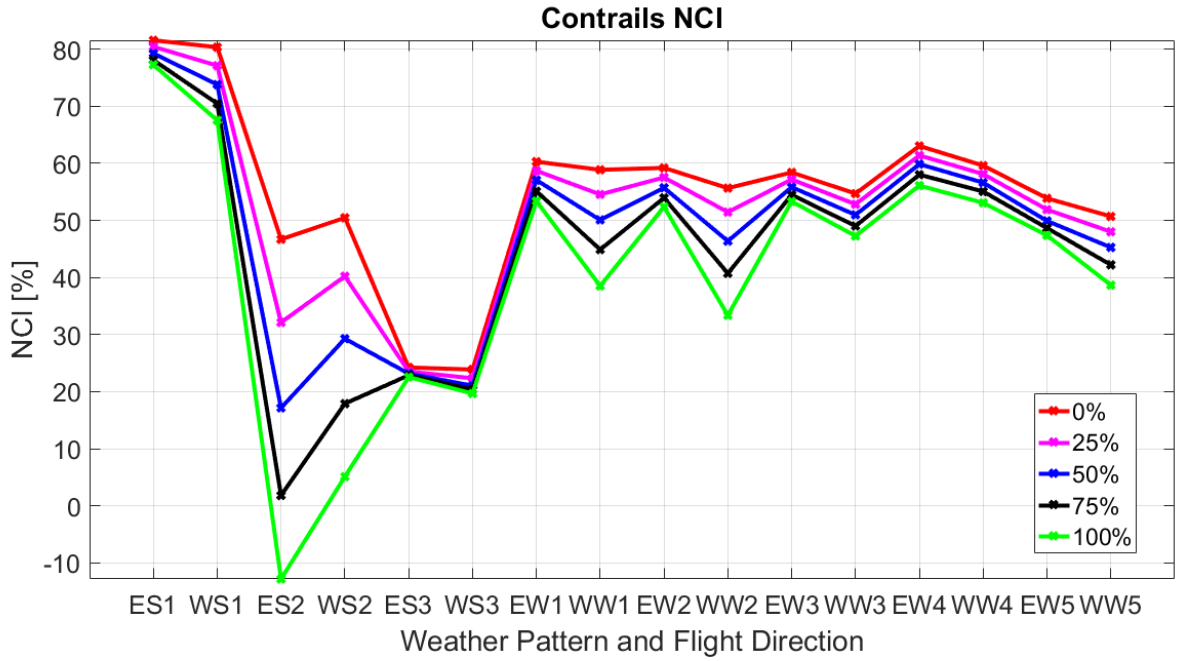

Figure 22. Comparison of contrails *NCI* for AGWP100 climate metric and different flight directions and weather patterns. The *NTCIC* values presented are 0%, 25%, 50%, 75%, and 100%.

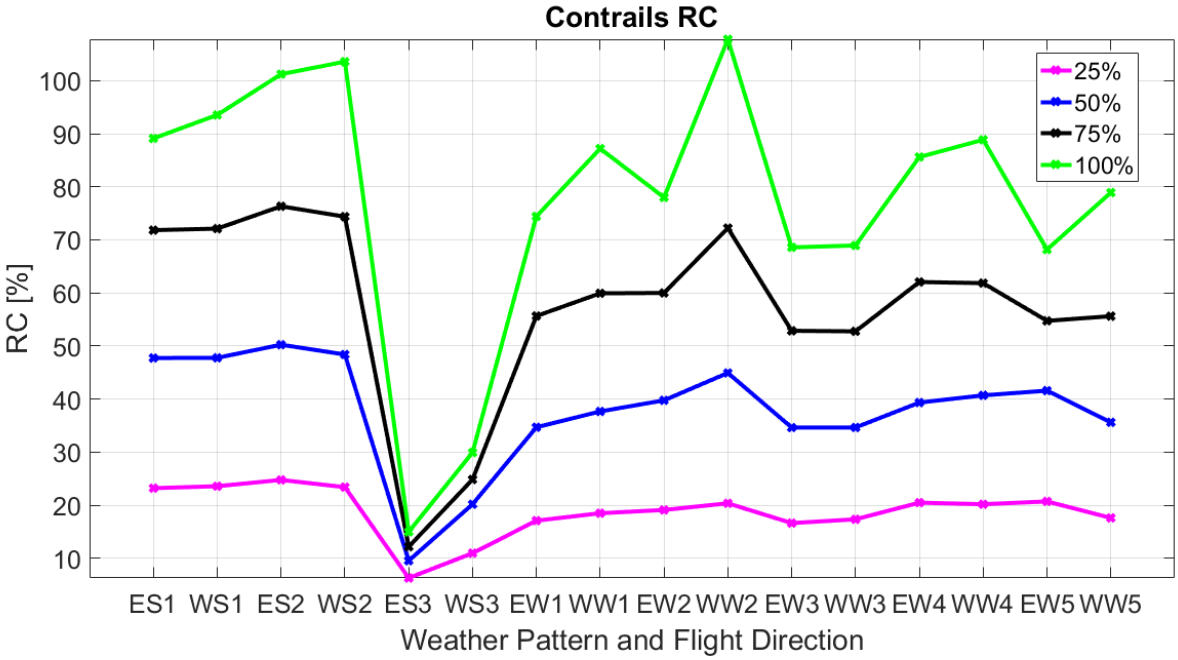

Figure 23. Comparison of contrails *RC* for AGWP100 climate metric and different flight directions and weather patterns. The *NTCIC* values presented are 25%, 50%, 75%, and 100%.

Figure 24 and Figure 25 show NO_x *NCI* and *RC* respectively. In the case of *Normalized Climate Impact*, its general tendency is to decrease during the optimization. This happens in every case except for Westbound-SP2 and Westbound-WP2. In these two cases ozone climate impact increases at a faster pace than the net-cooling produced by methane and PMO combined effects. In addition, summer pattern show great differences when compared to each other. However, winter patterns values are quite similar during all the optimization process remaining 20% and 30% during all the optimization and not changing more than 5% for each case.

The NO_x *Relative Contribution* is different for each case. It is never higher than the values shown for contrails in Figure 23 except for Summer Pattern 3. Only in that case, NO_x is driving the optimization. Moreover, all weather patterns increase or keep the *RC* constant when *NTCIC* is between 0% and 75%. For *NTCIC* equal to 100%, the

Relative Contribution values are higher than in the prior cases except for Westbound-SP2 and Westbound-WP2. In addition, summer patterns show high variability while winter patterns are quite similar. *RC* is never higher than 25% (for Westbound-WP3) when *NTCIC* is equal or less than 75%. For maximum *NTCIC* the *RC* values vary but they are never higher than 50% (for Eastbound-WP3). Furthermore, values for eastbound flights are always higher than for eastbound flights for same weather pattern for maximum *NTCIC*.

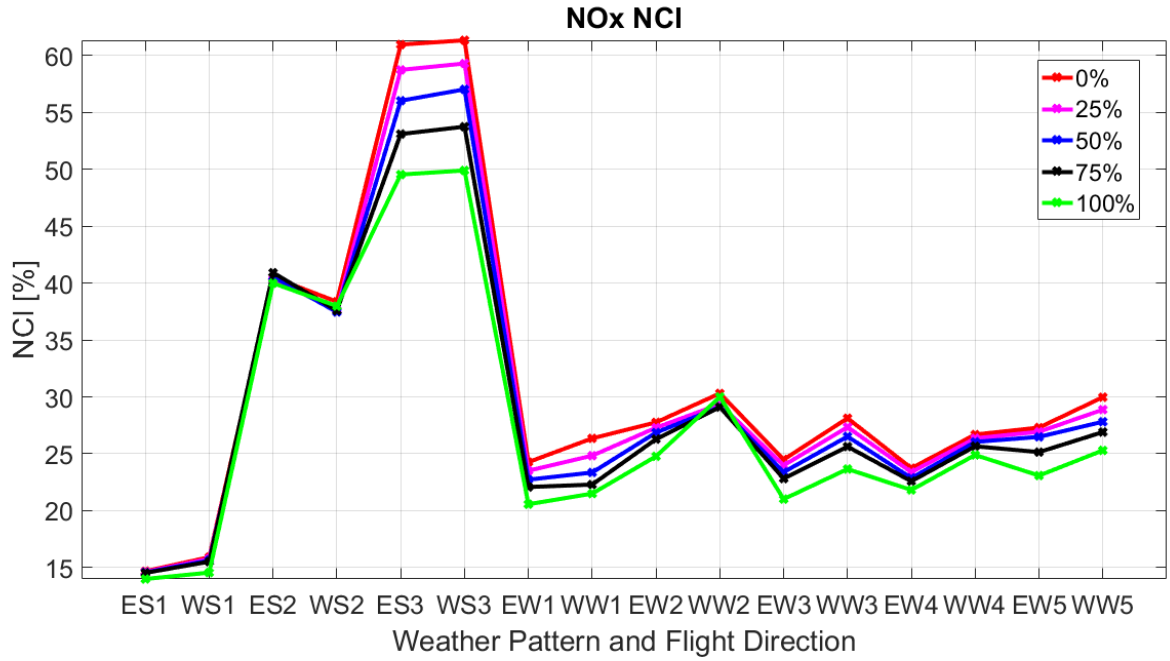

Figure 24. Comparison of NO_x *NCI* for AGWP100 climate metric and different flight directions and weather patterns. The *NTCIC* values presented are 0%, 25%, 50%, 75%, and 100%.

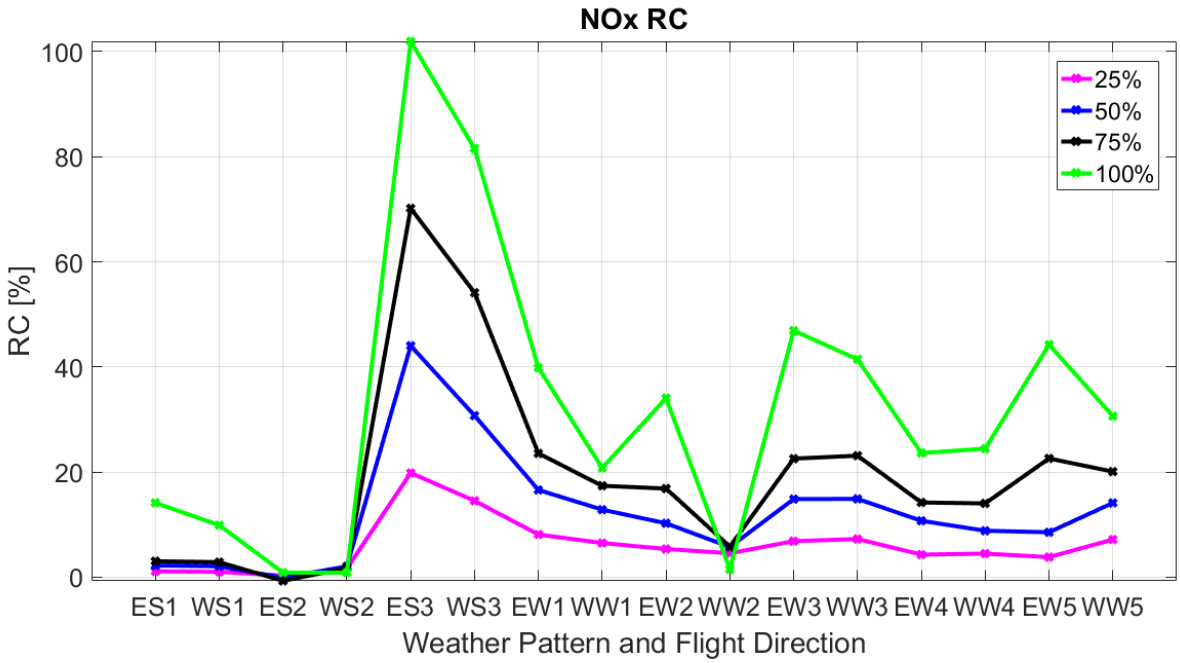

Figure 25. Comparison of NO_x *RC* for AGWP100 climate metric and different flight directions and weather patterns. The *NTCIC* values presented are 25%, 50%, 75%, and 100%.

Both ozone and methane *Normalized Climate Impact* have a similar behavior when increasing the *NTCIC*. Excluding SP3, changes are not very significant during the first 75% of the optimization. This is more notorious for ozone. However, in the last segment of the optimization, *NCI* values start changing more. For ozone, in all cases except Summer Pattern 1, the *NCI* increases. For methane, in all cases, the *NCI* decreases. These two effects are related with

the increment in fuel consumption that leads to higher emissions of NO_x. This means more ozone formation and more methane depletion. Moreover, ozone values are always notoriously higher than methane values for the same weather pattern and flight direction. This explains why NO_x has always a positive *Normalized Climate Impact*. For more details check Annex B.

In order to explain NO_x *Relative Contribution* values, Figure 26 and Figure 27 show ozone and methane *RC* respectively. As can be seen in ozone case, most cases are characterized by an increase in *Relative Contribution* during the first part of the optimization. This is caused by the avoidance of climate sensitive areas to this climate parameter. However, when increasing the *NTCIC*, it is clear that the *RC* falls in the majority of cases. This is caused by the higher emission of NO_x instigating more ozone formation. The values of *RC* for maximum *NTCIC* can drop to -35% (for Westbound-WP2).

The methane *RC* values are increasing the whole optimization for all cases. This is caused by two major reasons: firstly, the avoidance of climate sensitive regions of the atmosphere; and secondly, the increase in NO_x emissions when performing the optimization, that leads to more methane depletion and therefore an enhanced net-cooling. This second effect is more important in the last segment of the optimization. For *NTCIC* equal to 75%, the maximum *RC* value is smaller than 25% (for Eastbound-SP3). However, for *NTCIC* equal to 100%, the *Relative Contribution* increases up to 62% (for Eastbound-WP3).

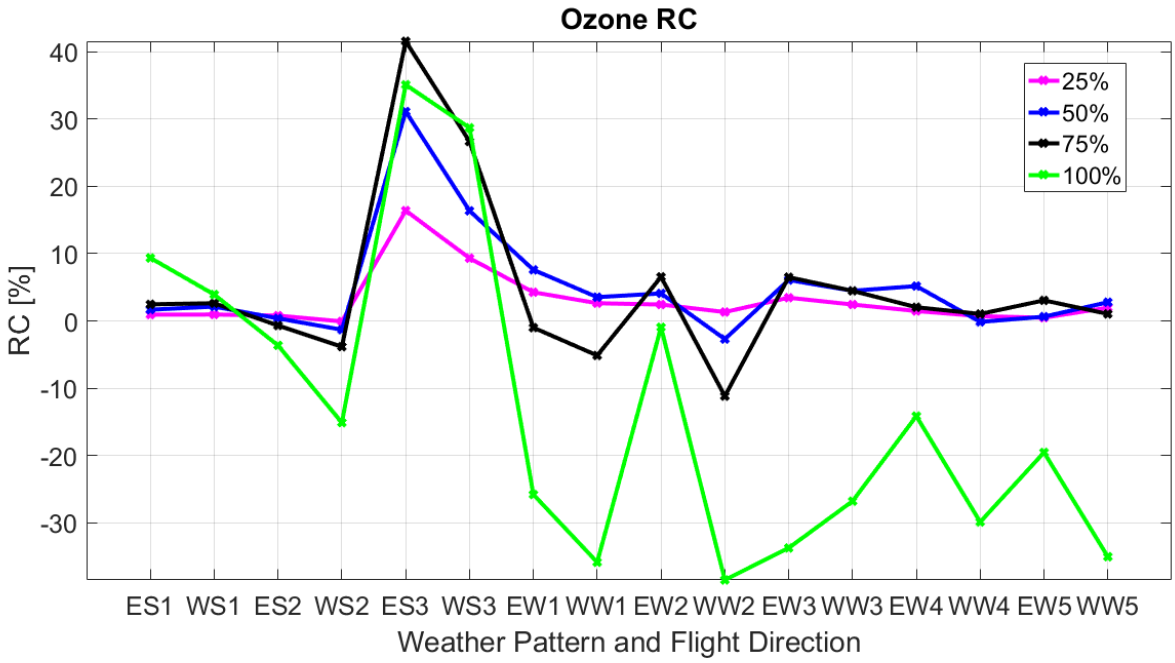

Figure 26. Comparison of ozone *RC* for AGWP100 climate metric and different flight directions and weather patterns. The *NTCIC* values presented are 25%, 50%, 75%, and 100%.

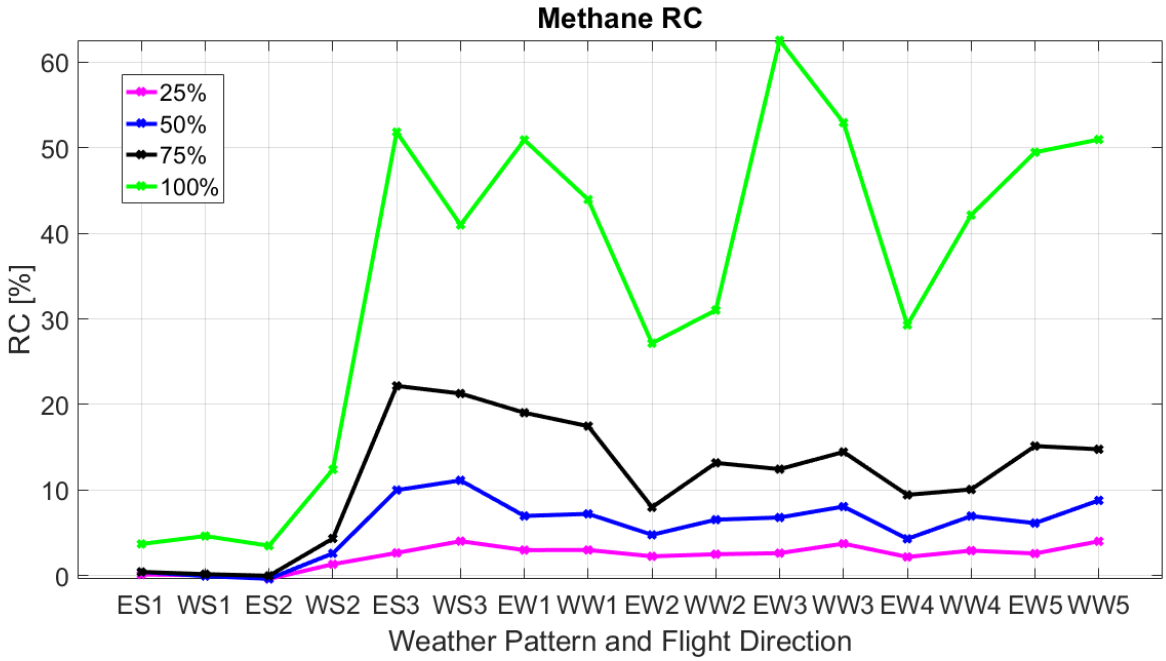

Figure 27. Comparison of methane *RC* for AGWP100 climate metric and different flight directions and weather patterns. The *NTCIC* values presented are 25%, 50%, 75%, and 100%.

4.7. Summary and Main Conclusions

After analyzing and comparing the different combinations of weather pattern, flight direction, and climate metric, some conclusions can be derived. This subsection summarizes the most important findings in Section 4.

In the case of carbon dioxide, the *Normalized Climate Impact* values are very similar for same weather pattern and climate metric. The flight direction is not very important. The maximum values are always associated with the long term climate metric, AGWP100 and always followed by AGWP20 and ATR20, in that order. This happens due to the long-term climate impact associated to CO_2; therefore its *NCI* is higher for longer time horizons. This can be seen as an increase in importance in comparison with other climate parameters.

Looking at carbon dioxide *Relative Contribution*, the behavior of the curve is the same in all cases. Values are always negative and the curve has a negative second derivative, meaning that the slope decreases for higher values of *NTCIC*. The value on each point is dependent on each case, but it never goes lower than -15%. The lowest values are only reached when using AGWP100. When analyzing cases with AGWP20 or ATR20, the *RC* is never lower than -5%. The shape of the curve is explained by considering the route changes required to reach the maximum total climate impact reduction. Changes in latitude and longitude lead to longer routes, especially for the last segment of the optimization. Changes in altitude lead to non-optimal engine operation, increasing its specific fuel consumption. Hence, the fuel consumption increases and it is accompanied with more carbon dioxide emissions. Moreover, the maximum values are always associated to AGWP100, then AGWP20, and finally ATR20.

The next climate parameter, water vapor, has a really short term climate impact. This, and the fact of using a pulse type emission for AGWP and a future air traffic scenario for ATR, makes AGWP20 the climate metric with higher *NCI*. It is followed by AGWP100, and then by ATR20. However, its *NCI* is very similar for the same weather pattern, and never higher than 2.5%. Its *Relative Contribution* is very similar for same weather pattern and direction. It increases slightly in the beginning and then goes down due to the higher fuel consumption. Nevertheless, its value is less important than carbon dioxide´s when using short-term climate parameters. Therefore, it can be considered negligible.

The third climate parameter is contrails. *Normalized Climate Impact* values are quite similar for same direction and weather pattern. These values change considerably during the optimization and always decrease. In addition, when

studying summer patterns, contrails have different importance. However, for winter patterns, the *NCI* is very similar in the minimum economic cost situation. Moreover, in all cases, the curve is almost a straight line. The order of importance between the climate metrics is the same than with water vapor. This is because contrails have a really short persistence and therefore they are more important for short-term time horizons.

Contrails *Relative Importance* is quite high for almost every single case, reaching at least a value of 70% when *NTCIC* is equal to 100% except for Summer Pattern 3. In that case, this climate parameter stays in 30% for westbound flights and 15% for eastbound flights. Moreover, *RC* is always higher for westbound flights than for eastbound flights at least in the last part of the optimization. Also, the highest *RC* is associated to ATR20, followed by AGWP20 and AGWP100. It is higher with the short-term climate metrics because contrails usually last for a few hours. Therefore they will become less important when the time horizon increases. Finally, the *Relative Contribution* is very similar for the same weather pattern and does not change that much with the direction. This can be explained taking into account the short duration of contrails, of the order of hours. If the considered climate metrics made use of time horizons of days, the difference would be noticeable. However, considering 20 or 100 years, the difference between *RC* values becomes smaller due to the difference in order of magnitude from hours to years-centuries.

The last of the main climate parameters is NO_x. Its *Normalized Climate Impact* is determined by ozone, methane and PMO. Depending on these climate parameters, different values for *NCI* are obtained. The values vary considerably when comparing summer patterns. They are higher when the contrails formation is less important. For winter patterns the *NCI* is quite similar at the minimum economic cost point. Moreover, depending on the weather pattern, flight direction and climate metric, *NCI* values change. In addition, for same weather pattern and flight direction, the climate metrics always follow the same order, been ATR20 the most important and AGWP100 the least. This occurs because of the values reached by ozone, methane and PMO. Ozone has a higher *NCI*, in absolute sense, than PMO and methane combined, which always have negative values. Remember that PMO radiative forcing was obtained as methane radiative forcing multiplied by a constant factor of 0.29. Moreover, the differences of ozone *NCI* are very small (perturbation lifetime of one year). For methane and PMO, these differences are higher (perturbation lifetime of twelve years) and therefore are going to lead the *NCI* order for NO_x. The order for ozone climate metrics *NCI* values is AGWP20 higher than AGWP100, and higher than ATR20. For methane and PMO, in absolute value, AGWP100 values are higher than AGWP20 values, which are higher than ATR20 ones. In addition, NO_x *Normalized Climate Impact* can increase, decrease, or remain constant during the optimization. However, it usually decreases.

NO_x *Relative Contribution* changes considerably depending on weather pattern, flight direction and climate metric. Most of the times, it is positive. This is not the case just in some configurations of SP2 and WP2. However, it does not decay under -10%. In addition, for same weather pattern and flight direction, there is a clear order in the importance of climate metrics *Relative Contribution.* AGWP100 has the highest value and ATR20 the lowest. This means that PMO and methane combined have usually more importance than ozone. This happens because ozone *RC* is always higher for ATR20 followed by AGWP20 and AGWP100 like in the contrails case. Methane and PMO *RC* is always higher for AGWP100 followed by AGWP20, and ATR20, like in carbon dioxide study. Finally, the climate parameters controlling NO_x *Relative Contribution* depend on each individual case for summer weather, but for winter weather methane and PMO are the most important during the whole process. However, in some cases, ozone becomes important in the last part of the optimization due to the increase in NO_x emissions, or in the first part of the optimization due to the avoidance of climate sensitive regions.

Ozone *Normalized Climate Impact* is primarily determined by the weather pattern. Moreover, when looking at the same direction and weather pattern, the curve shapes are similar and there are not bigger gaps than 5% between them. When looking at same weather pattern and climate metric, the gaps are not larger than 15%. In addition, the typical behavior of the curve is to first decrease kind of linearly and then to increase rapidly. The minimum point is located before for AGWP100, then for AGWP20 and ATR20. The slope after the minimum point is higher for ATR20 and then for AGWP20 and AGWP100.

For the major part of the optimization, the *Relative Contribution* for same weather pattern and direction is quite similar for the different climate metrics. The biggest differences are found in the last segment, where there is an increase in fuel consumption and therefore NO_x emission. The NO_x emission leads to higher levels of ozone in the atmosphere and therefore less *RC*. Furthermore, *RC* curve usually increases with a negative second derivative until it reaches a maximum value. This part is characterized by the importance of re-routing and its larger weight in comparison with the NO_x emission. After reaching the maximum point, the curve goes down rapidly especially in the last segment of the optimization. There, the fuel consumption increases considerably. In the case of SP1, the fuel

consumption does not vary very much (carbon dioxide maximum *RC* is 3.5%) and therefore the benefits of re-routing are more important than this increase in emissions.

The other climate parameter controlling NO_x is methane. Its *NCI* changes considerably depending on the weather pattern. For same weather pattern and climate metric the maximum differences are 5%, while for same weather pattern and flight direction the differences are around 10%. In addition, it is always negative and tends to decrease during the whole optimization.

Finally, methane *Relative Contribution* has a similar tendency for same weather pattern and same direction. However, the gaps between the curves for different climate metrics are noticeable due to its perturbation lifetime of 12 years. Usually, the curve behavior is to increase linearly until a point. After that, it increases more rapidly due to larger emissions of NO_x.

There are several reasons why there is more variability for summer patterns than for winter patterns when comparing the different cases. In summer the humidity of the atmosphere may vary more between the different weather patterns while in winter the humidity is quite similar for all of them. This leads to more variability in contrail formation for summer patterns. Other reason is that in winter there are more flights happening at night. The relative position of the Sun with respect to the Earth does not affect climate impact at night since there is not incoming sunlight.

To clarify all this details and have a more precise view of the *NCI* and *RC* values, some figures are presented. Figure 28 shows the *NCI* values for the different climate parameters for AGWP100 at the minimum economic cost point. Figure 29 stablishes a comparison between the *Relative Contribution* of the different climate parameters for AGWP100 climate metric and *NTCIC* equal to 50%. Figure 30 presents the same results but for maximum NTCIC. Finally, Figure 31 shows the maximum total climate impact reduction that can be achieved for each case. The results show that SP2 weather pattern and Westbound-SP1 are the best configurations to reduce the total climate impact, no matter the climate metric.

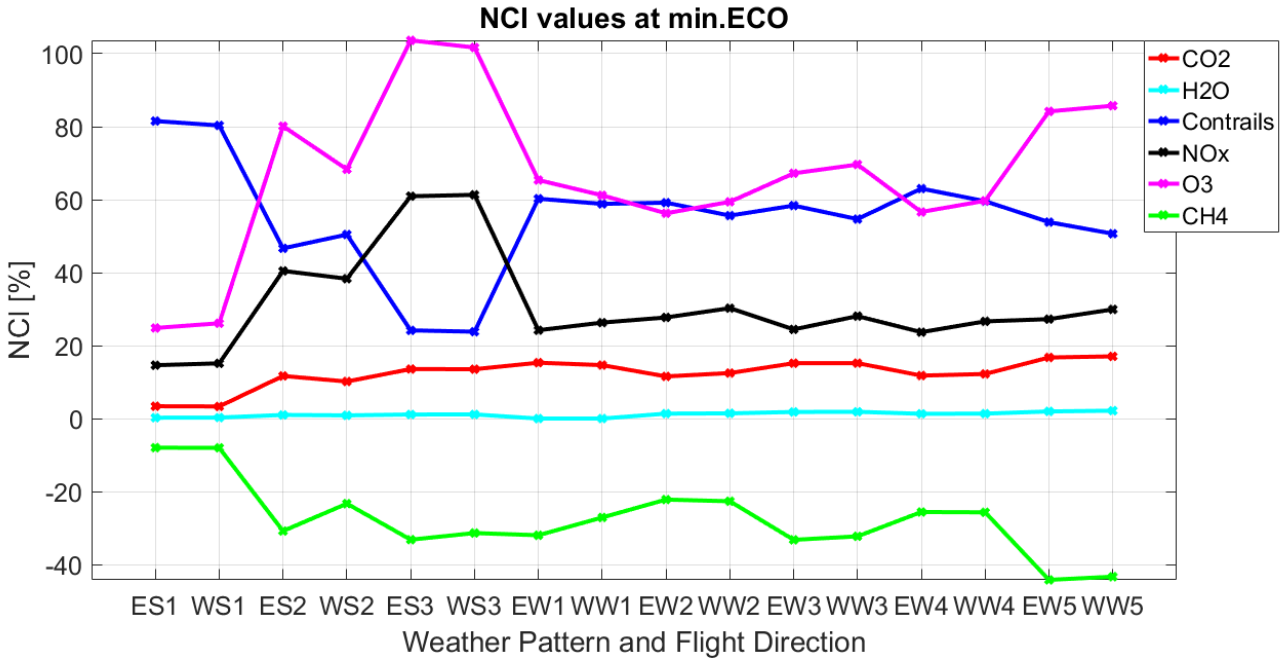

Figure 28. Comparison between the *Normalized Climate Impact* of the different climate parameters for AGWP100 and different weather patterns and flight directions. The values shown are for minimum economic cost situation. Results of carbon dioxide (red), water vapor (cyan), contrails (blue), NO_x (black), ozone (magenta), and methane (green) are shown.

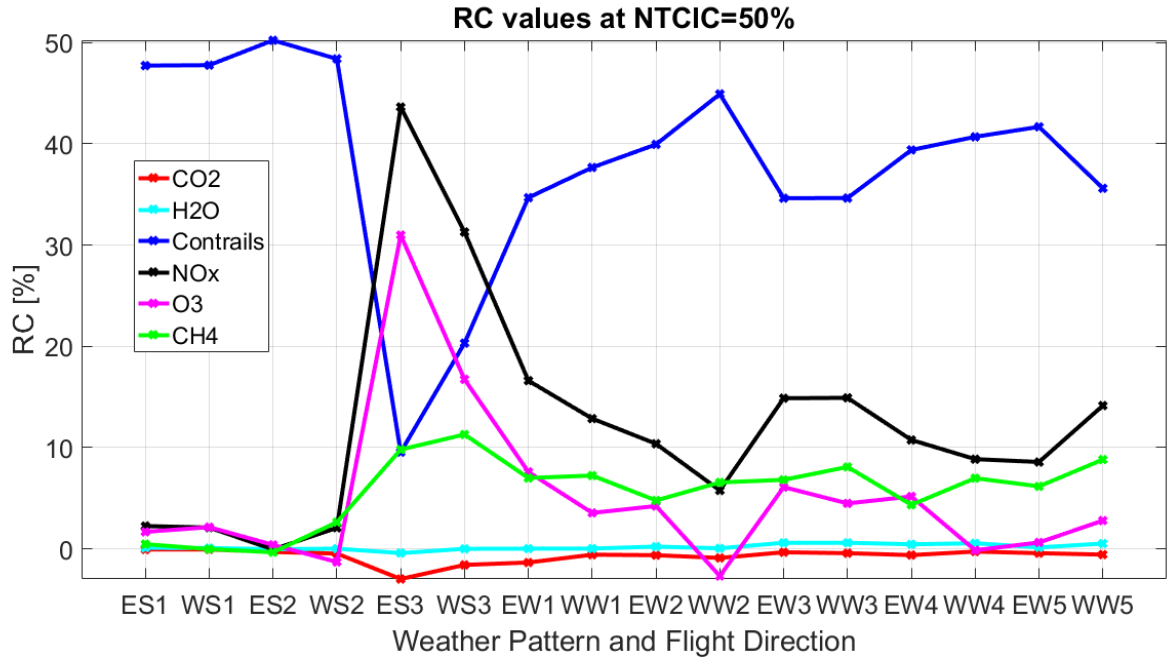

Figure 29. Comparison between the *Relative Contribution* of the different climate parameters for AGWP100 and different weather patterns and flight directions. The values shown are for *NTCIC*=50%. The climate parameters represented are carbon dioxide (red), water vapor (cyan), contrails (blue), NO_x (black), ozone (magenta), and methane (green).

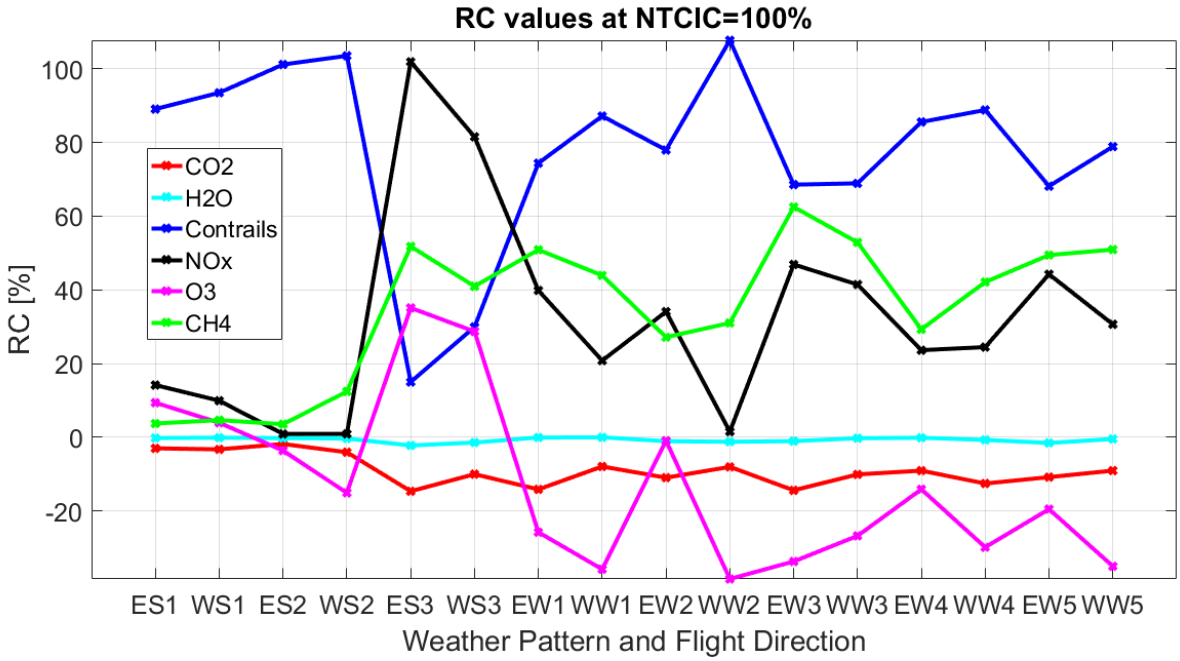

Figure 30. Comparison between the *Relative Contribution* of the different climate parameters for AGWP100 and different weather patterns and flight directions. The values shown are for *NTCIC*=100%. The climate parameters represented are carbon dioxide (red), water vapor (cyan), contrails (blue), NO_x (black), ozone (magenta), and methane (green).

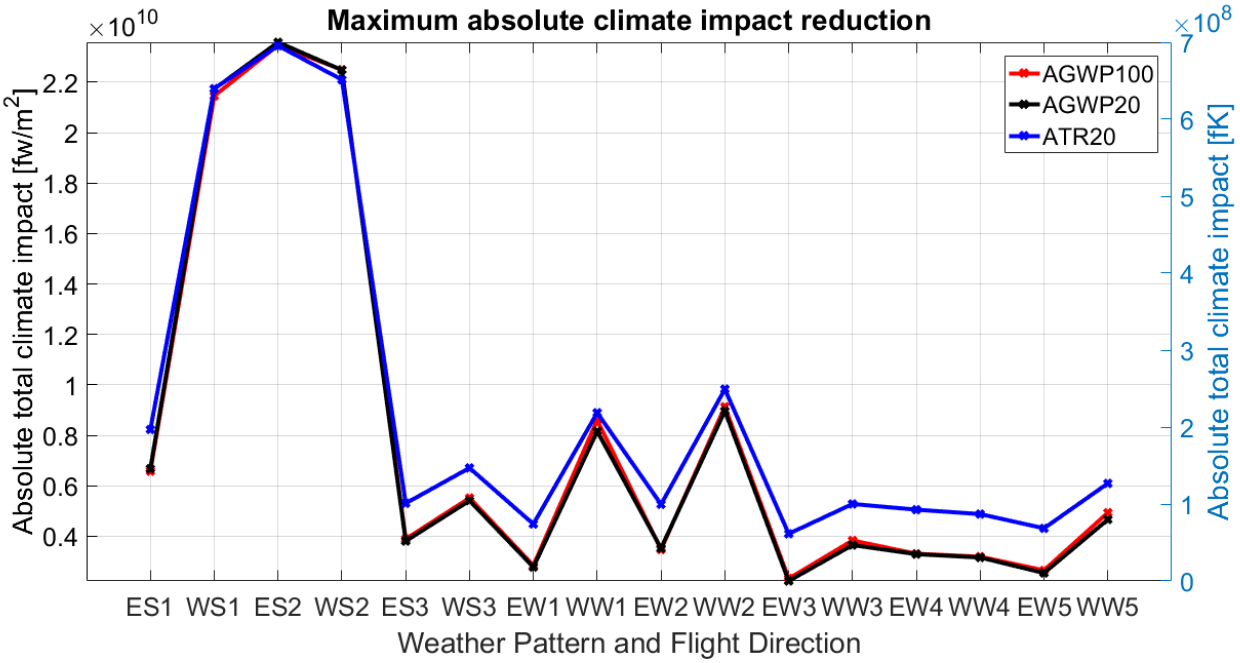

Figure 31. Absolute differences between the minimum economic cost point and the minimum climate impact point for each configuration. AGWP100 values are shown in red, AGWP20 in black, and ATR20 in blue.

5

Individual Flight Analysis

After analyzing the complete fleet results, it is interesting to see how the individual flights are contributing to the total climate impact reduction. To do so, two different figures are going to be presented. The first one will show the probability density functions (PDF) of the climate impact caused by each climate parameter. The second one will show the values of *RCIC* (explained in Section 3) for the different flights and climate parameters.

The analysis performed in Section 4 has shown that, for most of the cases, contrails are the driving parameter and NO_x effect has also an important effect especially when considering long-term impact scenarios. Moreover, NO_x behavior changes depending on each weather pattern, especially for summer type-days. Water vapor has been proven to be negligible and carbon dioxide emission is only related with fuel consumption and therefore with the selected route. Since this study is not trying to analyze the route changes but the driving parameters leading to these changes, carbon dioxide is not going to be analyzed in this part. Water vapor will not be considered due to its negligible impact. Hence, the analysis to be performed will focus on contrails, NO_x, ozone, and methane.

The case to be analyzed is the summer pattern 1 (SP1) for westbound direction and AGWP100 as climate metric. This case, as shown in Figure 31, presents one of the highest total climate impact reductions (only smaller than Summer Pattern 2). Moreover, NO_x *Relative Contribution* is higher for this case than in SP2. The reason to choose AGWP100 as climate metric is double: first to continue with the analysis of the same climate metric than in the prior section; and second, because the strategies should focus on reducing the long-term impact.

The first climate parameter to be analyzed is contrails. In Figure 32 is presented probability density function of the climate impact cause by contrails for 5 different values of *Normalized Total Climate Impact Change*. These values are 0% (red line with asterisks), 25% (magenta line with triangles), 50% (blue line with circles), 75% (black line with squares), and 100% (green line). Moreover, on the horizontal axis the climate impact mean value is represented with the same code of color and shape as the PDF curve. In Figure 33, the *RCIC* values are shown for each flight for different values of *NTCIC*. These values are 25% (magenta triangles), 50% (blue circles), 75% (black squares), and 100% (green crosses). These codes of colors and shapes will be used on all representations of this type.

Looking at the contrails PDF, the shapes of the different curves are quite similar, showing one important maximum close to the origin. Therefore the vast part of the flights will be located on that area. Moreover, there are some flights that have a negative climate impact as it can be seen on the left part of the graph. The way the curve behaves when performing the optimization tends to increase the height of the peak and move the curve to the left, meaning that there are some flights with high climate impact reducing it to smaller values. The maximum value has gone down in $5 \cdot 10^8$ fw/m^2 approximately. Therefore the general behavior of flights in this case is to move to smaller values of climate impact. This is better represented on Figure 33. During the optimization there are some flights that are decreasing its contrails climate impact and others which are maintaining it constant. For the first 25% there are not many changes and those are mainly caused by a small number of flights changing down to a *RCIC* of -40%. However, flight number 315 goes down to -90%. During the next steps of the optimization, flights reduce more and more its contrails climate impact down to -60% except for two flights. Flight 315 goes down to -115% and flight 172 to -100%. Looking at the line defined by *RCIC=0%*, many green crosses are really close to it. This means that changes are caused by some flights changing considerably its impact and a lot of flights that change very little but its summation is significant.

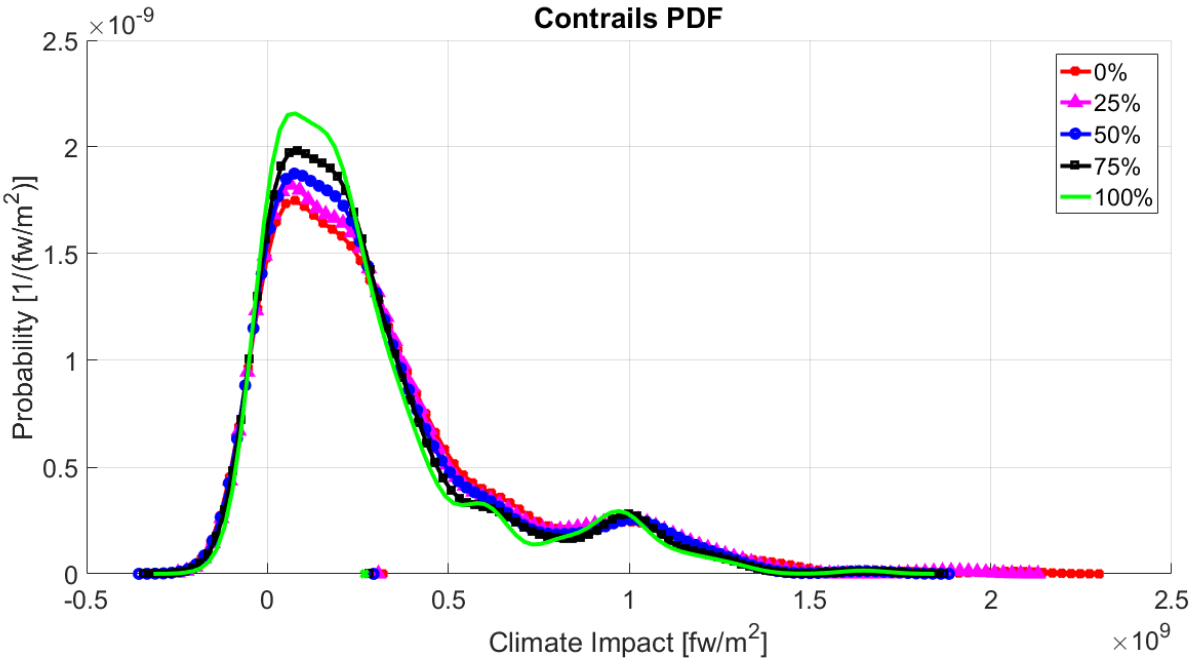

Figure 32. PDF of contrails for SP1-Westbound-AGWP100 case. The different curves and points represent the values for 0%, 25%, 50%, 75%, and 100% of *NTCIC*.

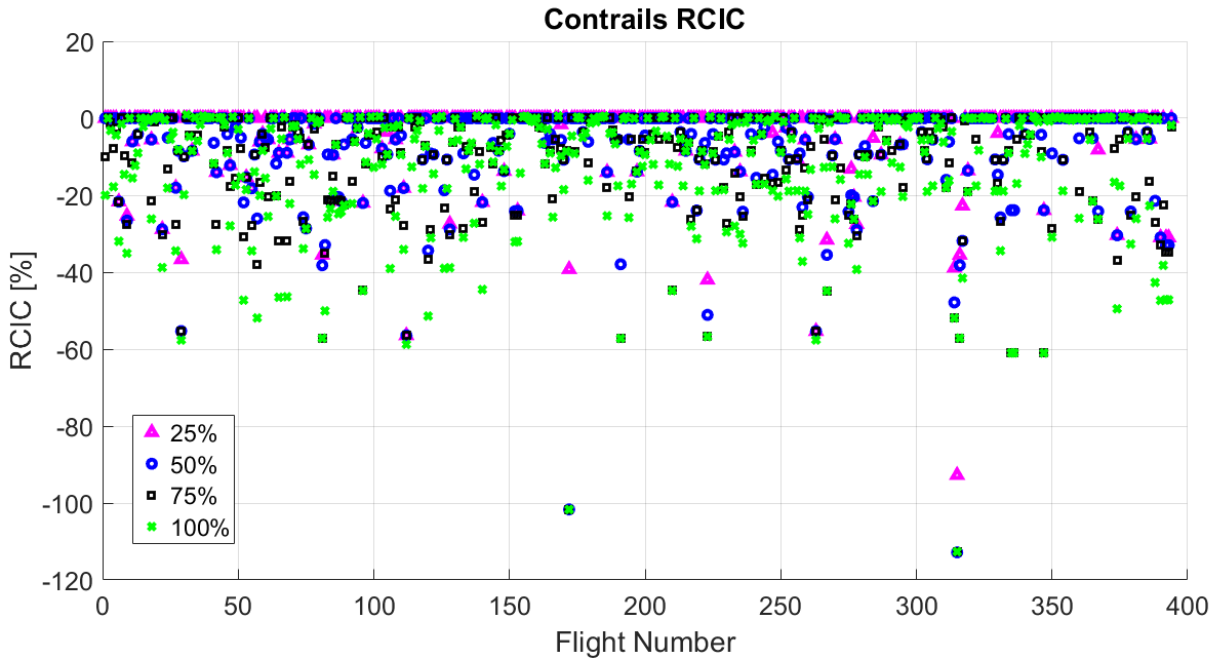

Figure 33. *RCIC* of contrails for SP1-Westbound-AGWP100 case. The different curves and points represent the values for 25%, 50%, 75%, and 100% of *NTCIC*.

The next climate parameter to consider is NO_x. Results of the PDF are shown in Figure 34. The probability density function, as in contrails case, shows only one peak. Also, there are some flights having a negative climate impact. The most important changes are occurring in the last segment of the optimization, from 75% to 100% of *NTCIC*. The peak increases a bit especially in this part and also the curve moves slightly to the left. This combination gives as a result a reduction in the mean value of NO_x emission as shown on the horizontal axis.

Moving to the *Relative Climate Impact Change* graph shown in Figure 35, there are not big changes during the first 75% of the optimization. There are some flights changing their NO_x climate impact but the values are less than -4% in absolute value except for flight number 315. In the last segment of the optimization there are many more changes occurring. There are some flights with a positive *RCIC*, but the general tendency is to decrease. This happens in the

vast majority of flights and almost all values are smaller, in absolute value, than -2%. However, flight 269 value goes down to -7% and flight number 315 to -9.5%.

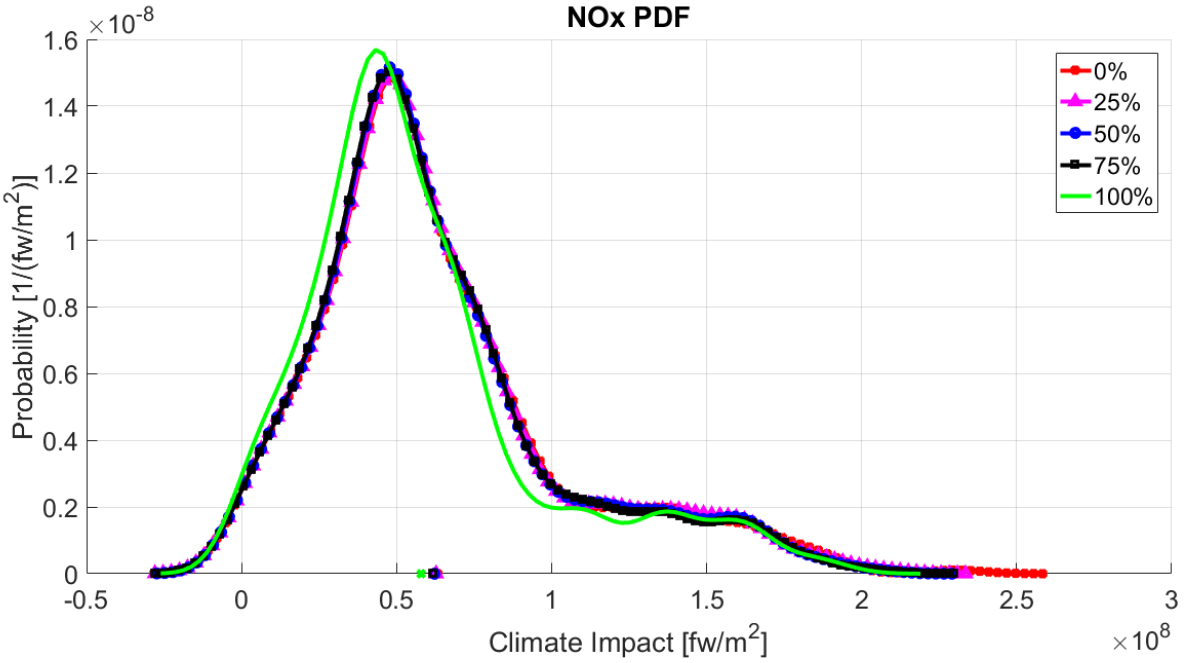

Figure 34. PDF of NO_x for SP1-Westbound-AGWP100 case. The different curves and points represent the values for 0%, 25%, 50%, 75%, and 100% of *NTCIC*.

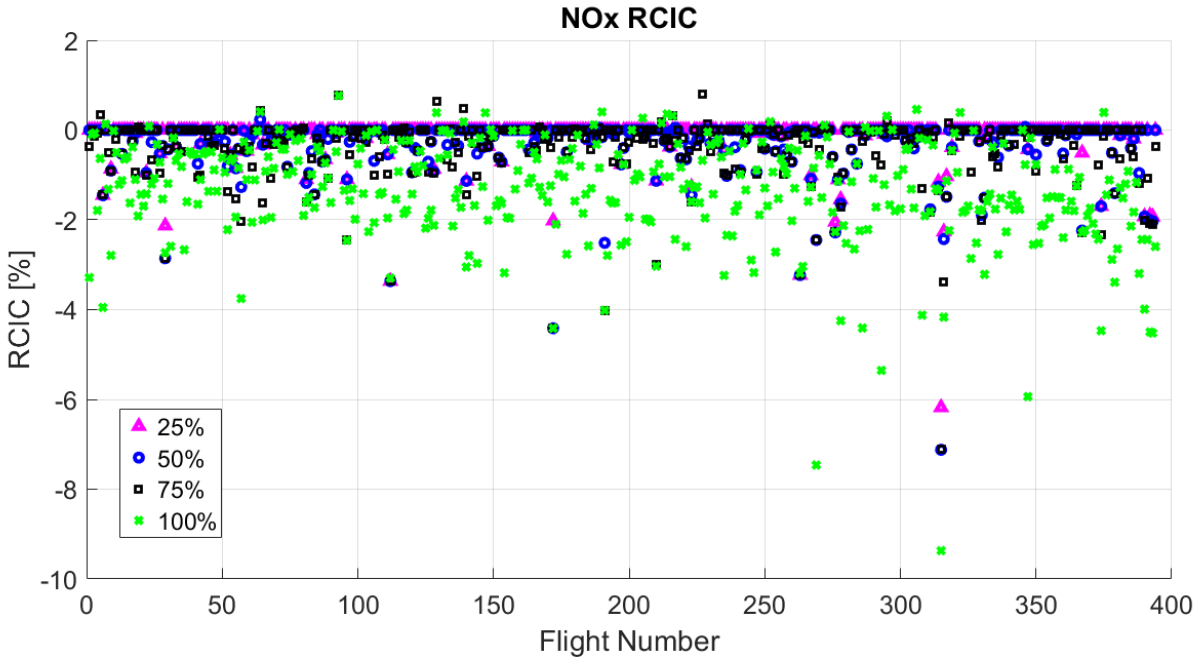

Figure 35. *RCIC* of NO_x for SP1-Westbound-AGWP100 case. The different curves and points represent the values for 25%, 50%, 75%, and 100% of *NTCIC*.

Figure 36 and Figure 37 show the results obtained for ozone and methane *RCIC* values respectively. For ozone, the PDF presents only one peak. The curve shape is almost the same during the whole optimization. Only some small changes appear that lead to the decrease in the mean value. However this change is very small. More interesting is to look at the *Relative Climate Impact Change*. Here again, there are not big changes happening during the first 75% of the optimization. In the last 25%, there are some flights increasing a bit their *RCIC* and others, more significantly,

making it lower. Nevertheless, the values are usually between 2% and -4%. There are only 4 flights with a larger *RCIC* than -4% in absolute sense. Those are flight 269 (-9.5%), 293 (-6%), 315 (-6.5%), and 347 (-9%).

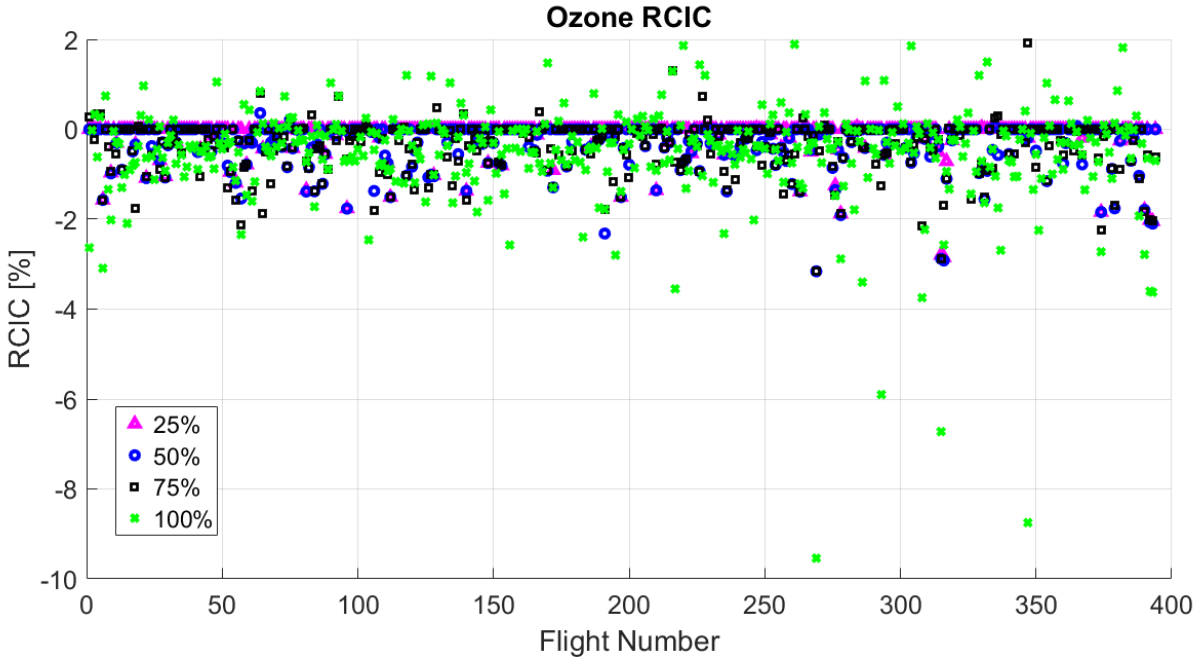

Figure 36. *RCIC* of ozone for SP1-Westbound-AGWP100 case. The different curves and points represent the values for 25%, 50%, 75%, and 100% of *NTCIC*.

For methane, the Probability Density Function shows 2 peaks, meaning that flights tend to group in two areas. Moreover, the values are most of the time negative. In addition, as in the case of ozone, the major change in curve shape occurs for the last segment of the optimization. This change mainly reduces the height of the peaks and moves the graph to the left, reshaping the climate impact distribution. The way flights change in order to promote this modification is shown on Figure 37. Only major changes occur in the last segment of the optimization, from *NTCIC* equal to 75% to 100%. Most flights present a negative *RCIC* between 0% and -3%. Some flights have positive values but they are a small portion of the total.

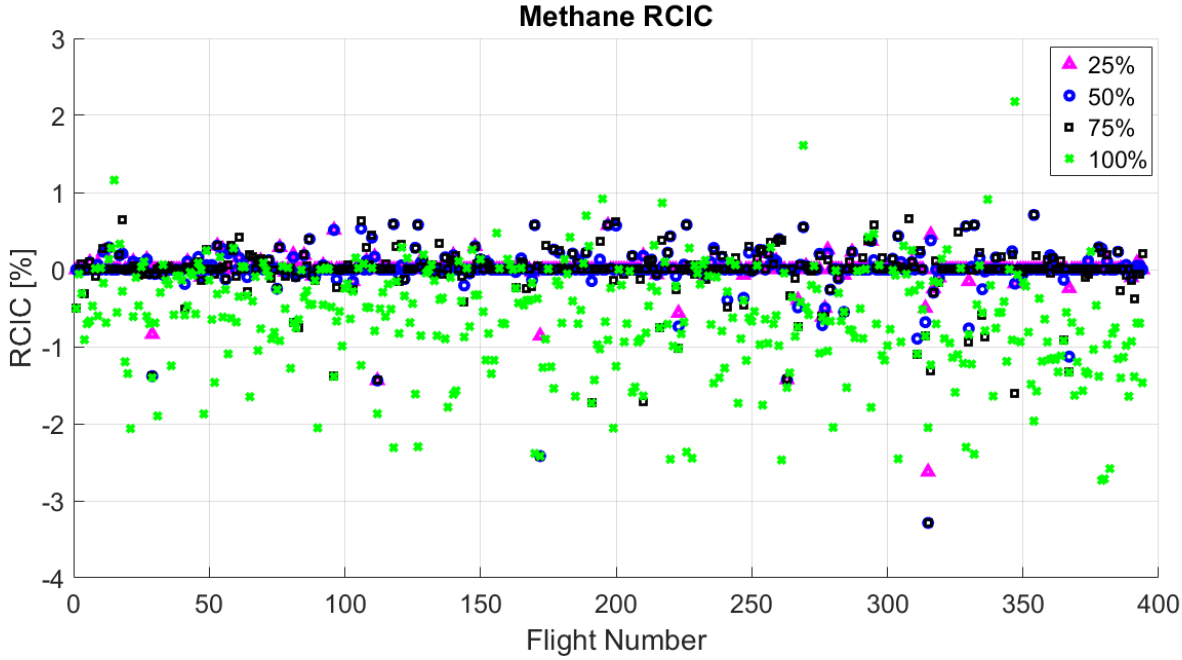

Figure 37. *RCIC* of methane for SP1-Westbound-AGWP100 case. The different curves and points represent the values for 25%, 50%, 75%, and 100% of *NTCIC*.

After analyzing a few more cases, the observation clearly shows that the Probability Density Function shape is quite similar than in the case presented. It always shows one peak for contrails, ozone, and NO_x; and two peaks for methane. This means that individual flight climate impact tends to concentrate around one or two values, respectively. Moreover, when looking at the same weather pattern, flight direction, and climate parameter, the distributions are very similar in terms of shape. The climate metric selected does not affect considerably. The same happens with the *Relative Climate Impact Change*. Hence, analyzing only one climate metric (AGWP100 in this case), is enough to explain the individual flight contribution. If the reader is interested, a complete list of PDF and *RCIC* graphs is presented in Annex C for AGWP100 climate metric.

In order to compare the results obtained for different flight direction and weather pattern, in the next figures some comparisons will be established. Figure 38 shows different values of *RCIC* for contrails when *NTCIC* is equal to 25%. The climate metric chosen is AGWP100. The values presented are the mean value (red), the 0.25 quantile (blue), the 0.5 quantile or median value (black), and the 0.75 quantile (green). Comparing them can be seen the distribution of flights changing the climate parameter climate impact. In this case, the 0.5 and 0.75 quantiles are equal to zero. This means that most of the flights have not changed their contrails climate impact. Moreover, except for Eastbound-SP2, Westbound-WP1, and Wesbound-WP5, the mean value is lower than the 0.75 quantile. This means that the climate impact reduction from contrails is caused by a small number of flights that are changing considerably, while the vast majority of flights do not change at all.

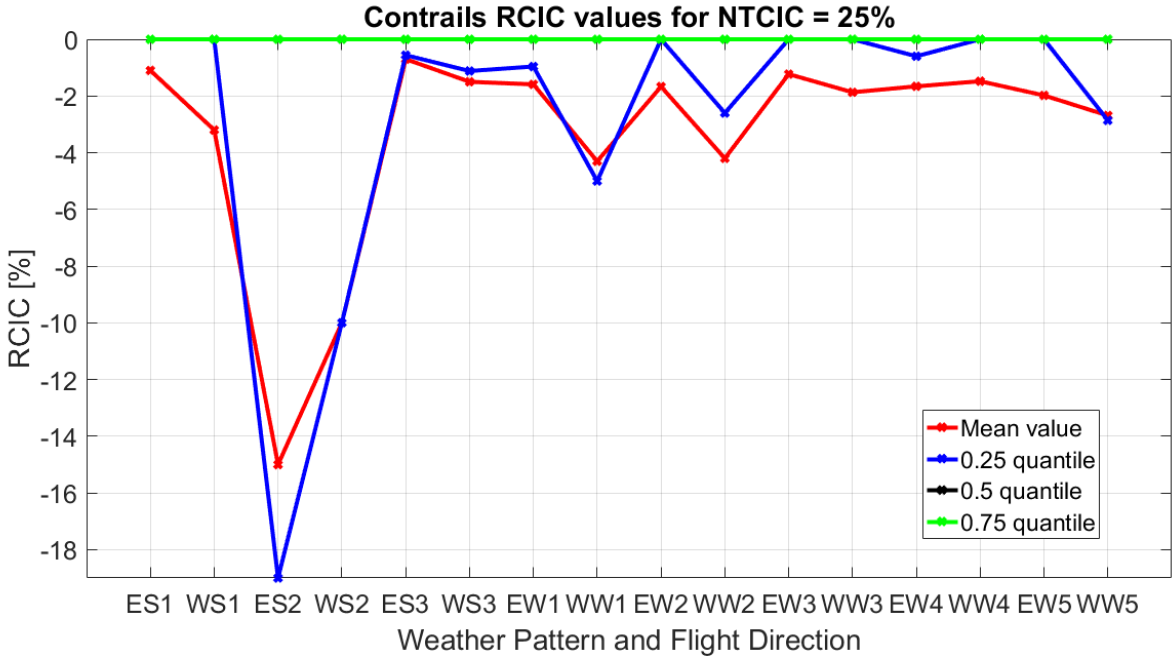

Figure 38. Comparison between mean value, 0.25 quantile, 0.5 quantile, and 0.75 quantile of *RCIC*. The climate parameter presented is contrails and *NTCIC* is equal to 25%. The climate metric is AGWP100.

In Figure 39 the same results are presented but for *NTCIC*=50%. In some of the cases the 0.5 quantile decreases. However, the 0.75 quantile value remains zero in all of them. In addition, the 0.25 quantile tends to be slightly lower than the mean value in most cases. Hence, there are more flights changing than in the prior case but there are many that have not changed at all. Therefore, the climate impact reduction of contrails is caused, for *NTCIC* equal to 50%, by a low number of flights reducing their contrails climate impact considerably, and higher number of flights just changing their contrails climate impact slightly. This is the tendency after this point as can be seen in Figure 40, where the *NTCIC* is equal to 100%. In this last case, the mean value can be found between the 0.25 quantile and the median value. Also, the 0.75 quantile is not zero anymore in the major part of configurations. Hence, the climate impact reduction caused by contrails during the optimization is carried out by a small number of flights changing their climate impact considerably, a slightly larger number of flights changing their climate impact around the mean value, and the vast majority of flights changing their contrails climate impact in a small quantity when compared to the mean value. In order to see the *RCIC* values when *NTCIC* is equal to 75% and see a complete list of figures, refer to Annex D.

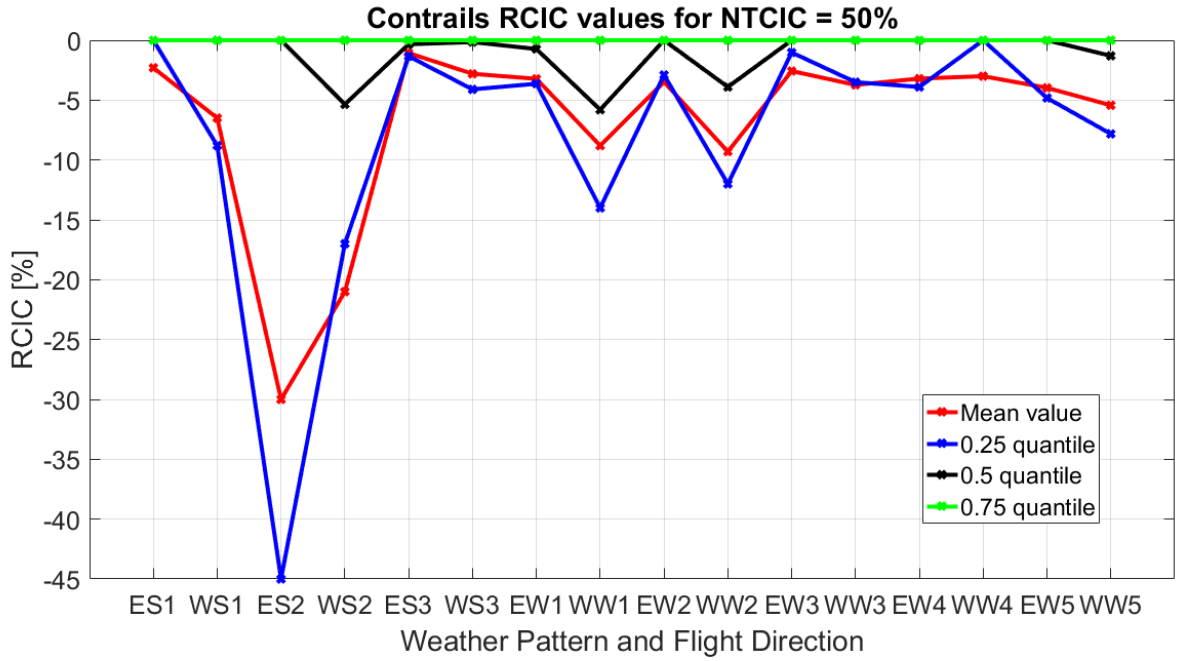

Figure 39. Comparison between mean value, 0.25 quantile, 0.5 quantile, and 0.75 quantile of *RCIC*. The climate parameter presented is contrails and *NTCIC* is equal to 50%. The climate metric is AGWP100.

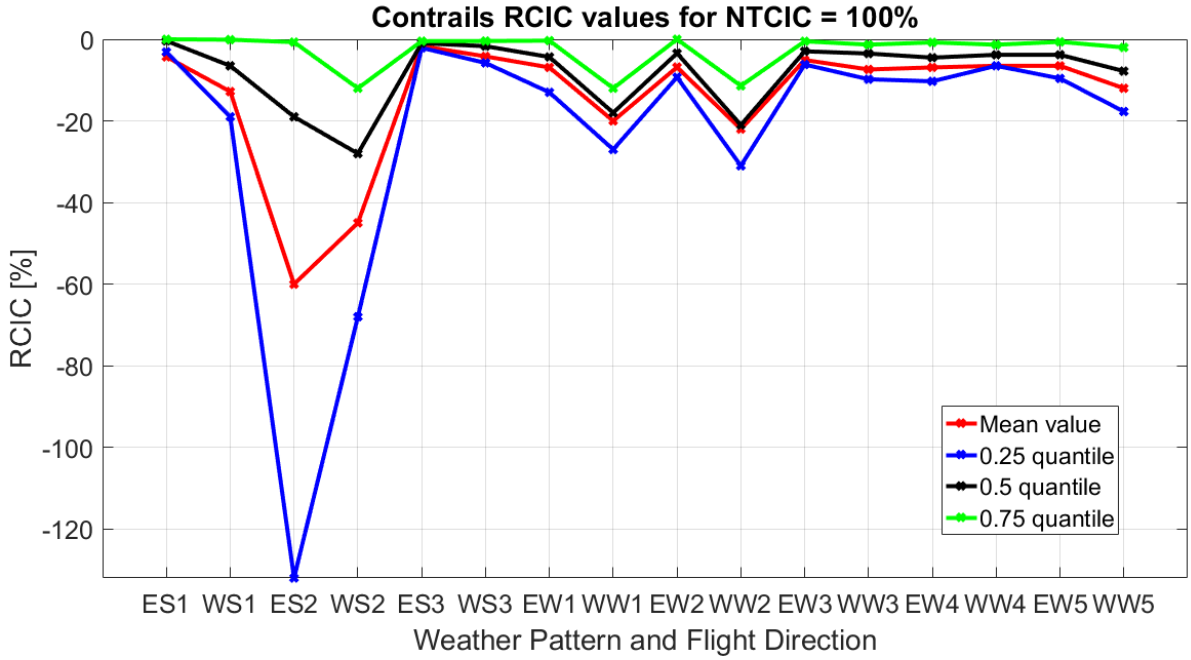

Figure 40. Comparison between mean value, 0.25 quantile, 0.5 quantile, and 0.75 quantile of *RCIC*. The climate parameter presented is contrails and *NTCIC* is equal to 100%. The climate metric is AGWP100.

NO_x *RCIC* follows a similar tendency than contrails. The values vary from each case to another due to the differences in *Relative Contribution* between both climate parameters as shown in Section 4. In Figure 41 *RCIC* values of NO_x are shown for a *NTCIC* equal to 25%. In most of the cases (excluding Westbound-SP2, Eastbound-SP3, Westbound-SP3, and Westbound-WP1) the mean value is lower than the 0.25 quantile. Moreover, in 10 out of the 16 configurations, the 0.25 quantile is zero. This means that the NO_x climate impact reduction is caused in this first segment by a tiny part of the fleet (usually less than 25%) changing its climate impact considerably in comparison with the mean value. When increasing the *NTCIC*, there are more flights affected but still the distribution found is quite similar than in the contrails case. In Figure 42 the NO_x *RCIC* values are shown for maximum *NTCIC*. It can be seen that the behavior is similar than in contrails case. Hence, there are a small amount of flights reducing their NO_x climate impact considerably, a larger number of flights changing around the mean value, and the vast majority only changing slightly.

Moreover, in some cases, the *RCIC* of the 0.75 quantile is positive. This happens because NO_x results are a combination of ozone, methane, and PMO. In the last segment of the optimization the ozone climate impact tends to increase due to the larger amount of NO_x emissions. Therefore, in some flights ozone effect is more dominant and this is shown in NO_x results.

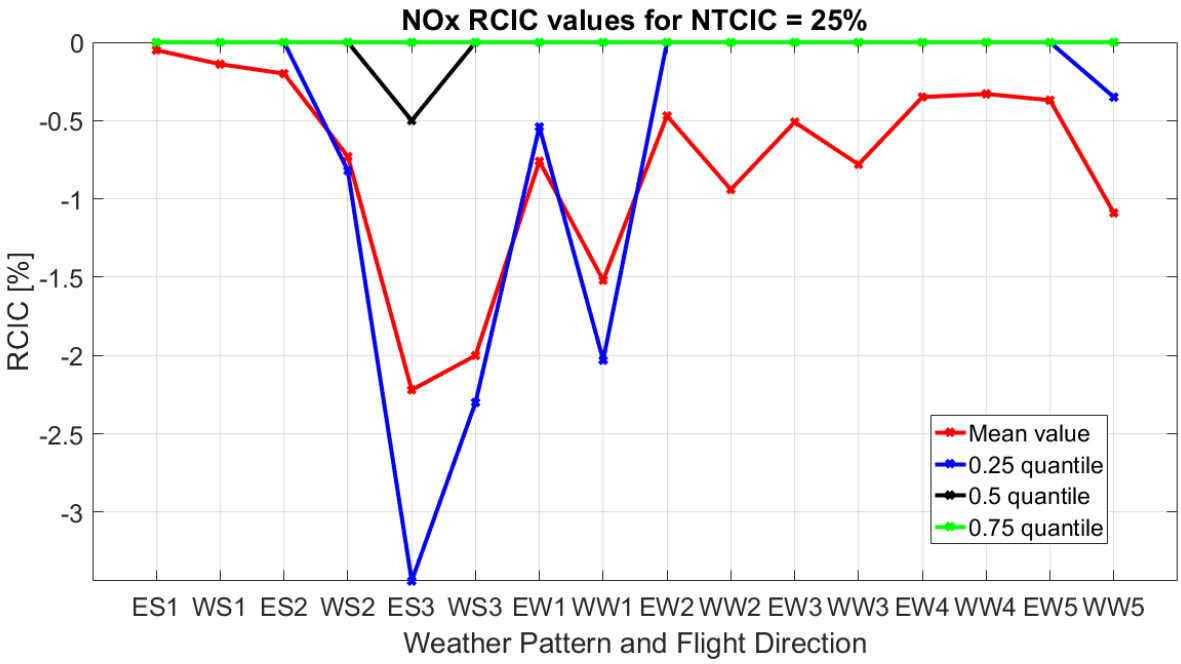

Figure 41. Comparison between mean value, 0.25 quantile, 0.5 quantile, and 0.75 quantile of *RCIC*. The climate parameter presented is NO_x and *NTCIC* is equal to 25%. The climate metric is AGWP100.

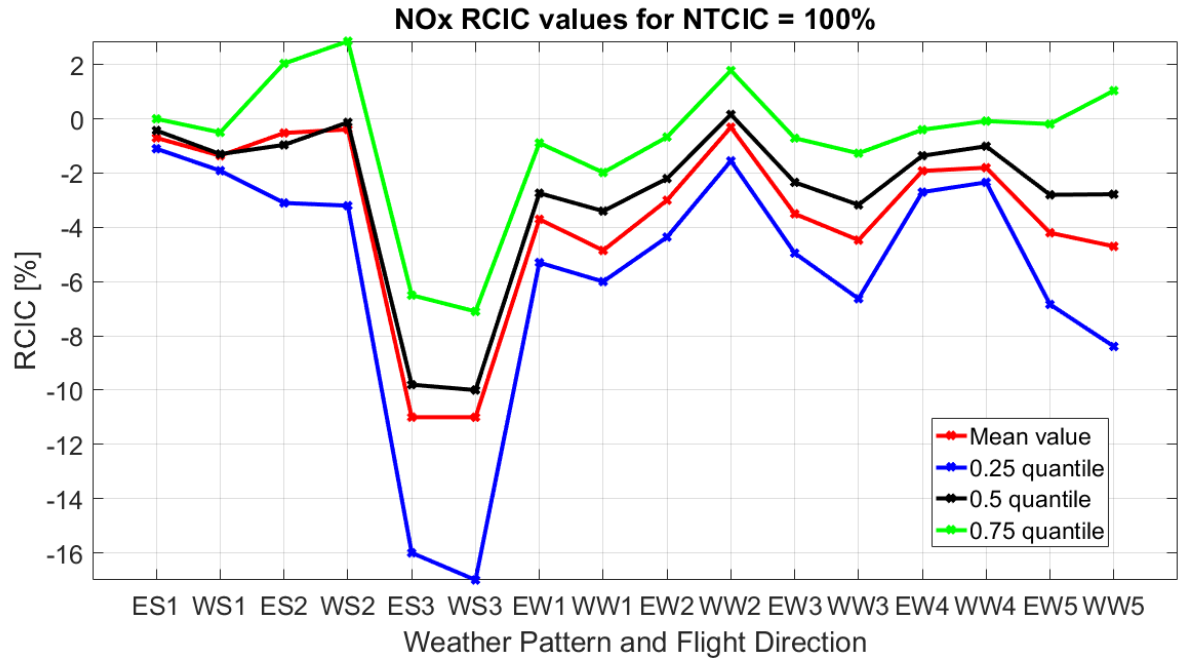

Figure 42. Comparison between mean value, 0.25 quantile, 0.5 quantile, and 0.75 quantile of *RCIC*. The climate parameter presented is NO_x and *NTCIC* is equal to 100%. The climate metric is AGWP100.

Both ozone and methane behavior are quite similar than NO_x conduct. Methane does not require any more explanations than NO_x. However, ozone is more interesting. In the first segment of the optimization it behaves like NO_x. Nevertheless, when increasing the *NTCIC*, the mean value and the 0.5 quantile start being closer. This happens because the last part of the optimization is characterized by an increment in ozone climate impact due the larger amount of NO_x emissions caused by the growth in fuel consumption. The results in the end of the optimization are

shown in Figure 43. The mean value is usually slightly larger than the 0.5 quantile. However, both values are very similar. Therefore, in this case the majority of flights are changing their ozone climate impact close to the mean value. In order to see a complete list of these figures, see Annex D.

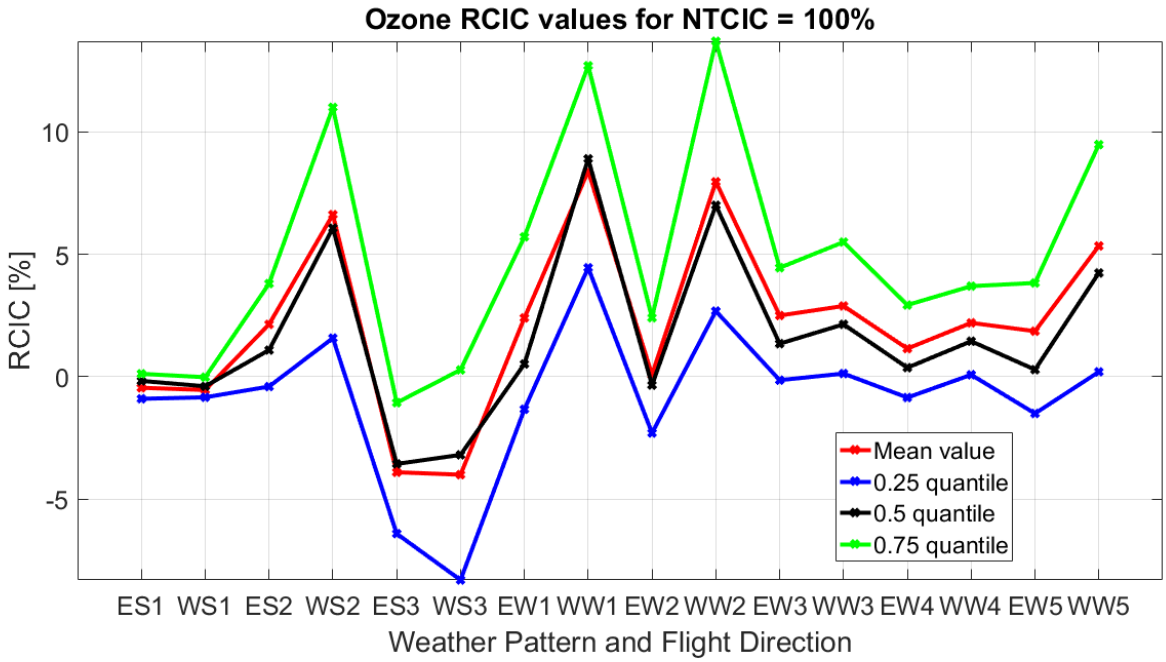

Figure 43. Comparison between mean value, 0.25 quantile, 0.5 quantile, and 0.75 quantile of *RCIC*. The climate parameter presented is ozone and *NTCIC* is equal to 100%. The climate metric is AGWP100.

Finally, Figure 44 shows the amount of flights with a *RCIC* for NO_x different than zero for different values of *NTCIC*. These values are 25% (magenta), 50% (blue), 75% (black), and 100% (green). Ozone and methane have the same value than NO_x and for that reason are not presented. The climate metric selected is AGWP100 again. In most cases the values are the same for contrails and NO_x. This means that changes in route have an effect in both climate parameters. However, there are other cases where the value for contrails is slightly smaller. Hence, there are route modifications that are changing the *Relative Climate Impact Change* of NO_x but not altering the contrails effect at all.

Moreover, when increasing the *NTCIC*, the amount of flights that see their route modified increases. The number of flights depends considerably on the weather pattern and direction for each *NTCIC*. However, the differences when *NTCIC* is equal to 25% are higher than when the optimization is completed. When *NTCIC=25%*, Eastbound-SP1 shows a value of 11.76% while Eastbound-SP3 shows a 57.29% for NO_x. Therefore the difference is 45.53%. These gap decreases to 13.81% when *NTCIC* is 100%. However, the differences for the *Normalized Total Climate Impact Changes* of 50% and 75% are 57.54% and 63.18% respectively. What can be derived from this analysis is that for the first 75% of the optimization the amount of flights changing their climate impact varies considerably depending on weather pattern and flight direction. However, in order to achieve the maximum possible climate impact reduction, the amount of flights changing their climate impact has to be quite high. This value is always higher than 94% except for Eastbound-SP1, where it is 86.19%.

In order to summarize the results obtained in this section, figure 45 is presented. It shows the amount of flights with a climate impact reduction higher than the mean climate reduction for each case. The different combinations of weather pattern and flight directions are presented for AGWP100 climate metric. The *NTCIC* values shown are 25%, 50%, 75%, and 100%. The figure shows that for most cases the amount of flights causing a climate impact reduction larger than the mean value increases during the optimization. However the amount of flights with this characteristic is always smaller than 45%. Moreover, the maximum variation appreciated in one configuration is never larger than 20% (Westbound-WP2). This shows, as mentioned before, that the amount of flights reducing the total climate impact is relatively small in comparison with the total amount of flights. This is more obvious when the *NTCIC* is low. The explanation for this behavior is related with the change in flight routes. In the minimum economic point, flights are organized so the operative costs are the smallest. This makes them to be flying through climate sensitive regions in general. When the optimization to reduce climate impact begins, the areas of the atmosphere where the different emissions have a smaller climate impact are free and the first flights changing their trajectory can freely move to

those regions. Therefore the climate impact reduction is caused by a small number of flights reducing their climate impact considerably, while the vast majority of flights are not modified. As the optimization progresses the flights move to the regions where the emissions cause less climate impact. However, these regions become busier and the following flights to be modified do not achieve a climate impact reduction as larger as in the first cases because they cannot freely change their trajectory. The possible collisions have to be considered. Therefore there are a larger number of flights that are reducing their climate impact in comparison with the mean value.

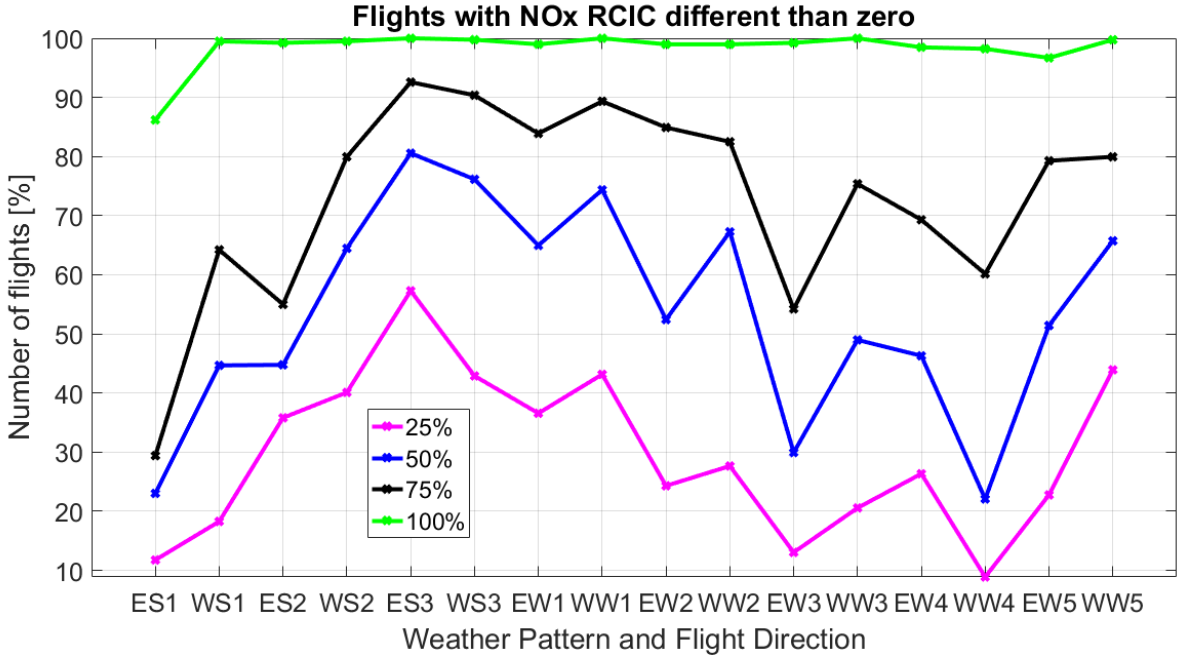

Figure 44. Comparison between the amount of flights with NO_x *RCIC* different than zero for different *NTCIC* values. The climate metric chosen is AGWP100.

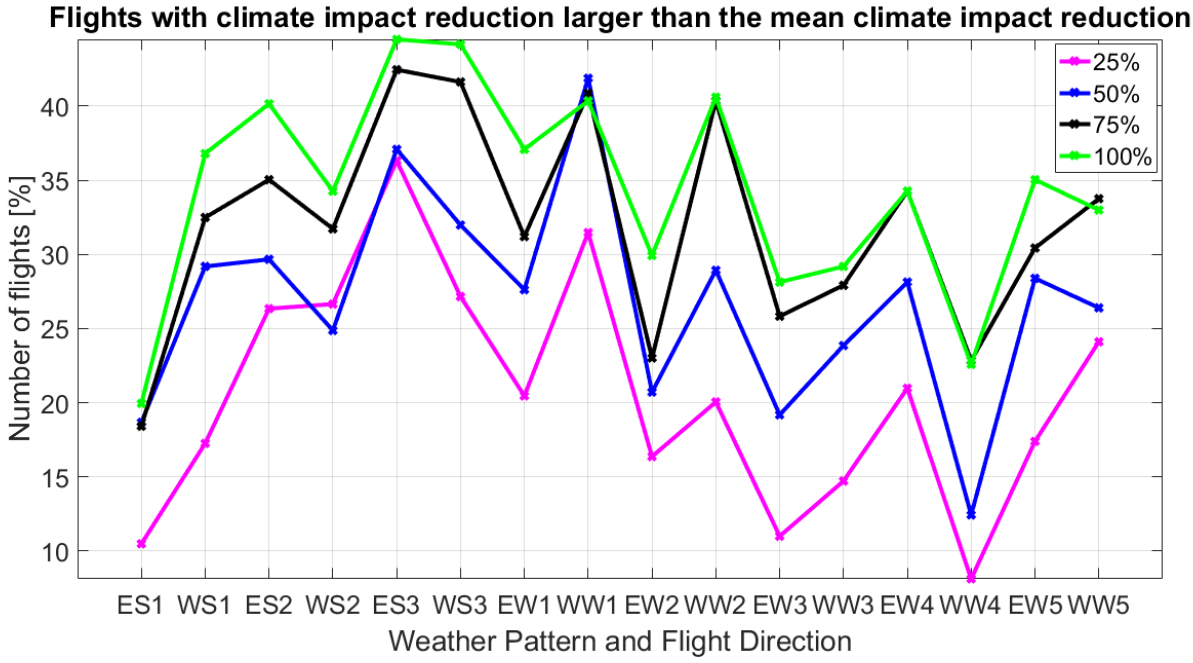

Figure 45. Number of flights that show a climate impact reduction larger than the mean climate impact reduction for different weather patterns and flight directions. The climate metric considered is AGWP100. The *NTCIC* values presented are 25%, 50%, 75%, and 100%.

To sum up, the number of flights that change their trajectory increase during the optimization. In the first part, the optimization is driven by a small number of flights achieving a great climate impact reduction because their

trajectories can be easily changed to regions of the atmosphere where the emissions have less climate impact. When the optimization progresses the total climate impact reduction is achieved thanks to a small number of flights reducing their climate impact considerably and a large proportion of flights reducing their climate impact slightly. This occurs because the last flights changing their trajectory cannot occupy the regions of the atmosphere where the emissions have lower climate impact since the prior flights are already occupying those regions. Therefore their climate impact reduction is lower.

6

Conclusions

The analysis performed had as objective to answer the following question: *What are the driving climate parameters when optimizing green flight trajectories as a result of the REACT4C project in the North Atlantic flight corridor for the eight different weather patterns, two flight directions, and three climate metrics?* In order to answer this question, two major analyses have been performed. In the first one, the complete fleet has been considered. Both the importance of the climate impact (using the *NCI*) and its change and contribution to the optimization (using the *RC*) have been studied. In the second analysis, an individual flight study has been performed. The probability density functions for the different climate parameters, as well as their relative change compared to the minimum economic cost point (using the *RCIC*) have been studied. Moreover, in both major analyses, some comparisons have been stablished in order to see differences and similarities for different weather patterns, flight directions, and climate metrics.

After performing the analysis, some conclusions can be derived from it. First of all, water vapor has a negligible effect in both climate impact and *Relative Contribution* to the optimization in comparison with the other climate parameters. Carbon dioxide shows different *Normalized Climate Impact* depending mainly on the climate metric chosen for each weather pattern. Same happens with its *Relative Contribution* to the optimization. Mainly the AGWP100 climate metric has more importance than AGWP20 and ATR20, being ATR20 values the least important ones. Moreover, its *Relative Contribution* is always negative and decreasing during the optimization. The increase in fuel consumption caused by route changes leads to this effect.

Contrails climate impact change is driving the optimization on each case except Summer Pattern 3. For that particular configuration, NO_x *RC* is the most important during the whole optimization. Contrails have a higher *Relative Contribution* when looking at a short-term time horizon due to its short-term climate impact. Their *RC* increases during the whole optimization except in the last part for some of the configurations. The shape of the curve is almost a straight line. Therefore, the route changes performed are focused on reducing contrails climate impact for most part of the optimization. However, in the last segment, the *Relative Contribution* tends to stagnate, meaning that total climate impact reduction is achieved by other means. Moreover, its *Relative Contribution* is higher for westbound flights than for eastbound flights with same weather pattern and climate metric.

NO_x climate impact, which is obtained as the summation of ozone, methane, and PMO climate impacts, has a higher relative contribution for long-term time horizons due to the net-cooling effect caused by methane depletion. Its *Normalized Climate Impact* is always positive due to the higher climate impact caused by ozone than by methane depletion and PMO in absolute sense. Moreover, *NCI* values are the highest for ATR20 climate metric and the lowest for AGWP100 due to the differences in *NCI* values for ozone and methane, and their perturbation lifetime in the atmosphere. In addition, *RC* varies significantly in value and tendency for summer weather patterns. However, for winter weather patterns, the behavior is very similar on each case. It is characterized by an increase in the first part of the optimization due to, probably, the avoidance of climate sensitive regions for ozone and methane. In the mid part of the optimization, the increment in *RC* is caused by a greater depletion of methane due to the increase in fuel consumption and therefore higher amounts of emitted NO_x. This part is also accompanied with an enhancement in ozone formation and therefore a warming effect. However, the methane depletion is more important than the ozone enhancement. Finally, in the last part of the optimization, ozone keeps increasing and methane decreasing their climate impact. Usually methane has a higher *RC* but in some cases, especially with the ATR20 climate metric, ozone can cause an important drop in NO_x *Relative Contribution*. This is caused by the rapid increase in NO_x emission that overrules the reduction obtained from the re-routing strategy. In addition, its *Relative Contribution* is, in most cases, larger in eastbound flights than in westbound flights for same weather pattern and climate metric.

Ozone presents one of the highest climate impacts in comparison with other climate parameters. Due to its short term climate impact, the values are higher for AGWP20. Its *Relative Contribution* varies depending mainly on the weather pattern. Its value depends on the location of the emission, but also on the amount of NO_x emitted. More emissions mean more ozone production and warming effect. For the summer patterns the importance of these two effects varies from case to case, but for winter patterns they follow a similar behavior. This behavior is driven in the first part of the optimization by climate-sensitive regions avoidance while in the last part is determined by the increasing amount of NO_x emissions.

Methane climate impact is always negative and has a net-cooling effect because methane is depleted. It is more important in long-term time scenarios due to its relative high perturbation lifetime in comparison with contrails, ozone, and water vapor. Its *Relative Contribution* is usually positive; therefore it reduces the total climate impact. As in ozone case, first is controlled by the avoidance of climate-sensitive areas of the atmosphere, and then by the rise in NO_x emission due to higher fuel consumption.

It is important to note that summer weather patterns present more variability in the results than winter pattern. This may be caused by two major reasons. The first one is that relative humidity in the atmosphere differs more for summer patterns while for winter patterns the humidity does not change considerably. Therefore the contrails formation largely varies for summer patterns while is quite similar for winter patterns. The second reason is the amount of flights performed during the day. For summer patterns there are more flights during the day while for winter patterns the flights tend to occur during night. During the day there is more variability due to the relative position of the Sun respect to the Earth, while at night, since there is not incoming sunlight, this does not happen.

The climate impact caused by the individual flights for each climate parameter always shows a Probability Density Function with one peak for contrails, NO_x, and ozone; and two peaks for methane. This means that the individual climate impacts from the different flights tend to accumulate around one or two values respectively. The individual contribution of each flight to the climate impact change follows a similar behavior for each climate parameter presented: contrails, NO_x, ozone, and methane. The first part of the optimization, up to 25% or even 50% depending on the case, is driven by a few changes on flights that modify their climate impact considerably. From that point until the end of the optimization, the changes in climate impact are controlled by a few flights changing considerably, a larger number of flights closed to the mean value, and the vast majority of them changing only slightly. This is more obvious for contrails, NO_x, and methane. To sum up, the number of flights that change their trajectory increase during the optimization. The first part of the optimization is driven by a small number of flights achieving a great climate impact reduction because their trajectories can be easily changed to regions of the atmosphere where the emissions have less climate impact. When the optimization progresses the total climate impact reduction is achieved thanks to a small number of flights reducing their climate impact considerably and a large proportion of flights reducing their climate impact slightly. This occurs because the last flights changing their trajectory cannot occupy the regions of the atmosphere where the emissions have lower climate impact since the prior flights are already occupying those regions. Therefore their climate impact reduction is lower.

Finally, the study shows that the results obtained for different climate metrics when comparing same time horizons (AGWP20 and ATR20) are not very different. This happens because the metrics were chosen in order to describe in the best mathematical possible way the overall objective of the optimization.

7

Recommendations

The study presented has shown that water vapor plays a non-important role in the optimization. Therefore it does not really require to be considered when analyzing subsonic aircraft fleets flying in the North Atlantic flight corridor. More important is to consider contrails (especially for westbound flights) and NO_x effect (especially for eastbound flights), and how this affects the atmosphere via ozone production, methane depletion, and PMO. Carbon dioxide should be studied and payed close attention to especially when considering long-term time horizons. Moreover, the studies in the future should focus in long-term impact rather than short-term. The reason to do that is the overall long term climate impact caused by carbon dioxide emission. The time this pollutant will be present in the atmosphere is several orders of magnitude larger than for the other climate parameters.

Considering that the re-routing approach may be applied to actual fleets, the recommendation is to achieve *Normalized Total Climate Impact Change* values between 25% and 50% and no further than that. There are some reasons to support this from different perspectives:

- The increment in economic costs will be low in comparison with the climate impact reduction. After that, the re-routing approach becomes less efficient in terms of climate impact reduction to economic cost increase ratio.
- The increase in fuel consumption will be small, and therefore the carbon dioxide emission will increase only slightly. Since carbon dioxide will remain in the atmosphere for centuries, reducing its emission amount is a good strategy.
- The increase in fuel consumption will lead to a growth in NO_x emissions. Since this value will be small, the effect from avoiding the sensitive-climate regions will be more important than the increase in NO_x emissions. Therefore, fewer problems caused by NO_x emissions are occurring than in the minimum climate impact situation.
- Fewer flights need to see its trajectory altered. Hence, from an organizational point of view, the changes are easier to apply.

Finally, the most interesting cases where this can be applied are westbound flights in Summer Pattern 1, and eastbound and westbound flights in Summer Pattern 2. Here, the total climate impact reduction that can be obtained is around three times higher than in all other cases.

A

Annex A

A complete list of figures comparing the *Normalized Climate Impact* and the *Relative Contribution* of the different climate parameters for the same weather pattern, but different flight direction and climate metric, is shown in this section. Moreover, the Pareto fronts are presented as well. Westbound flights (W) appear in red color while eastbound flights (E) are presented in blue color. In the case of climate metrics, AGWP100 is presented with a solid line, AGWP20 with a dotted line, and finally ATR20 with a dashed line.

A.1. Summer Pattern 1

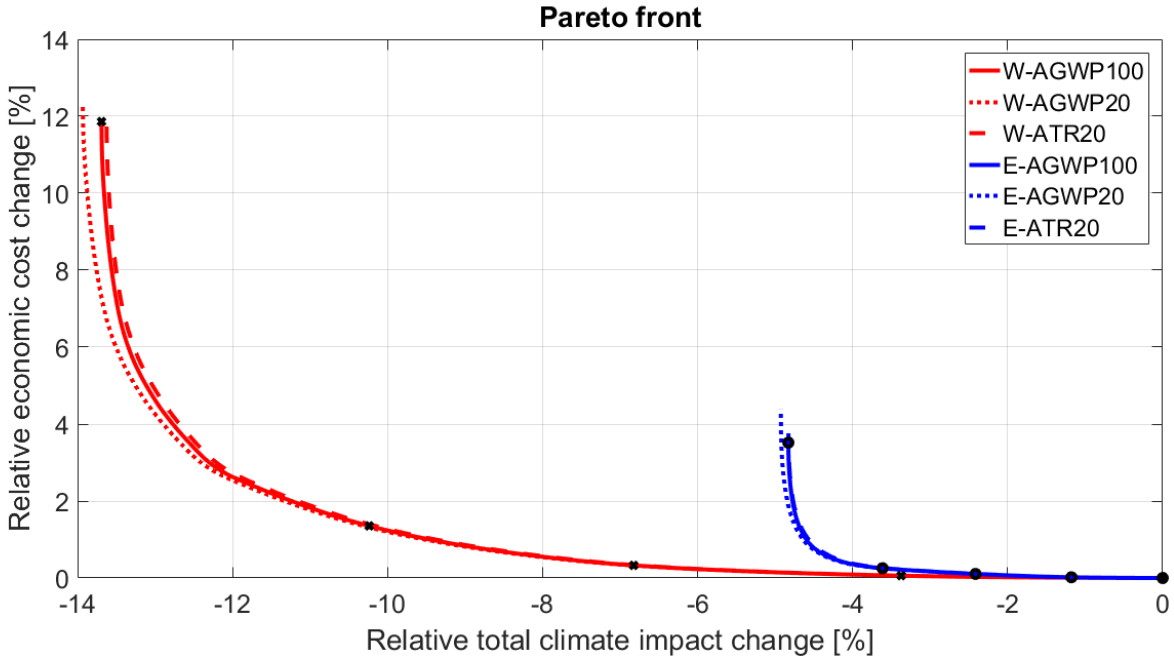

Figure 46. Comparison of Pareto Fronts for Summer Pattern 1 and different flight directions and climate metrics.

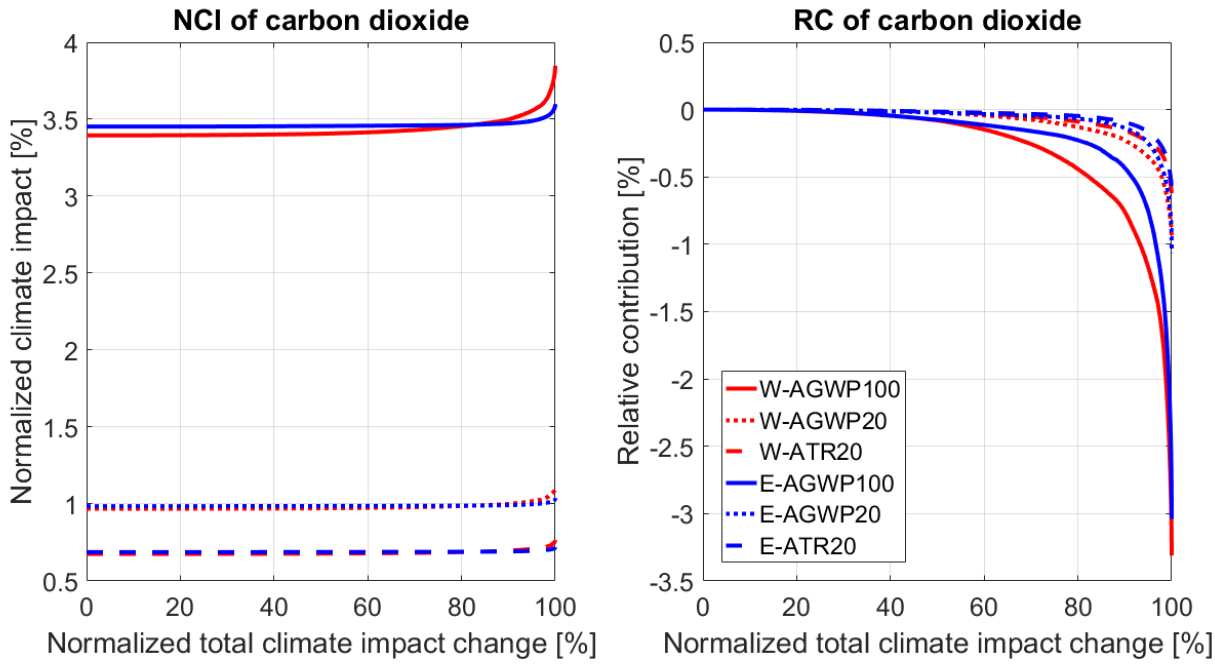

Figure 47. Comparison of carbon dioxide *NCI* and *RC* for Summer Pattern 1 and different flight directions and climate metrics.

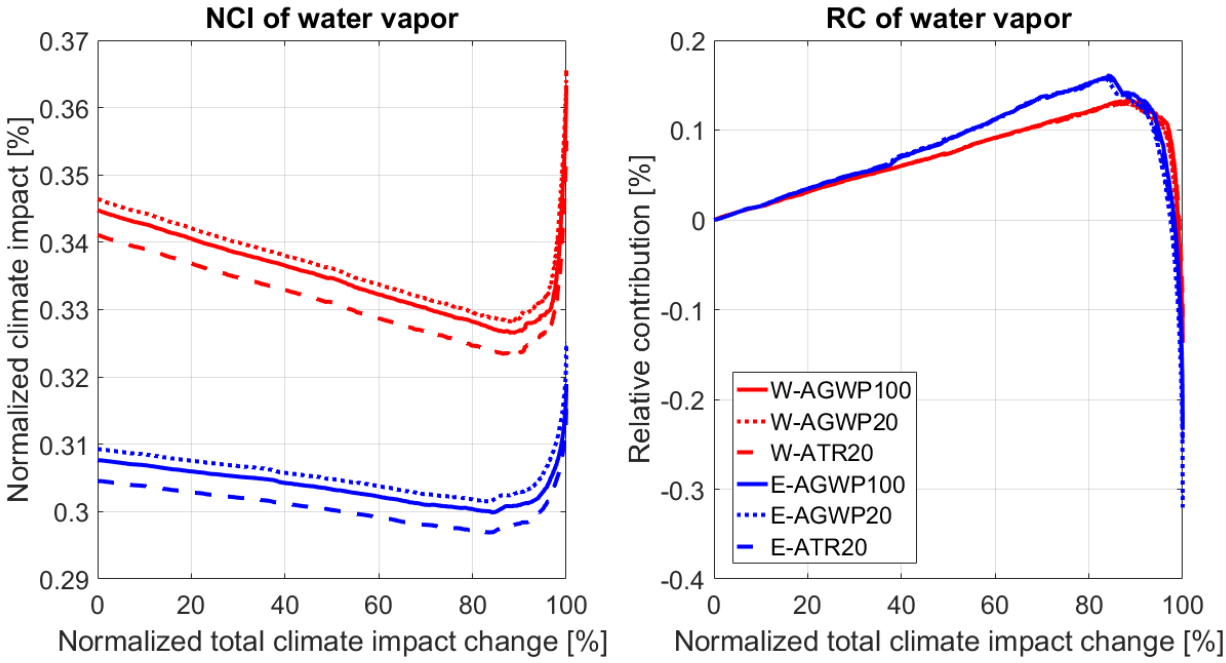

Figure 48. Comparison of water vapor *NCI* and *RC* for Summer Pattern 1 and different flight directions and climate metrics.

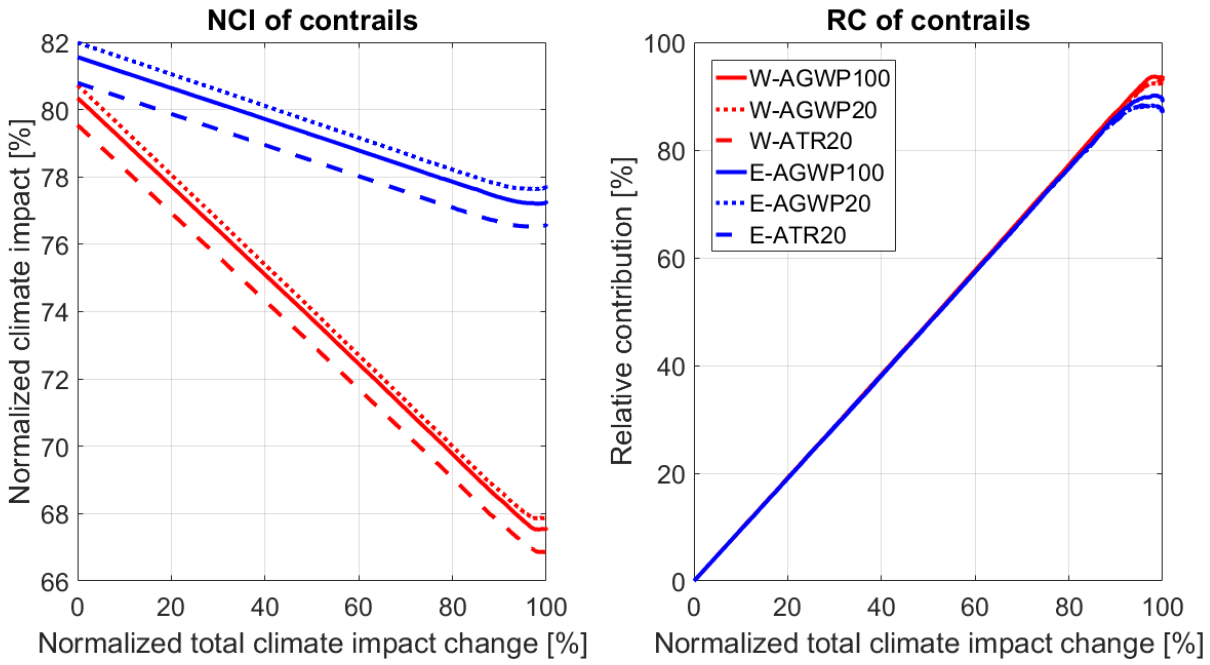

Figure 49. Comparison of contrails *NCI* and *RC* for Summer Pattern 1 and different flight directions and climate metrics.

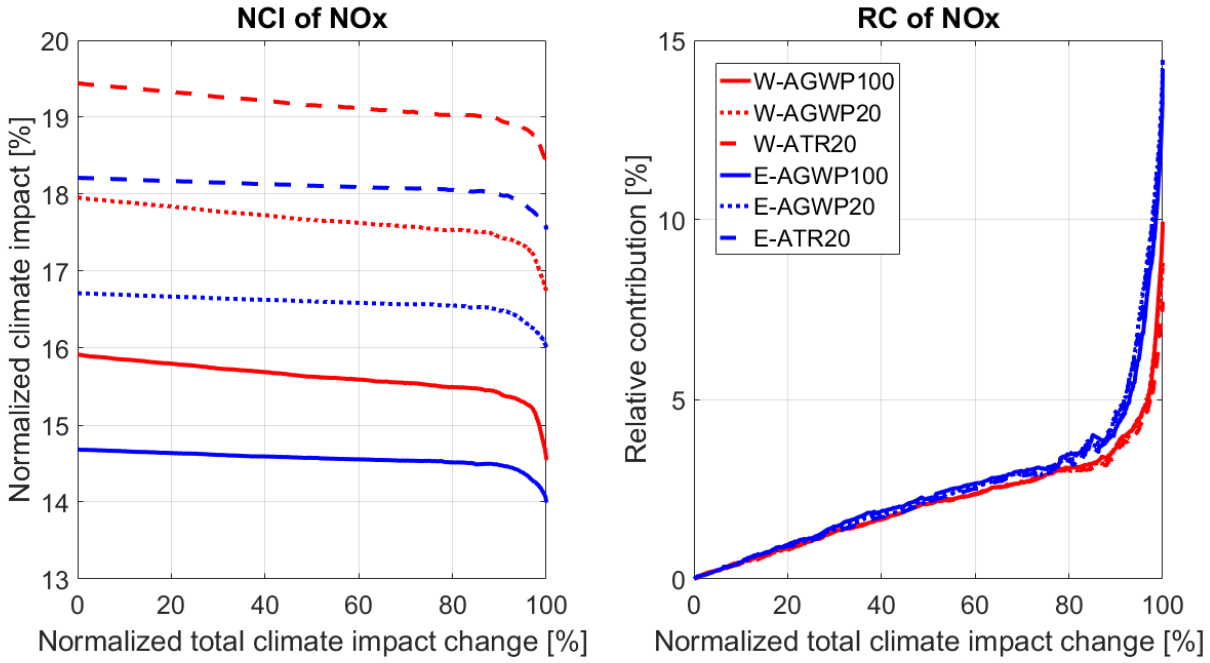

Figure 50. Comparison of NO_x *NCI* and *RC* for Summer Pattern 1 and different flight directions and climate metrics.

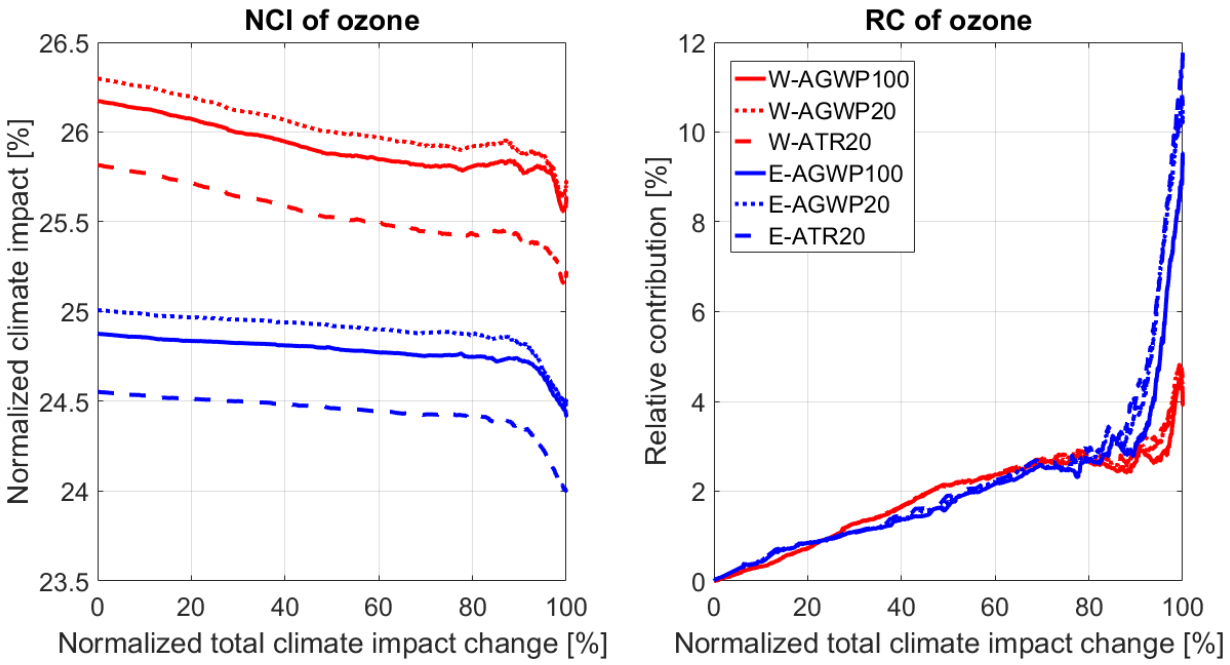

Figure 51. Comparison of ozone *NCI* and *RC* for Summer Pattern 1 and different flight directions and climate metrics.

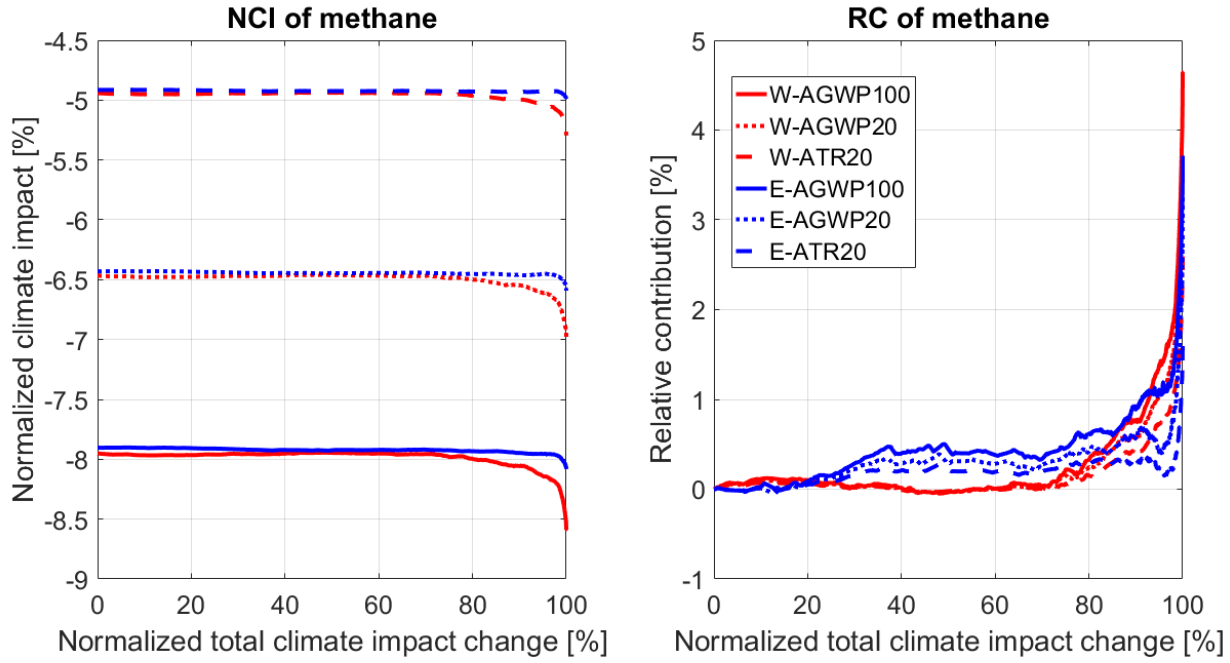

Figure 52. Comparison of methane *NCI* and *RC* for Summer Pattern 1 and different flight directions and climate metrics.

A.2. Summer Pattern 2

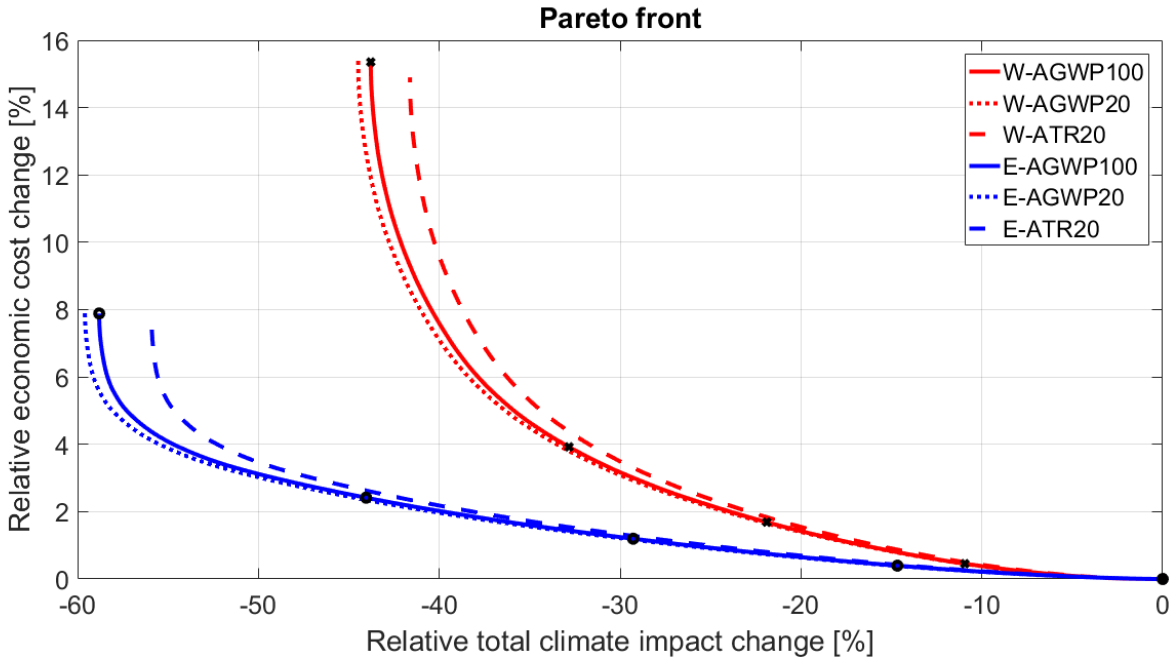

Figure 53. Comparison of Pareto Fronts for Summer Pattern 2 and different flight directions and climate metrics.

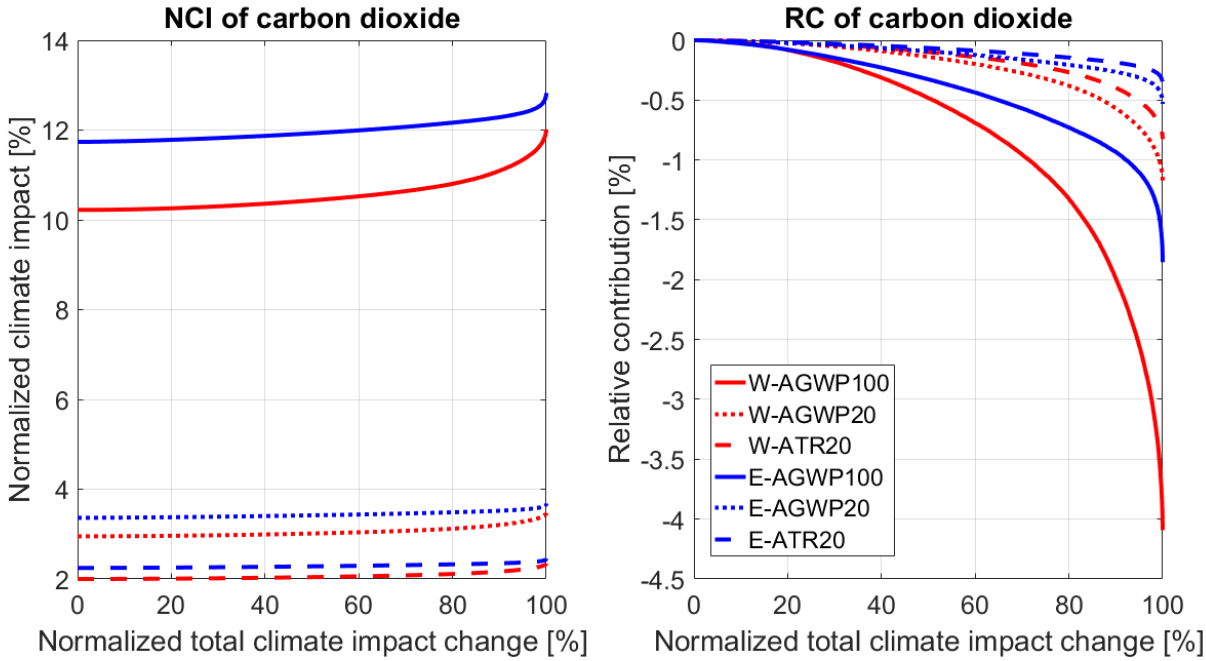

Figure 54. Comparison of carbon dioxide *NCI* and *RC* for Summer Pattern 2 and different flight directions and climate metrics.

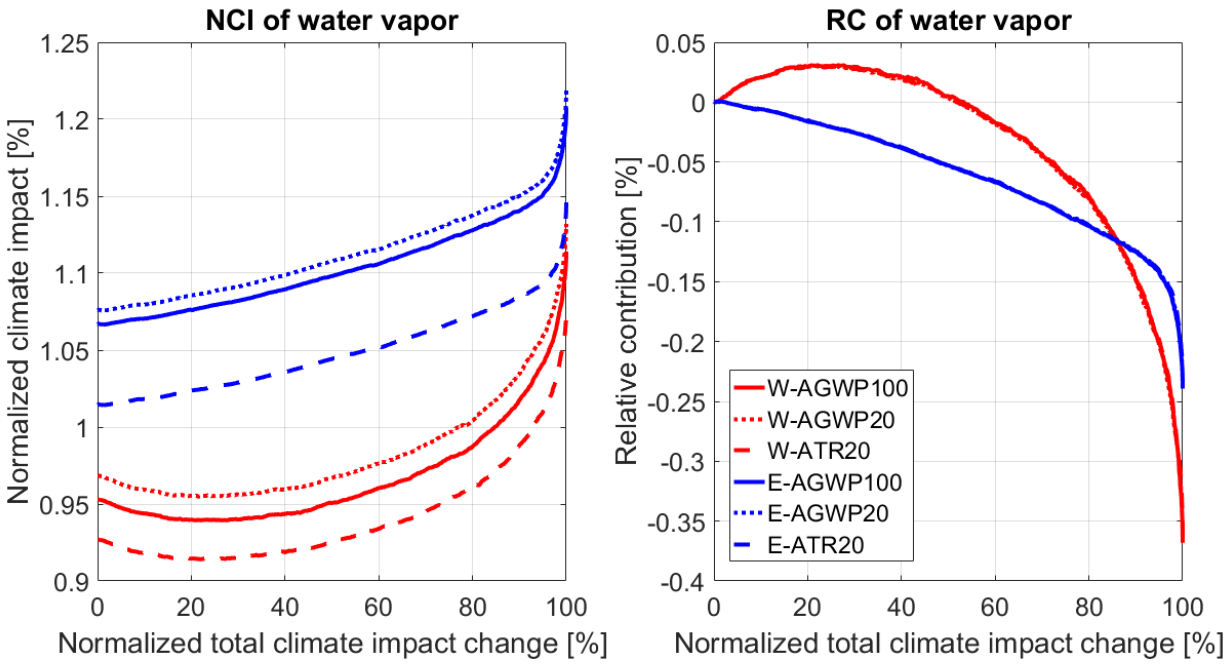

Figure 55. Comparison of water vapor *NCI* and *RC* for Summer Pattern 2 and different flight directions and climate metrics.

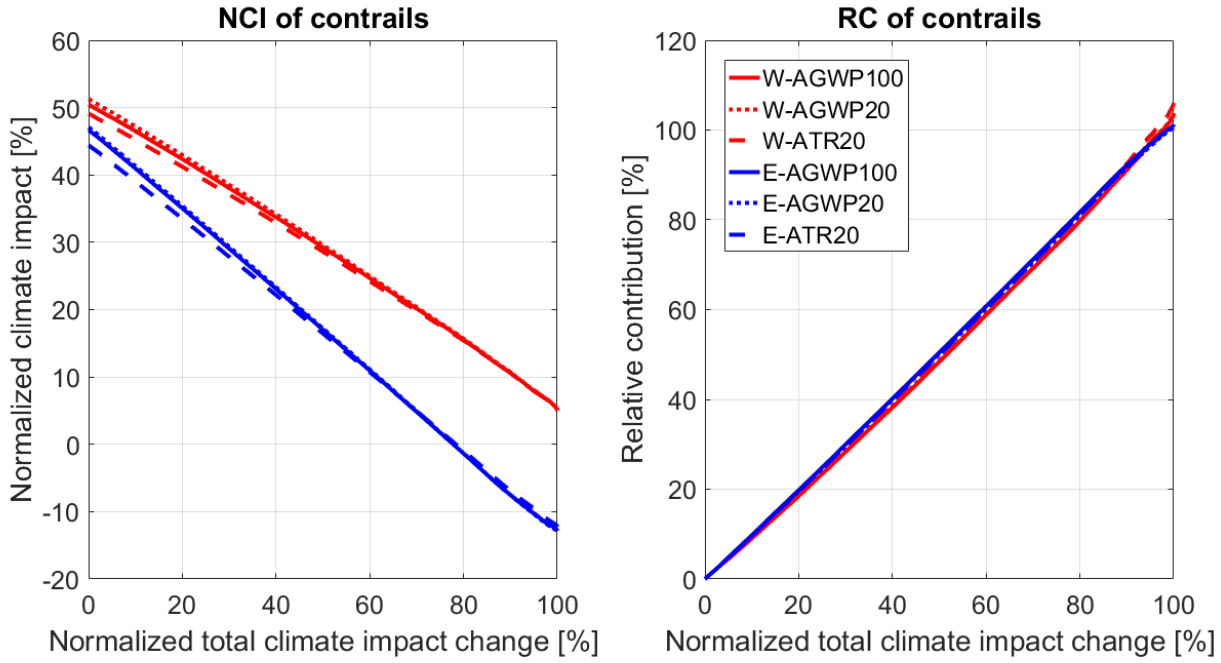

Figure 56. Comparison of contrails *NCI* and *RC* for Summer Pattern 2 and different flight directions and climate metrics.

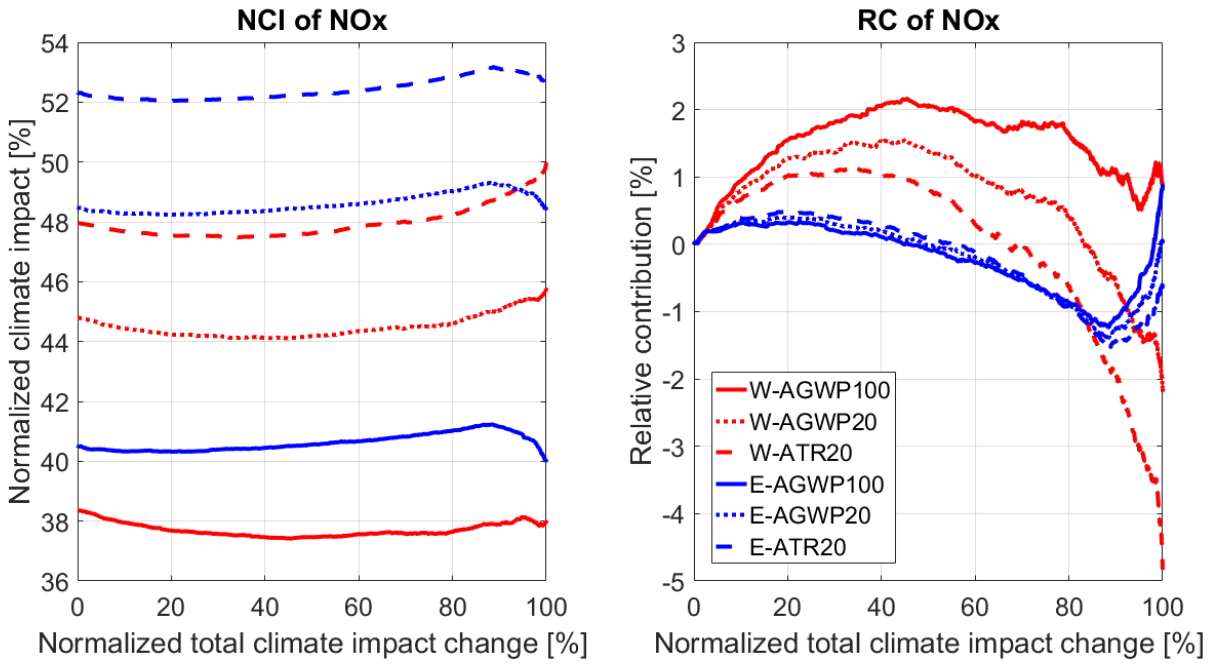

Figure 57. Comparison of NO_x *NCI* and *RC* for Summer Pattern 2 and different flight directions and climate metrics.

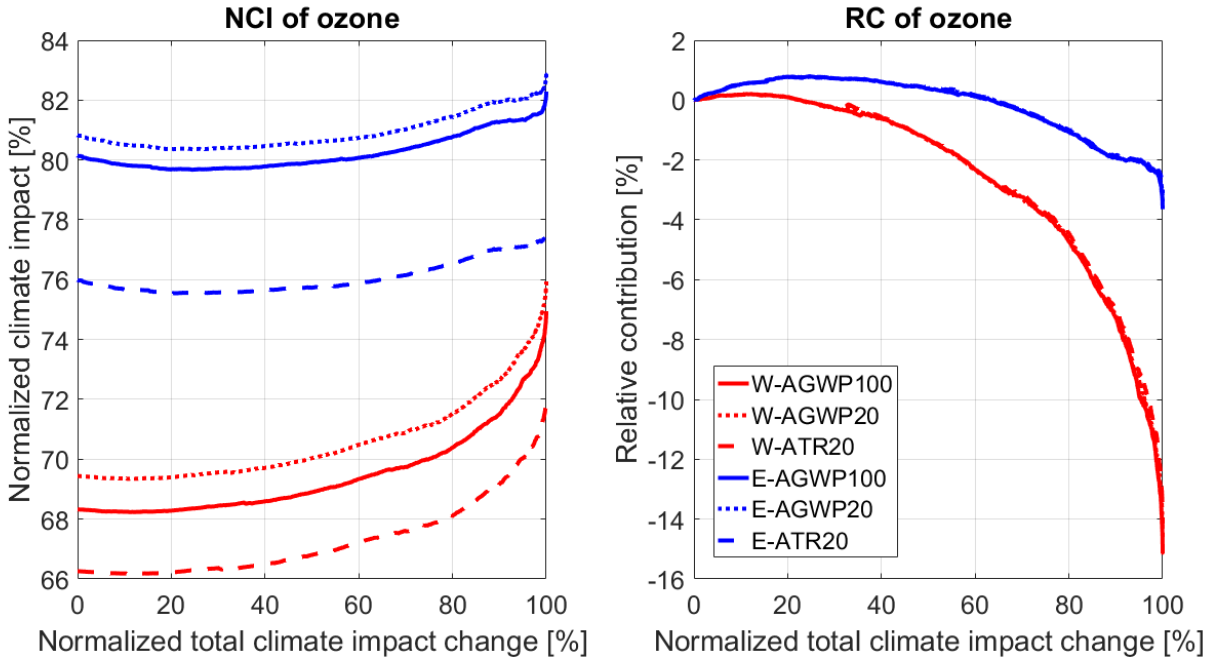

Figure 58. Comparison of ozone *NCI* and *RC* for Summer Pattern 2 and different flight directions and climate metrics.

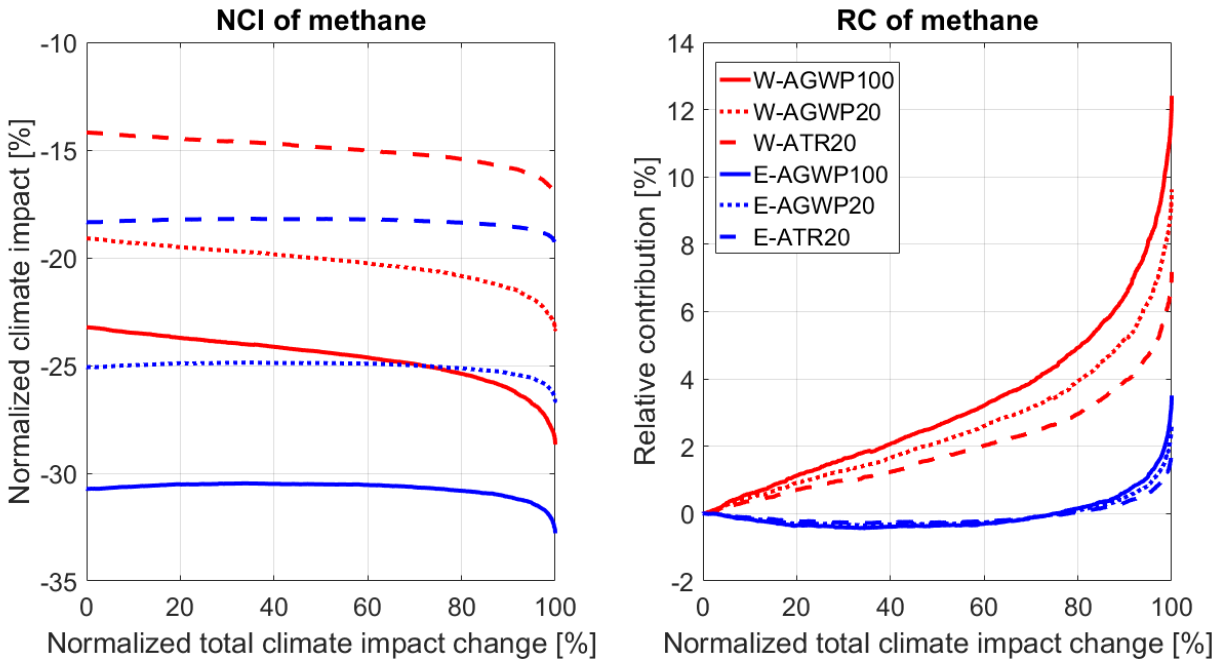

Figure 59. Comparison of methane *NCI* and *RC* for Summer Pattern 2 and different flight directions and climate metrics.

A.3. Summer Pattern 3

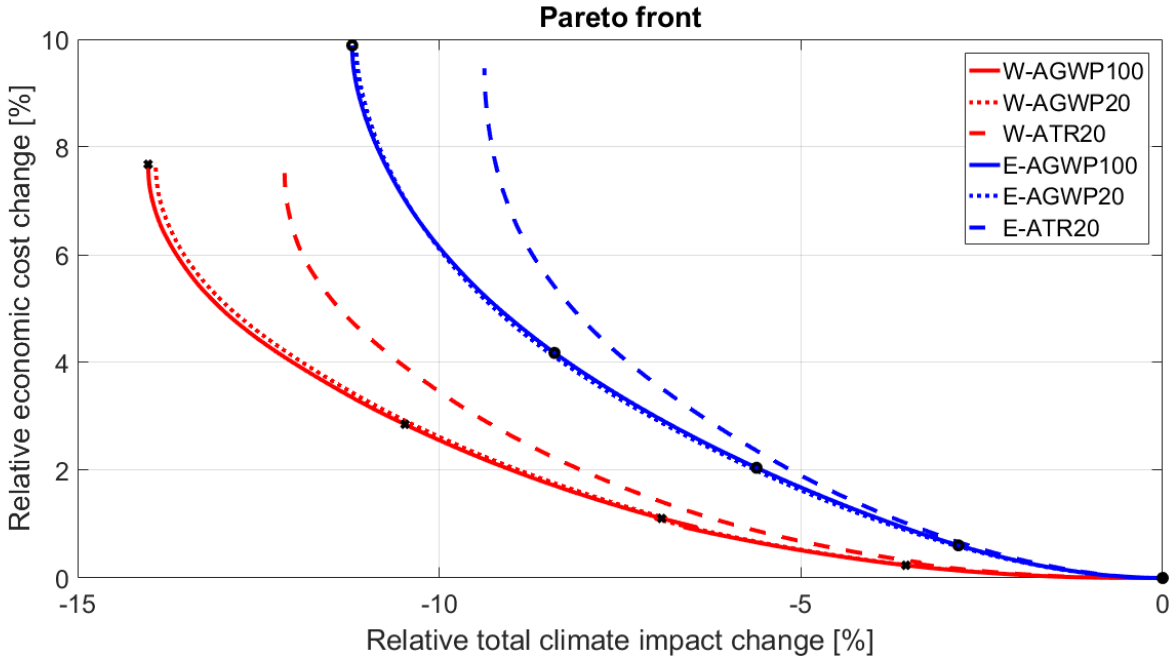

Figure 60. Comparison of Pareto Fronts for Summer Pattern 3 and different flight directions and climate metrics.

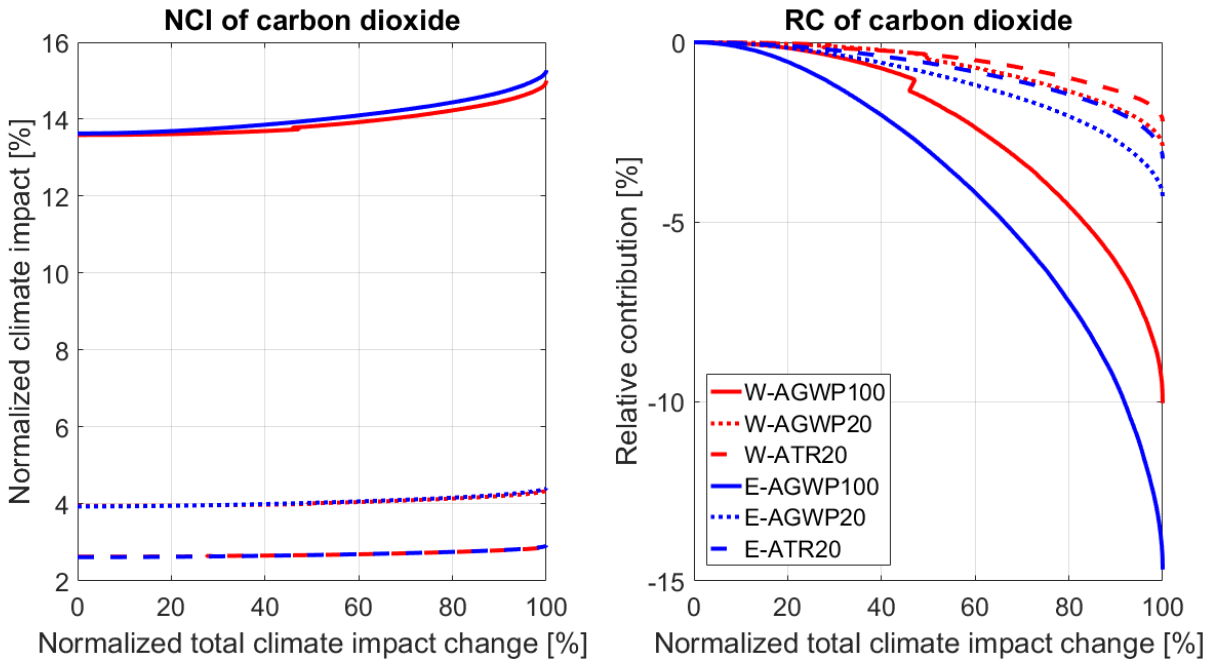

Figure 61. Comparison of carbon dioxide *NCI* and *RC* for Summer Pattern 3 and different flight directions and climate metrics.

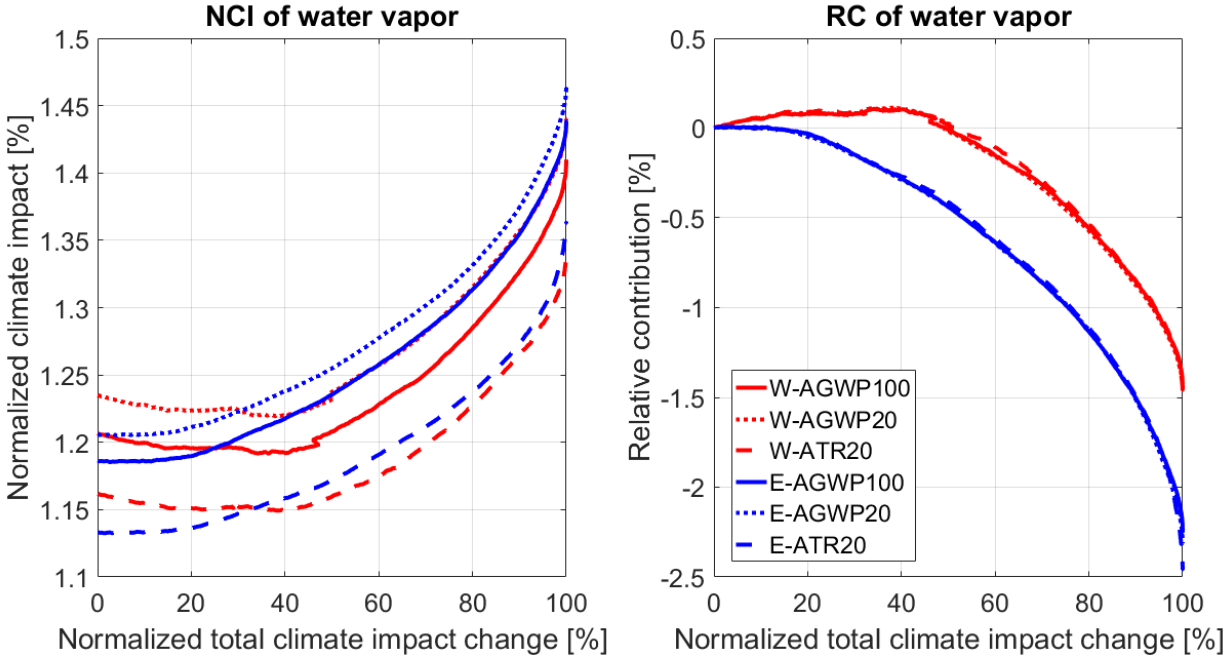

Figure 62. Comparison of water vapor *NCI* and *RC* for Summer Pattern 3 and different flight directions and climate metrics.

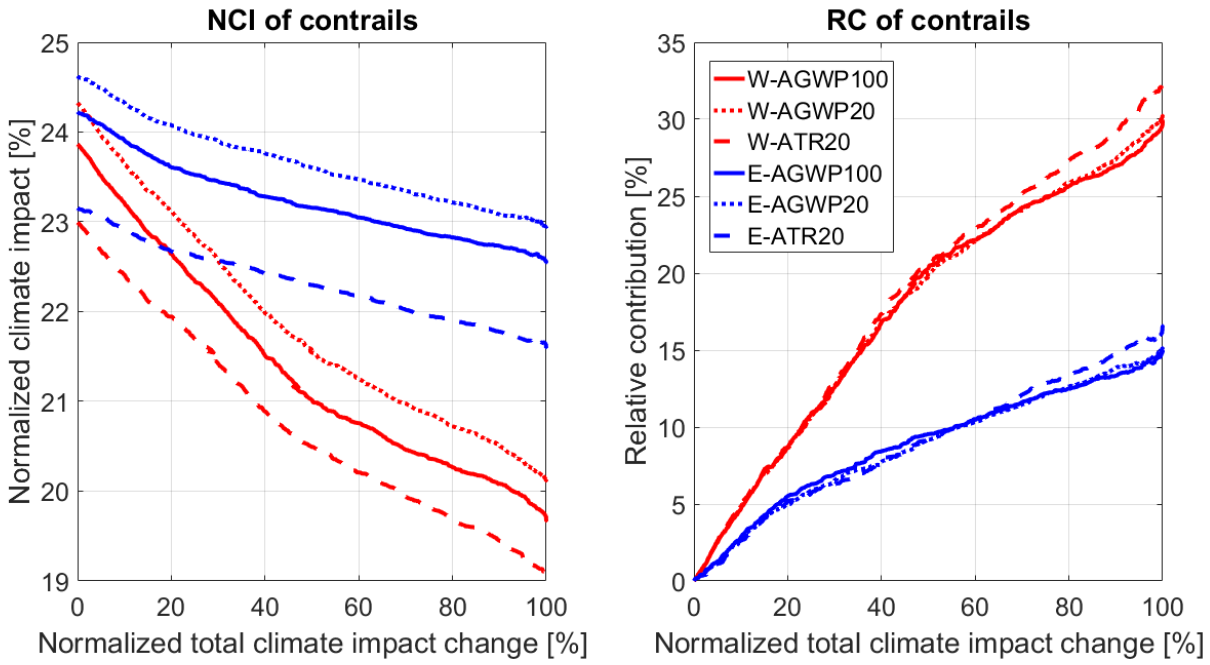

Figure 63. Comparison of contrails *NCI* and *RC* for Summer Pattern 3 and different flight directions and climate metrics.

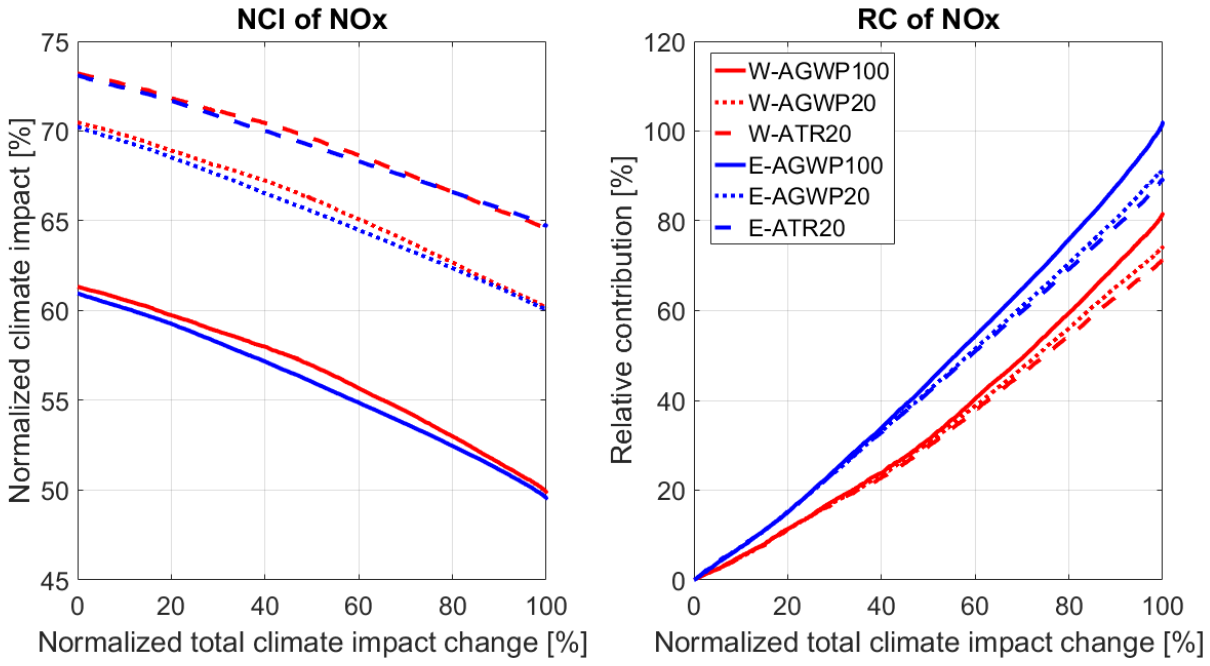

Figure 64. Comparison of NO_x *NCI* and *RC* for Summer Pattern 3 and different flight directions and climate metrics.

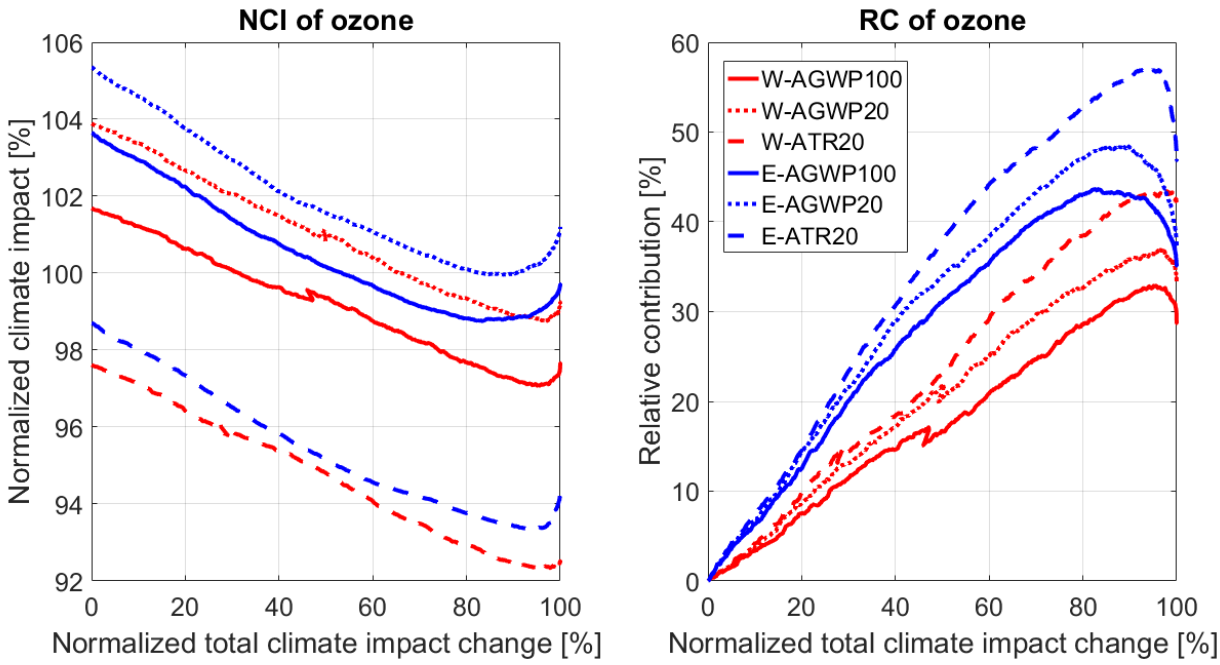

Figure 65. Comparison of ozone *NCI* and *RC* for Summer Pattern 3 and different flight directions and climate metrics.

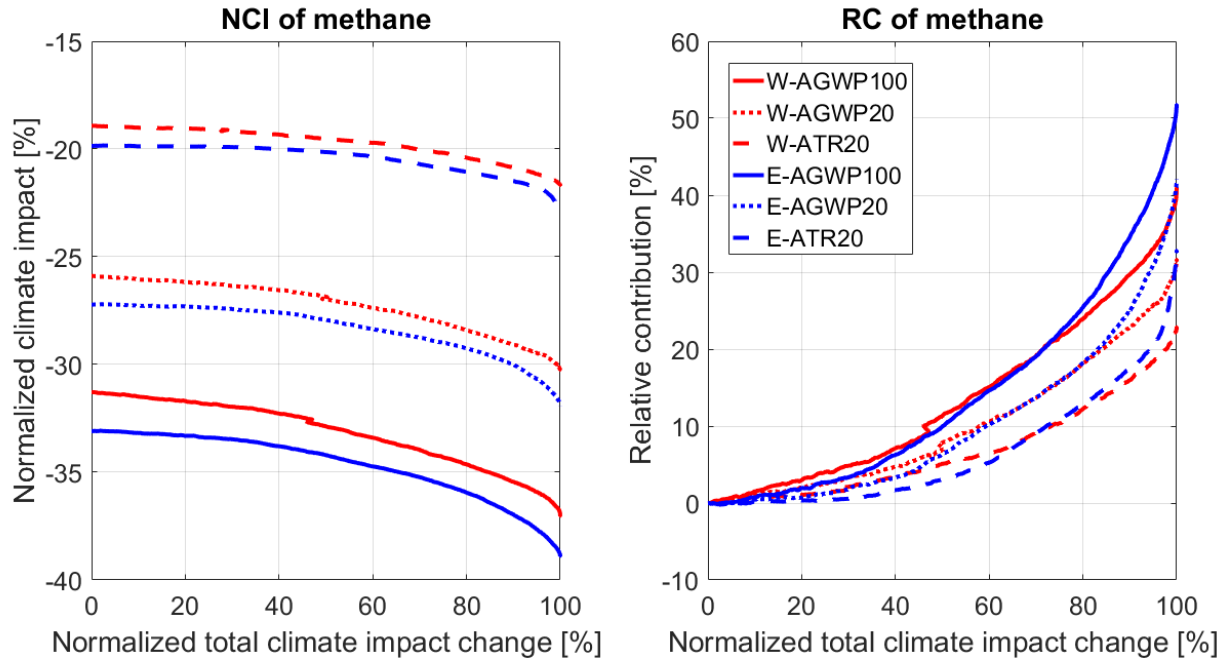

Figure 66. Comparison of methane *NCI* and *RC* for Summer Pattern 3 and different flight directions and climate metrics.

A.4. Winter Pattern 1

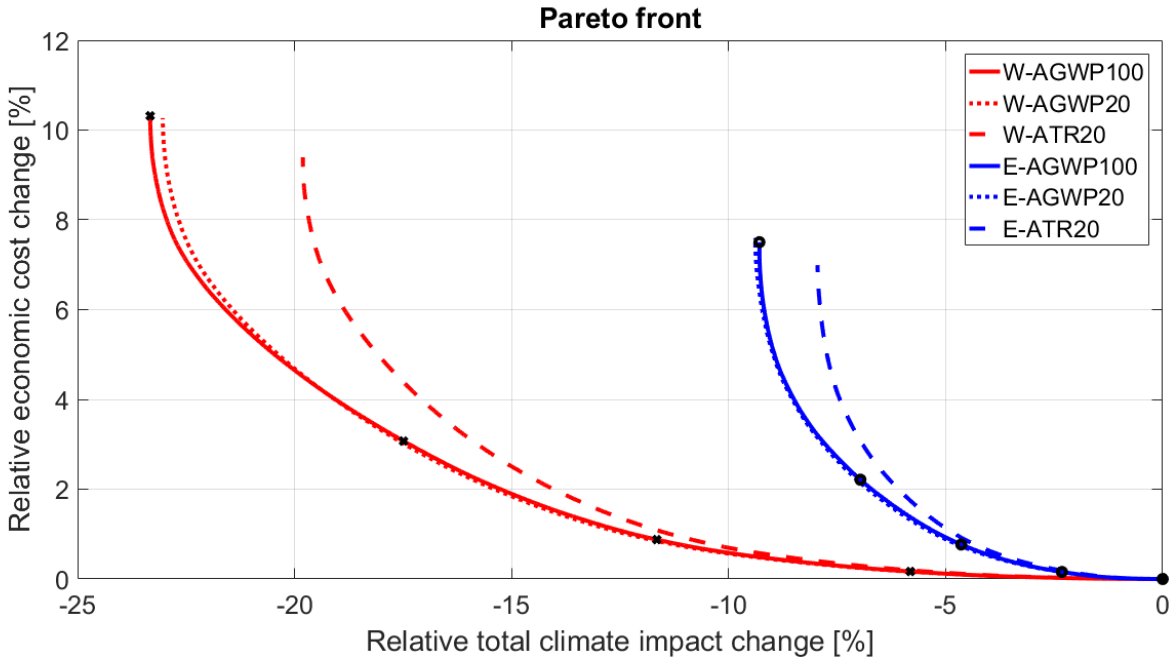

Figure 67. Comparison of Pareto Fronts for Winter Pattern 1 and different flight directions and climate metrics.

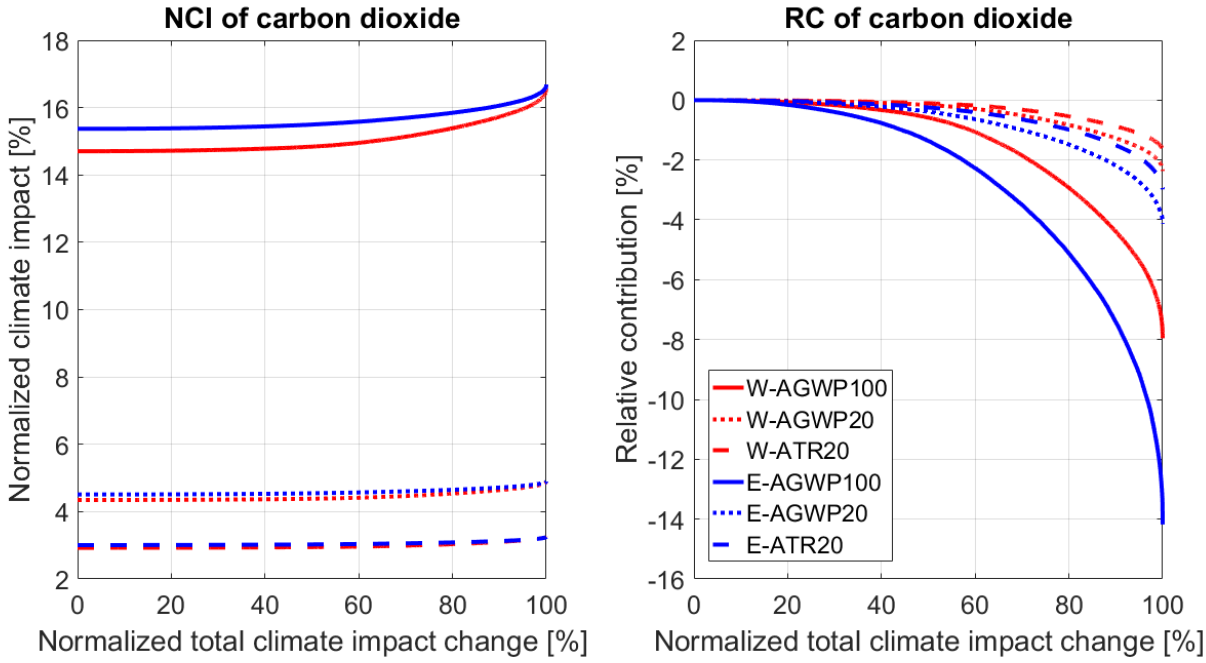

Figure 68. Comparison of carbon dioxide *NCI* and *RC* for Winter Pattern 1 and different flight directions and climate metrics.

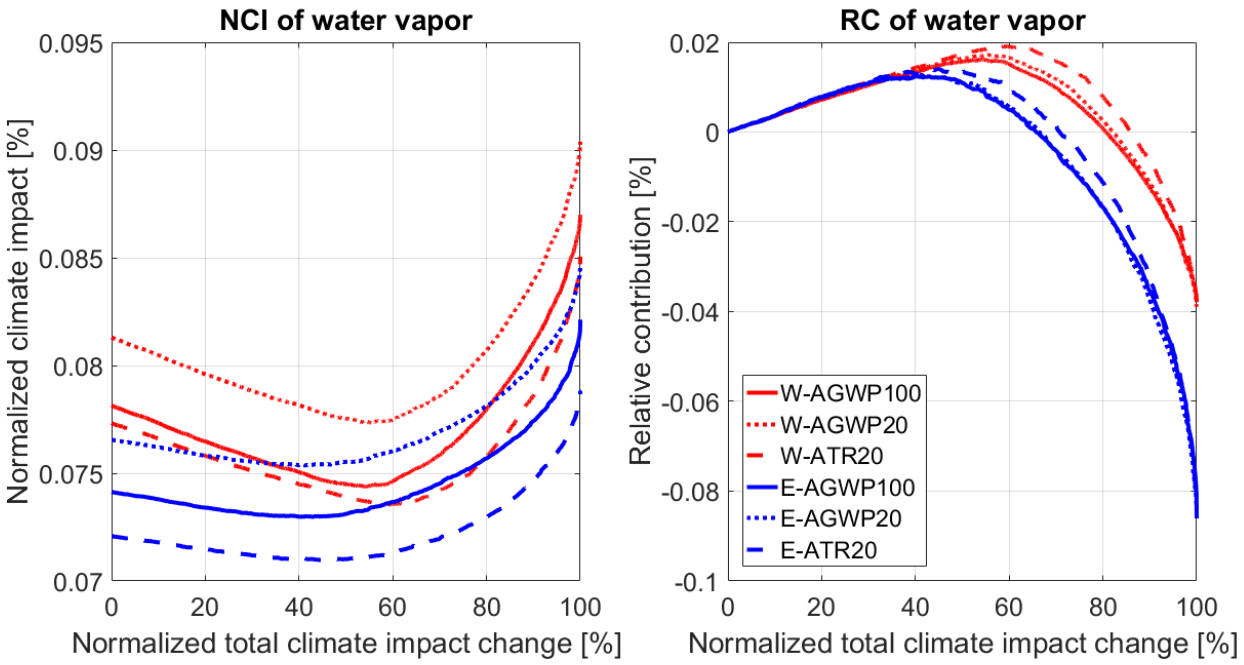

Figure 69. Comparison of water vapor *NCI* and *RC* for Winter Pattern 1 and different flight directions and climate metrics.

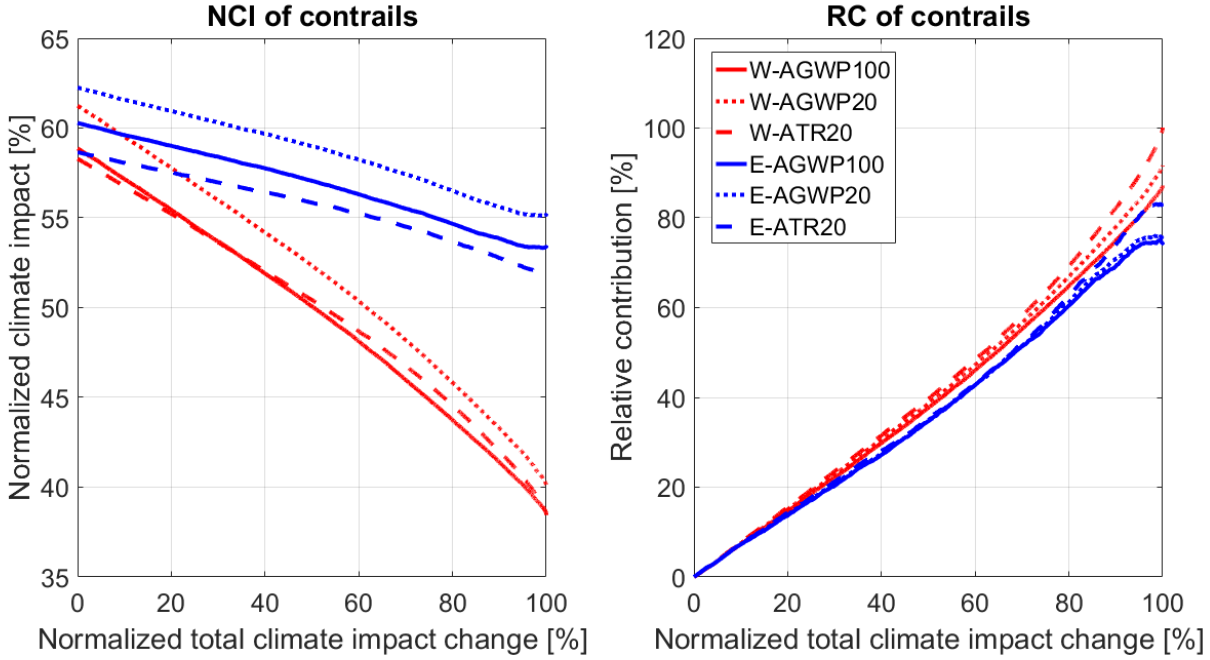

Figure 70. Comparison of contrails *NCI* and *RC* for Winter Pattern 1 and different flight directions and climate metrics.

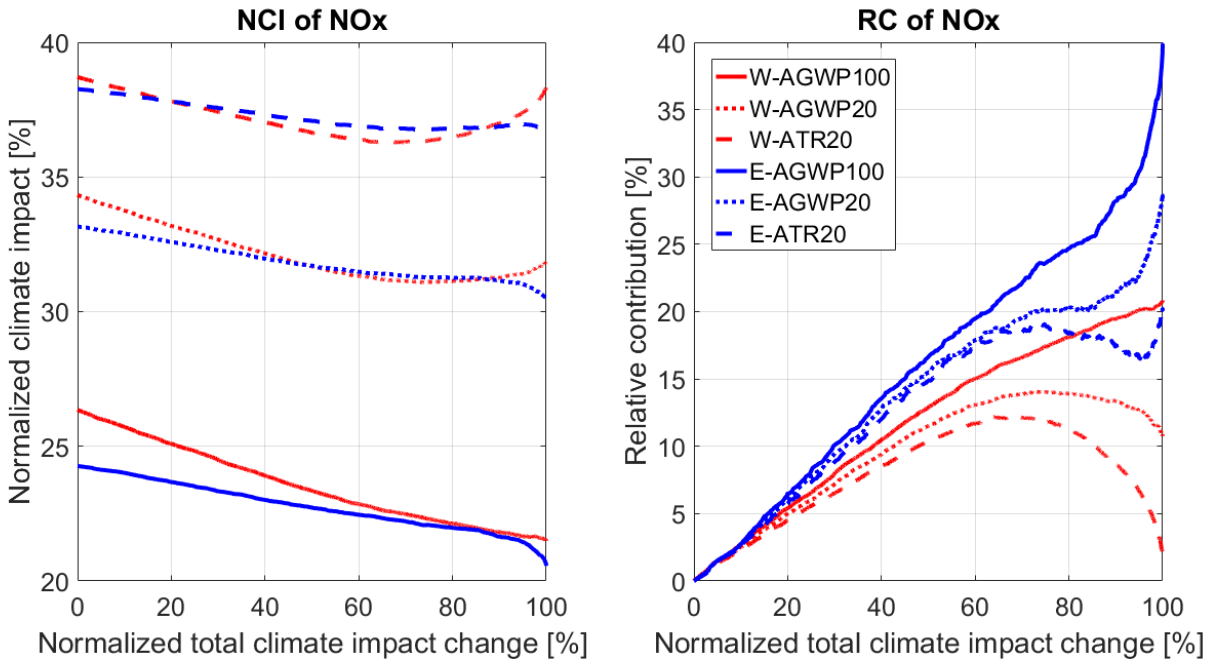

Figure 71. Comparison of NO_x *NCI* and *RC* for Winter Pattern 1 and different flight directions and climate metrics.

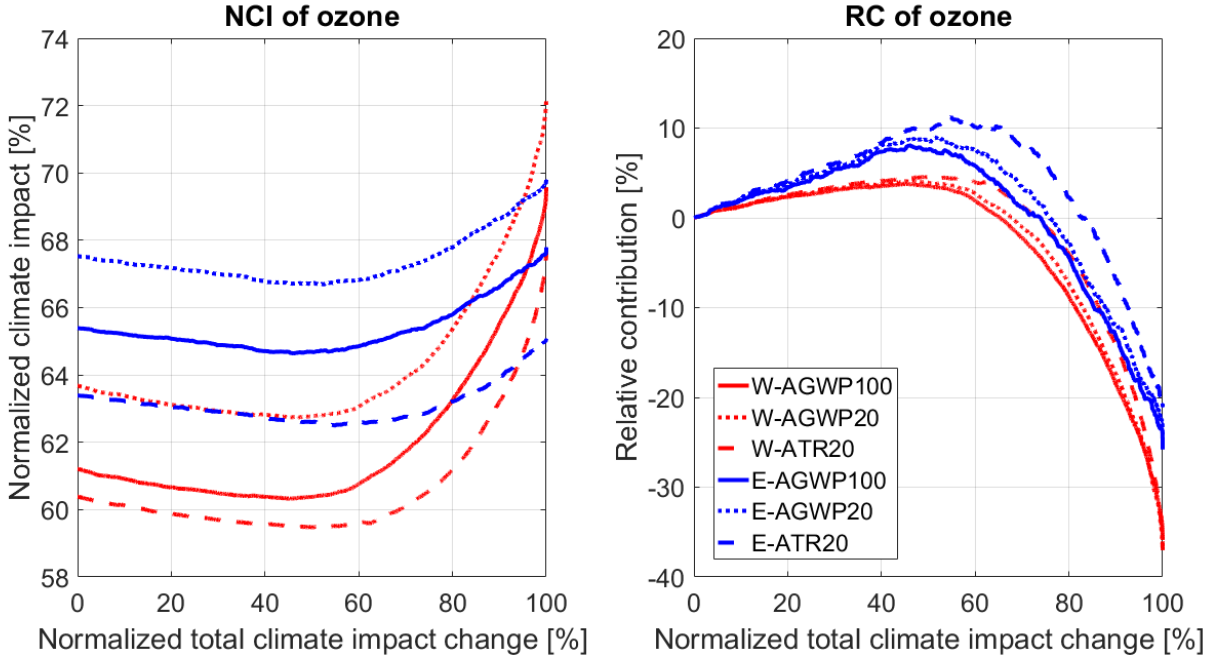

Figure 72. Comparison of ozone *NCI* and *RC* for Winter Pattern 1 and different flight directions and climate metrics.

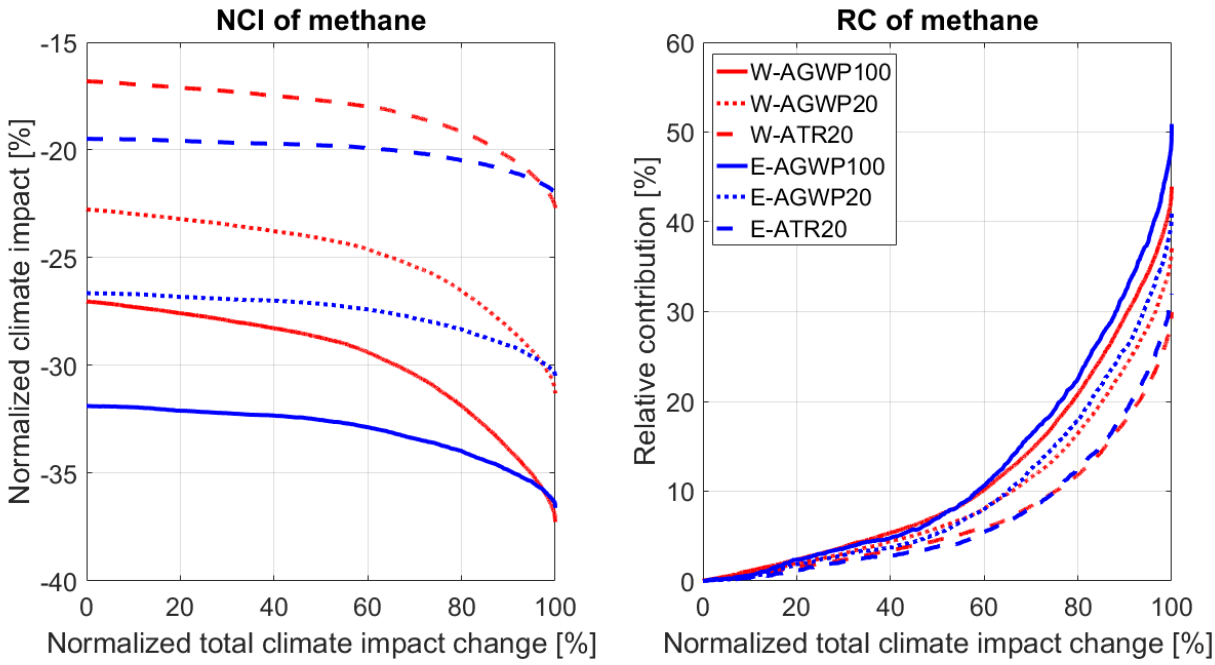

Figure 73. Comparison of methane *NCI* and *RC* for Winter Pattern 1 and different flight directions and climate metrics.

A.5. Winter Pattern 2

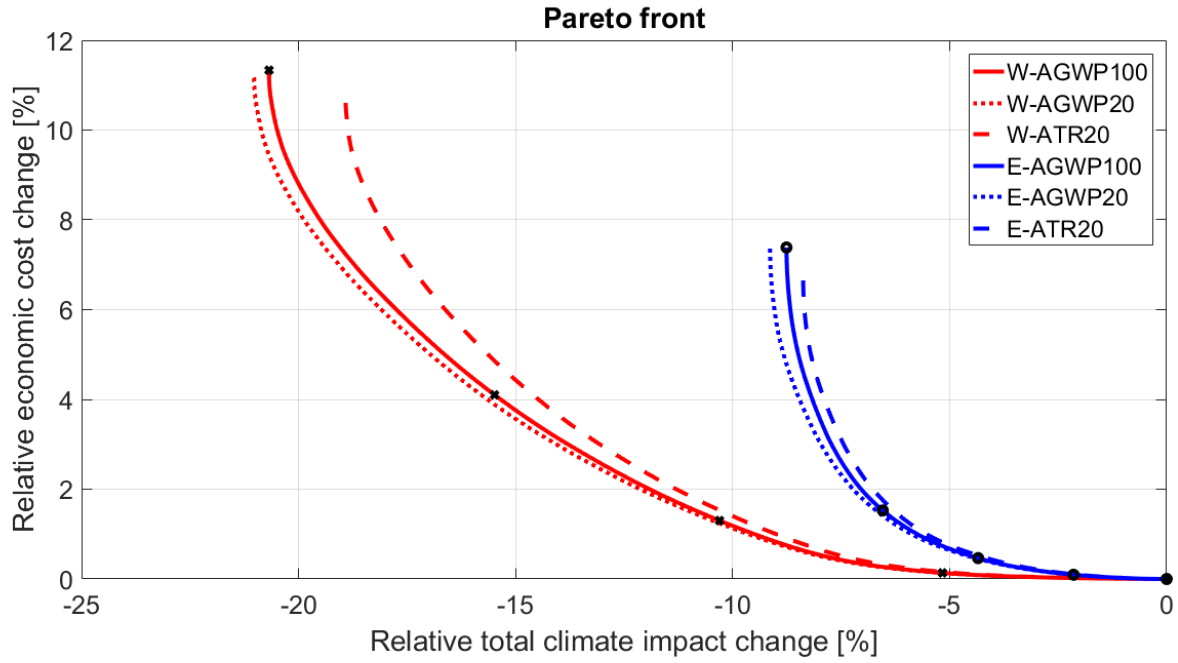

Figure 74. Comparison of Pareto Fronts for Winter Pattern 2 and different flight directions and climate metrics.

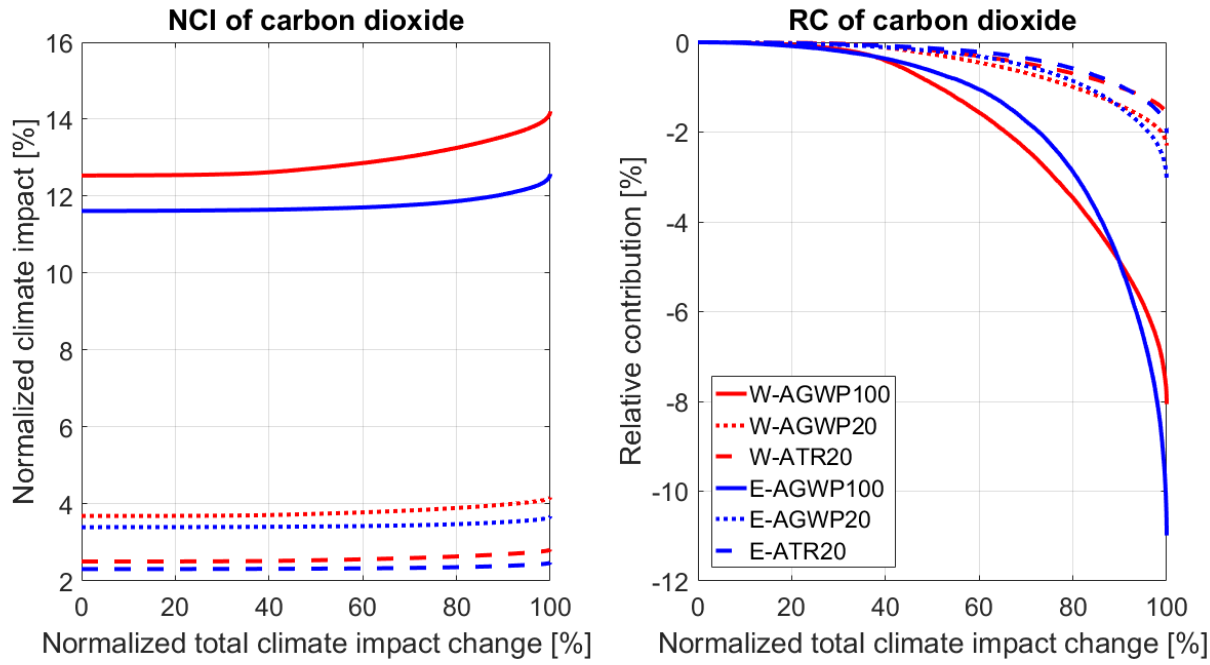

Figure 75. Comparison of carbon dioxide *NCI* and *RC* for Winter Pattern 2 and different flight directions and climate metrics.

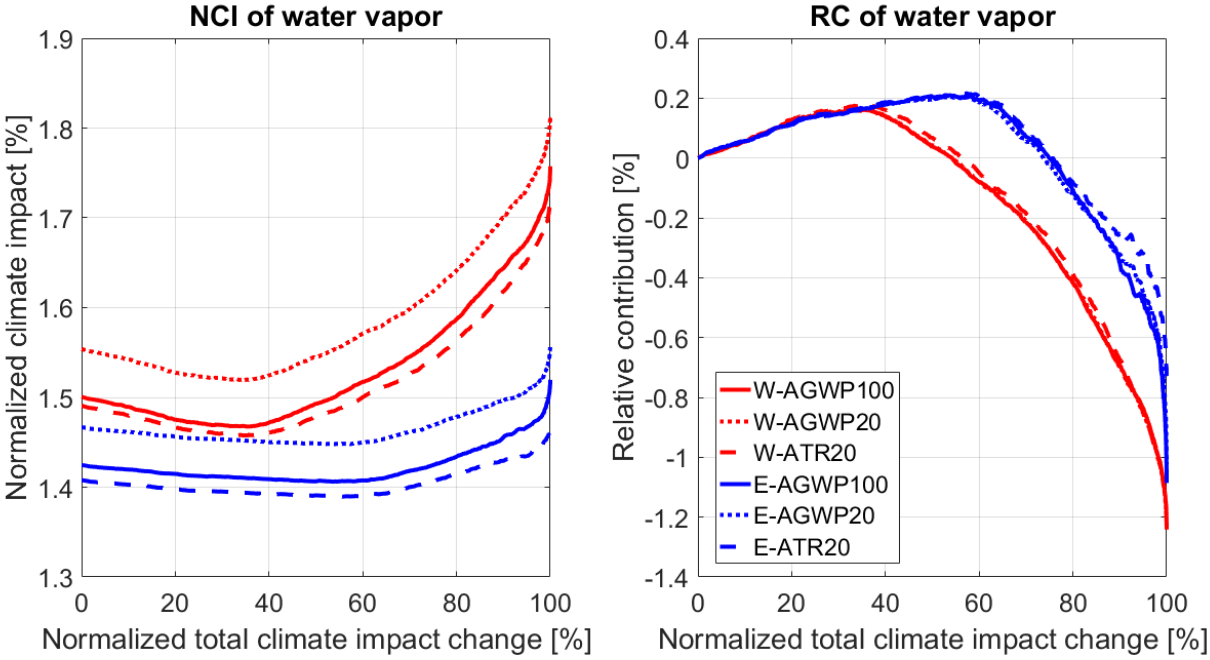

Figure 76. Comparison of water vapor *NCI* and *RC* for Winter Pattern 2 and different flight directions and climate metrics.

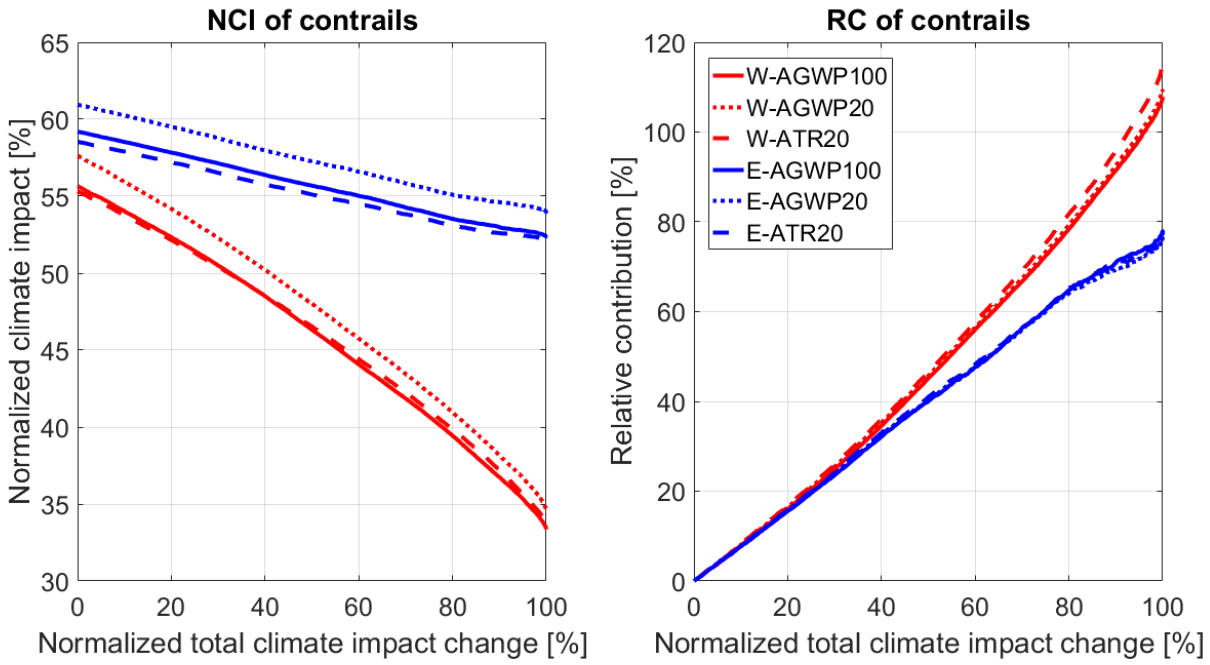

Figure 77. Comparison of contrails *NCI* and *RC* for Winter Pattern 2 and different flight directions and climate metrics.

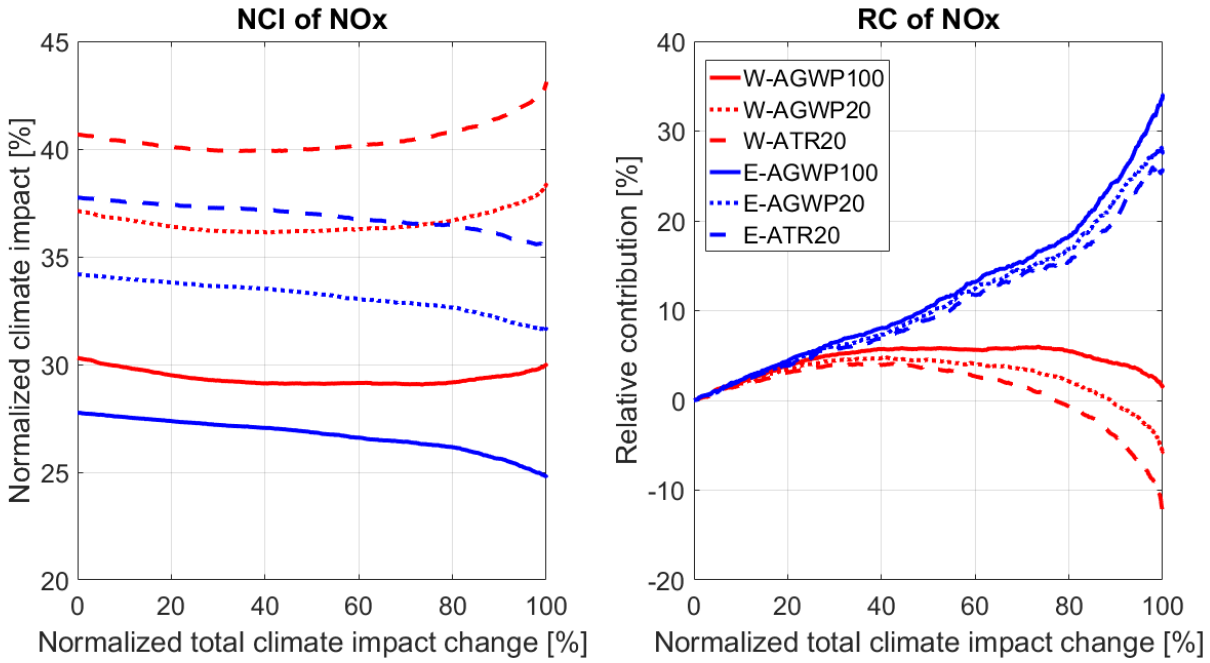

Figure 78. Comparison of NO_x *NCI* and *RC* for Winter Pattern 2 and different flight directions and climate metrics.

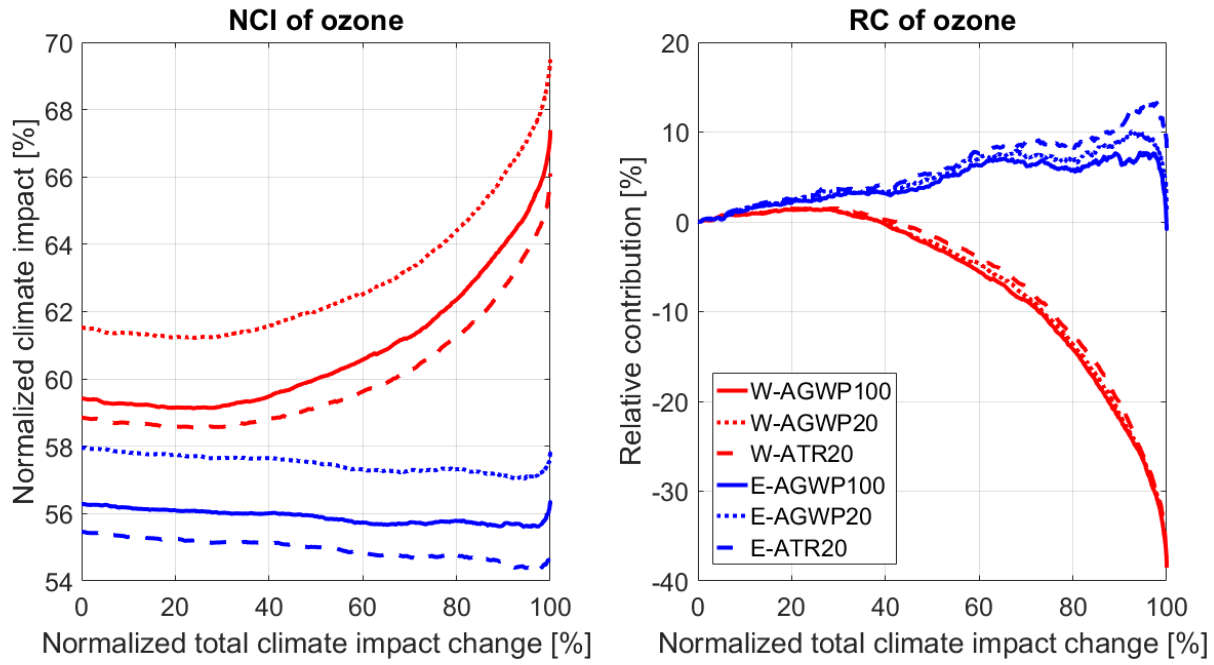

Figure 79. Comparison of ozone *NCI* and *RC* for Winter Pattern 2 and different flight directions and climate metrics.

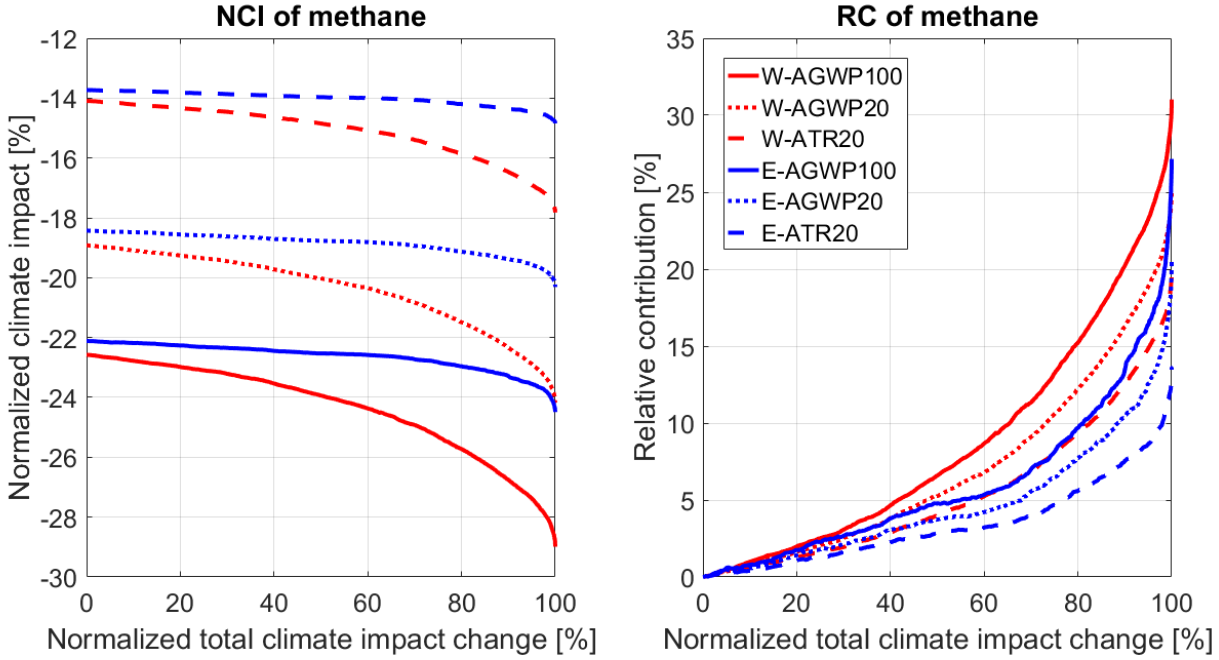

Figure 80. Comparison of methane *NCI* and *RC* for Winter Pattern 2 and different flight directions and climate metrics.

A.6. Winter Pattern 3

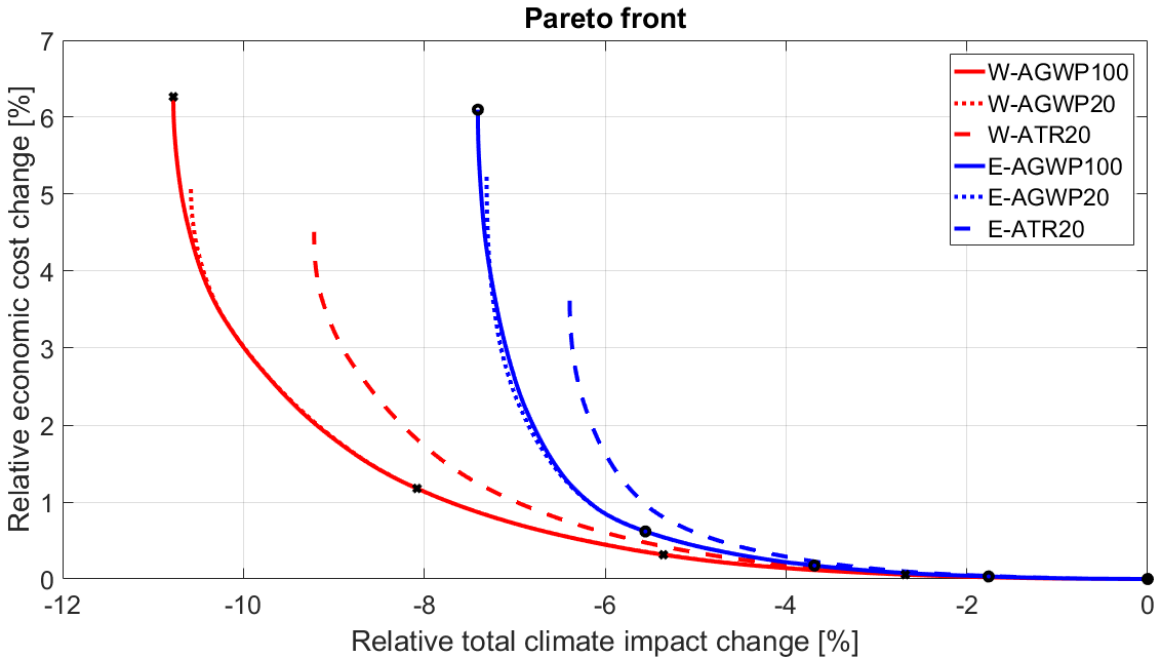

Figure 81. Comparison of Pareto Fronts for Winter Pattern 3 and different flight directions and climate metrics.

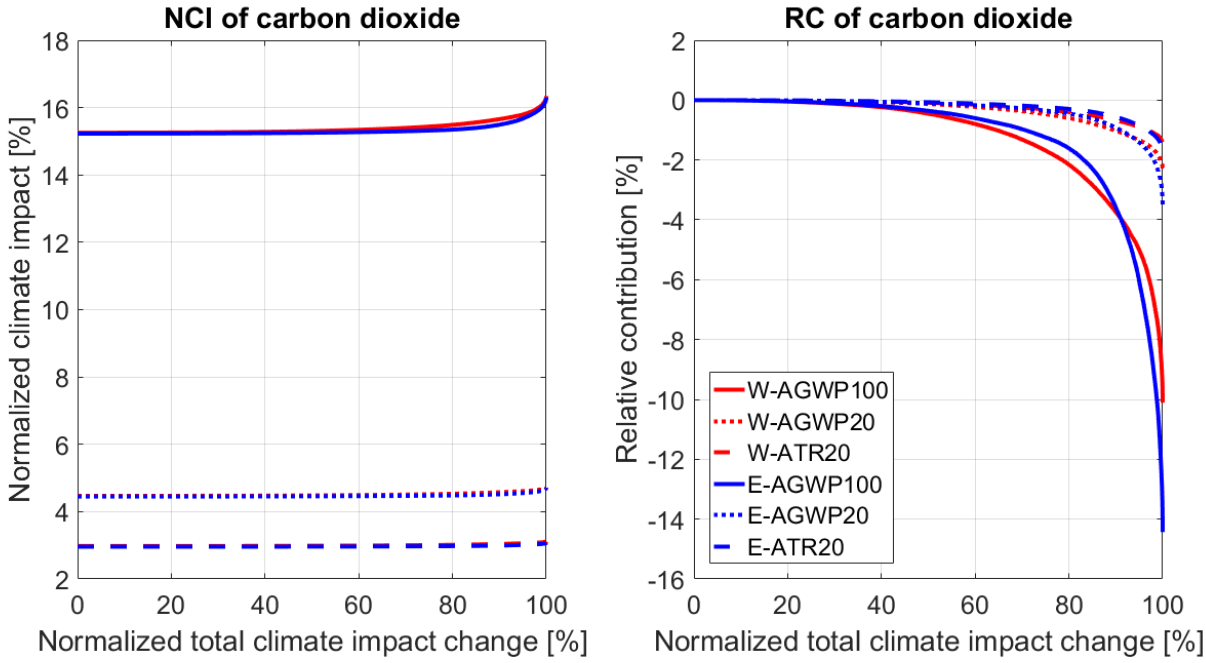

Figure 82. Comparison of carbon dioxide *NCI* and *RC* for Winter Pattern 3 and different flight directions and climate metrics.

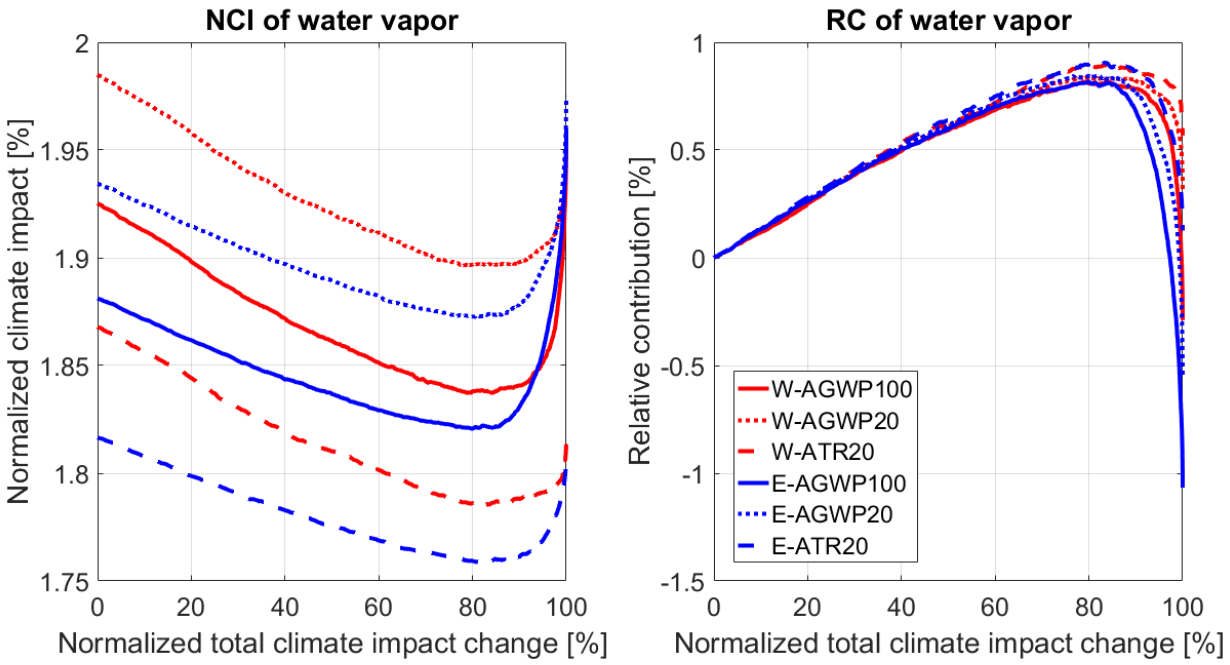

Figure 83. Comparison of water vapor *NCI* and *RC* for Winter Pattern 3 and different flight directions and climate metrics.

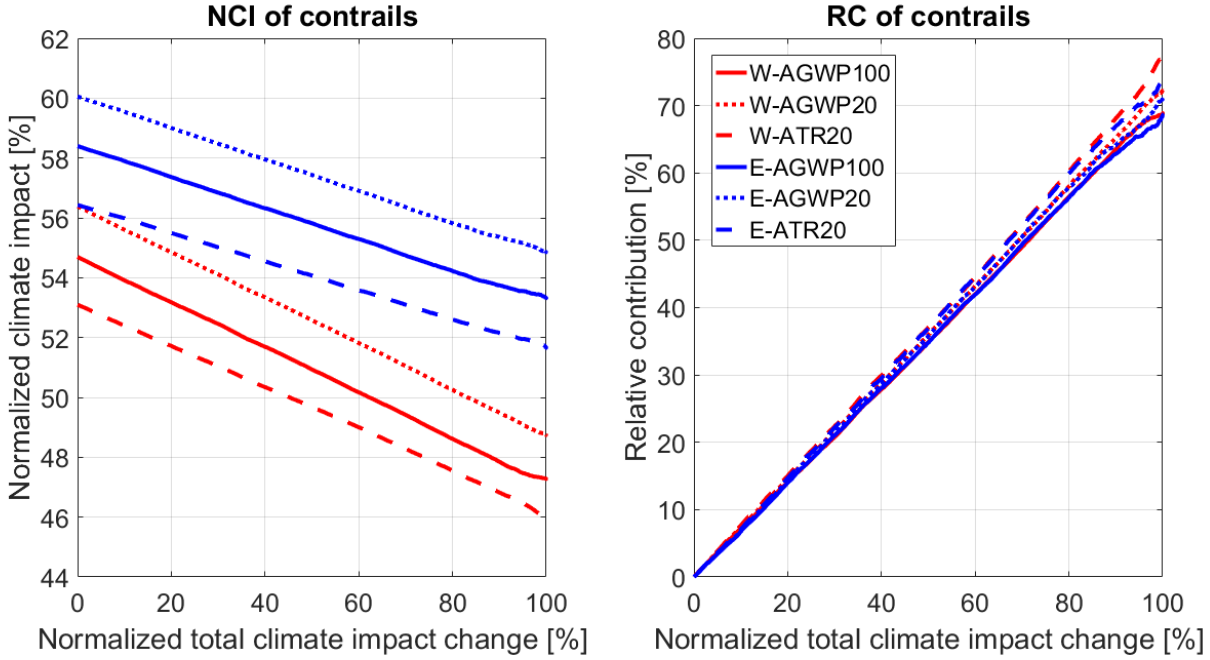

Figure 84. Comparison of contrails *NCI* and *RC* for Winter Pattern 3 and different flight directions and climate metrics.

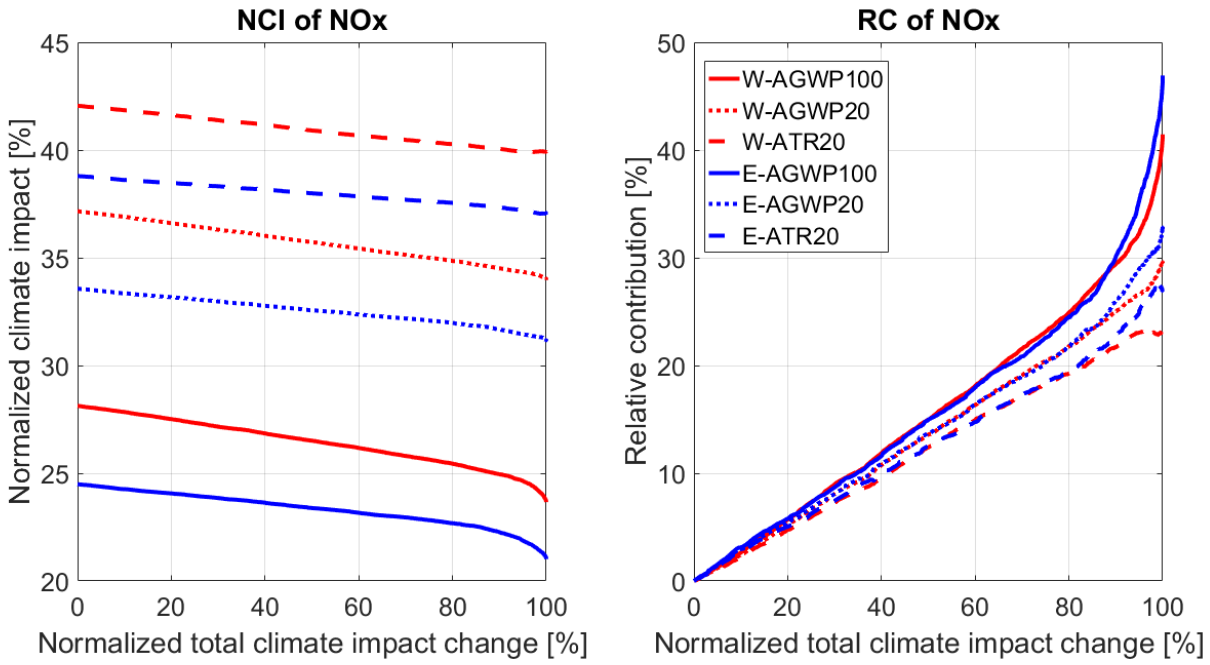

Figure 85. Comparison of NO_x *NCI* and *RC* for Winter Pattern 3 and different flight directions and climate metrics.

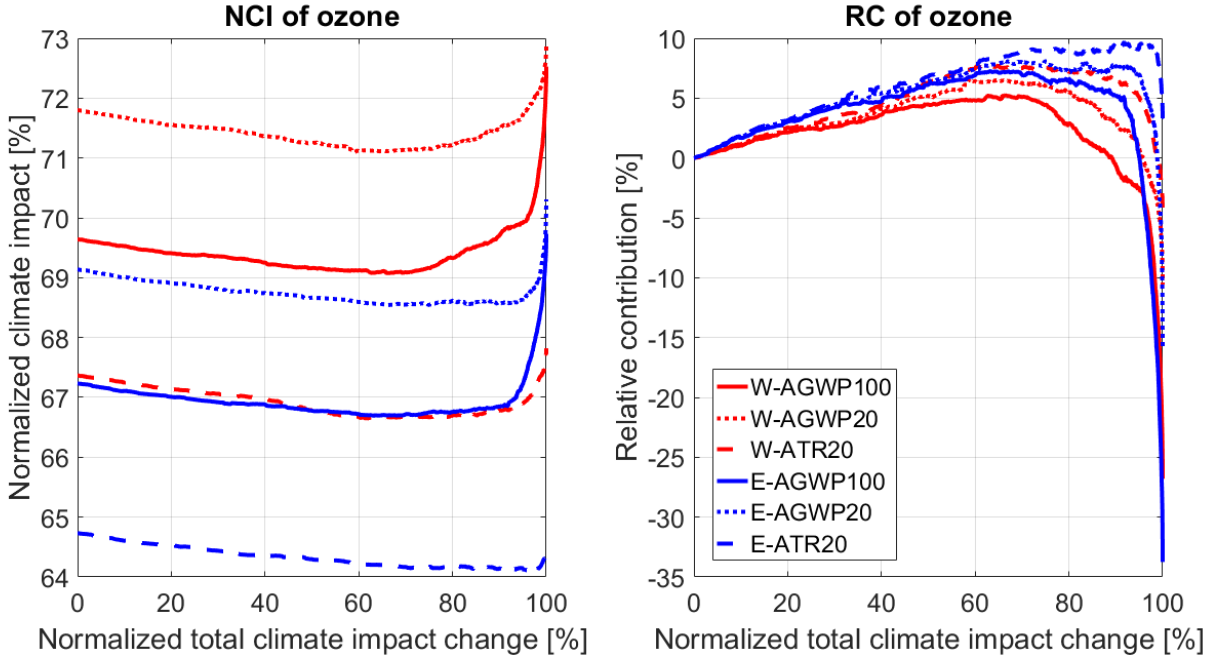

Figure 86. Comparison of ozone *NCI* and *RC* for Winter Pattern 3 and different flight directions and climate metrics.

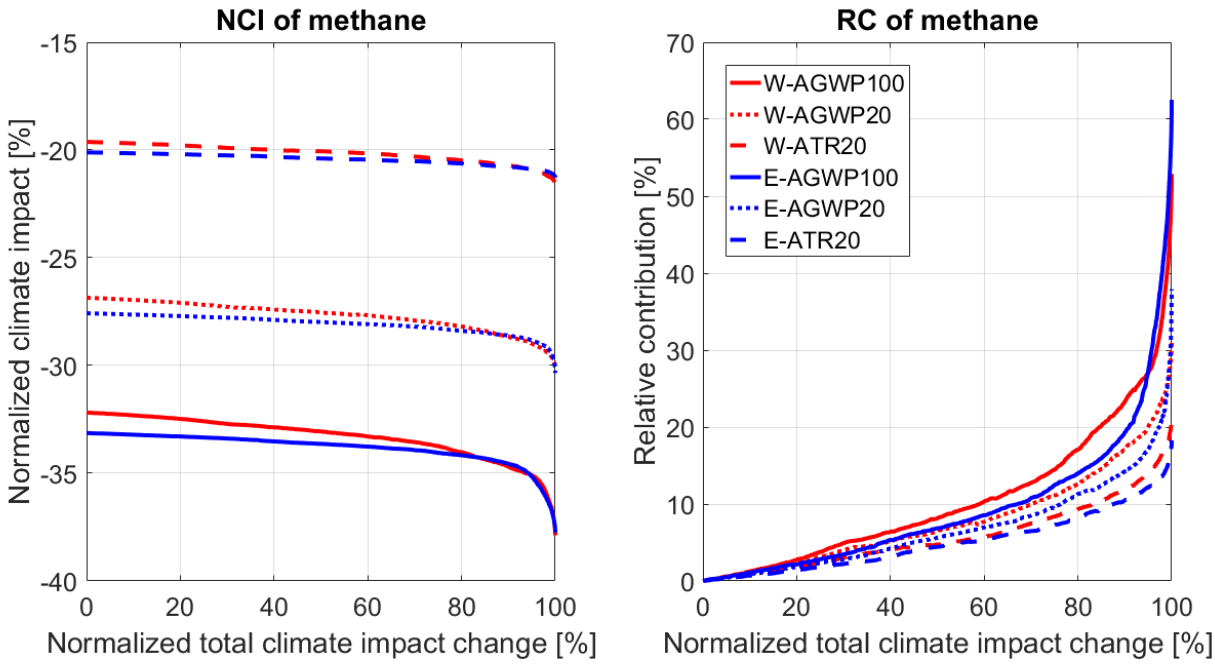

Figure 87. Comparison of methane *NCI* and *RC* for Winter Pattern 3 and different flight directions and climate metrics.

A.7. Winter Pattern 4

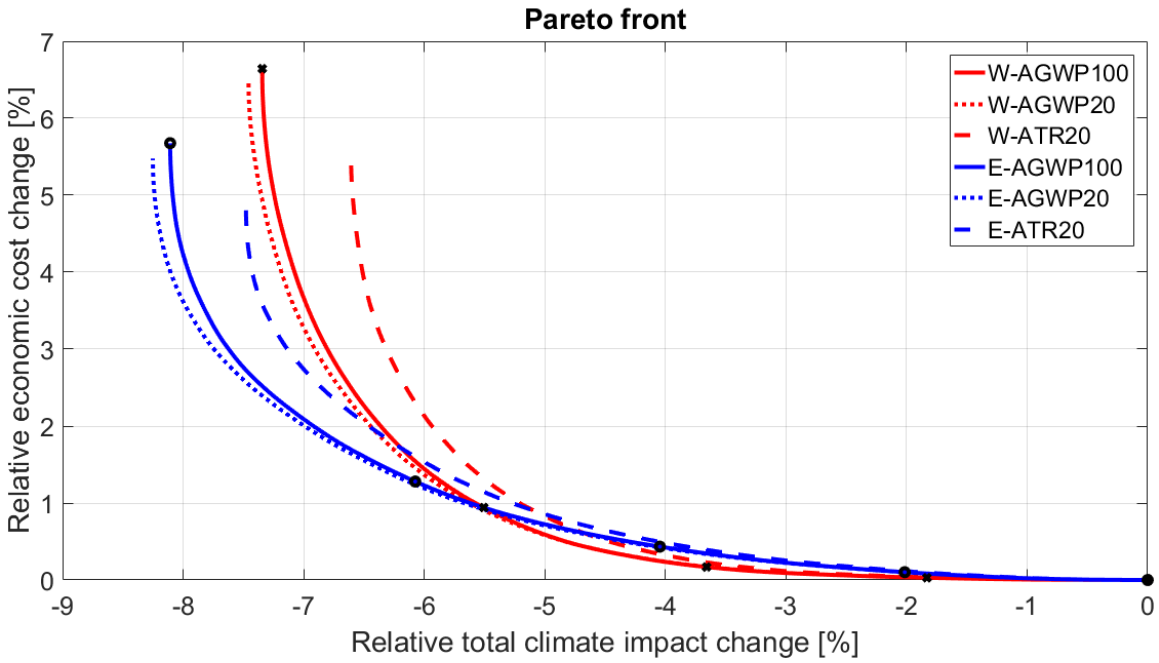

Figure 88. Comparison of Pareto Fronts for Winter Pattern 4 and different flight directions and climate metrics.

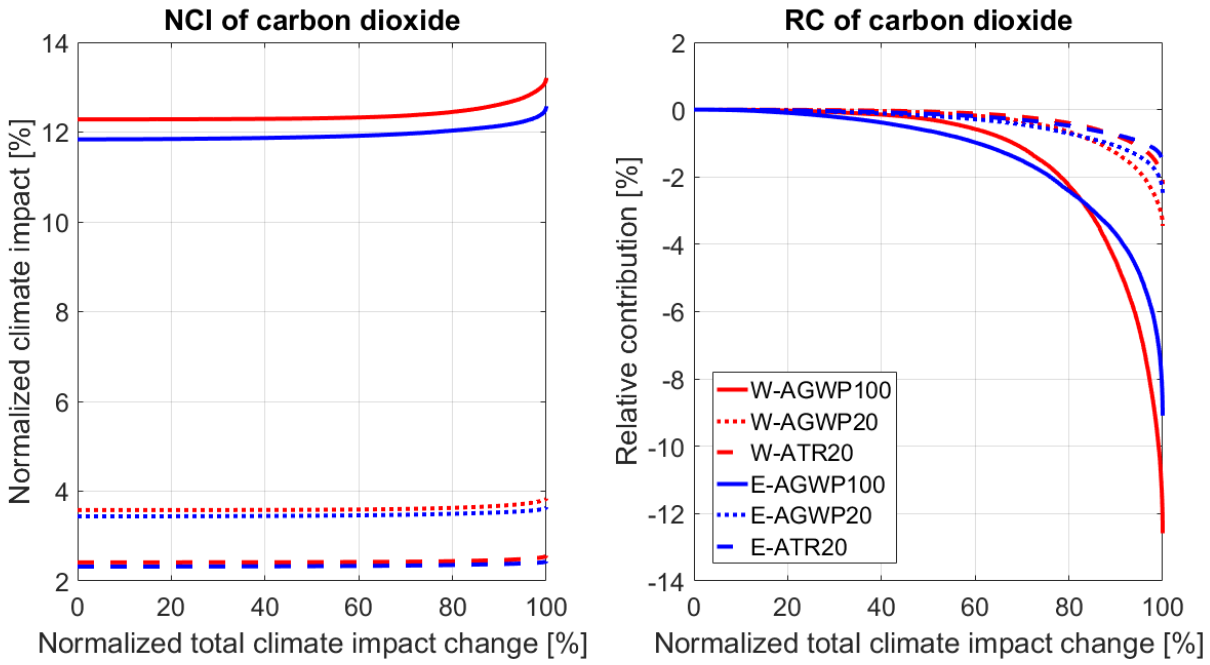

Figure 89. Comparison of carbon dioxide *NCI* and *RC* for Winter Pattern 4 and different flight directions and climate metrics.

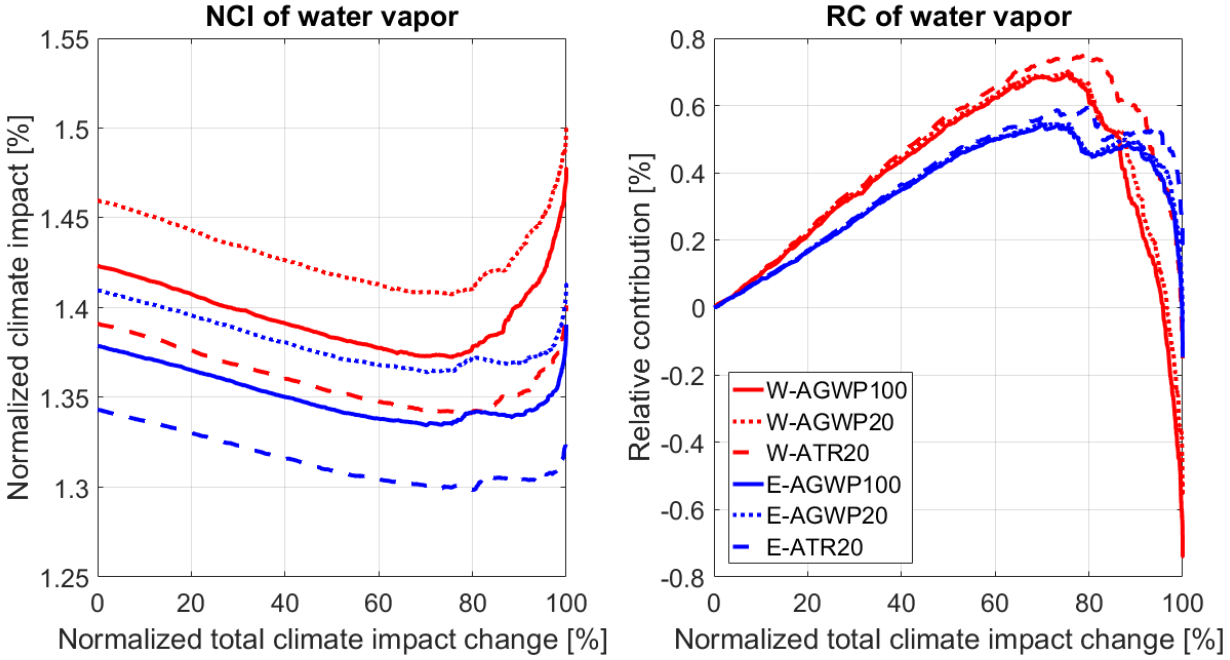

Figure 90. Comparison of water vapor *NCI* and *RC* for Winter Pattern 4 and different flight directions and climate metrics.

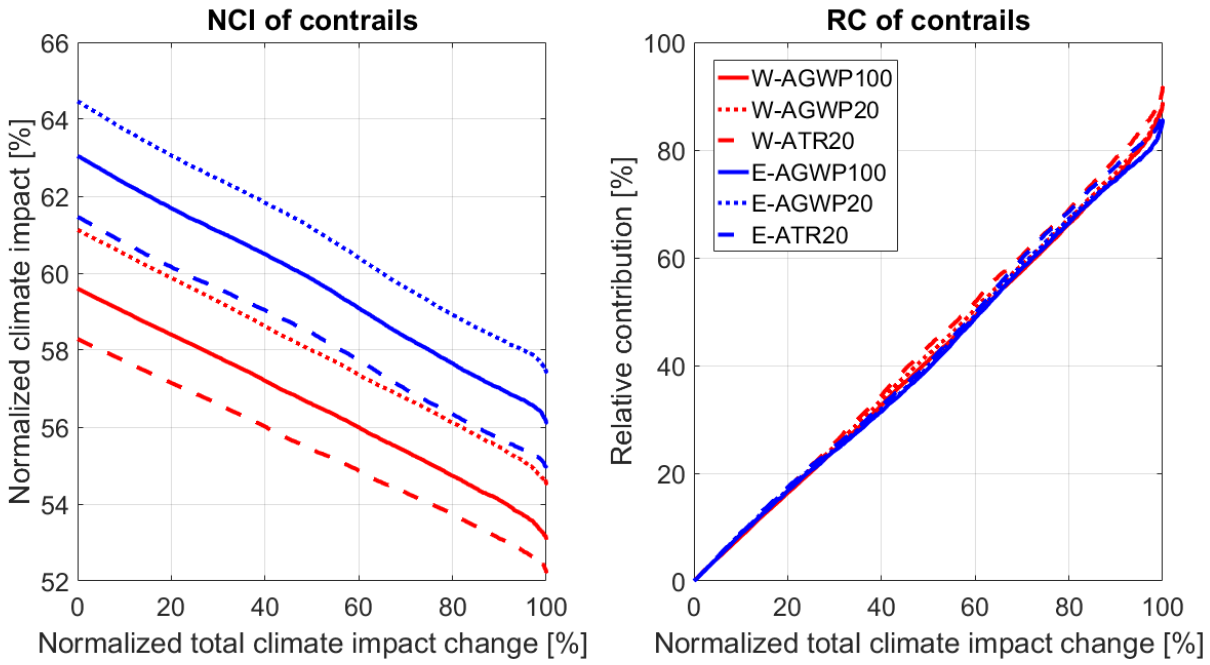

Figure 91. Comparison of contrails *NCI* and *RC* for Winter Pattern 4 and different flight directions and climate metrics.

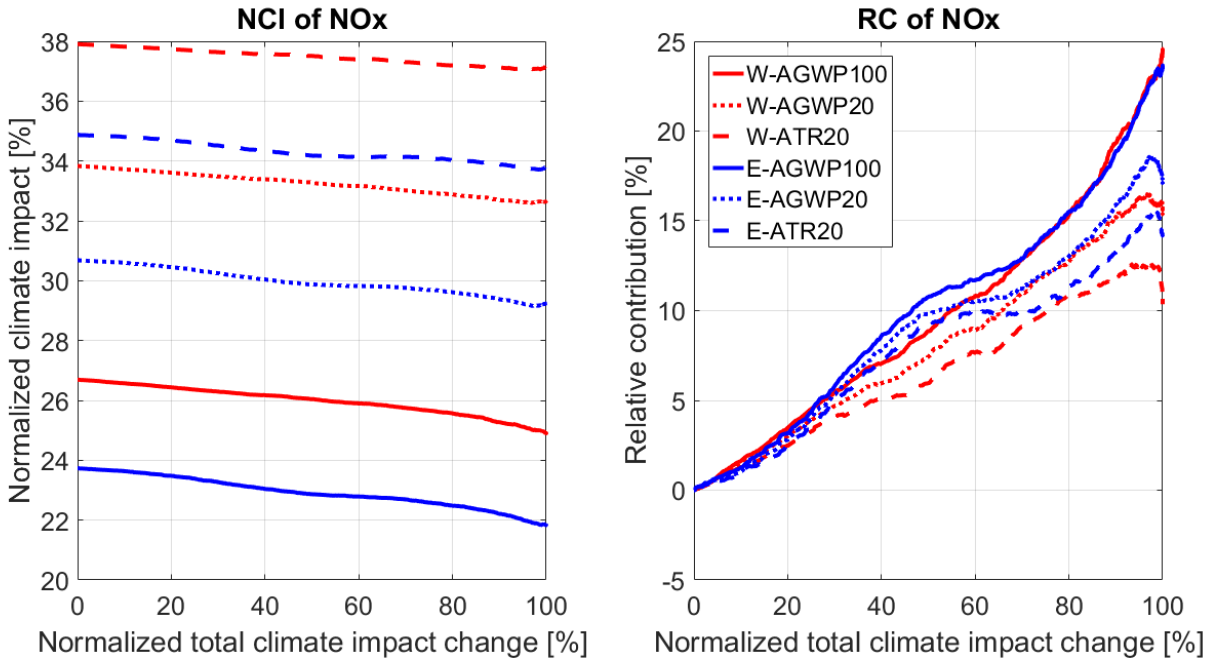

Figure 92. Comparison of NO_x *NCI* and *RC* for Winter Pattern 4 and different flight directions and climate metrics.

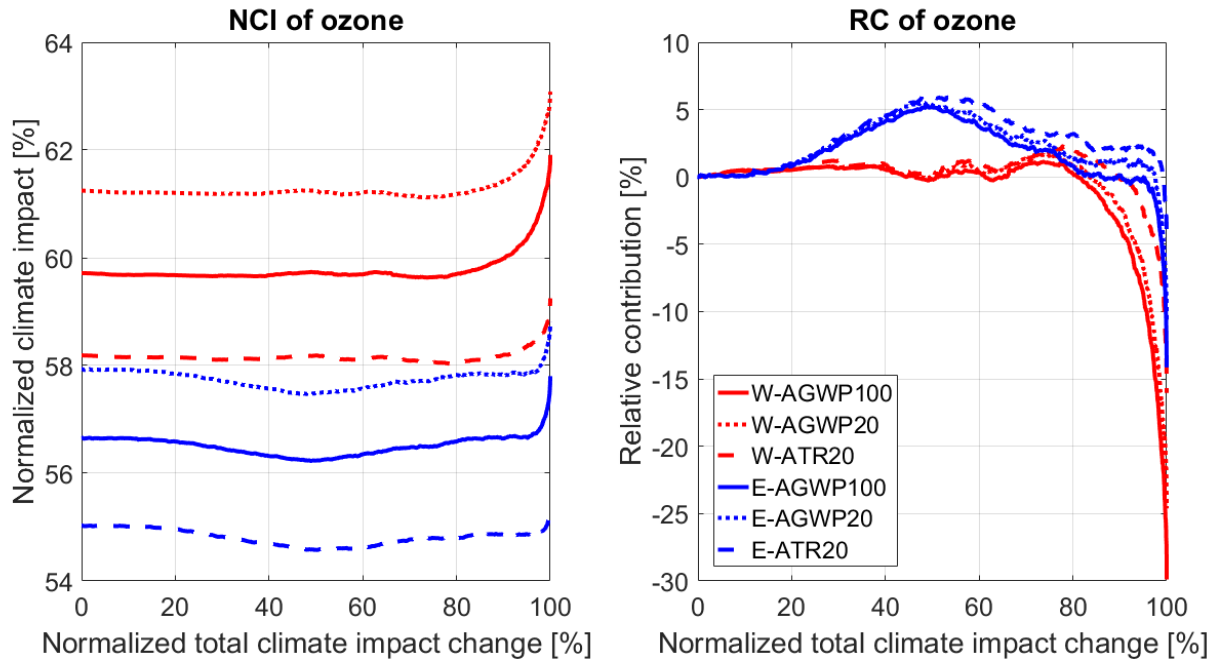

Figure 93. Comparison of ozone *NCI* and *RC* for Winter Pattern 4 and different flight directions and climate metrics.

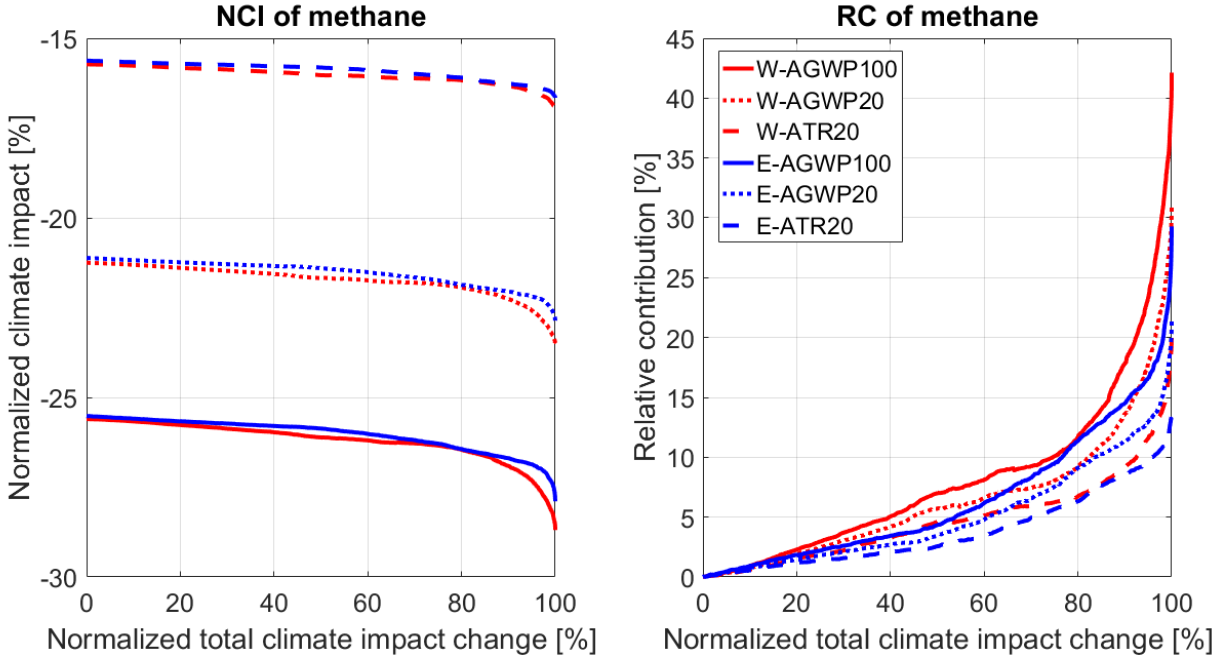

Figure 94. Comparison of methane *NCI* and *RC* for Winter Pattern 4 and different flight directions and climate metrics.

A.8. Winter Pattern 5

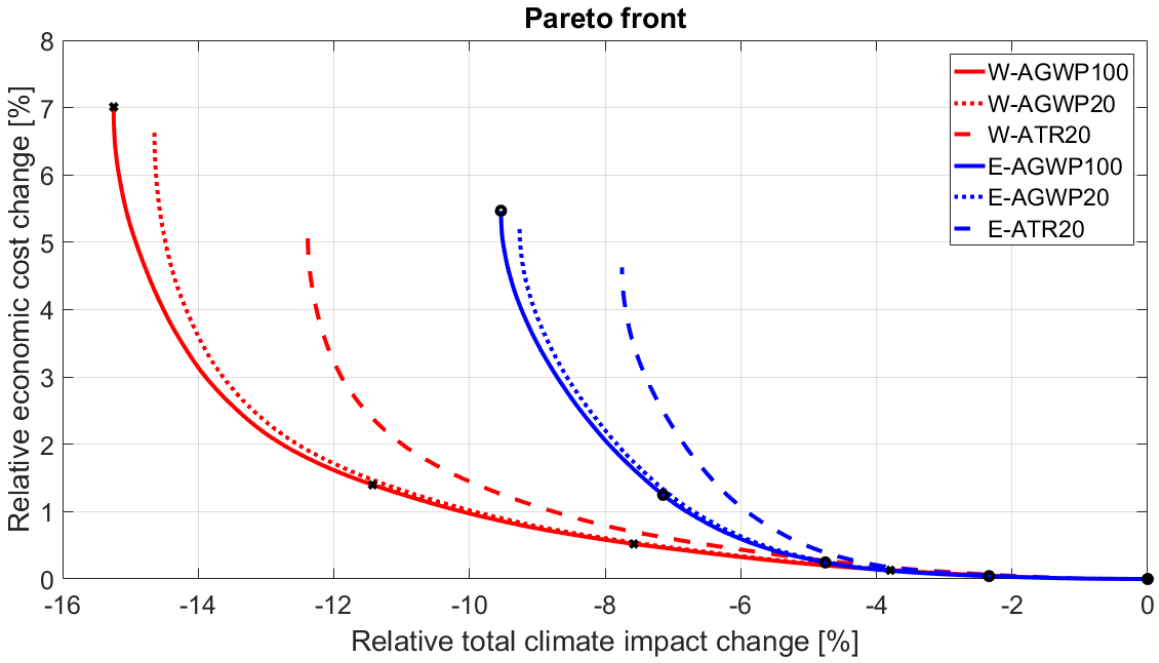

Figure 95. Comparison of Pareto Fronts for Winter Pattern 5 and different flight directions and climate metrics.

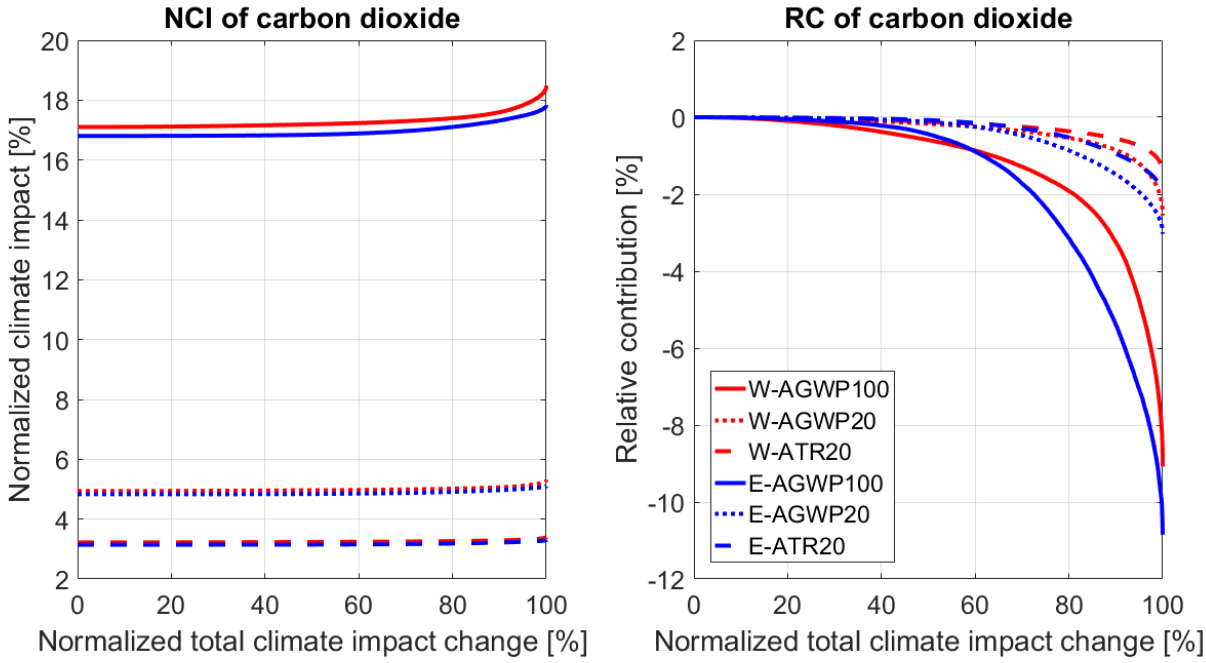

Figure 96. Comparison of carbon dioxide *NCI* and *RC* for Winter Pattern 5 and different flight directions and climate metrics.

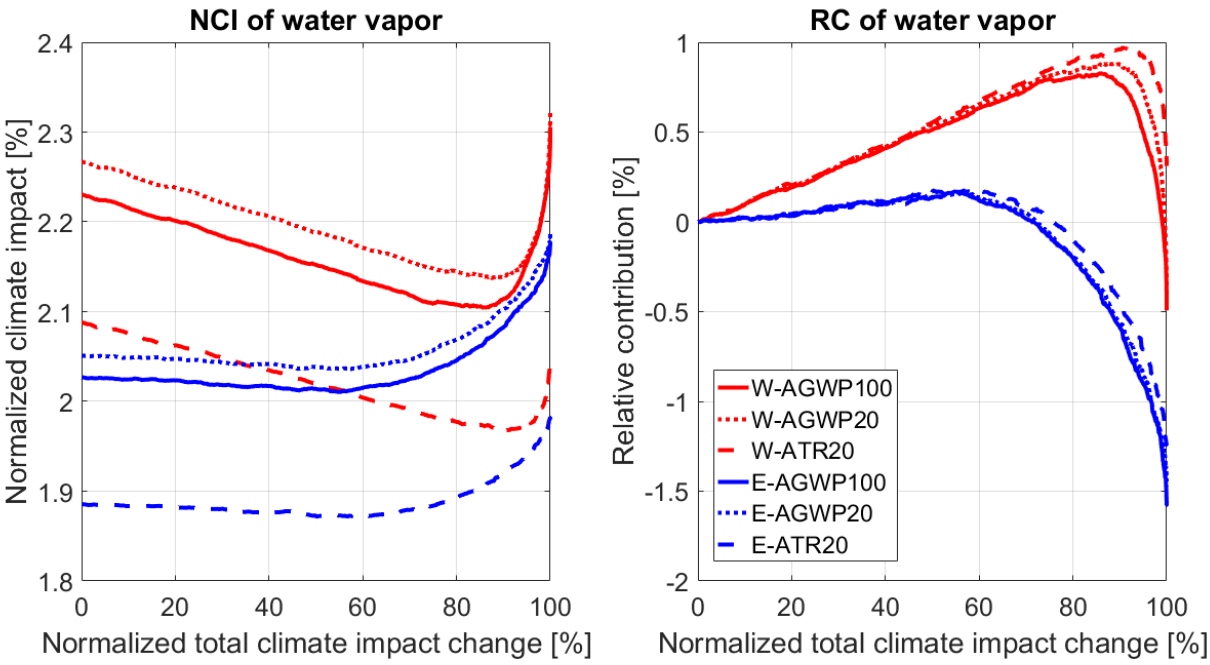

Figure 97. Comparison of water vapor *NCI* and *RC* for Winter Pattern 5 and different flight directions and climate metrics.

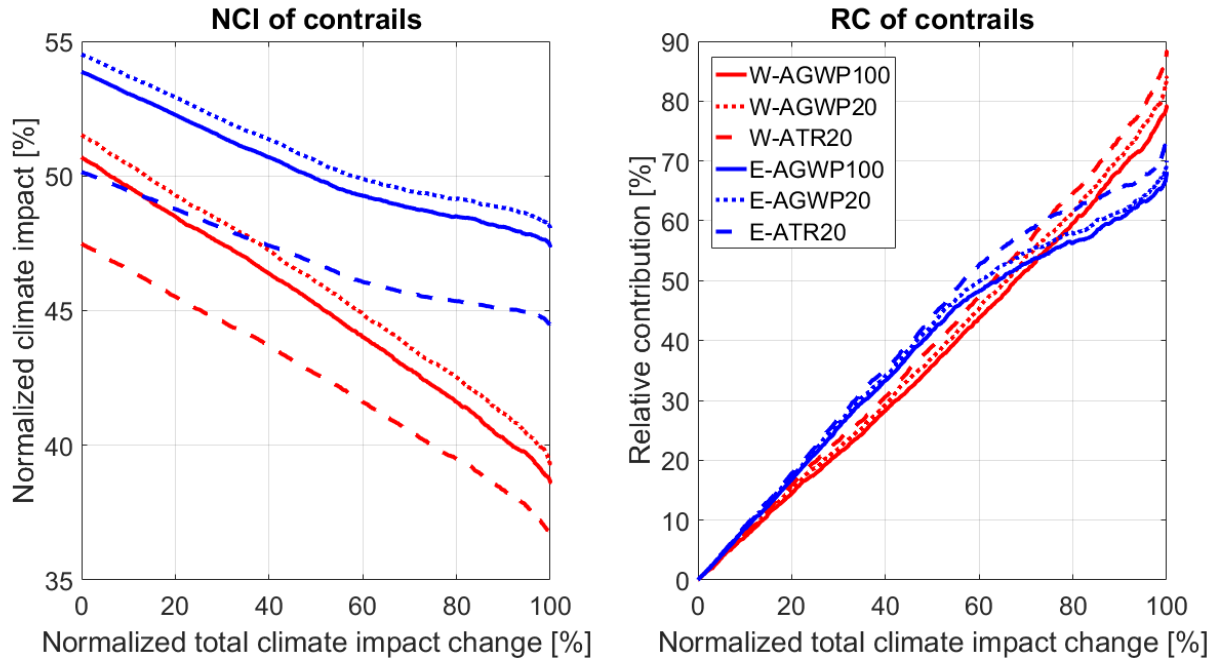

Figure 98. Comparison of contrails *NCI* and *RC* for Winter Pattern 5 and different flight directions and climate metrics.

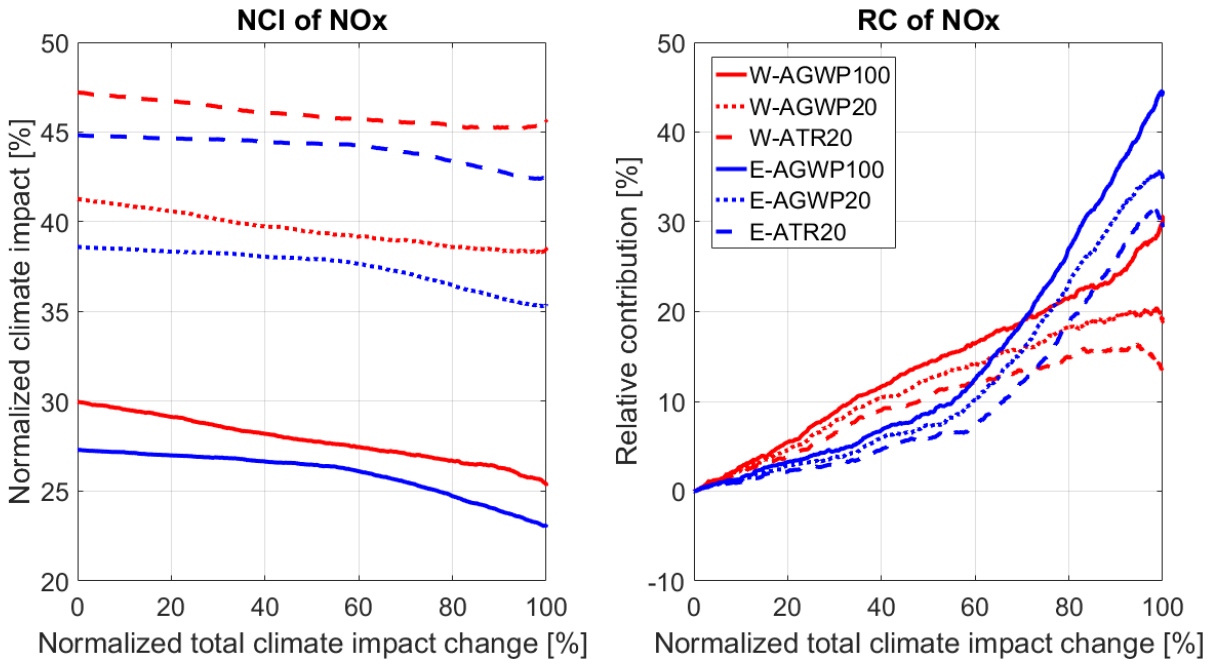

Figure 99. Comparison of NO_x *NCI* and *RC* for Winter Pattern 5 and different flight directions and climate metrics.

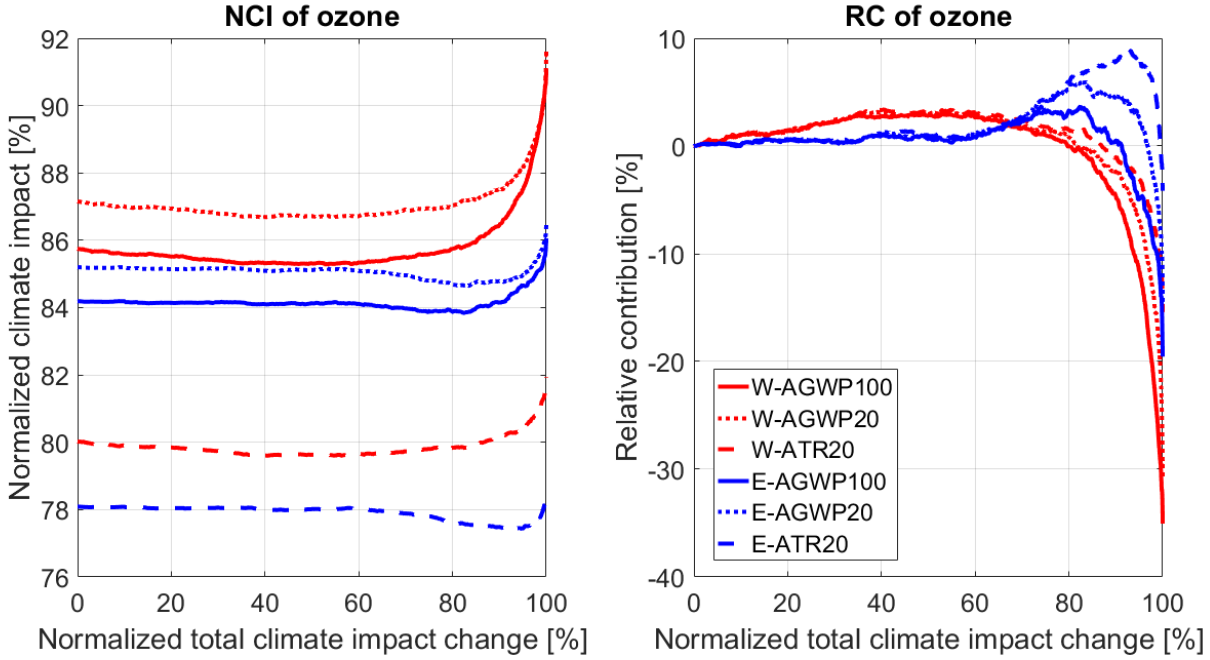

Figure 100. Comparison of ozone *NCI* and *RC* for Winter Pattern 5 and different flight directions and climate metrics.

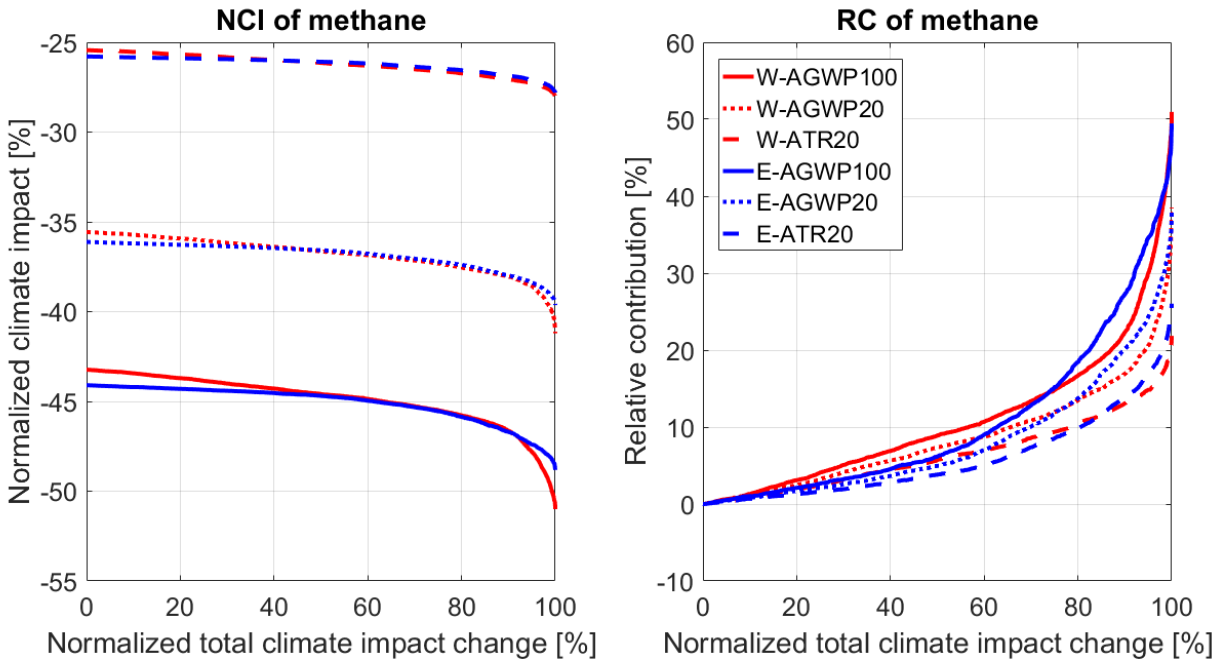

Figure 101. Comparison of methane *NCI* and *RC* for Winter Pattern 5 and different flight directions and climate metrics.

B

Annex B

A complete list with the figures comparing different values of *Normalized Climate Impact* and *Relative Contribution* for different flight directions and weather patterns is presented in this section. The climate metric is AGWP100. The different curves represent several values of *NTCIC*. These values are 0% (red), 25% (magenta), 50% (blue), 75% (black), 100% (green).

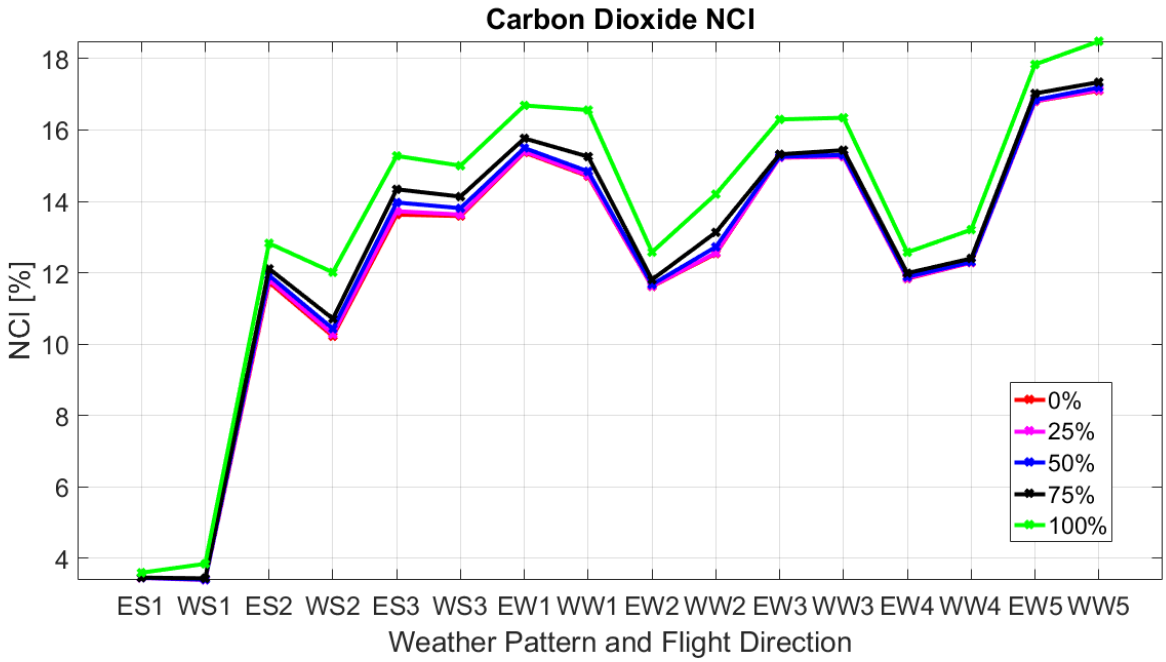

Figure 102. Comparison of carbon dioxide *NCI* for AGWP100 climate metric and different flight directions and weather patterns. The *NTCIC* values presented are 0%, 25%, 50%, 75%, and 100%.

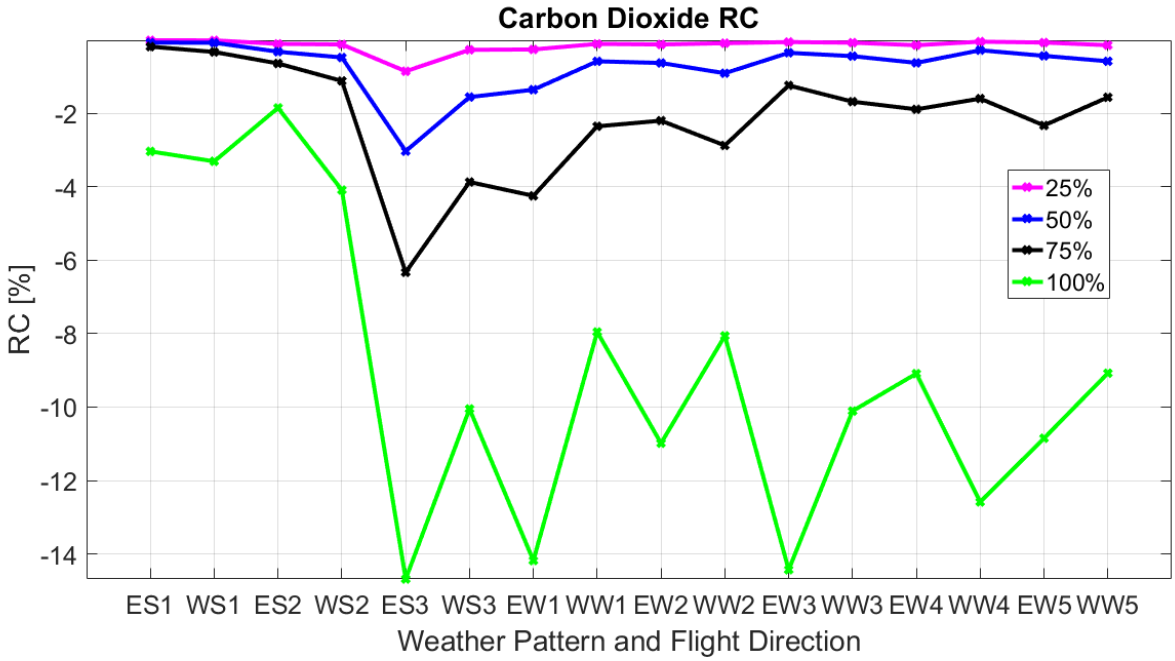

Figure 103. Comparison of carbon dioxide *RC* for AGWP100 climate metric and different flight directions and weather patterns. The *NTCIC* values presented are 25%, 50%, 75%, and 100%.

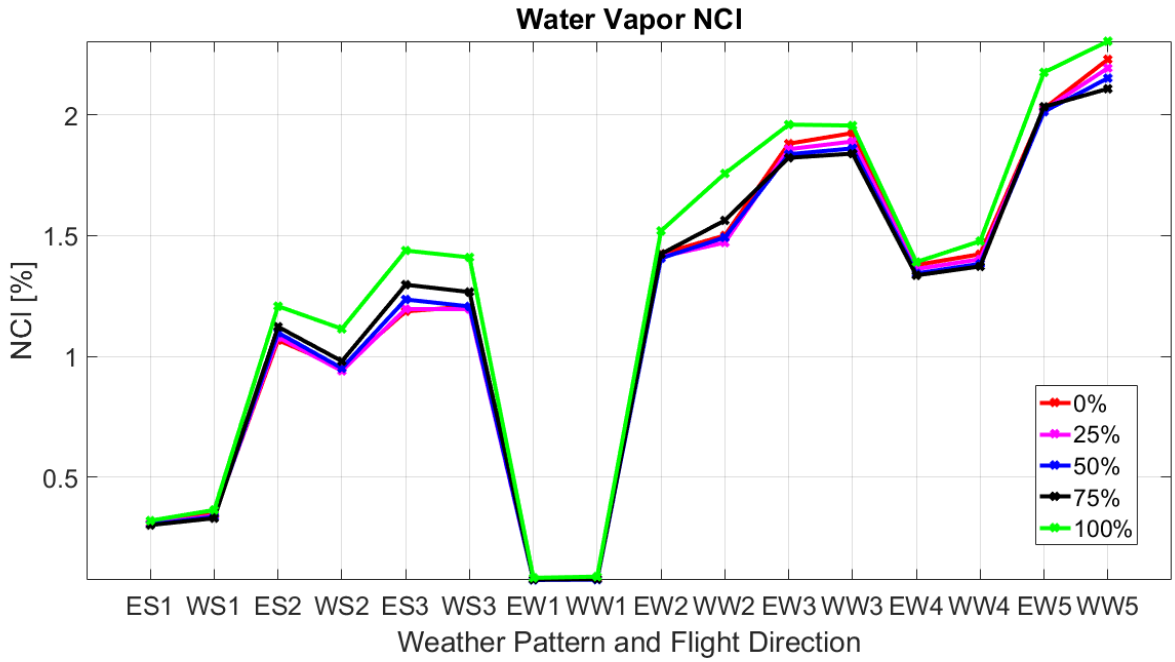

Figure 104. Comparison of water vapor *NCI* for AGWP100 climate metric and different flight directions and weather patterns. The *NTCIC* values presented are 0%, 25%, 50%, 75%, and 100%.

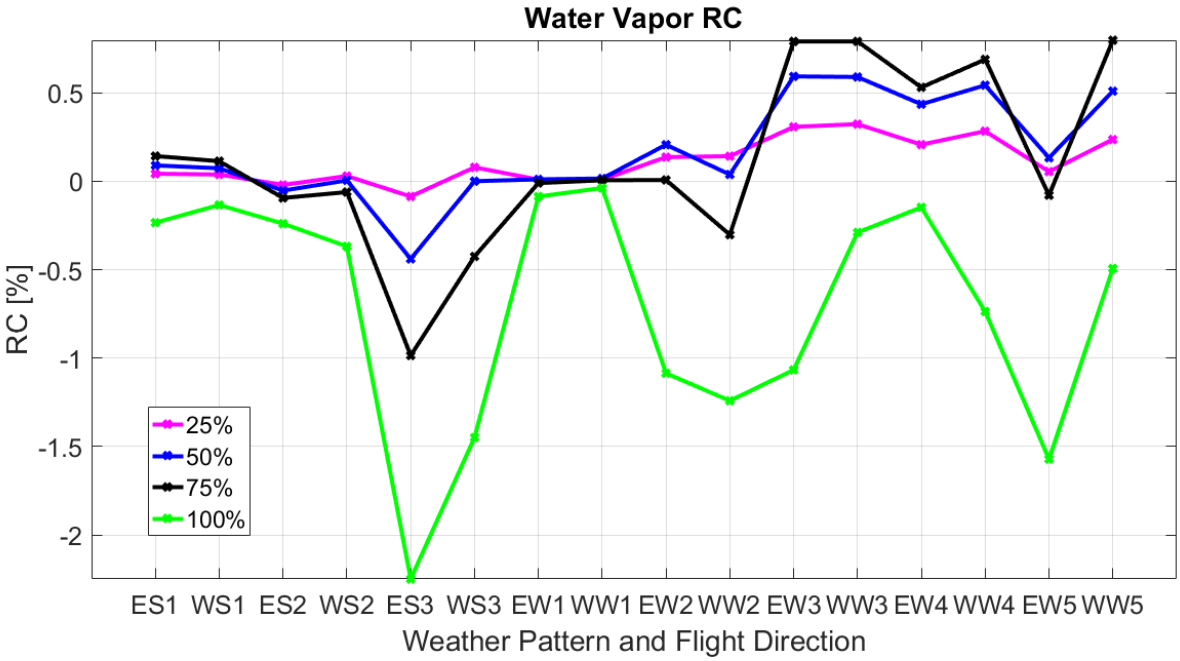

Figure 105. Comparison of water vapor *RC* for AGWP100 climate metric and different flight directions and weather patterns. The *NTCIC* values presented are 25%, 50%, 75%, and 100%.

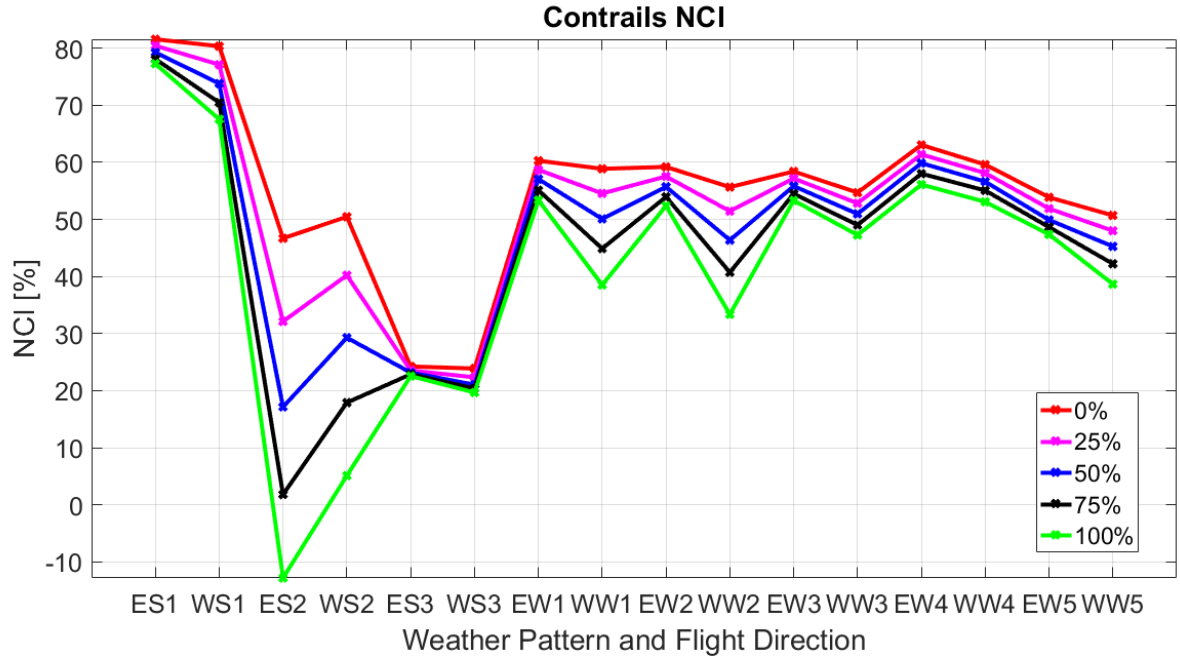

Figure 106. Comparison of contrails *NCI* for AGWP100 climate metric and different flight directions and weather patterns. The *NTCIC* values presented are 0%, 25%, 50%, 75%, and 100%.

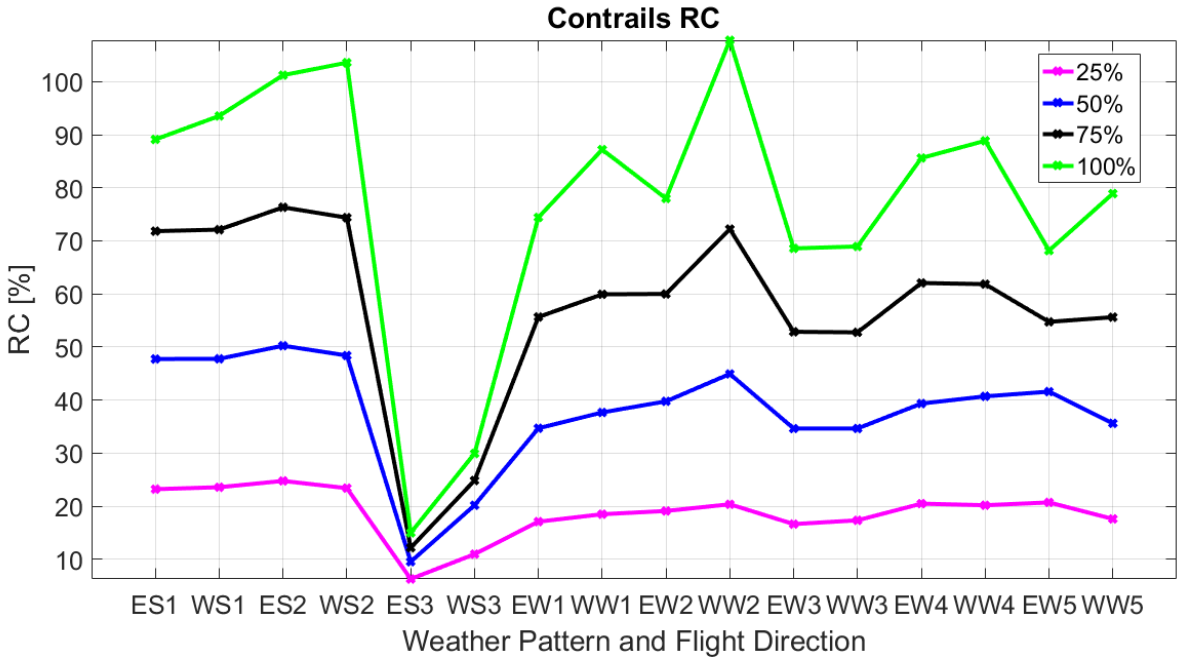

Figure 107. Comparison of contrails *RC* for AGWP100 climate metric and different flight directions and weather patterns. The *NTCIC* values presented are 25%, 50%, 75%, and 100%.

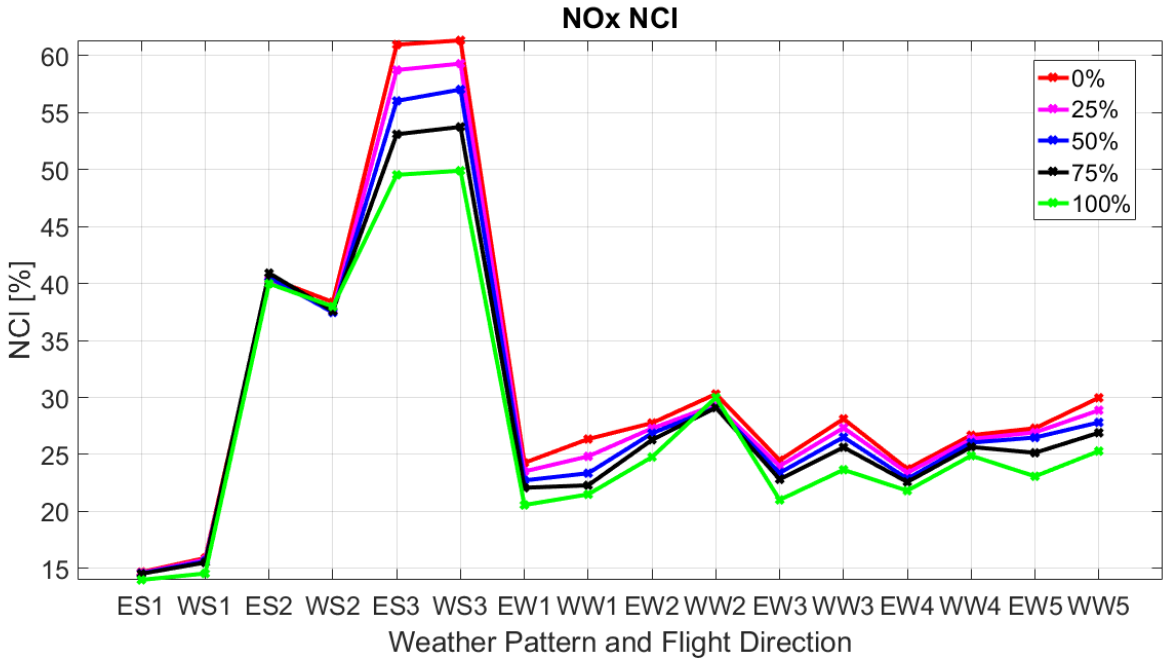

Figure 108. Comparison of NO_x *NCI* for AGWP100 climate metric and different flight directions and weather patterns. The *NTCIC* values presented are 0%, 25%, 50%, 75%, and 100%.

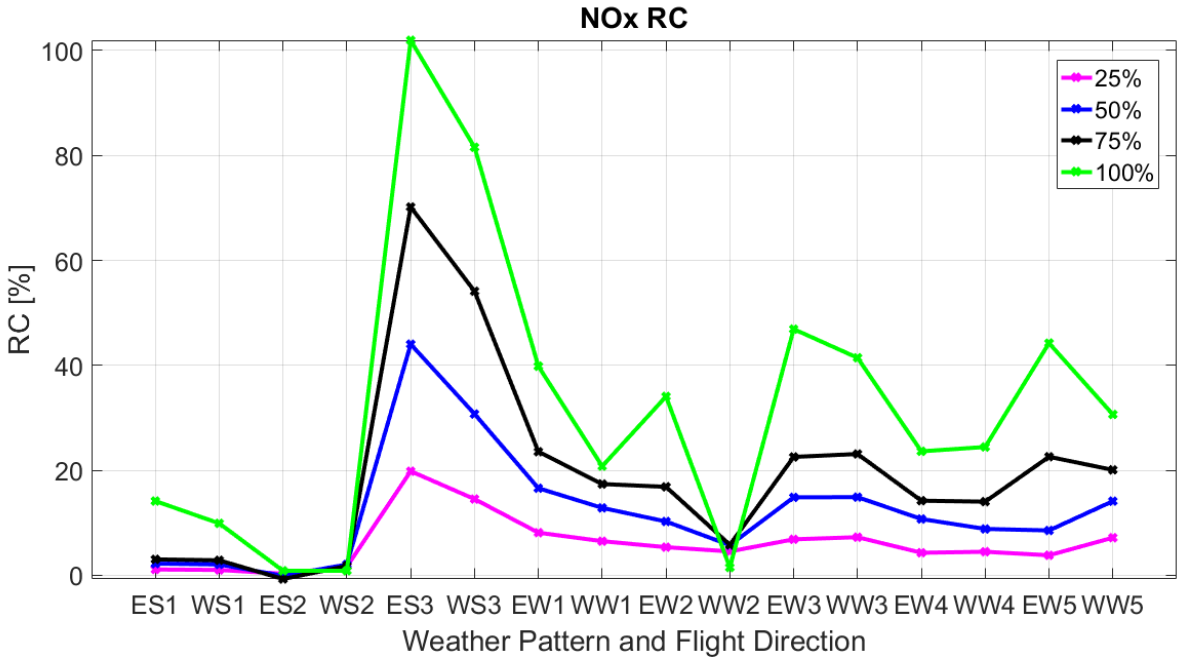

Figure 109. Comparison of NO_x *RC* for AGWP100 climate metric and different flight directions and weather patterns. The *NTCIC* values presented are 25%, 50%, 75%, and 100%.

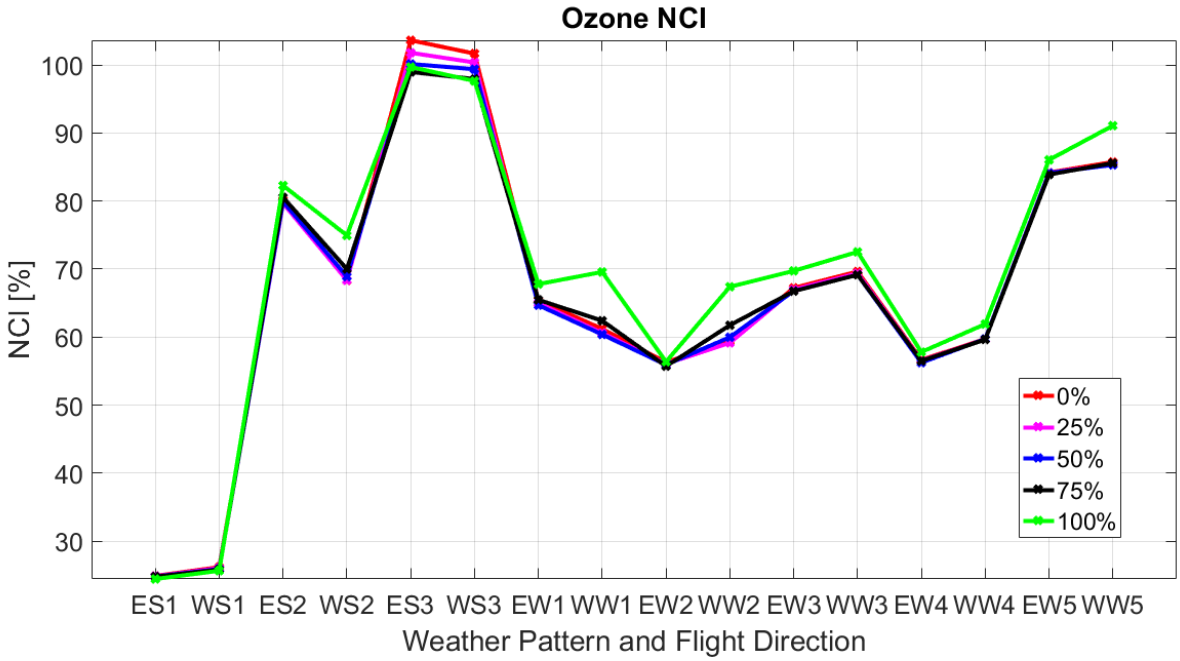

Figure 110. Comparison of ozone *NCI* for AGWP100 climate metric and different flight directions and weather patterns. The *NTCIC* values presented are 0%, 25%, 50%, 75%, and 100%.

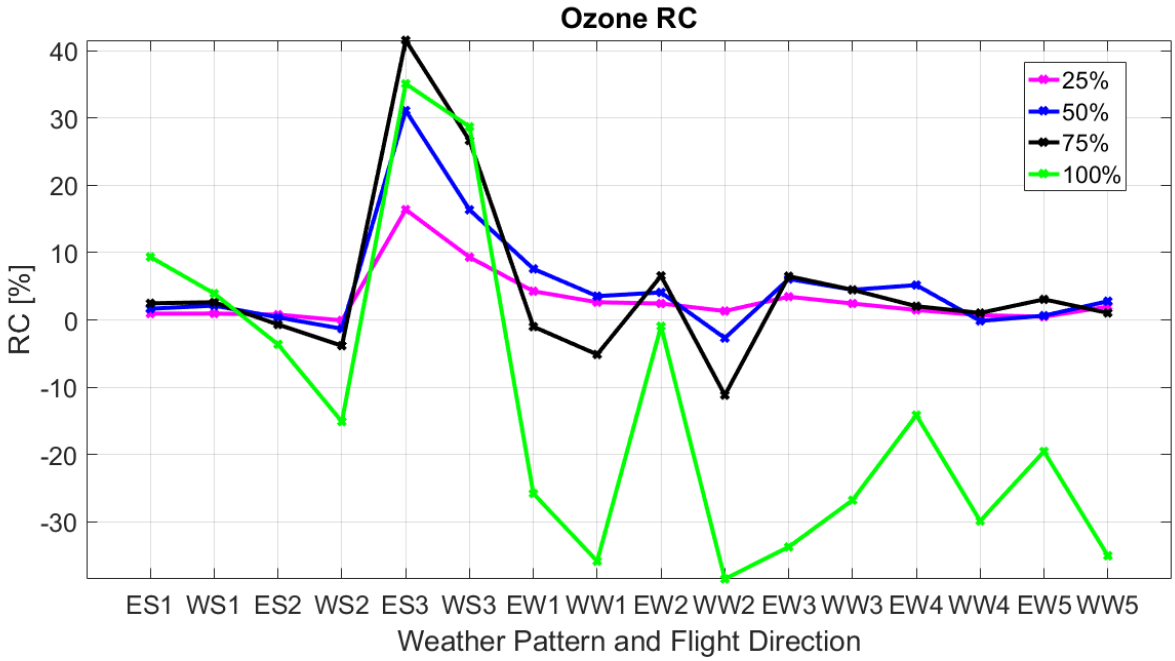

Figure 111. Comparison of ozone *RC* for AGWP100 climate metric and different flight directions and weather patterns. The *NTCIC* values presented are 25%, 50%, 75%, and 100%.

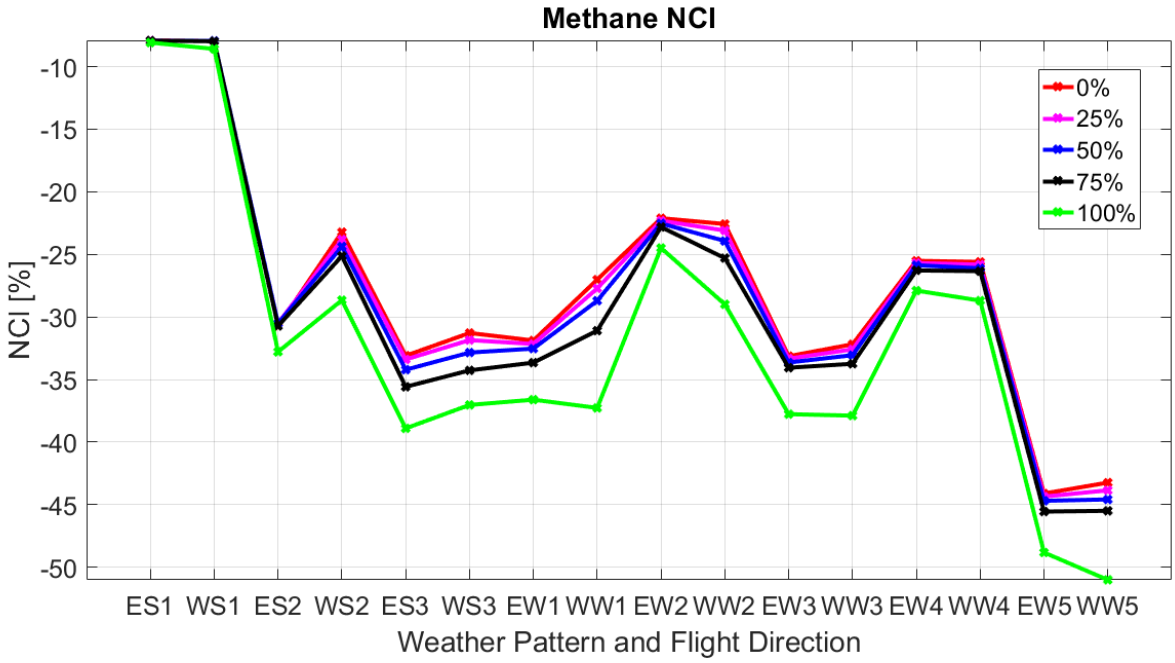

Figure 112. Comparison of methane *NCI* for AGWP100 climate metric and different flight directions and weather patterns. The *NTCIC* values presented are 0%, 25%, 50%, 75%, and 100%.

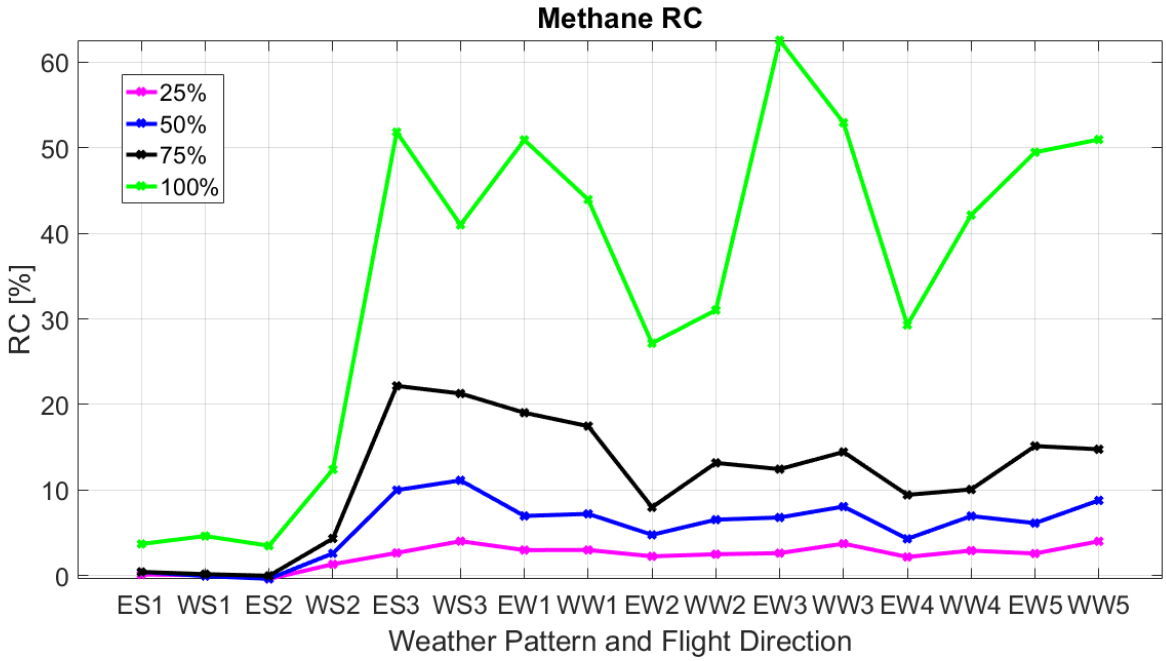

Figure 113. Comparison of methane *RC* for AGWP100 climate metric and different flight directions and weather patterns. The *NTCIC* values presented are 25%, 50%, 75%, and 100%.

C

Annex C

Here is presented a complete list with the Probability Density Functions and the values of *Relative Climate Impact Change* obtained in the individual flight analysis. The presented climate metric is AGWP100. The plot on top shows the probability density function of the climate impact cause by each climate parameter (contrails, NO_x, ozone, and methane) for 5 different values of *Normalized Total Climate Impact Change*. These values are 0% (red line with asterisks), 25% (magenta line with triangles), 50% (blue line with circles), 75% (black line with squares), and 100% (green line). Moreover, on the horizontal axis the climate impact mean value is represented with the same code of color and shape as the PDF curve. On the other plot, the *RCIC* is shown for each flight for different values of *NTCIC*. These values are 25% (magenta triangles), 50% (blue circles), 75% (black squares), and 100% (green crosses). These codes of colors and shapes will be used on all representations of this type.

C.1. Summer Pattern 1 – Eastbound

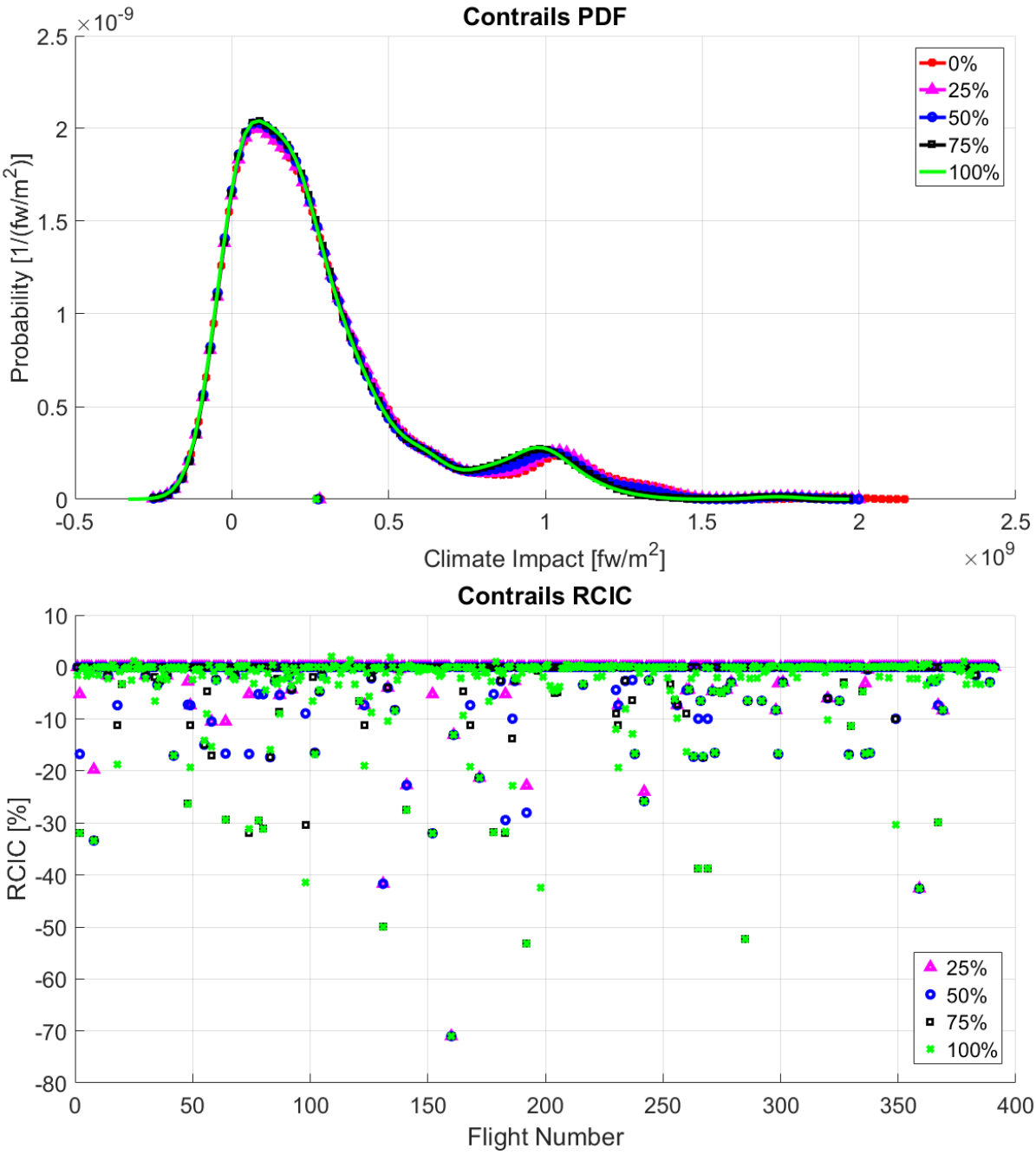

Figure 114. Probability Density Function and *RCIC* of contrails for SP1-Eastbound-AGWP100 case. The different curves and points represent the values for 0%, 25%, 50%, 75% and 100% of *NTCIC*.

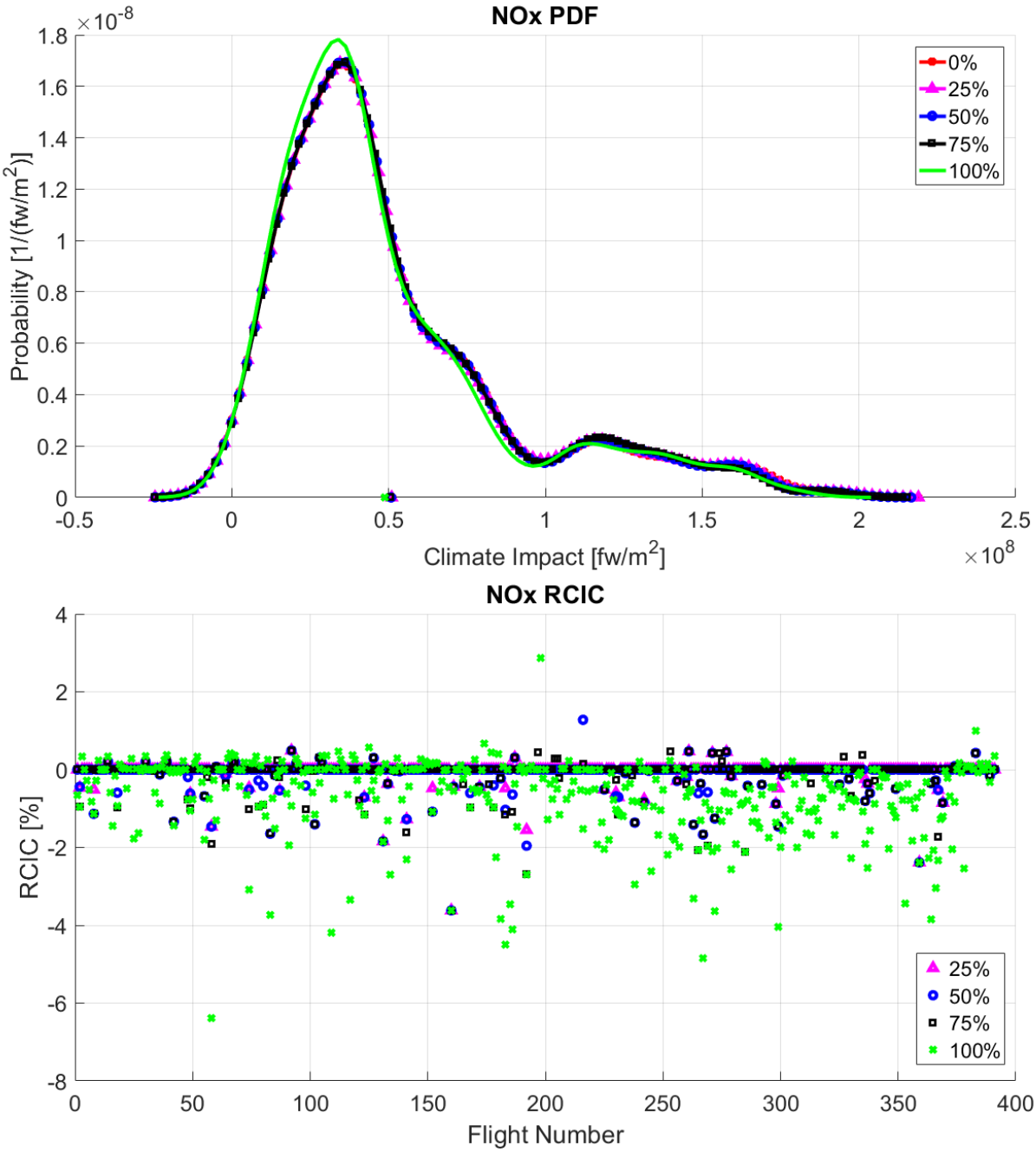

Figure 115. Probability Density Function and *RCIC* of NO_x for SP1-Eastbound-AGWP100 case. The different curves and points represent the values for 0%, 25%, 50%, 75% and 100% of *NTCIC*.

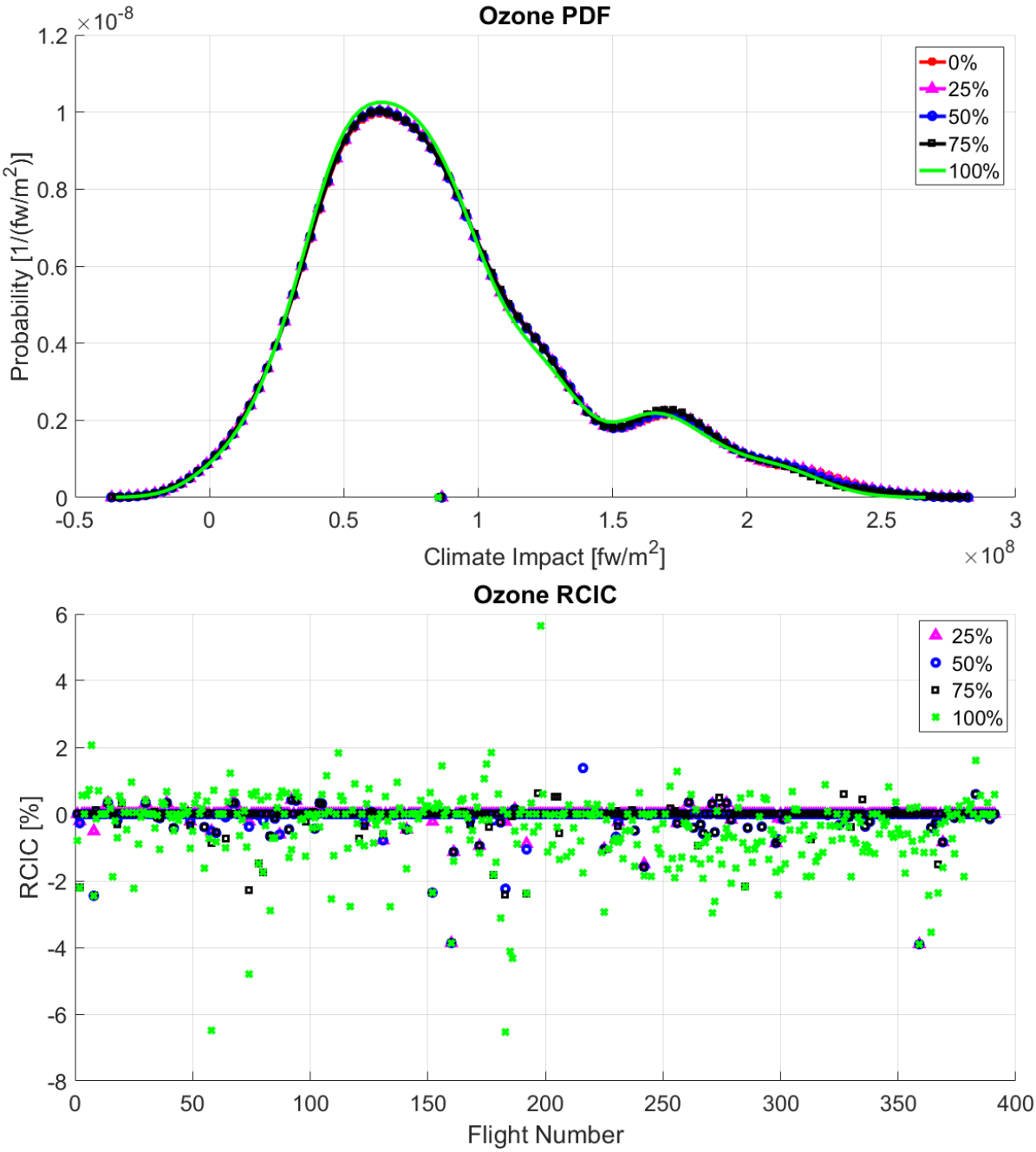

Figure 116. Probability Density Function and *RCIC* of ozone for SP1-Eastbound-AGWP100 case. The different curves and points represent the values for 0%, 25%, 50%, 75% and 100% of *NTCIC*.

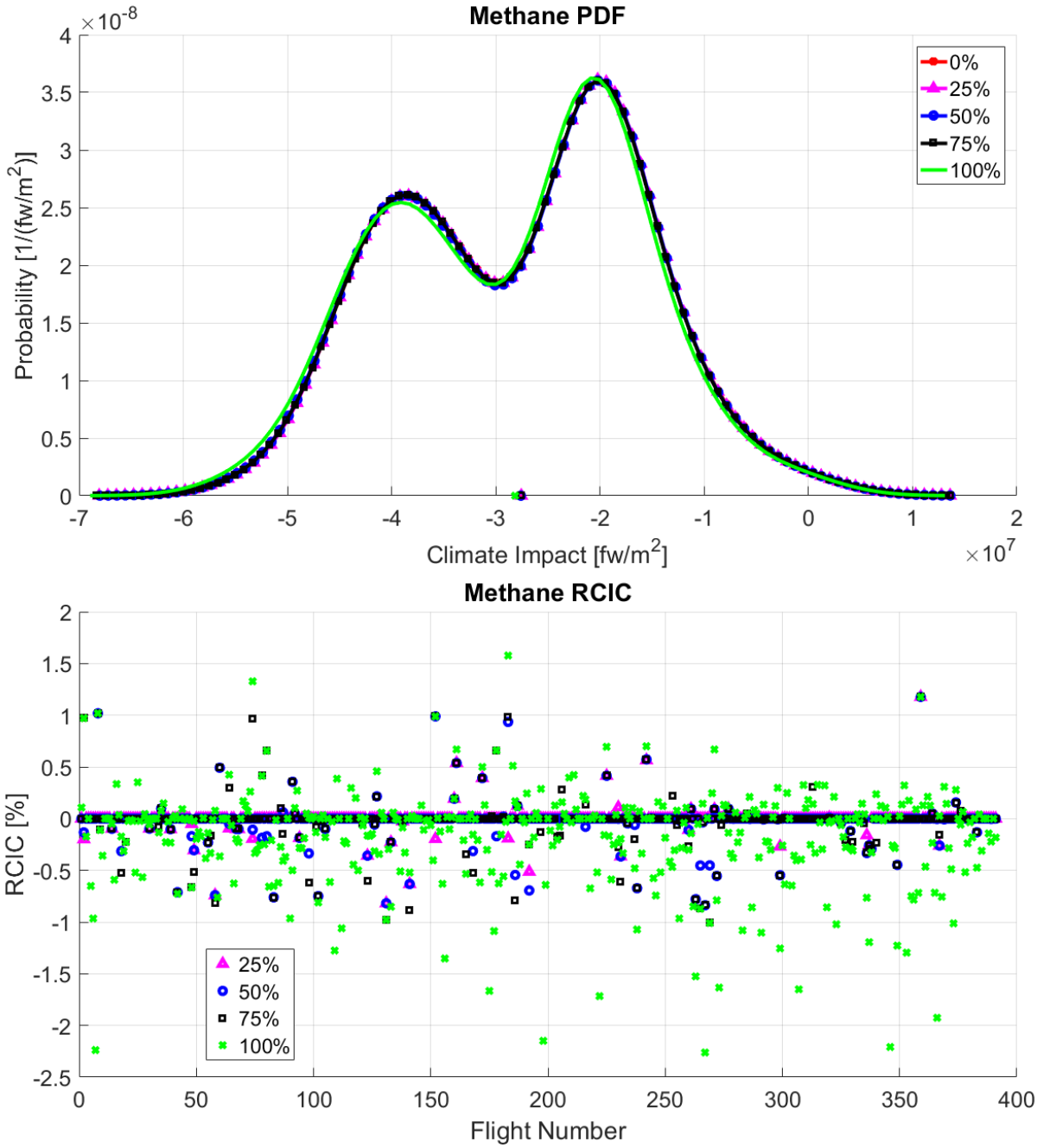

Figure 117. Probability Density Function and *RCIC* of methane for SP1-Eastbound-AGWP100 case. The different curves and points represent the values for 0%, 25%, 50%, 75% and 100% of *NTCIC*.

C.2. Summer Pattern 1 – Westbound

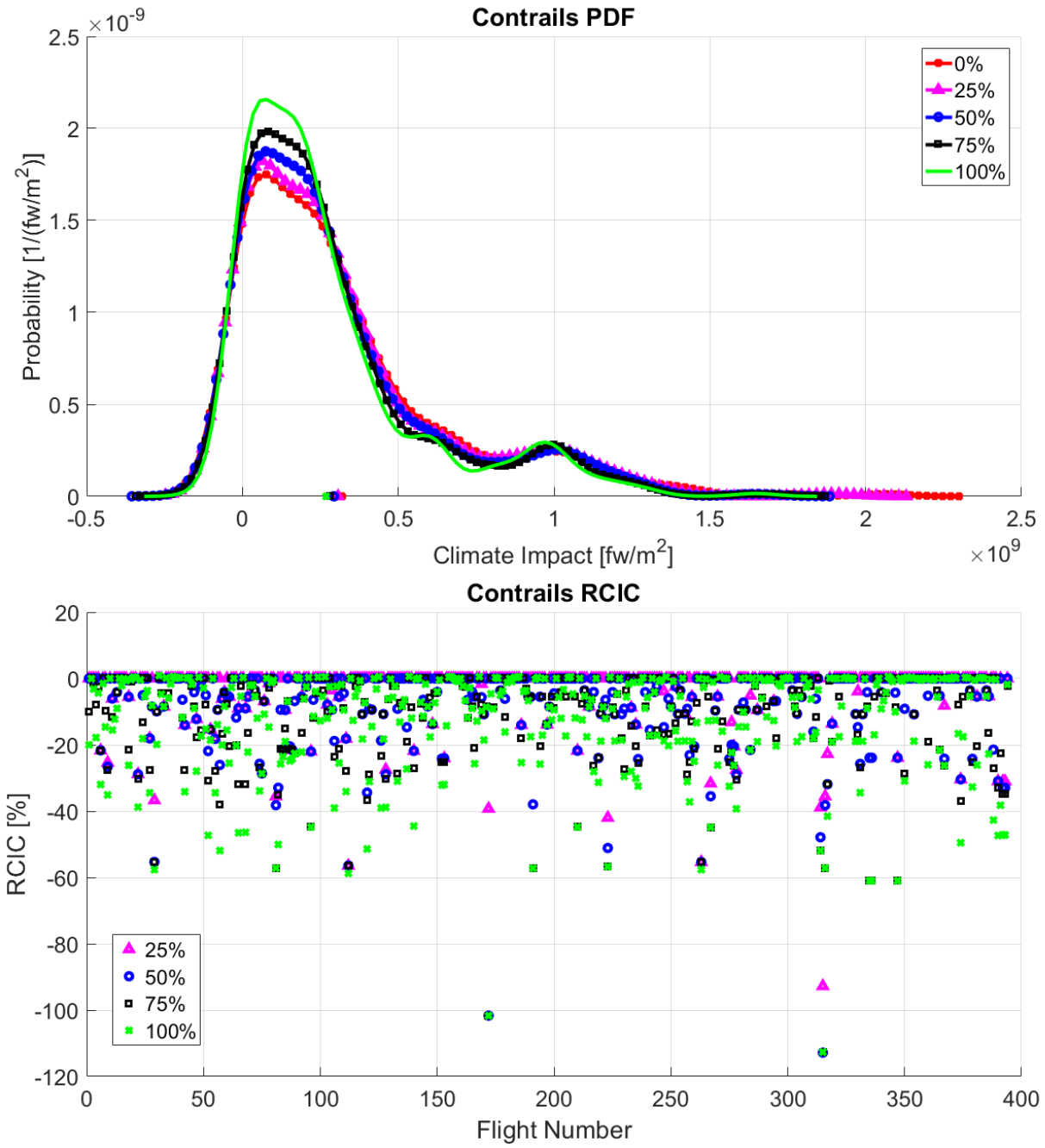

Figure 118. Probability Density Function and *RCIC* of contrails for SP1-Westbound-AGWP100 case. The different curves and points represent the values for 0%, 25%, 50%, 75% and 100% of *NTCIC*.

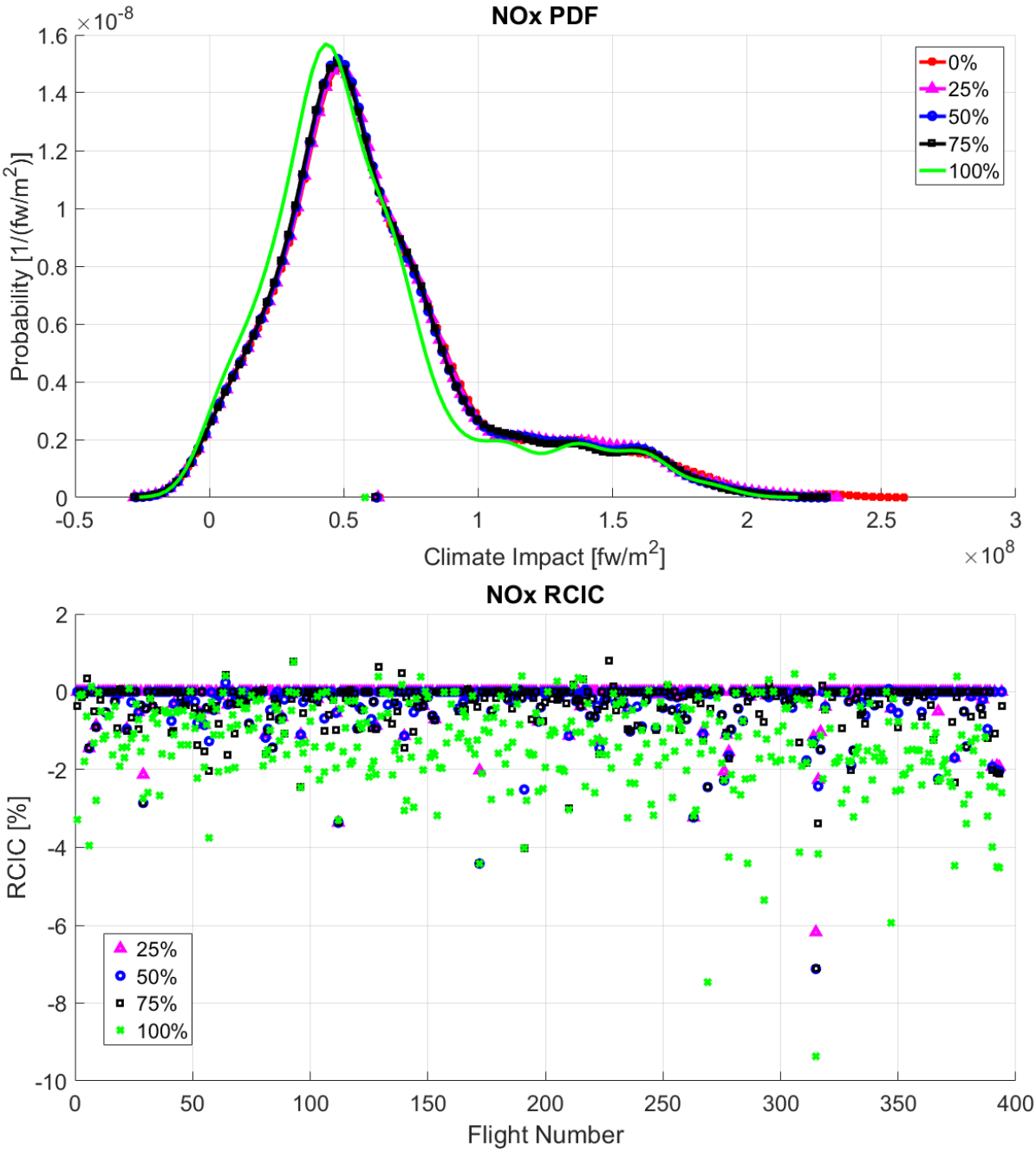

Figure 119. Probability Density Function and *RCIC* of NO_x for SP1-Westbound-AGWP100 case. The different curves and points represent the values for 0%, 25%, 50%, 75% and 100% of *NTCIC*.

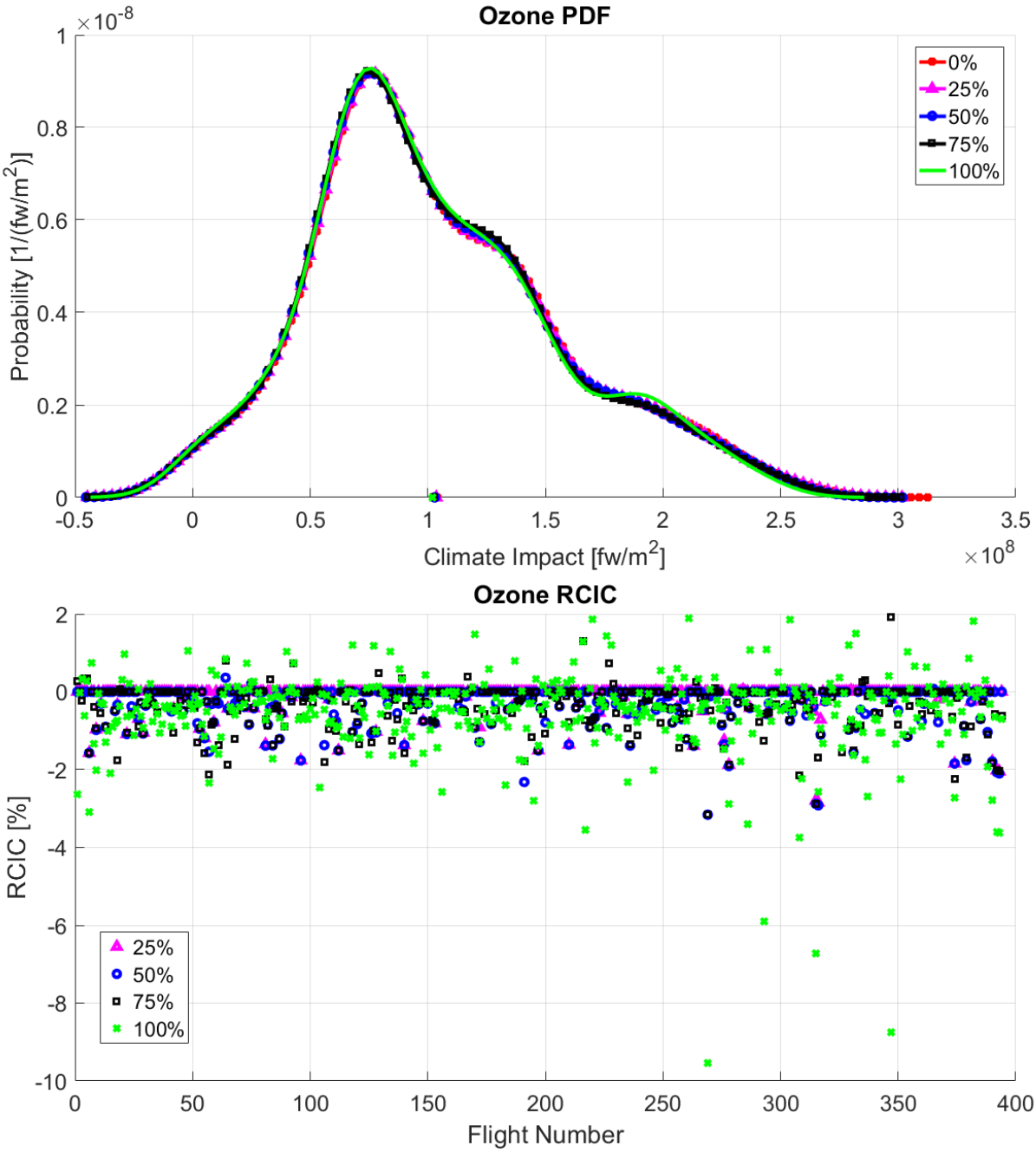

Figure 120. Probability Density Function and *RCIC* of ozone for SP1-Westbound-AGWP100 case. The different curves and points represent the values for 0%, 25%, 50%, 75% and 100% of *NTCIC*.

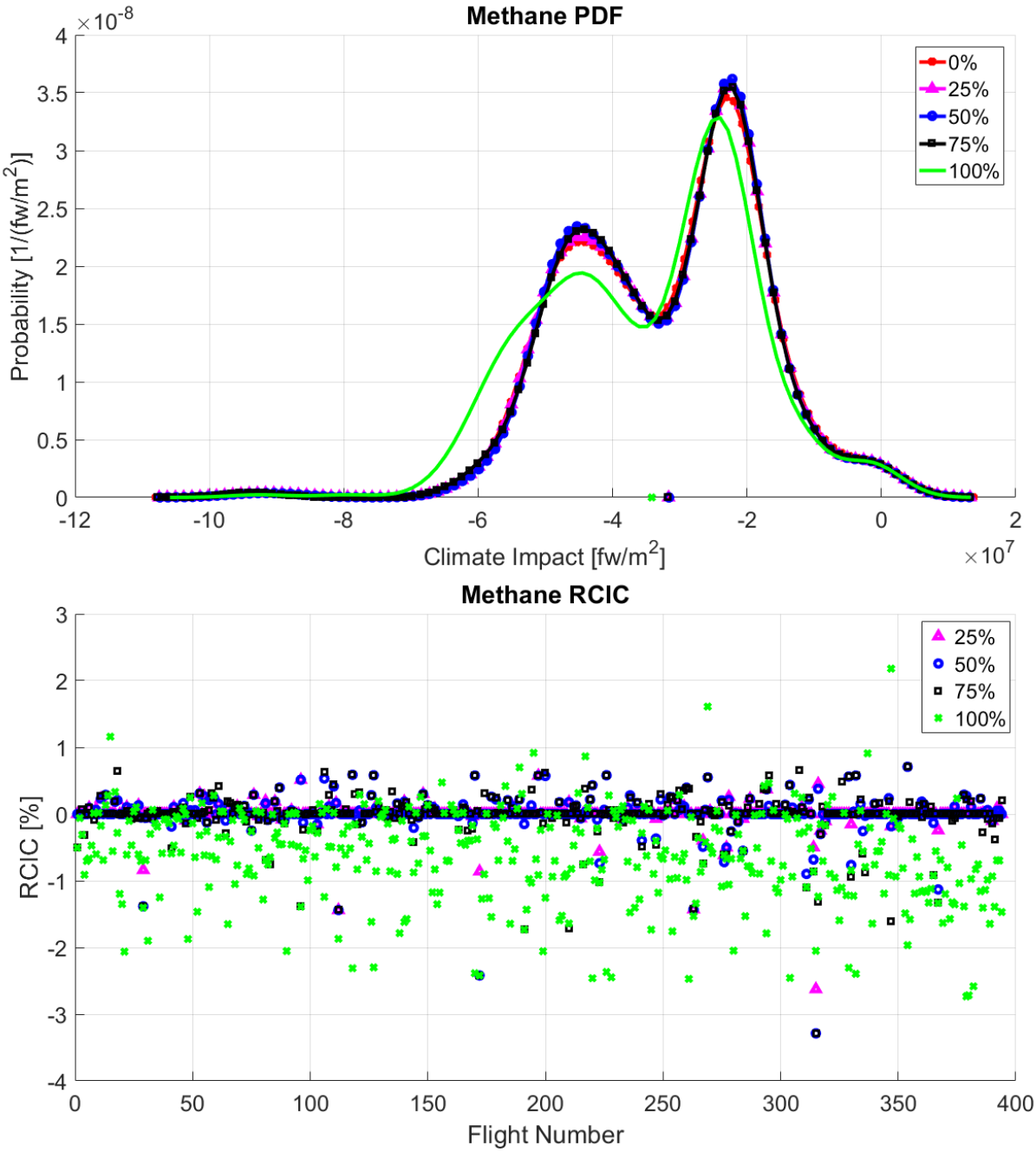

Figure 121. Probability Density Function and *RCIC* of methane for SP1-Westbound-AGWP100 case. The different curves and points represent the values for 0%, 25%, 50%, 75% and 100% of *NTCIC*.

C.3. Summer Pattern 2 – Eastbound

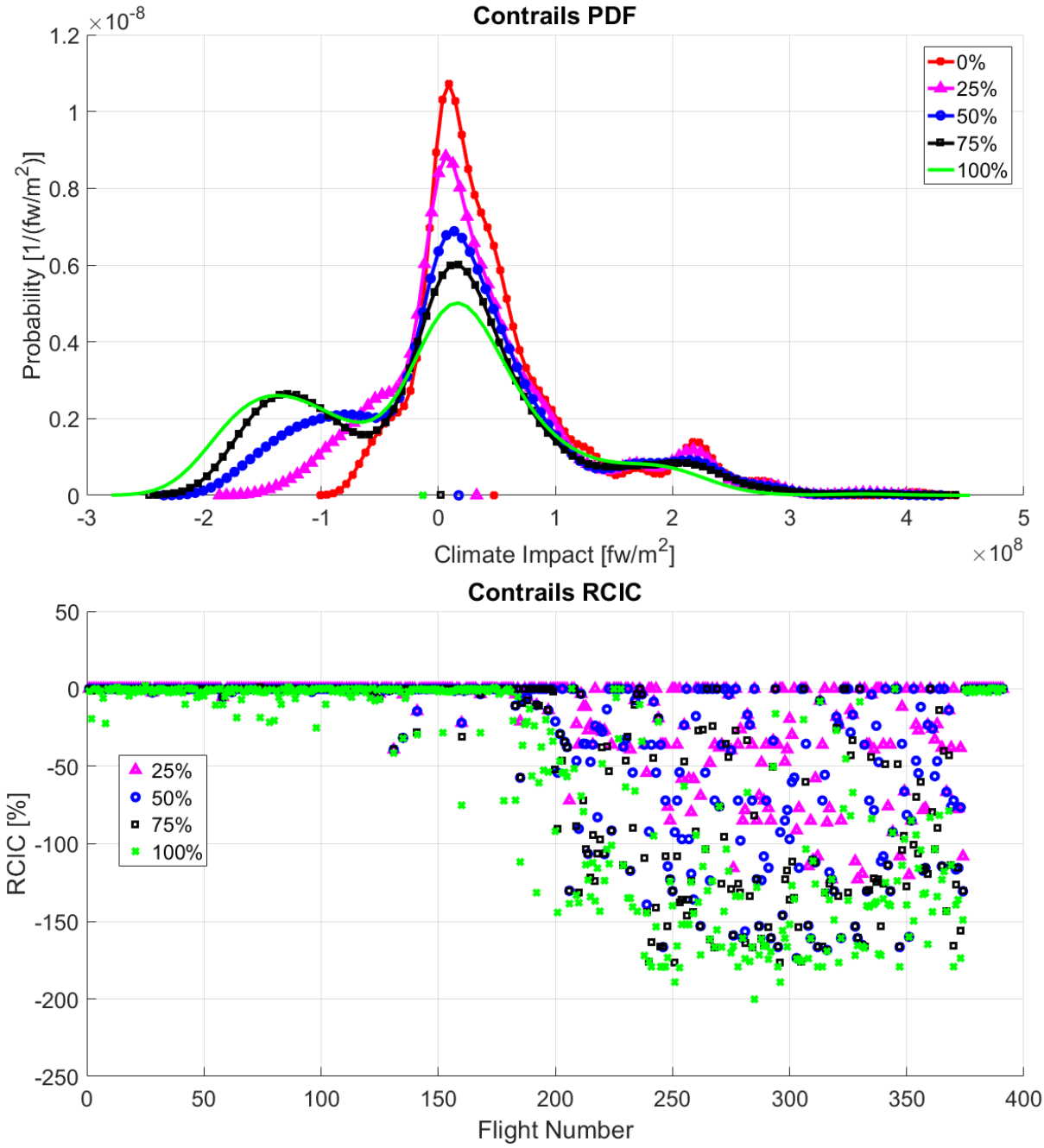

Figure 122. Probability Density Function and *RCIC* of contrails for SP2-Eastbound-AGWP100 case. The different curves and points represent the values for 0%, 25%, 50%, 75% and 100% of *NTCIC*.

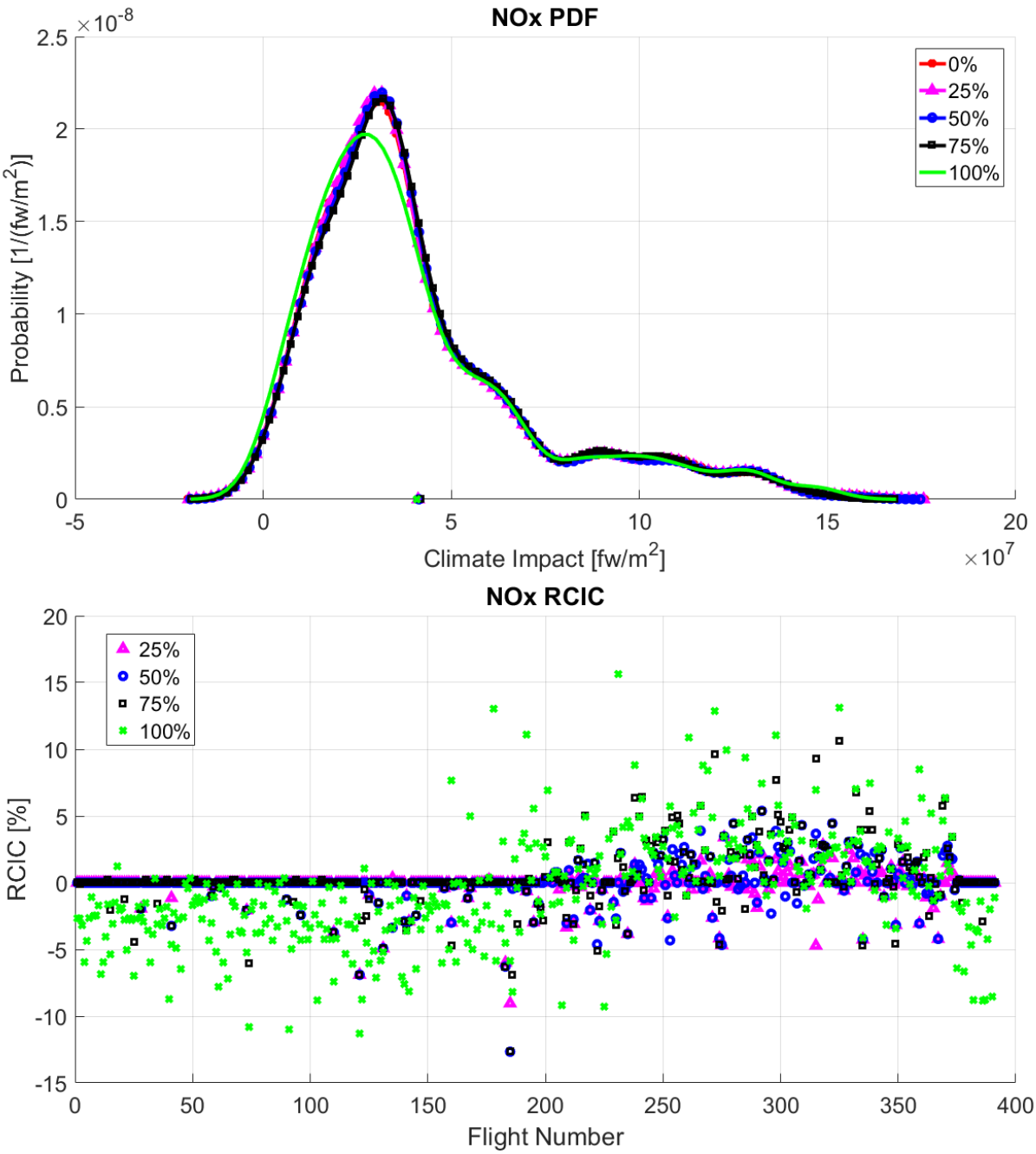

Figure 123. Probability Density Function and *RCIC* of NO_x for SP2-Eastbound-AGWP100 case. The different curves and points represent the values for 0%, 25%, 50%, 75% and 100% of *NTCIC*.

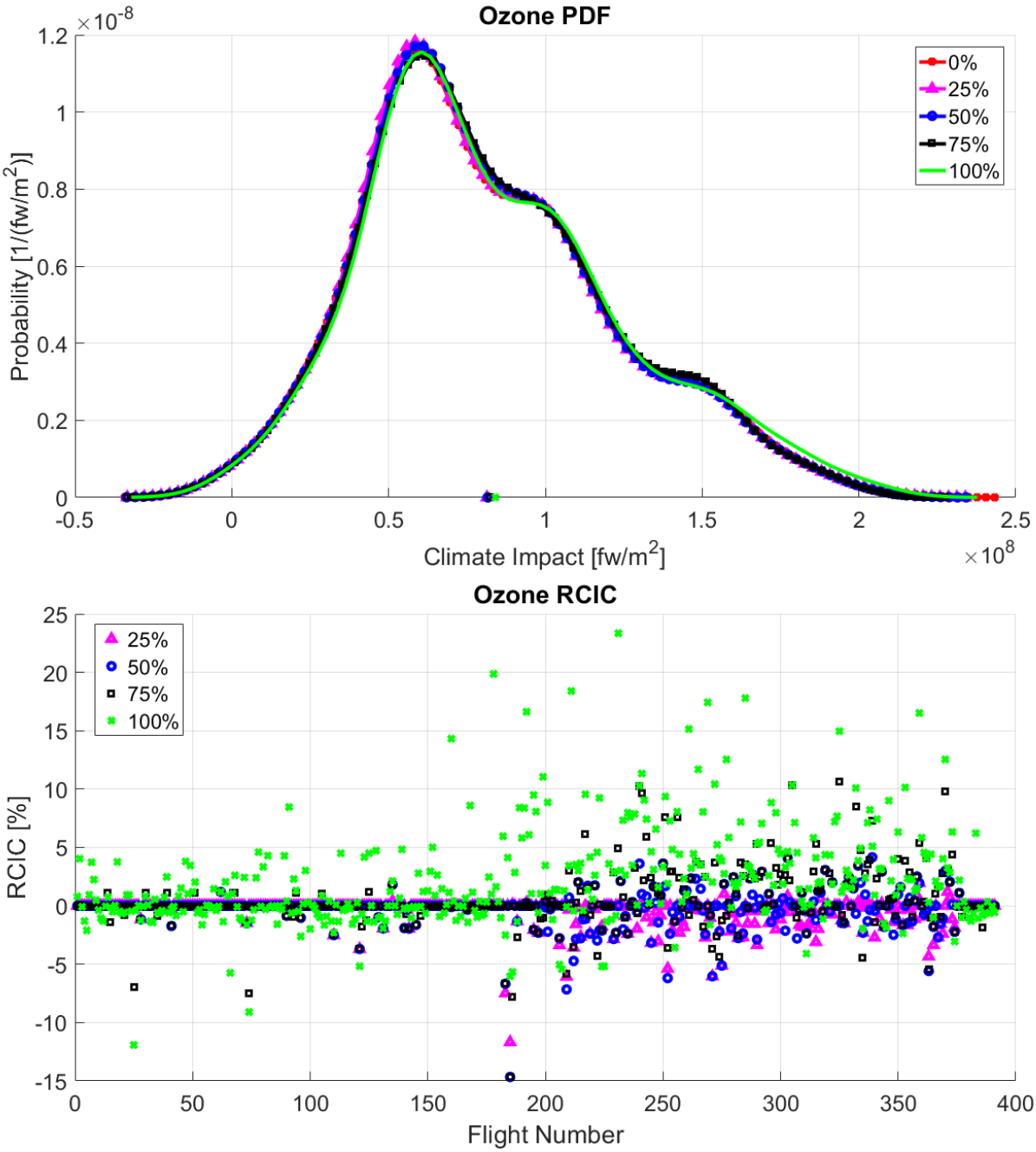

Figure 124. Probability Density Function and *RCIC* of ozone for SP2-Eastbound-AGWP100 case. The different curves and points represent the values for 0%, 25%, 50%, 75% and 100% of *NTCIC*.

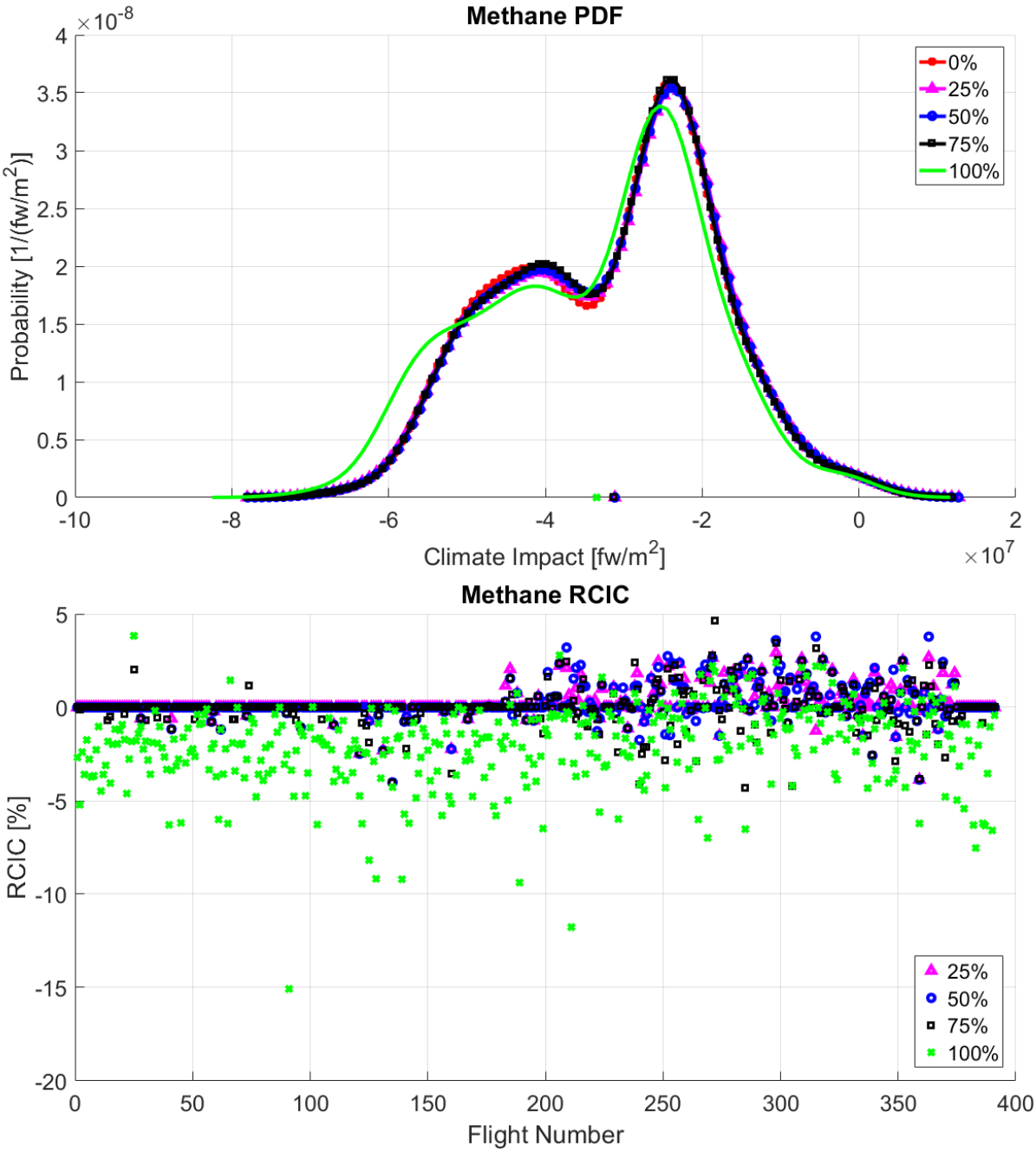

Figure 125. Probability Density Function and *RCIC* of methane for SP2-Eastbound-AGWP100 case. The different curves and points represent the values for 0%, 25%, 50%, 75% and 100% of *NTCIC*.

C.4. Summer Pattern 2 – Westbound

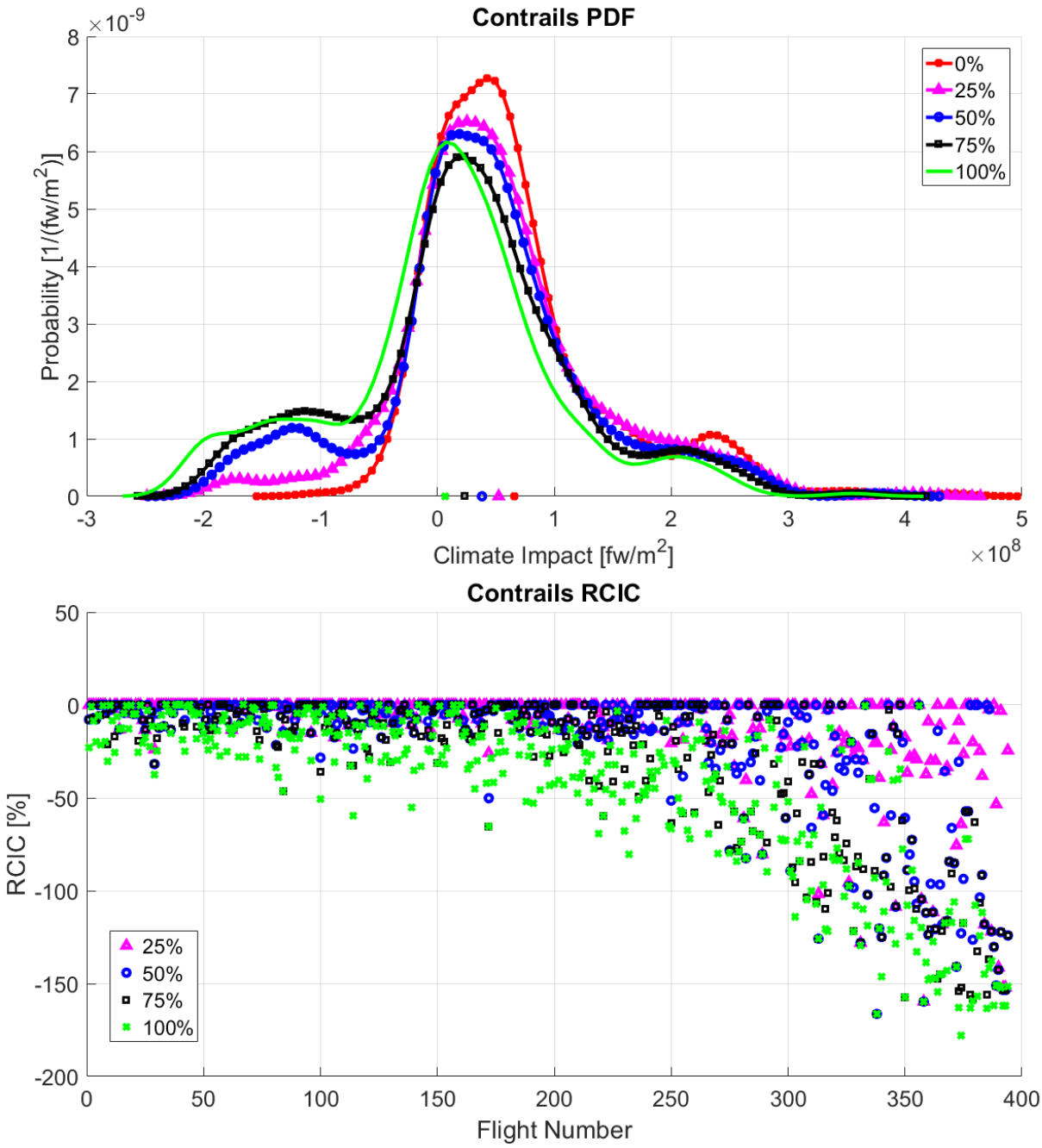

Figure 126. Probability Density Function and *RCIC* of contrails for SP2-Westbound-AGWP100 case. The different curves and points represent the values for 0%, 25%, 50%, 75% and 100% of *NTCIC*.

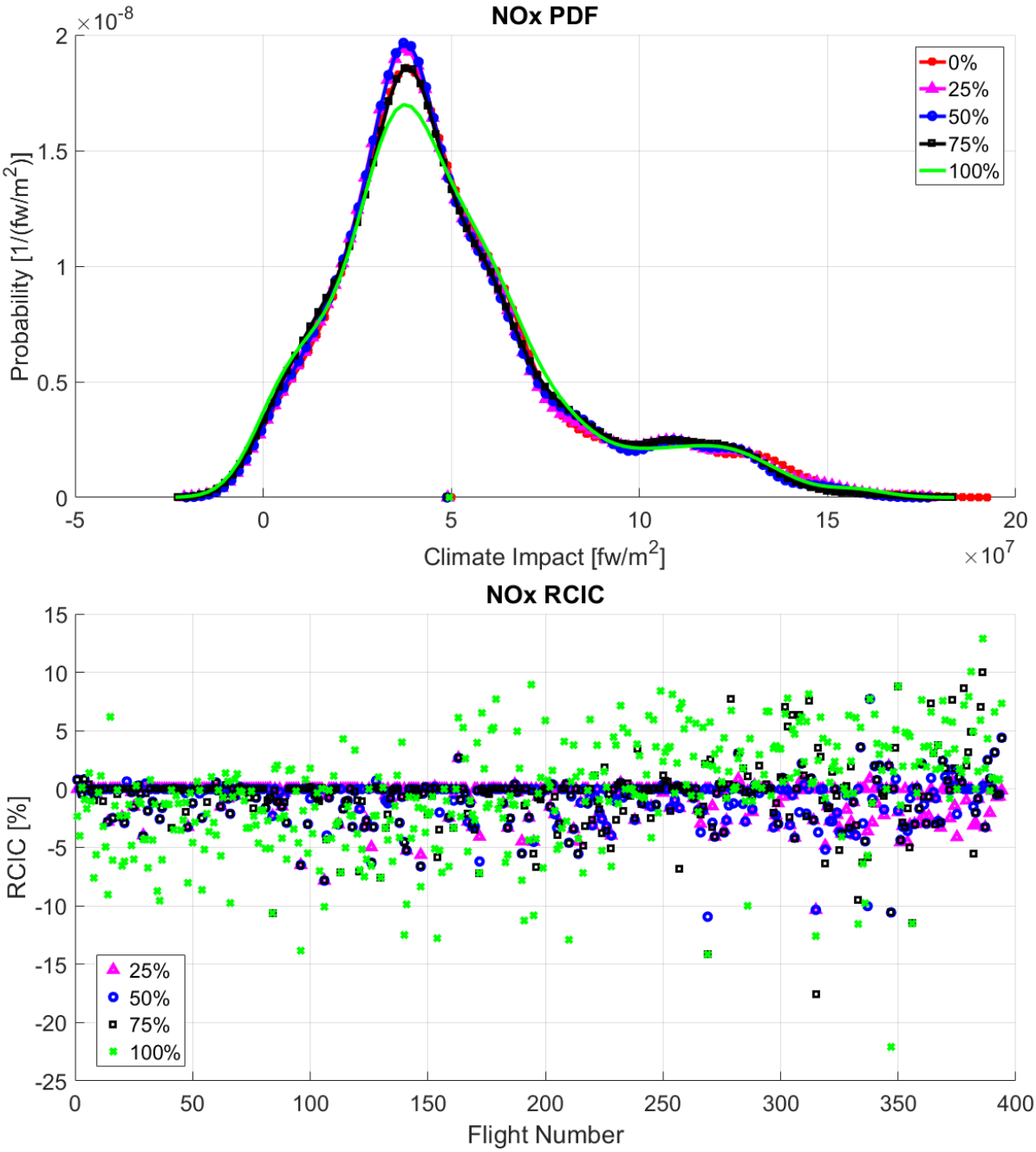

Figure 127. Probability Density Function and *RCIC* of NO_x for SP2-Westbound-AGWP100 case. The different curves and points represent the values for 0%, 25%, 50%, 75% and 100% of *NTCIC*.

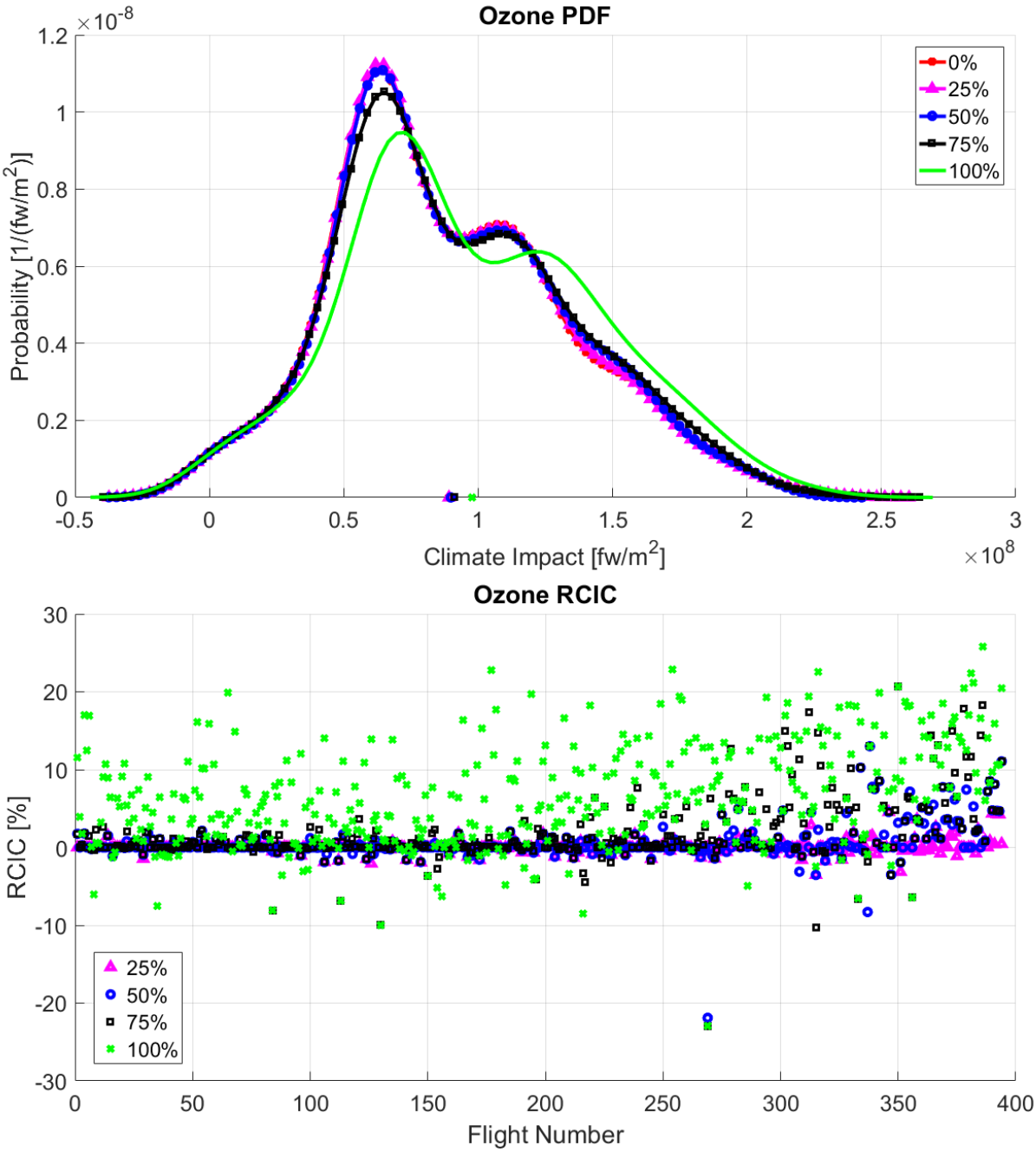

Figure 128. Probability Density Function and *RCIC* of ozone for SP2-Westbound-AGWP100 case. The different curves and points represent the values for 0%, 25%, 50%, 75% and 100% of *NTCIC*.

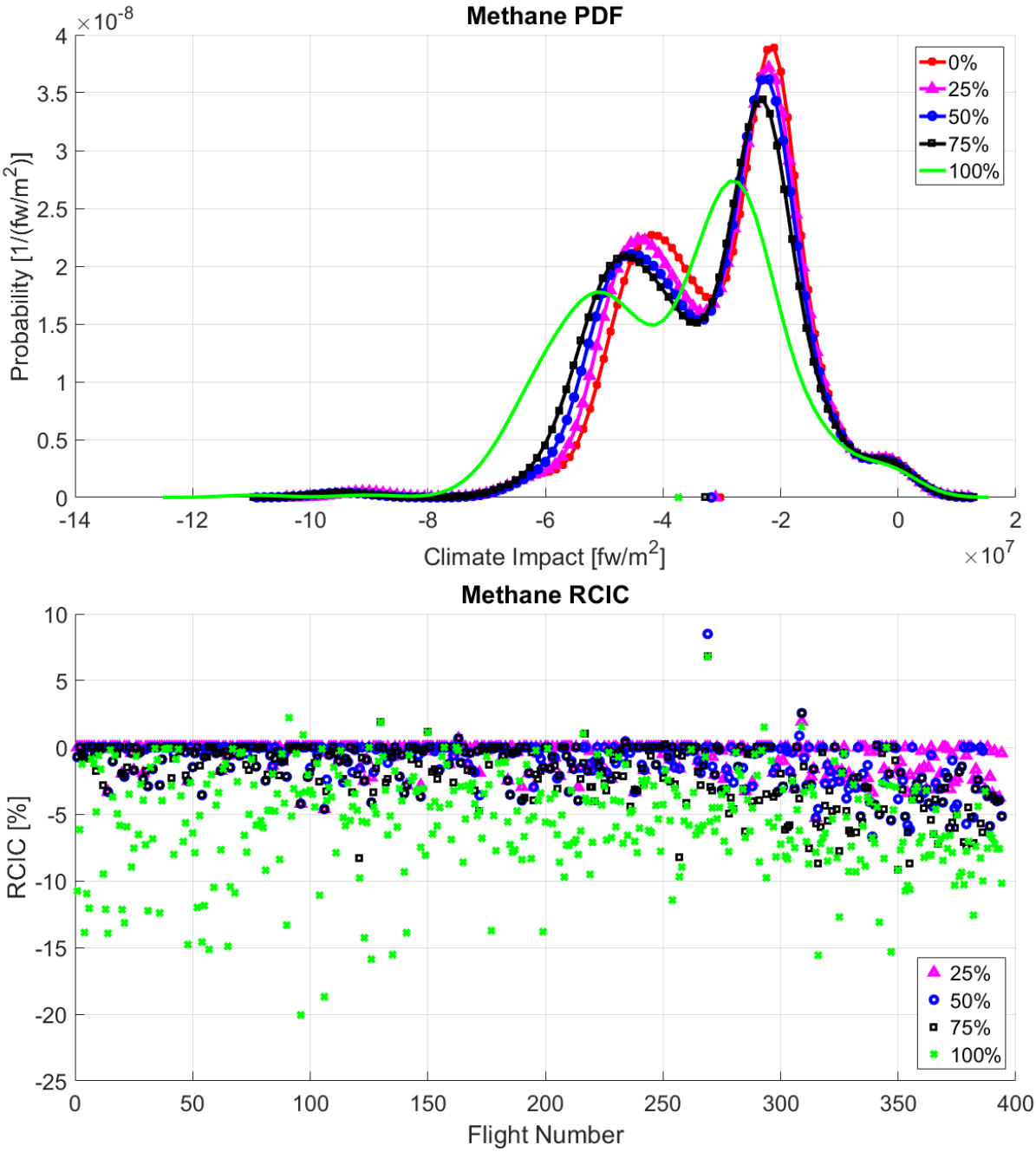

Figure 129. Probability Density Function and *RCIC* of methane for SP2-Westbound-AGWP100 case. The different curves and points represent the values for 0%, 25%, 50%, 75% and 100% of *NTCIC*.

C.5. Summer Pattern 3 – Eastbound

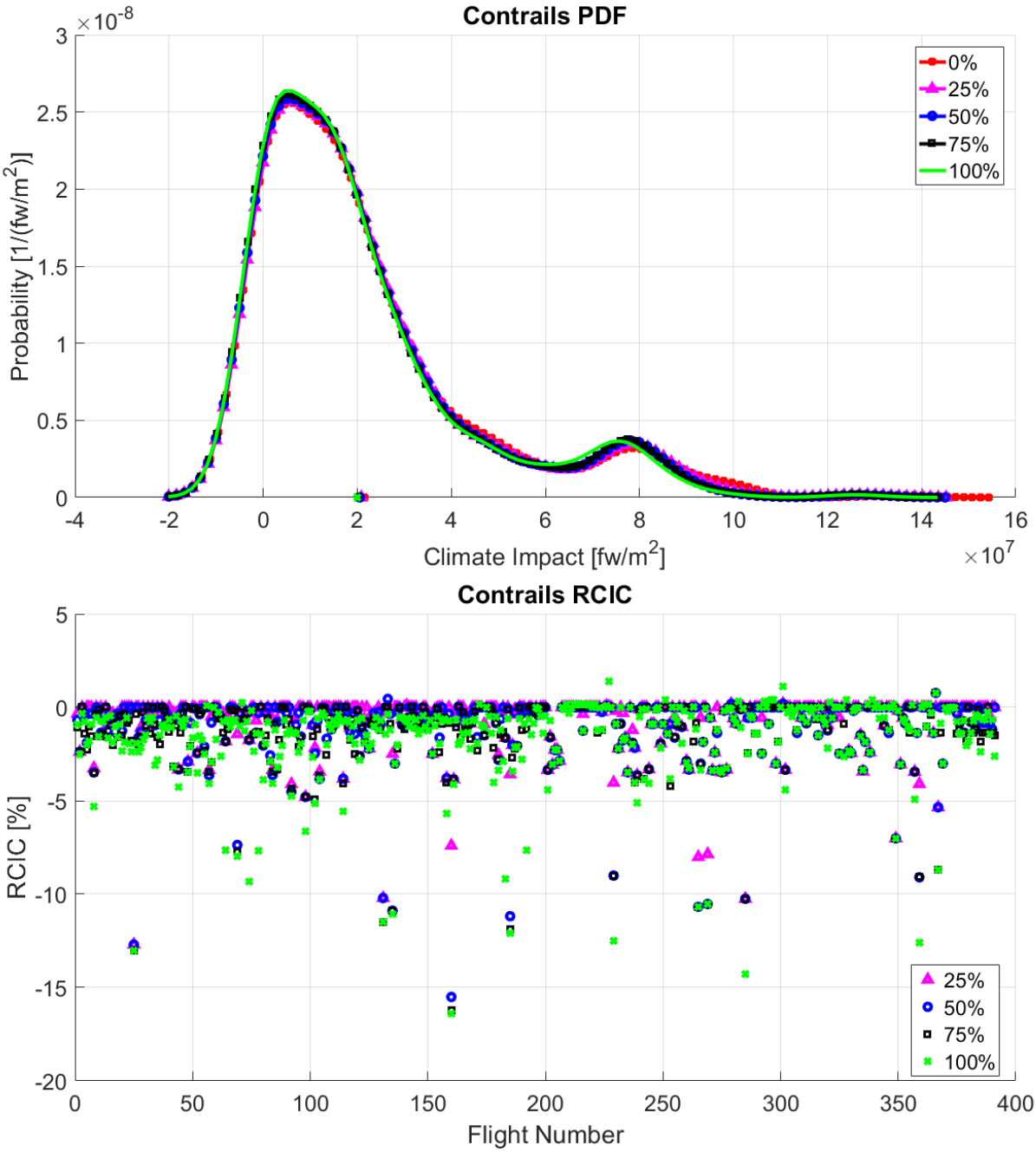

Figure 130. Probability Density Function and *RCIC* of contrails for SP3-Eastbound-AGWP100 case. The different curves and points represent the values for 0%, 25%, 50%, 75% and 100% of *NTCIC*.

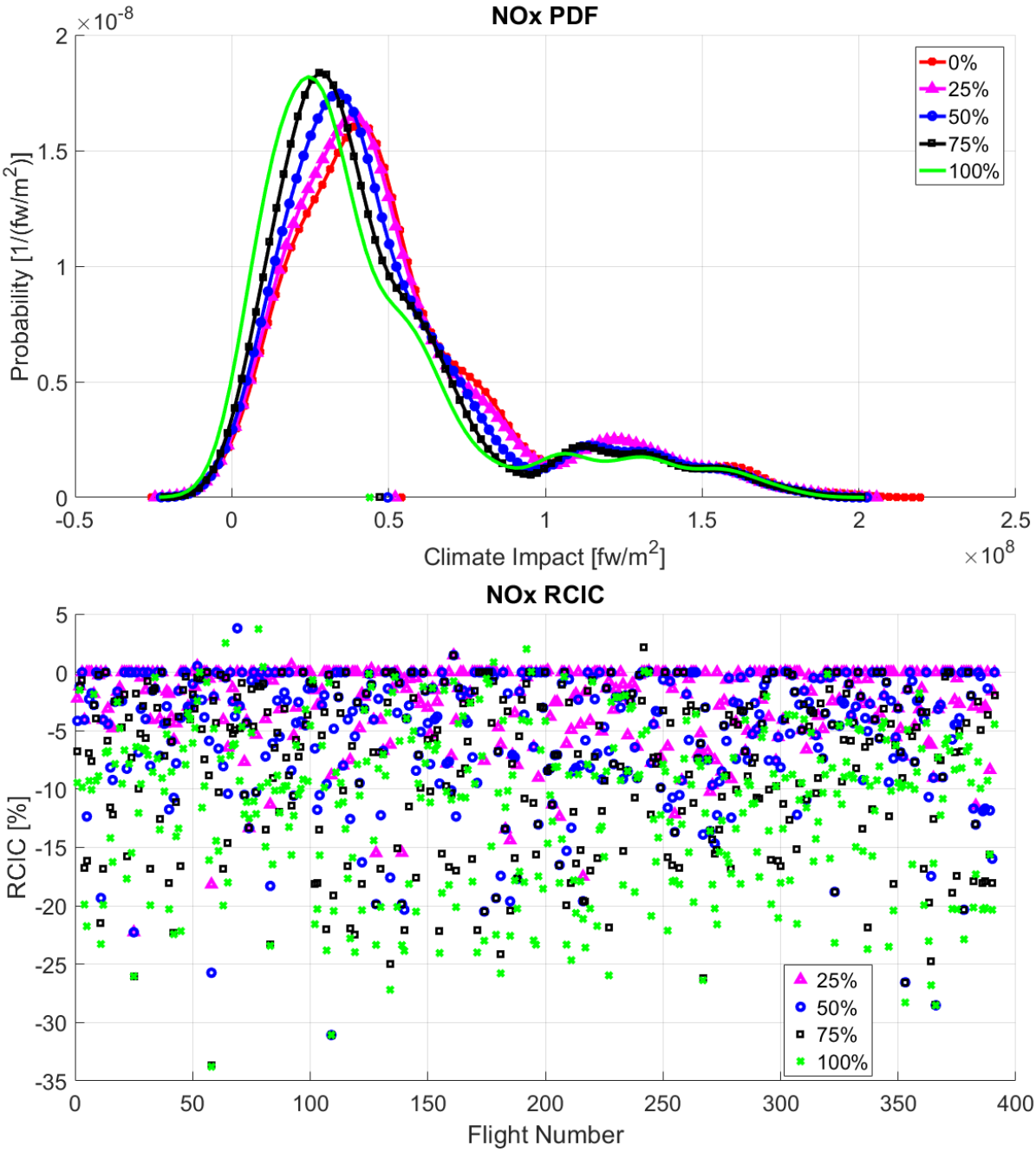

Figure 131. Probability Density Function and *RCIC* of NO_x for SP3-Eastbound-AGWP100 case. The different curves and points represent the values for 0%, 25%, 50%, 75% and 100% of *NTCIC*.

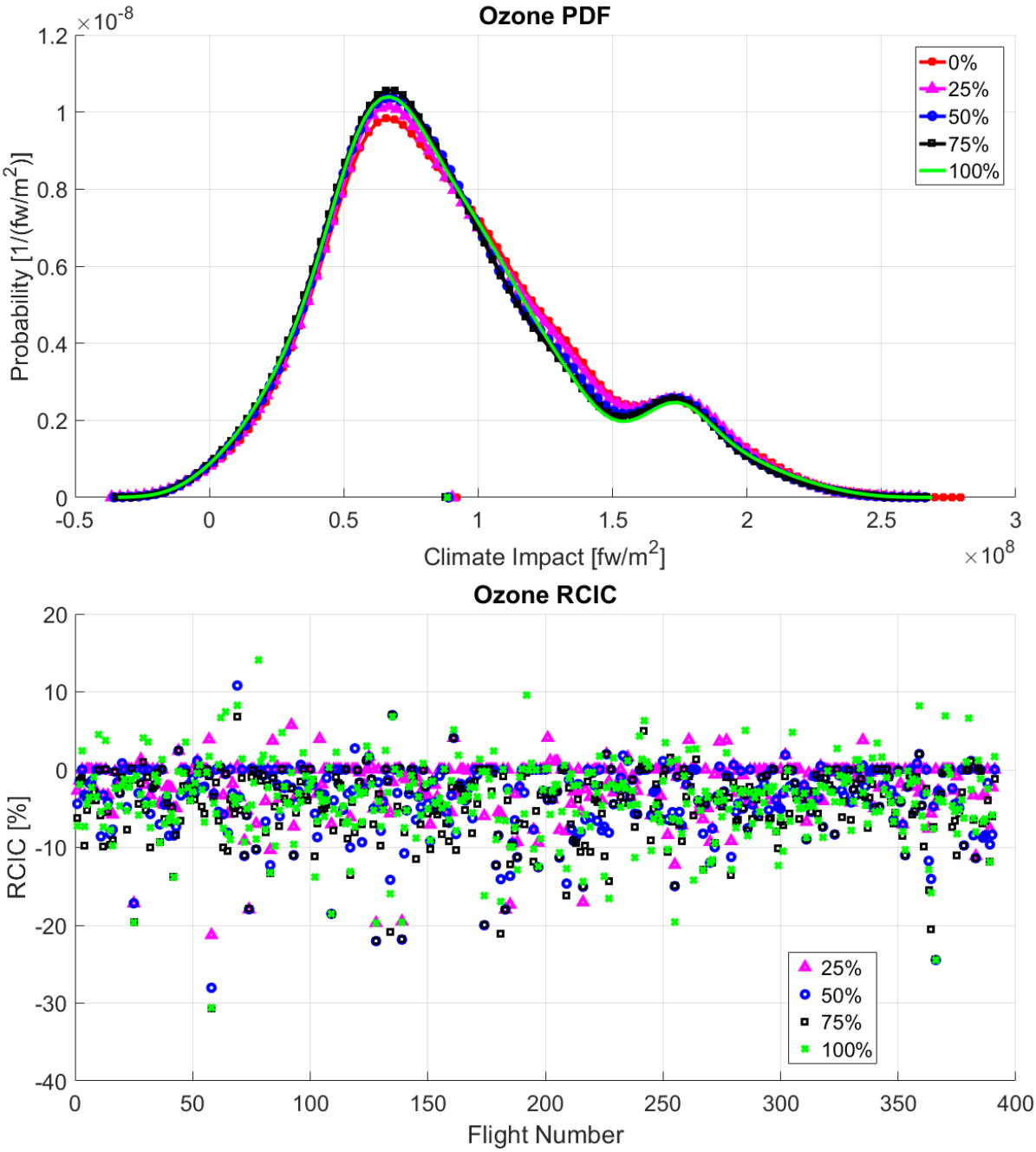

Figure 132. Probability Density Function and *RCIC* of ozone for SP3-Eastbound-AGWP100 case. The different curves and points represent the values for 0%, 25%, 50%, 75% and 100% of *NTCIC*.

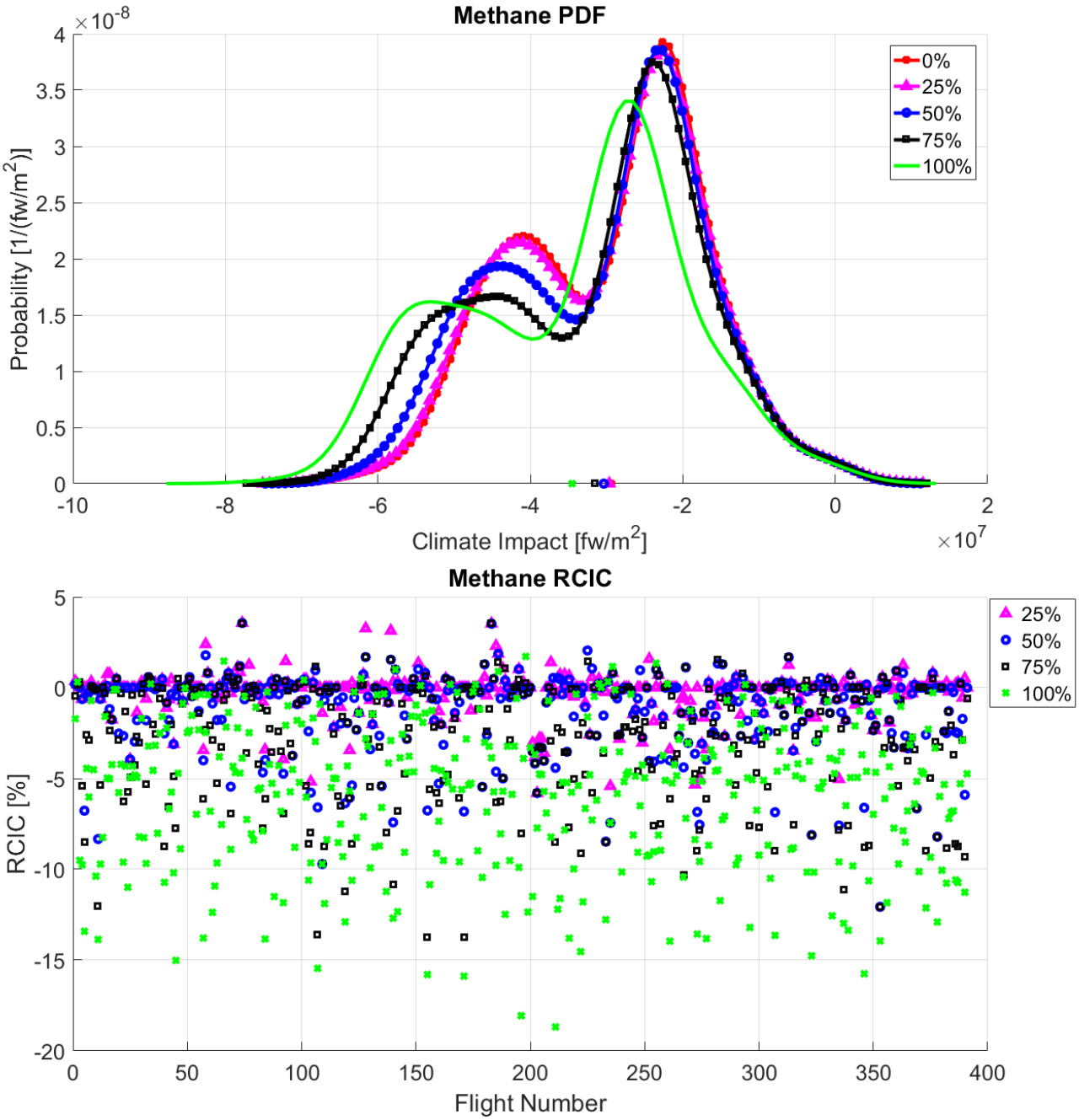

Figure 133. Probability Density Function and *RCIC* of methane for SP3-Eastbound-AGWP100 case. The different curves and points represent the values for 0%, 25%, 50%, 75% and 100% of *NTCIC*.

C.6. Summer Pattern 3 – Westbound

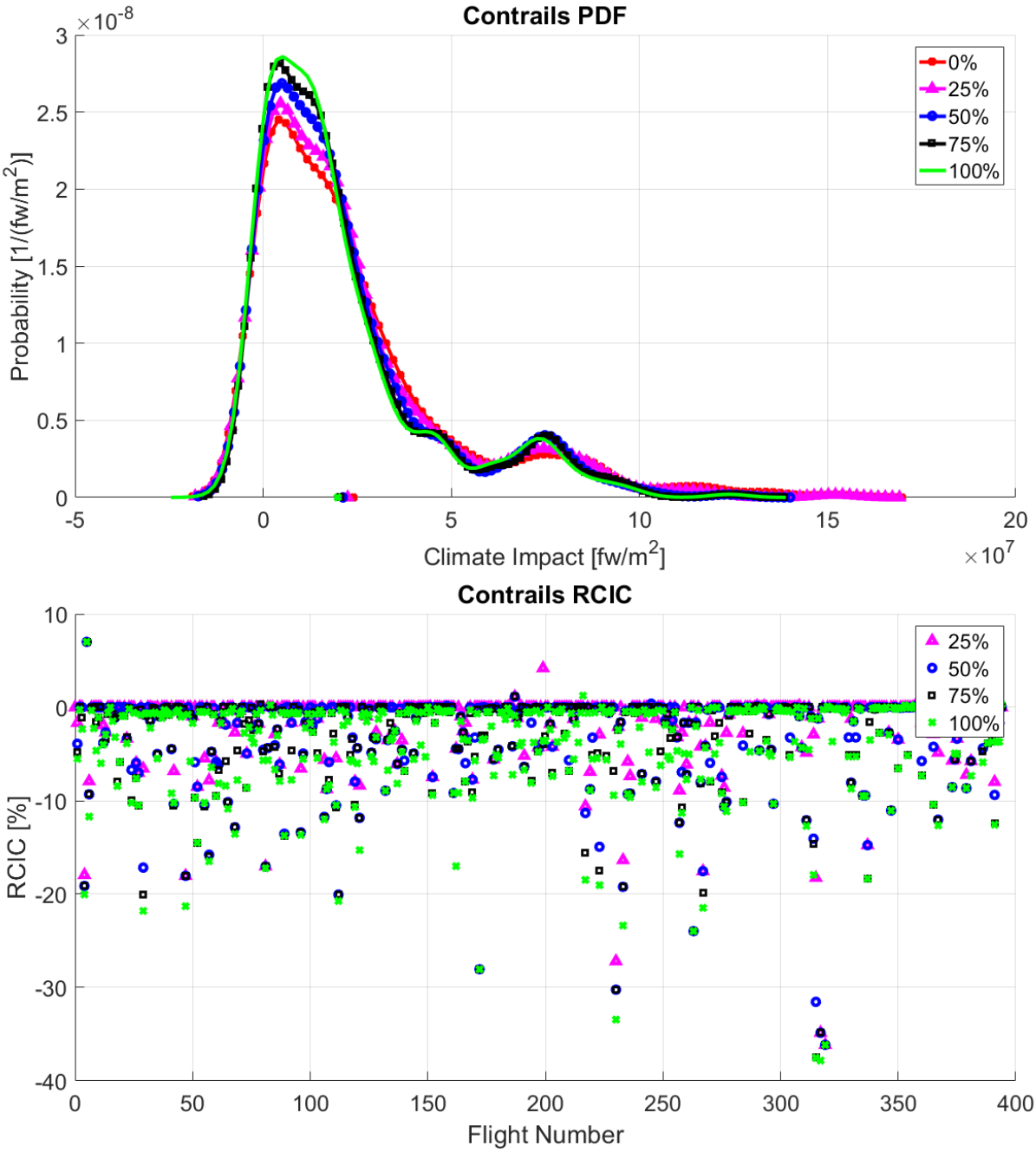

Figure 134. Probability Density Function and *RCIC* of contrails for SP3-Westbound-AGWP100 case. The different curves and points represent the values for 0%, 25%, 50%, 75% and 100% of *NTCIC*.

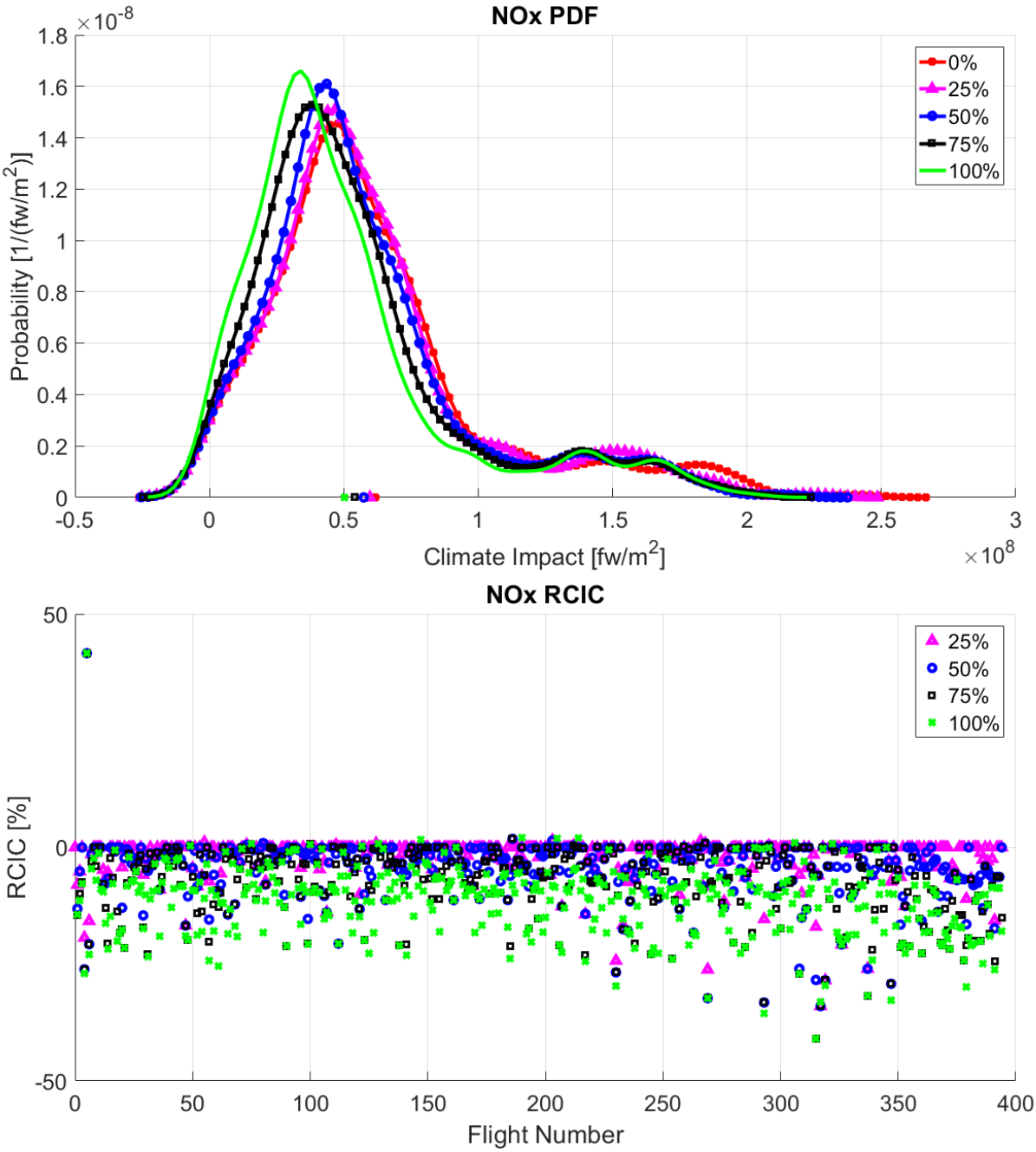

Figure 135. Probability Density Function and *RCIC* of NO_x for SP3-Westbound-AGWP100 case. The different curves and points represent the values for 0%, 25%, 50%, 75% and 100% of *NTCIC*.

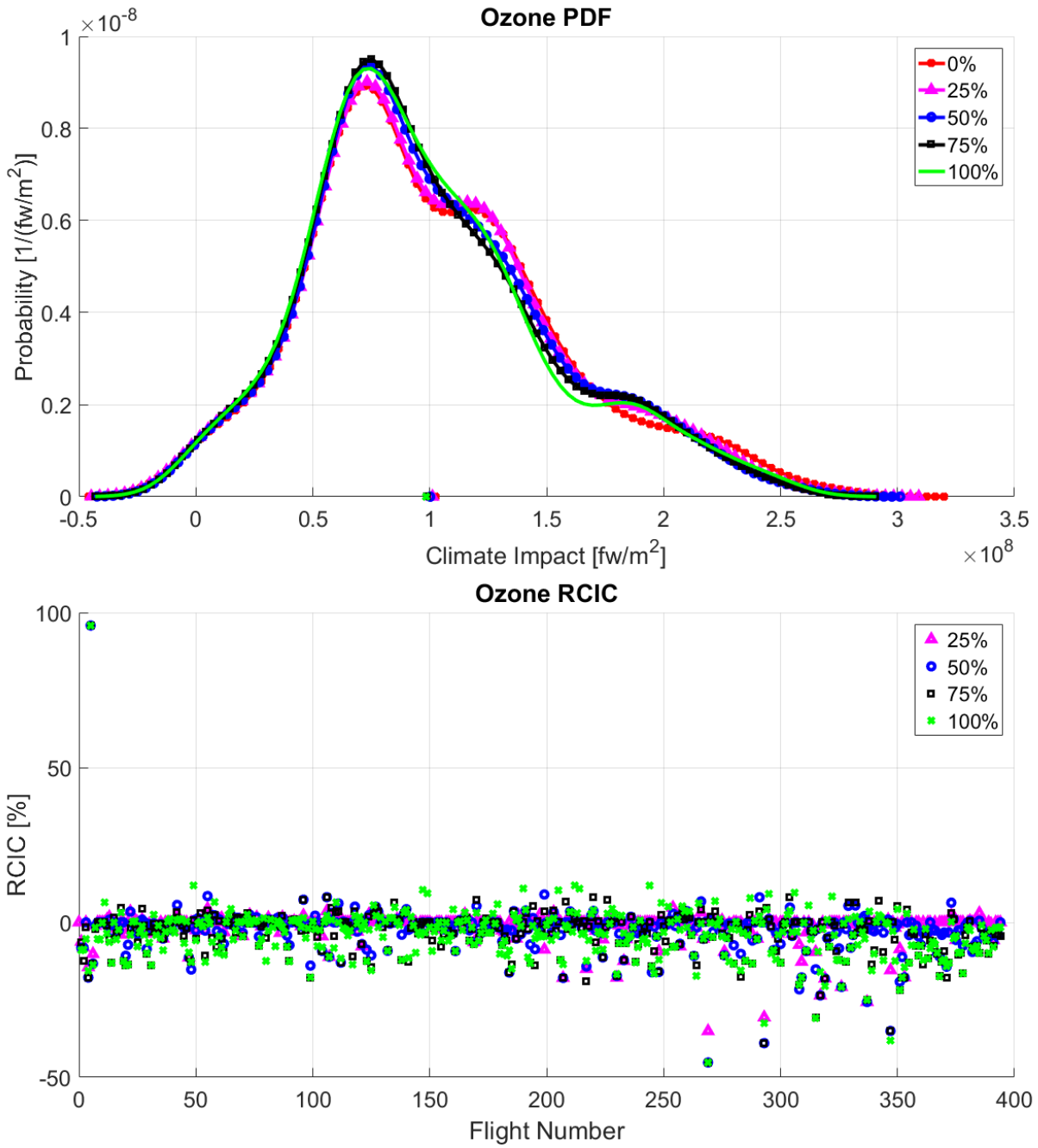

Figure 136. Probability Density Function and *RCIC* of ozone for SP3-Westbound-AGWP100 case. The different curves and points represent the values for 0%, 25%, 50%, 75% and 100% of *NTCIC*.

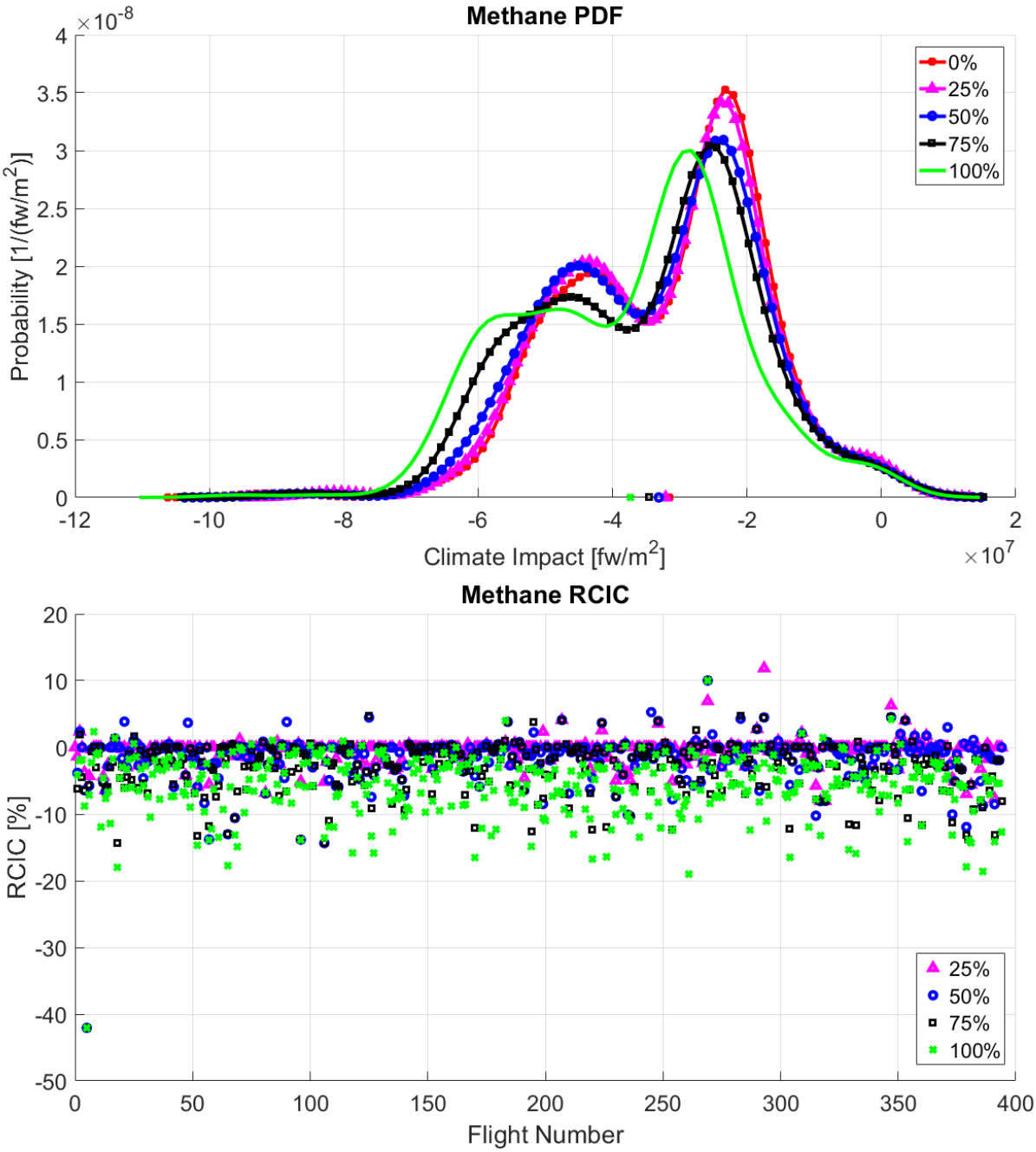

Figure 137. Probability Density Function and *RCIC* of ozone for SP3-Westbound-AGWP100 case. The different curves and points represent the values for 0%, 25%, 50%, 75% and 100% of *NTCIC*.

C.7. Winter Pattern 1 – Eastbound

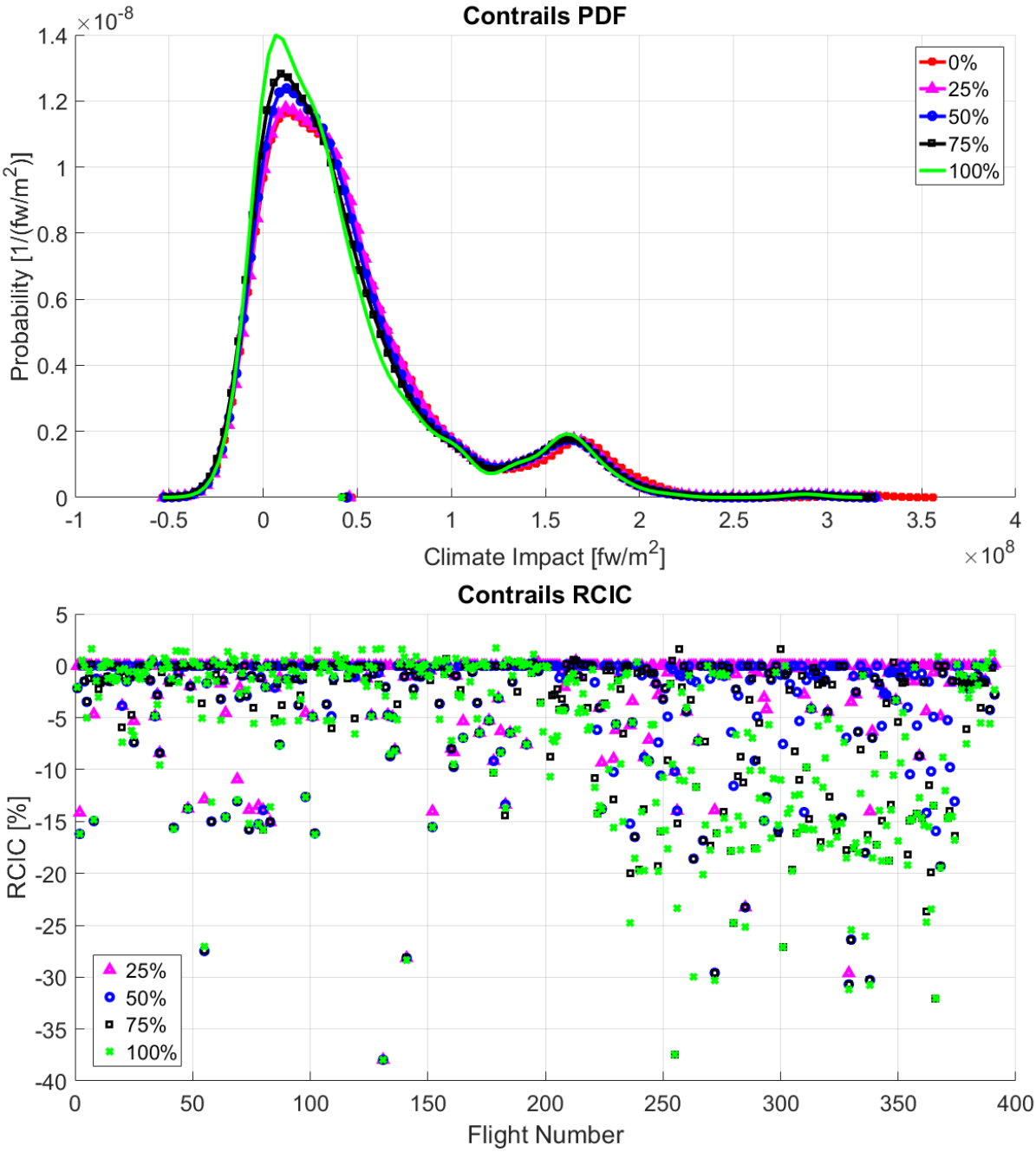

Figure 138. Probability Density Function and *RCIC* of contrails for WP1-Eastbound-AGWP100 case. The different curves and points represent the values for 0%, 25%, 50%, 75% and 100% of *NTCIC*.

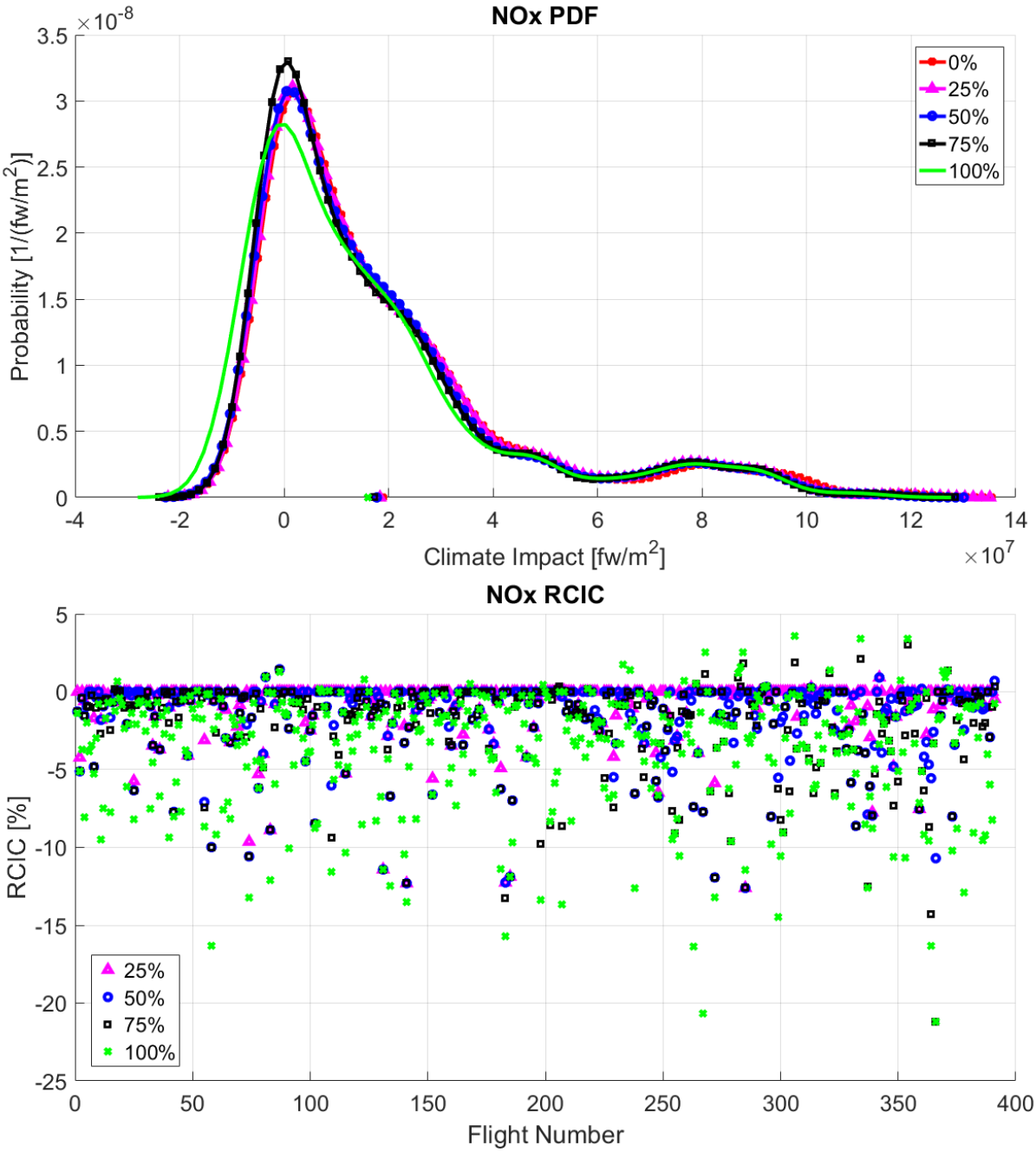

Figure 139. Probability Density Function and *RCIC* of NO_x for WP1-Eastbound-AGWP100 case. The different curves and points represent the values for 0%, 25%, 50%, 75% and 100% of *NTCIC*.

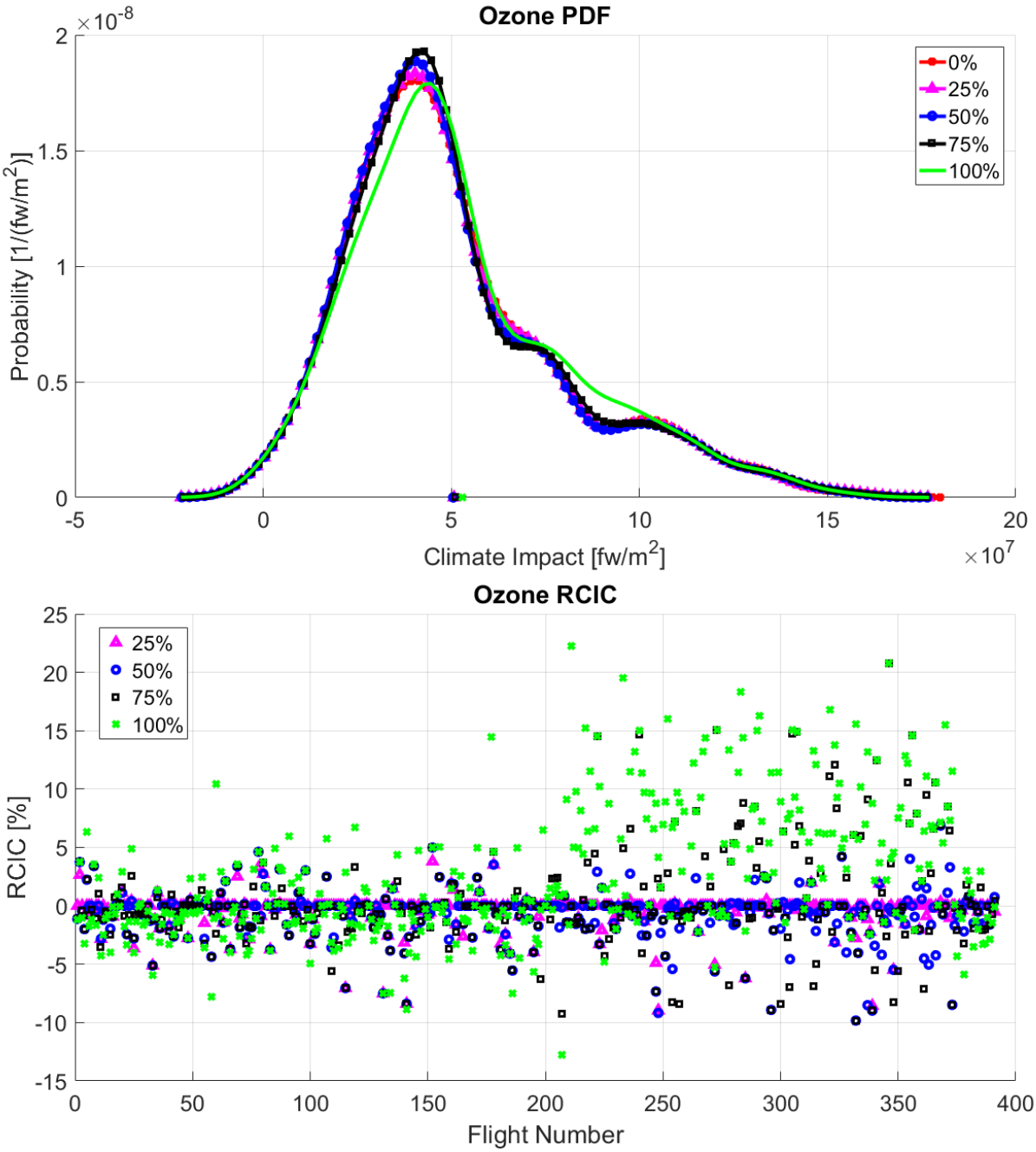

Figure 140. Probability Density Function and *RCIC* of ozone for WP1-Eastbound-AGWP100 case. The different curves and points represent the values for 0%, 25%, 50%, 75% and 100% of *NTCIC*.

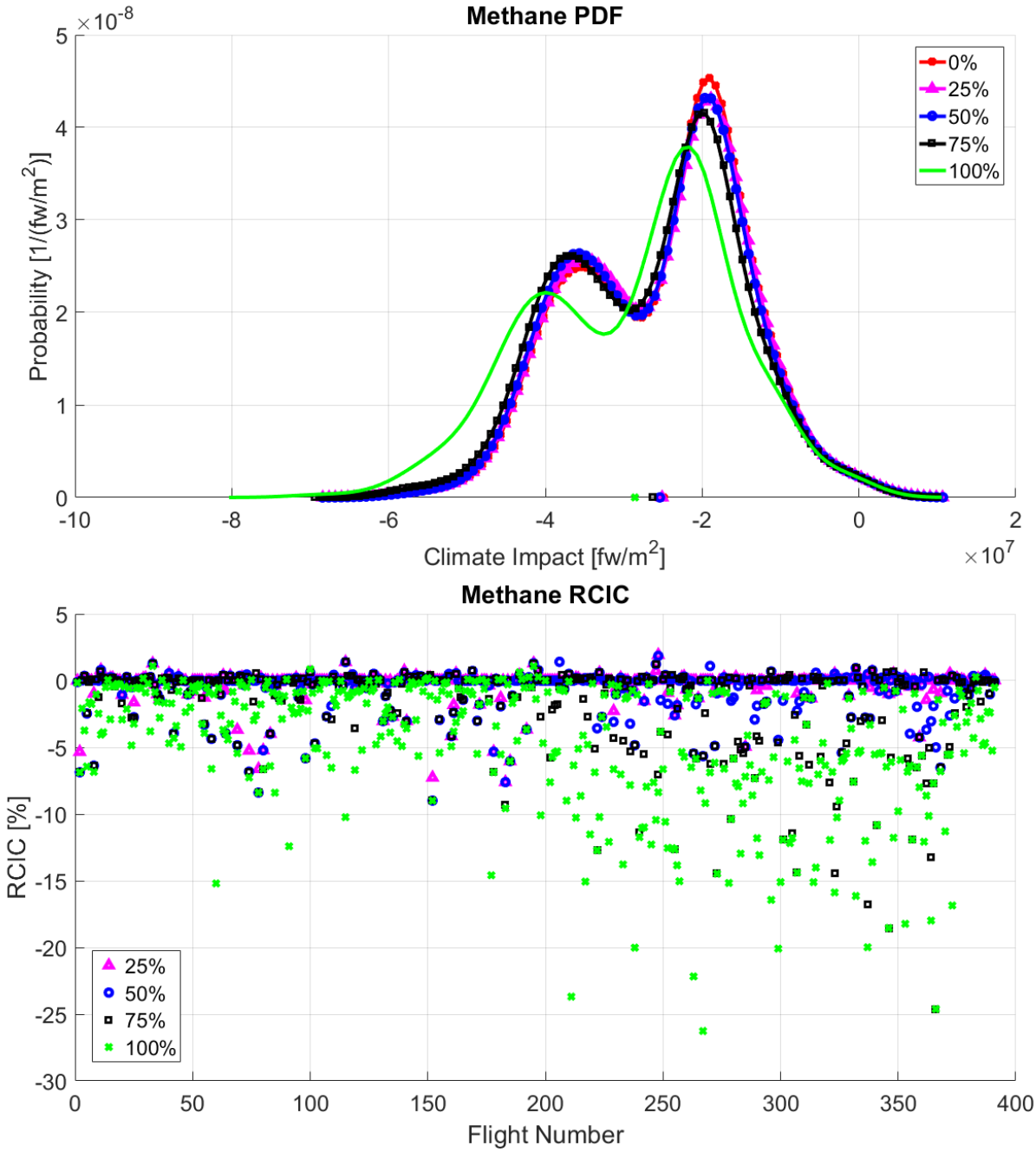

Figure 141. Probability Density Function and *RCIC* of methane for WP1-Eastbound-AGWP100 case. The different curves and points represent the values for 0%, 25%, 50%, 75% and 100% of *NTCIC*.

C.8. Winter Pattern 1 – Westbound

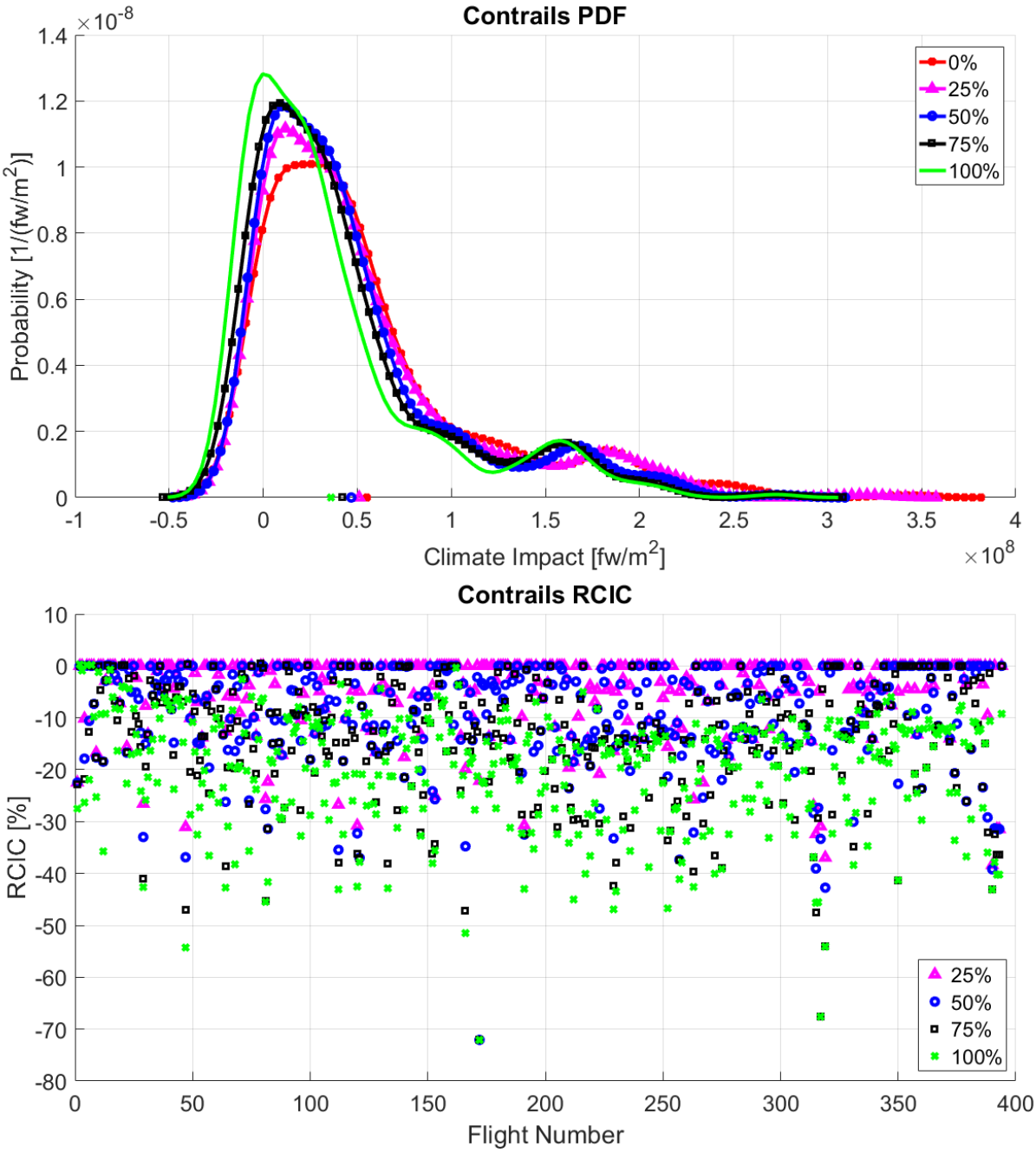

Figure 142. Probability Density Function and *RCIC* of contrails for WP1-Westbound-AGWP100 case. The different curves and points represent the values for 0%, 25%, 50%, 75% and 100% of *NTCIC*.

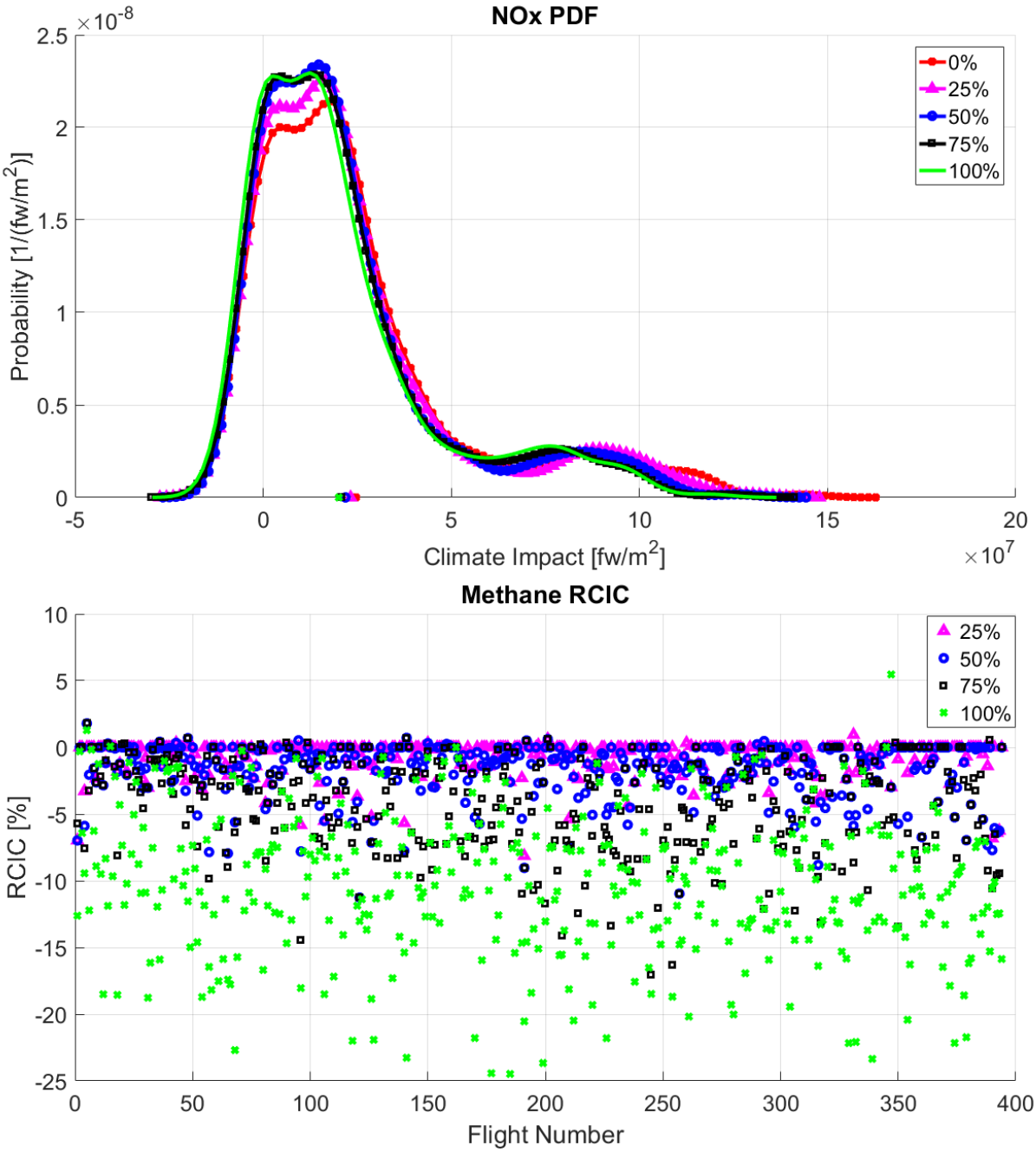

Figure 143. Probability Density Function and *RCIC* of NO_x for WP1-Westbound-AGWP100 case. The different curves and points represent the values for 0%, 25%, 50%, 75% and 100% of *NTCIC*.

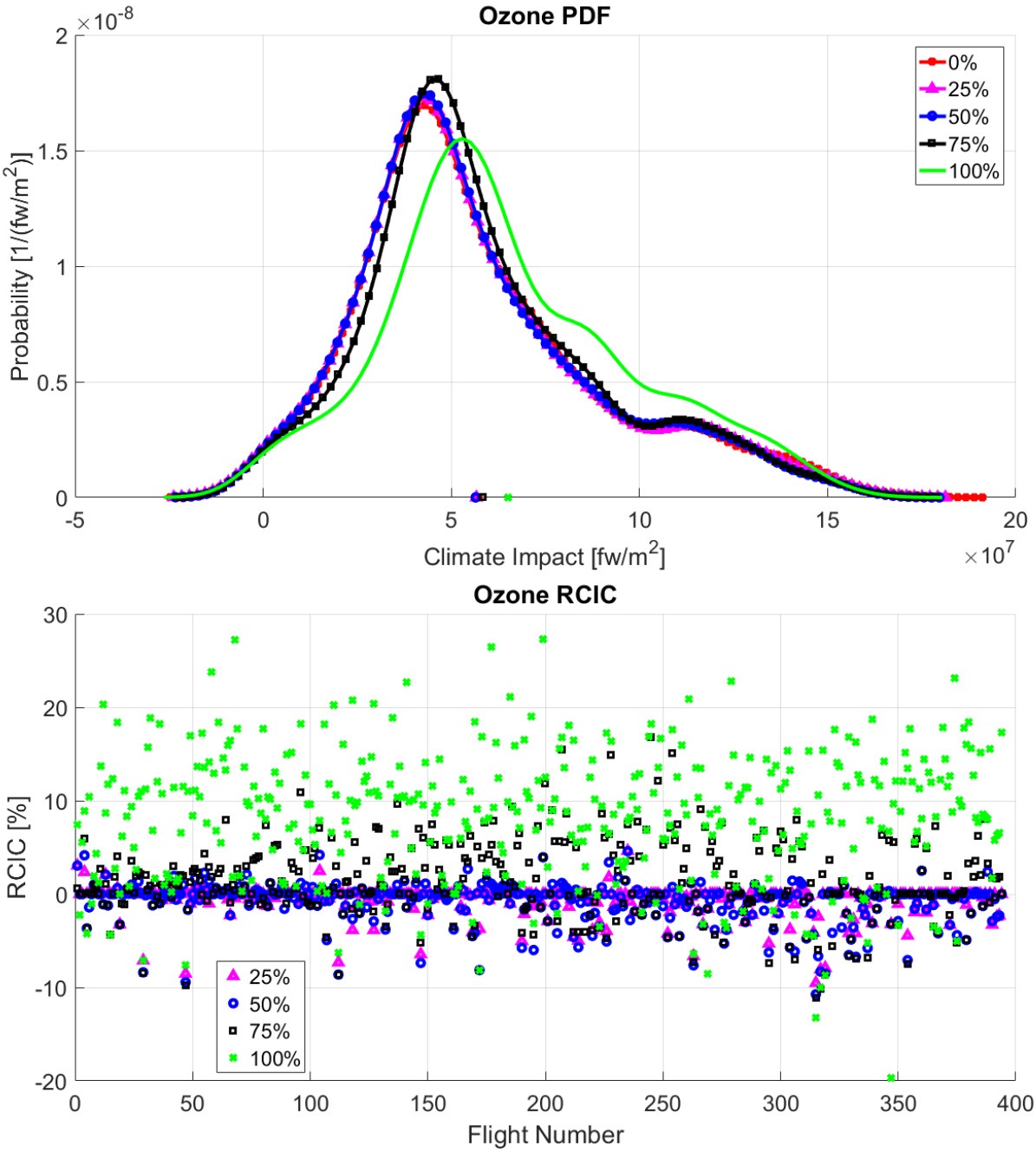

Figure 144. Probability Density Function and *RCIC* of ozone for WP1-Westbound-AGWP100 case. The different curves and points represent the values for 0%, 25%, 50%, 75% and 100% of *NTCIC*.

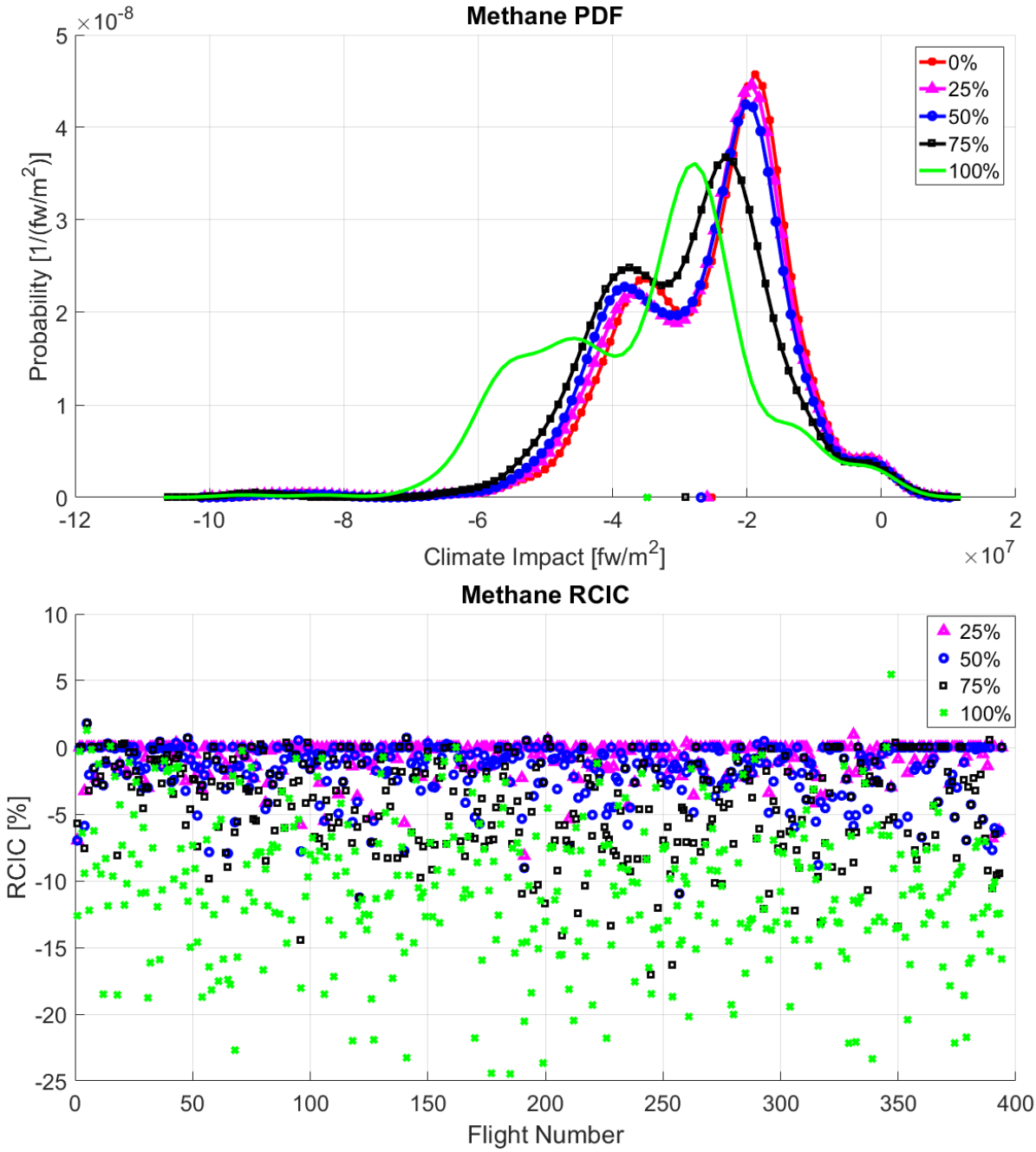

Figure 145. Probability Density Function and *RCIC* of methane for WP1-Westbound-AGWP100 case. The different curves and points represent the values for 0%, 25%, 50%, 75% and 100% of *NTCIC*.

C.9. Winter Pattern 2 – Eastbound

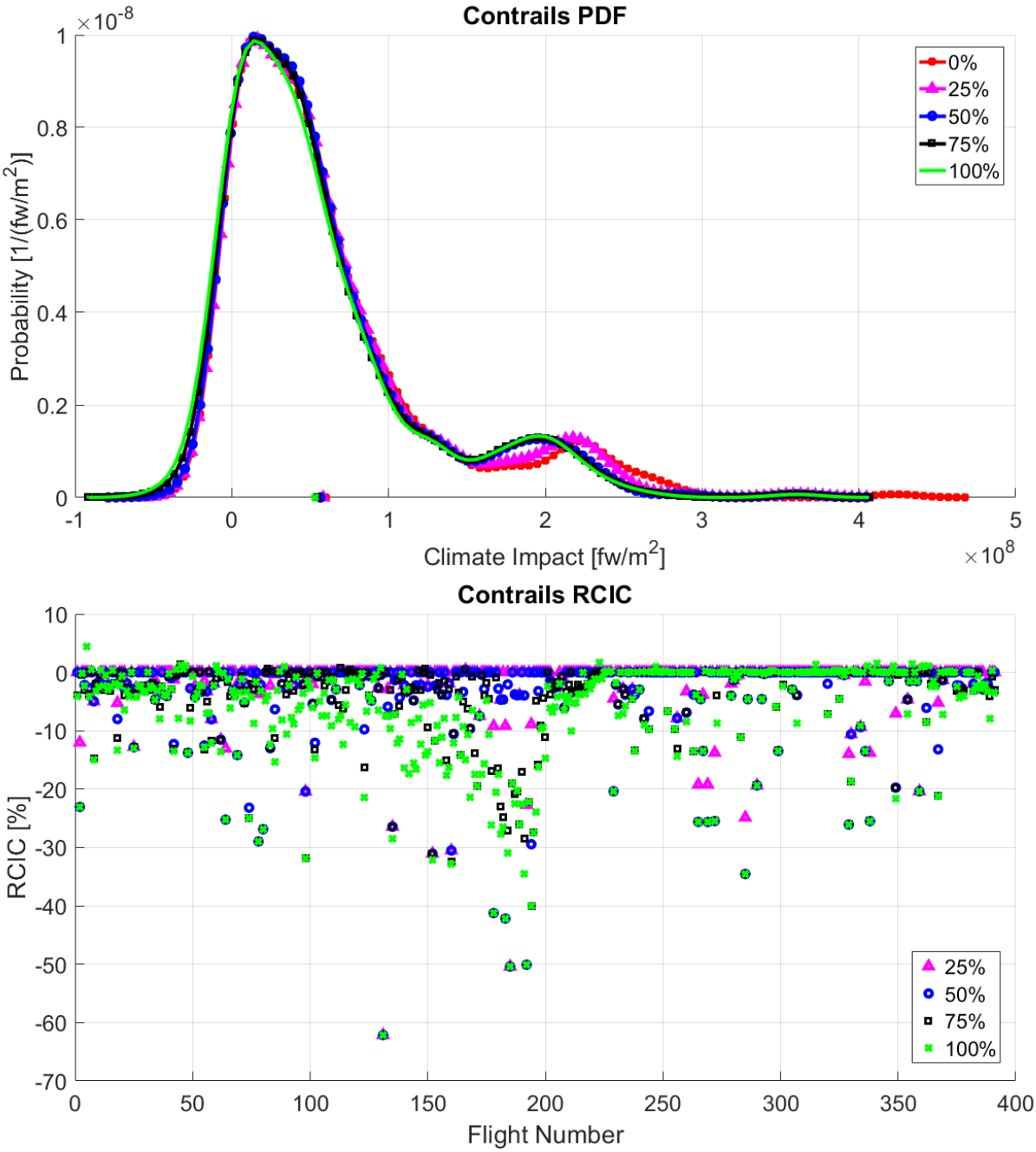

Figure 146. Probability Density Function and *RCIC* of contrails for WP2-Eastbound-AGWP100 case. The different curves and points represent the values for 0%, 25%, 50%, 75% and 100% of *NTCIC*.

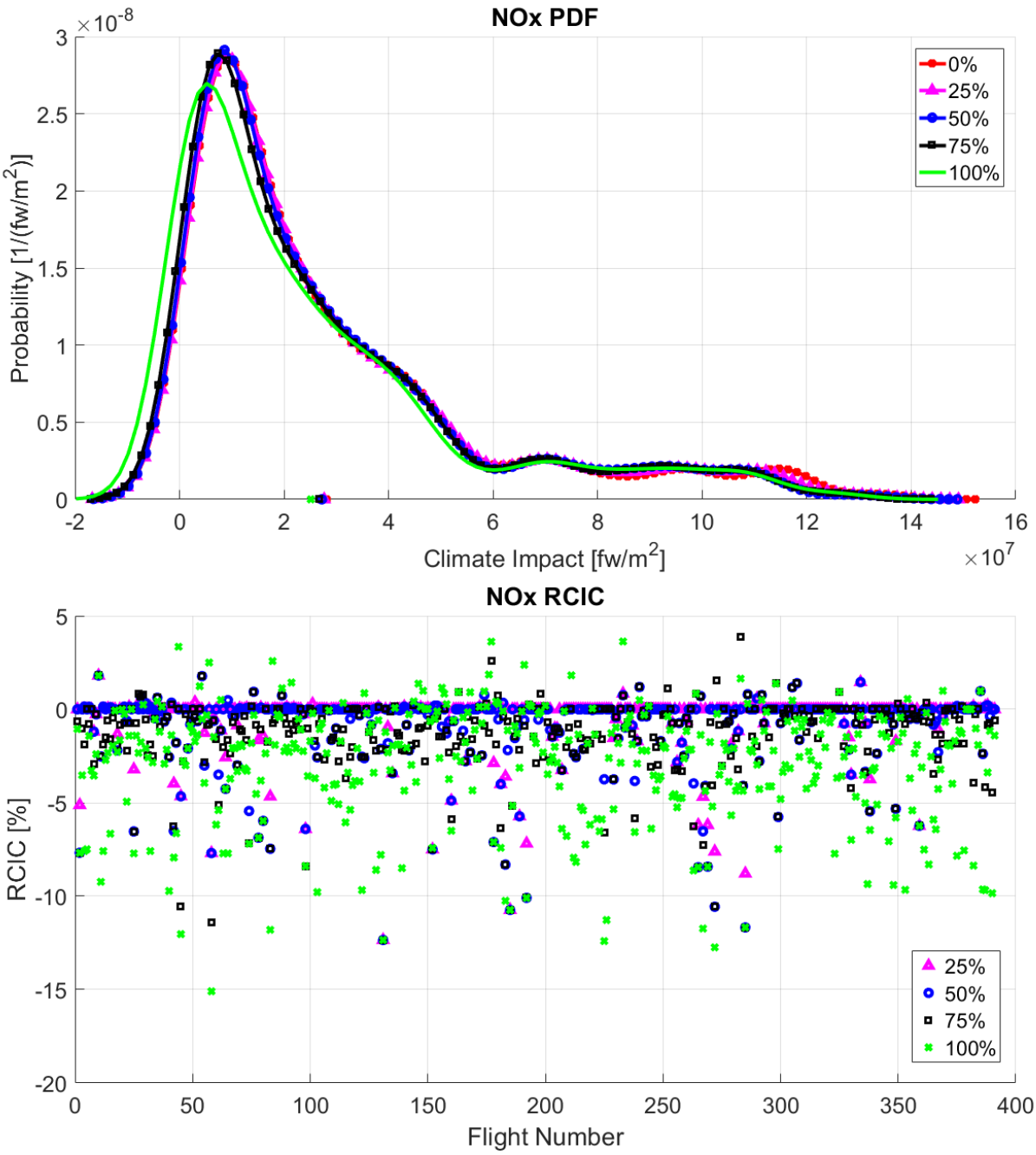

Figure 147. Probability Density Function and *RCIC* of NO_x for WP2-Eastbound-AGWP100 case. The different curves and points represent the values for 0%, 25%, 50%, 75% and 100% of *NTCIC*.

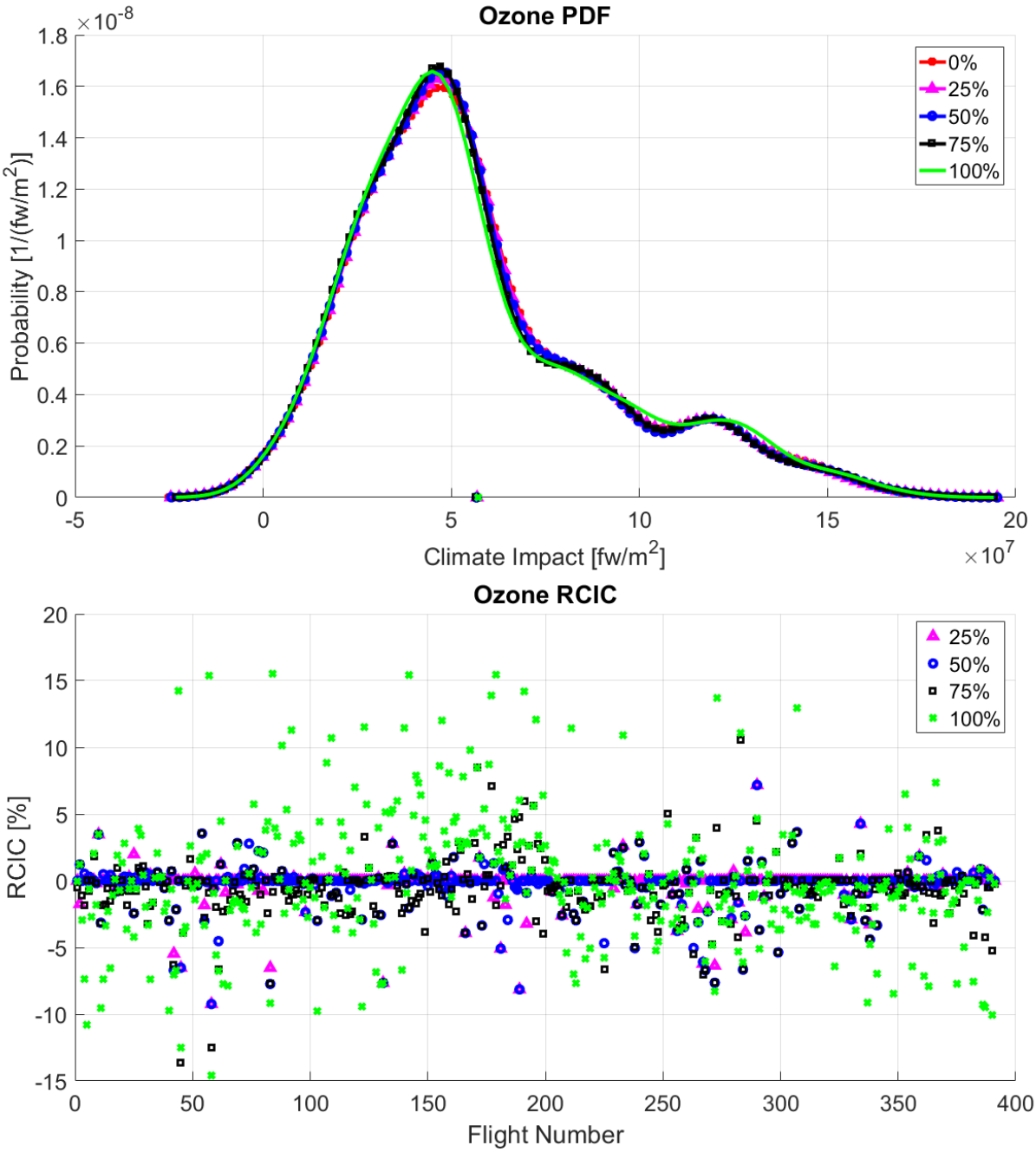

Figure 148. Probability Density Function and *RCIC* of ozone for WP2-Eastbound-AGWP100 case. The different curves and points represent the values for 0%, 25%, 50%, 75% and 100% of *NTCIC*.

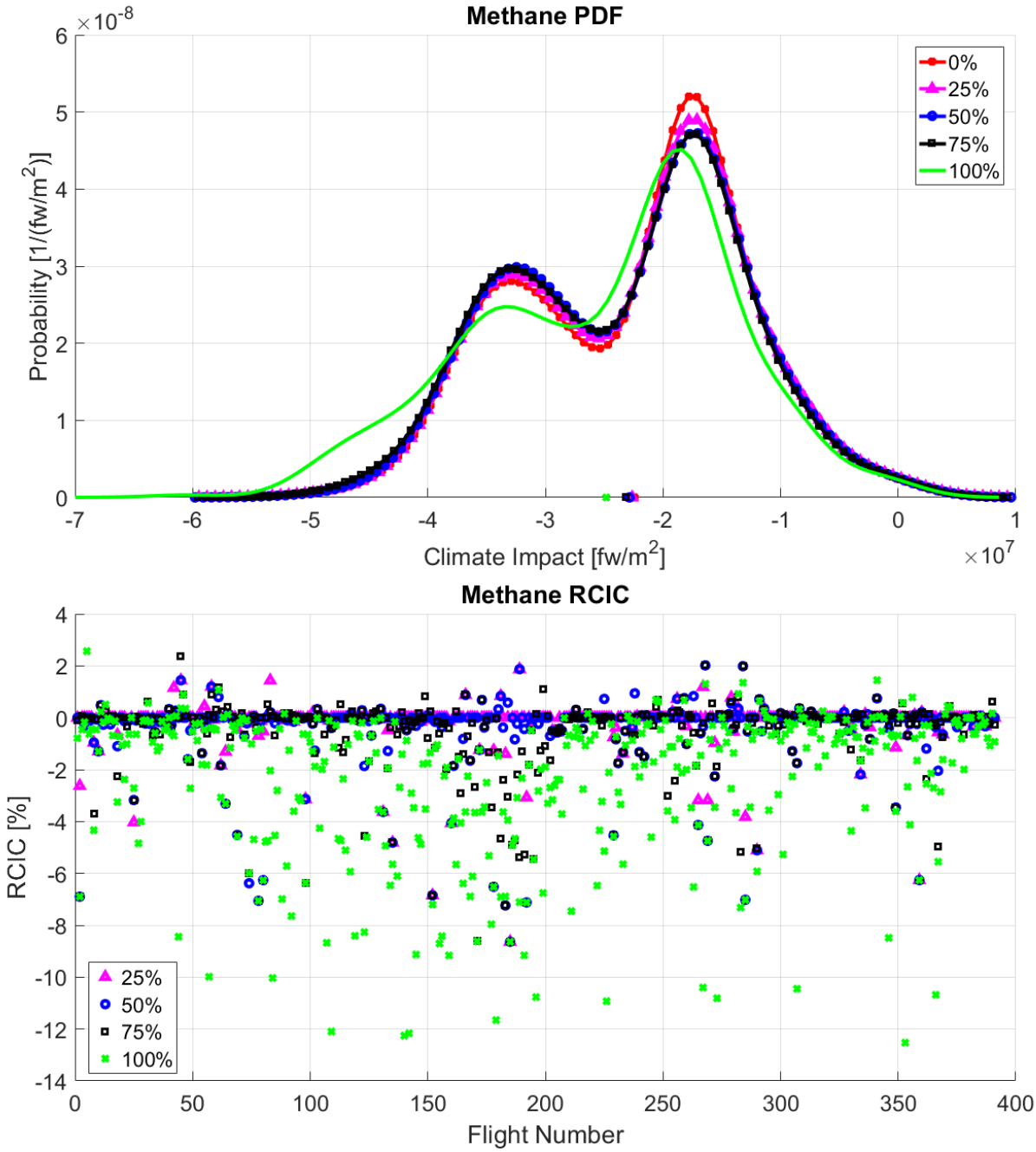

Figure 149. Probability Density Function and *RCIC* of methane for WP2-Eastbound-AGWP100 case. The different curves and points represent the values for 0%, 25%, 50%, 75% and 100% of *NTCIC*.

C.10. Winter Pattern 2 – Westbound

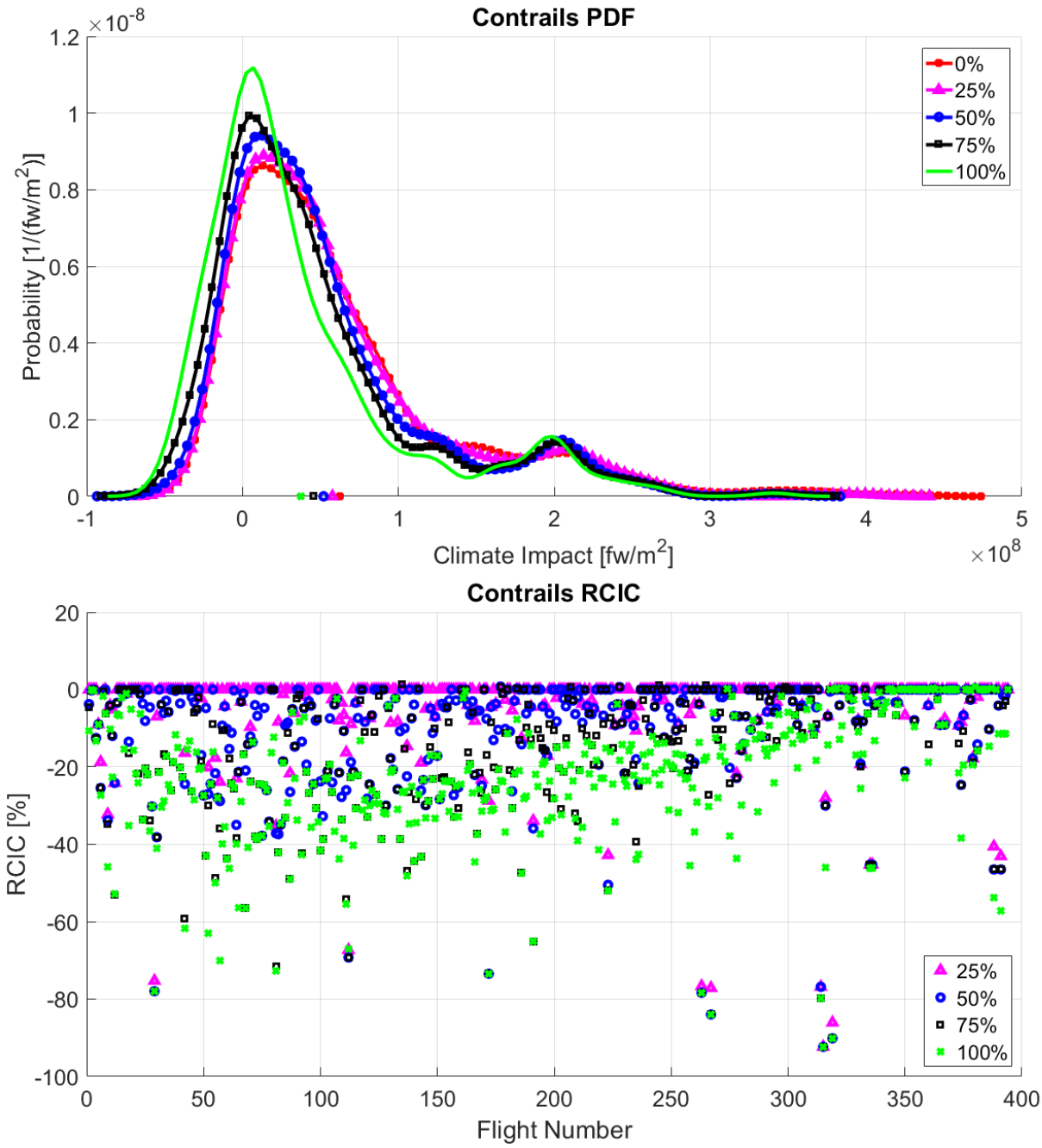

Figure 150. Probability Density Function and *RCIC* of contrails for WP2-Westbound-AGWP100 case. The different curves and points represent the values for 0%, 25%, 50%, 75% and 100% of *NTCIC*.

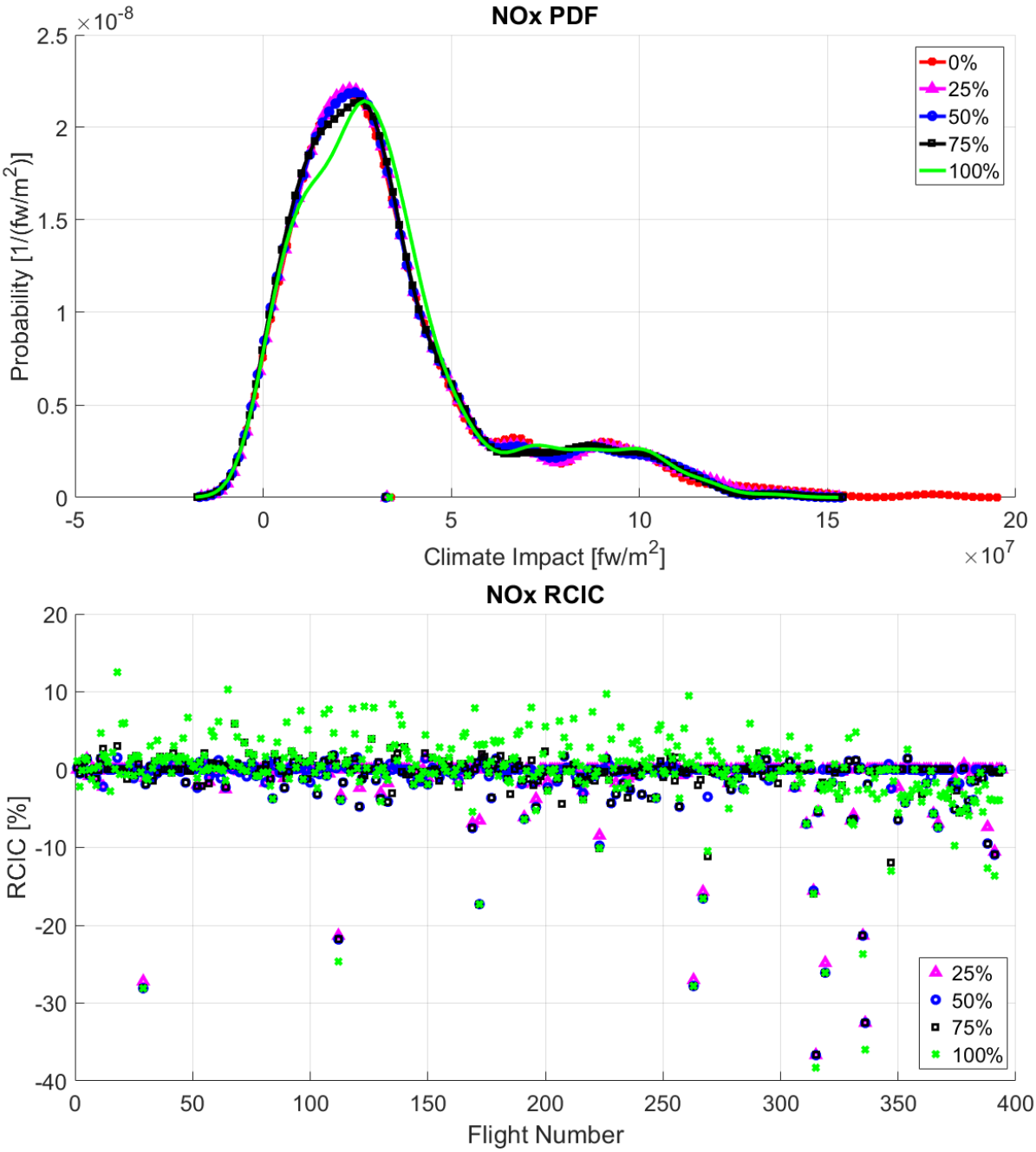

Figure 151. Probability Density Function and *RCIC* of NO_x for WP2-Westbound-AGWP100 case. The different curves and points represent the values for 0%, 25%, 50%, 75% and 100% of *NTCIC*.

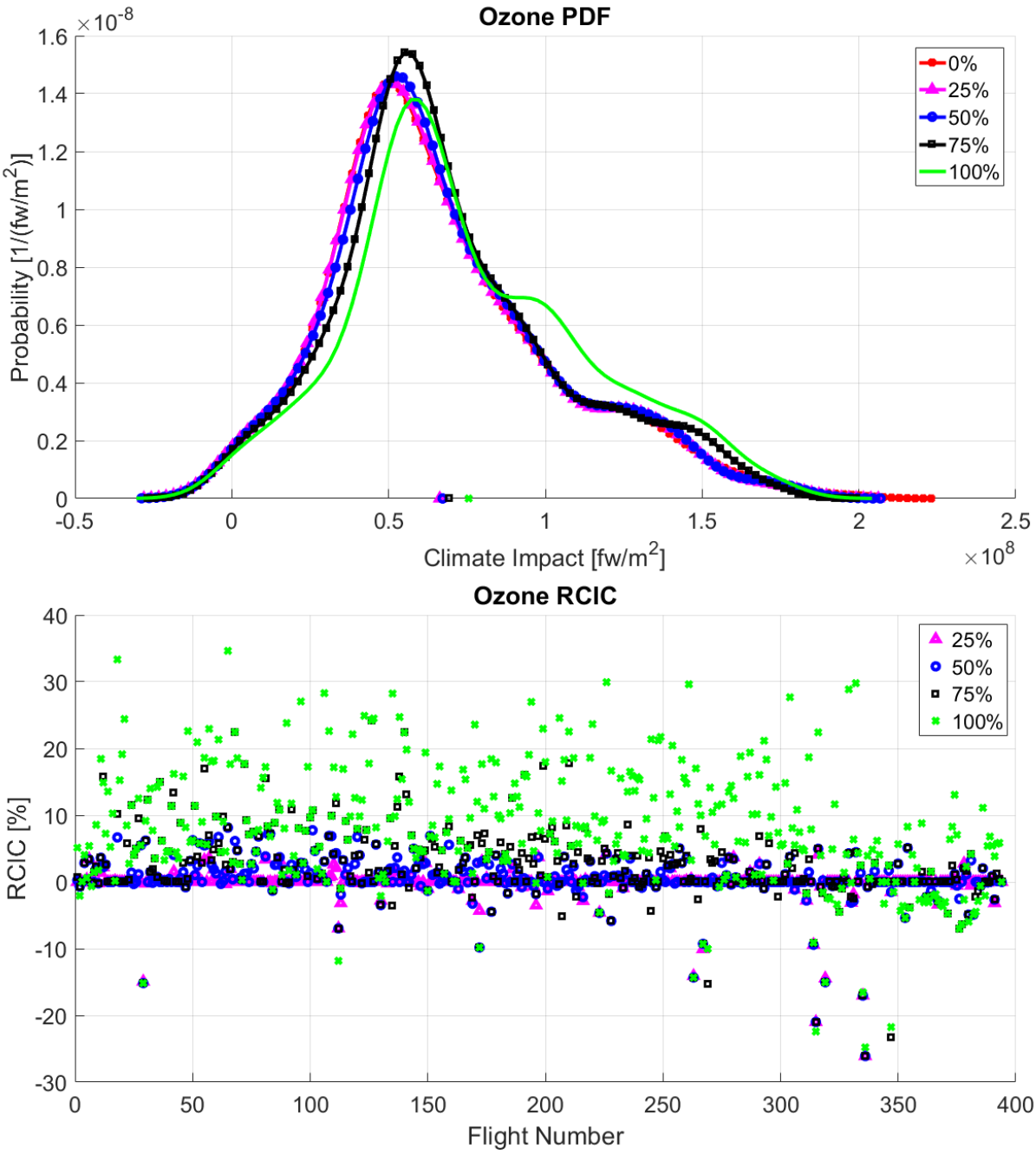

Figure 152. Probability Density Function and *RCIC* of ozone for WP2-Westbound-AGWP100 case. The different curves and points represent the values for 0%, 25%, 50%, 75% and 100% of *NTCIC*.

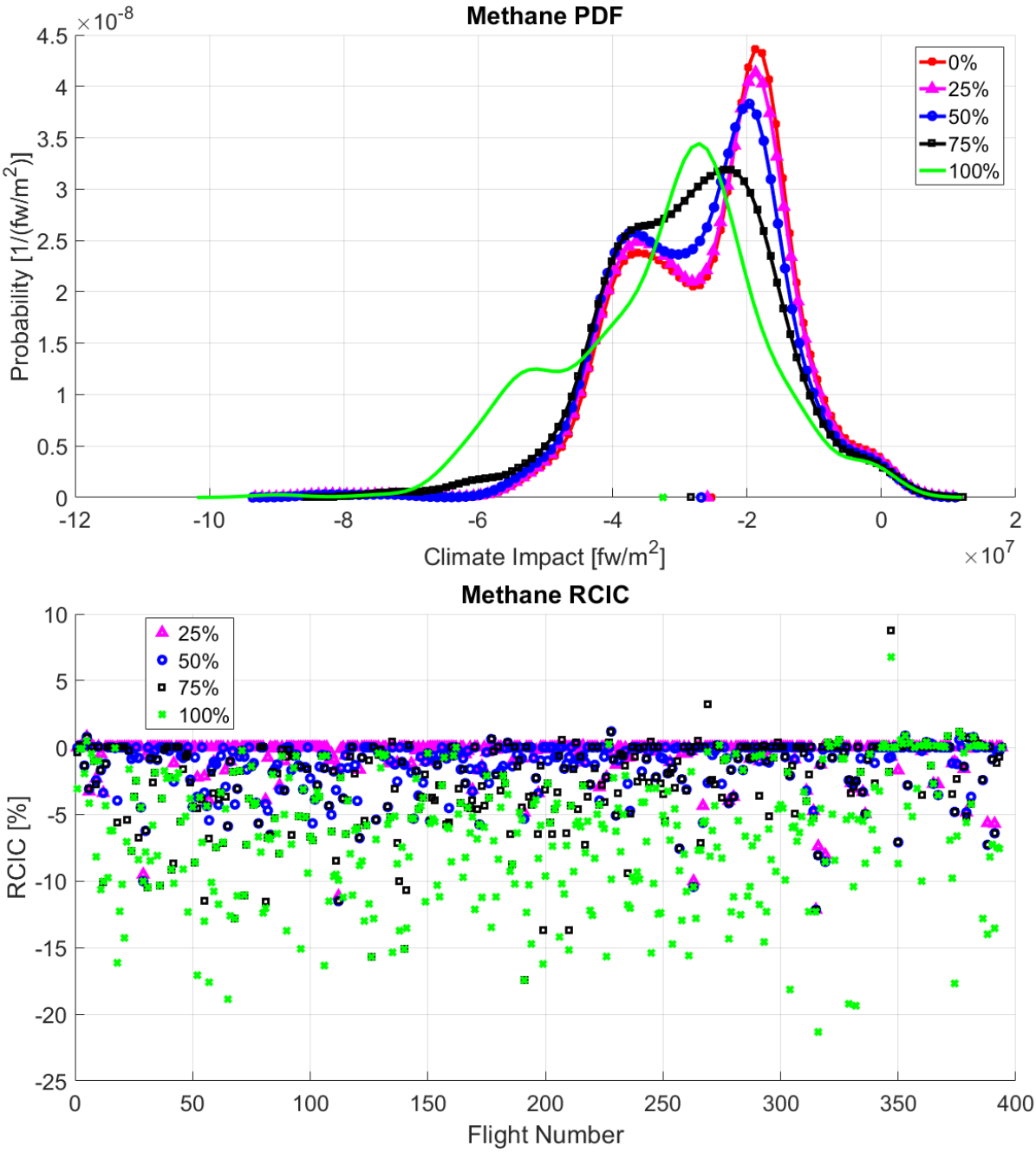

Figure 153. Probability Density Function and *RCIC* of methane for WP2-Westbound-AGWP100 case. The different curves and points represent the values for 0%, 25%, 50%, 75% and 100% of *NTCIC*.

C.11. Winter Pattern 3 – Eastbound

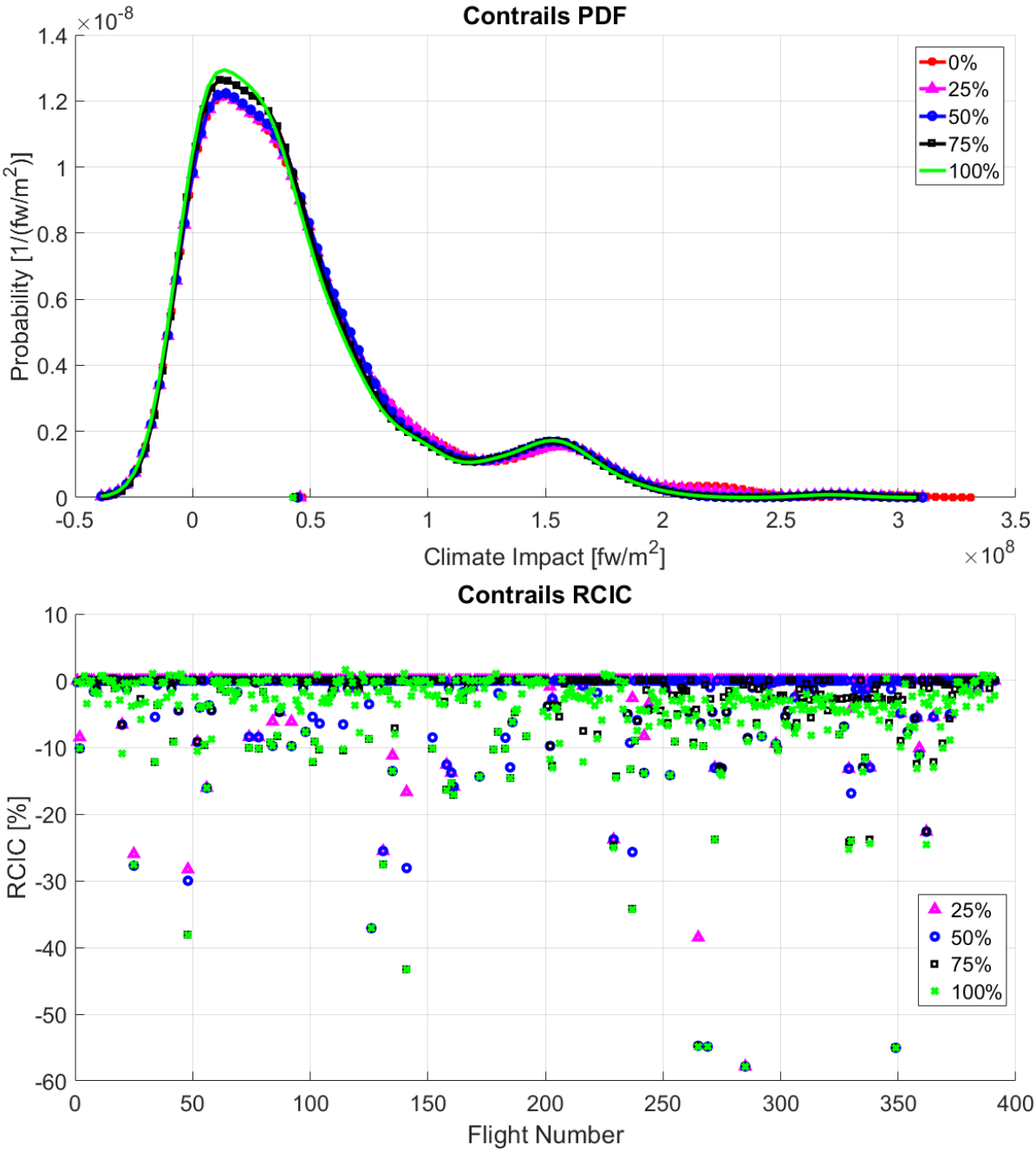

Figure 154. Probability Density Function and *RCIC* of contrails for WP3-Eastbound-AGWP100 case. The different curves and points represent the values for 0%, 25%, 50%, 75% and 100% of *NTCIC*.

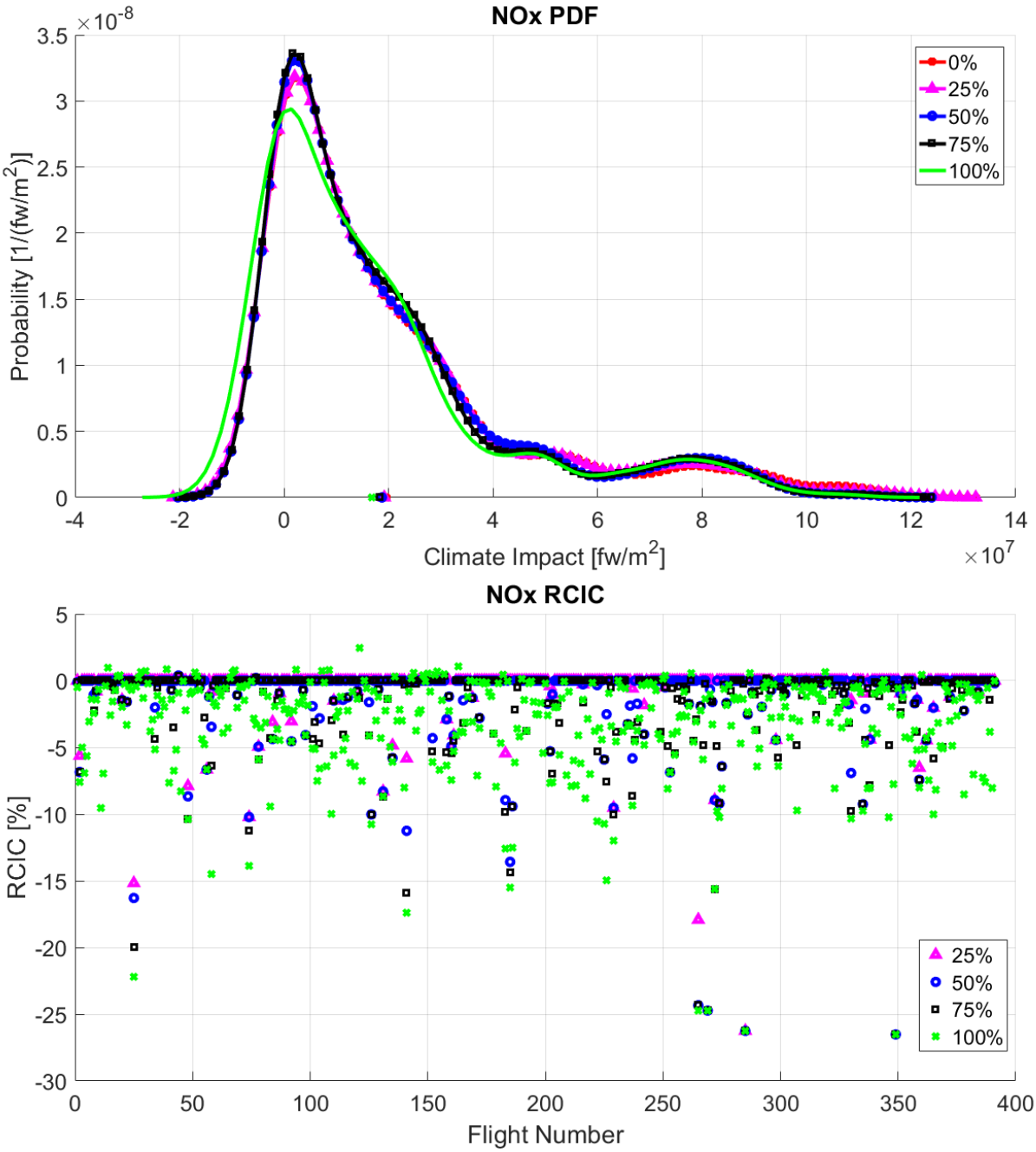

Figure 155. Probability Density Function and *RCIC* of NO_x for WP3-Eastbound-AGWP100 case. The different curves and points represent the values for 0%, 25%, 50%, 75% and 100% of *NTCIC*.

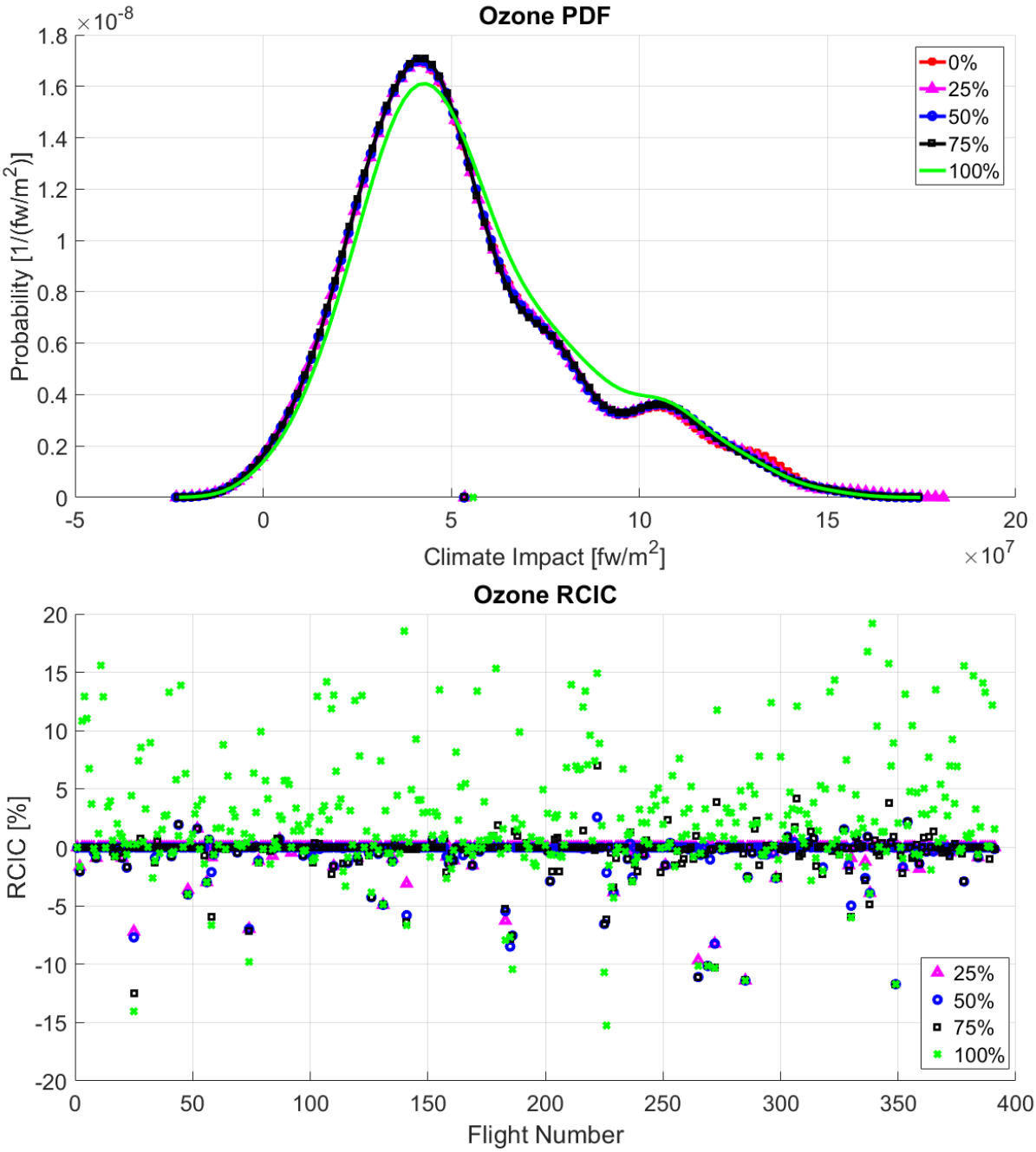

Figure 156. Probability Density Function and *RCIC* of ozone for WP3-Eastbound-AGWP100 case. The different curves and points represent the values for 0%, 25%, 50%, 75% and 100% of *NTCIC*.

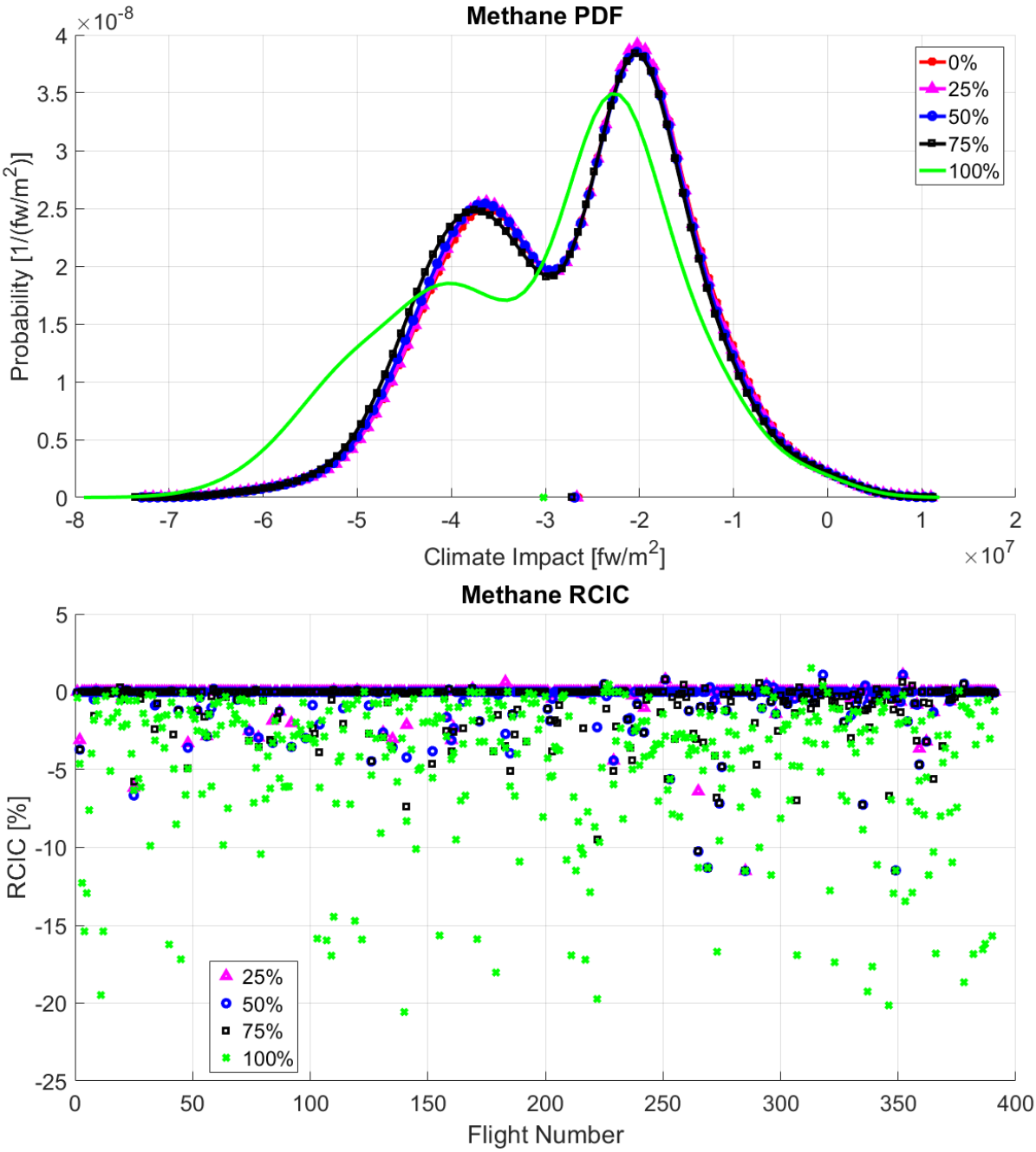

Figure 157. Probability Density Function and *RCIC* of methane for WP3-Eastbound-AGWP100 case. The different curves and points represent the values for 0%, 25%, 50%, 75% and 100% of *NTCIC*.

C.12. Winter Pattern 3 – Westbound

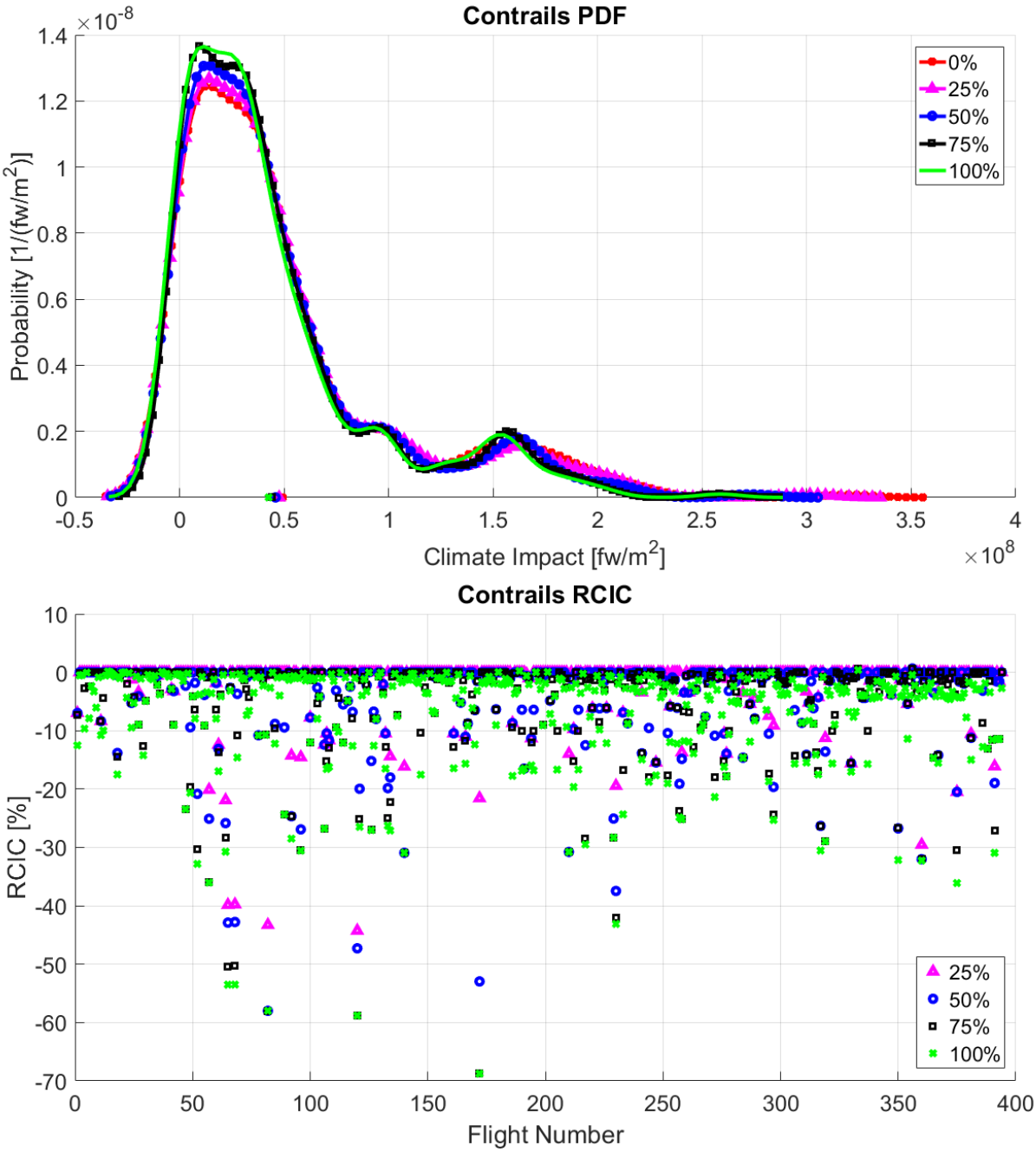

Figure 158. Probability Density Function and *RCIC* of contrails for WP3-Westbound-AGWP100 case. The different curves and points represent the values for 0%, 25%, 50%, 75% and 100% of *NTCIC*.

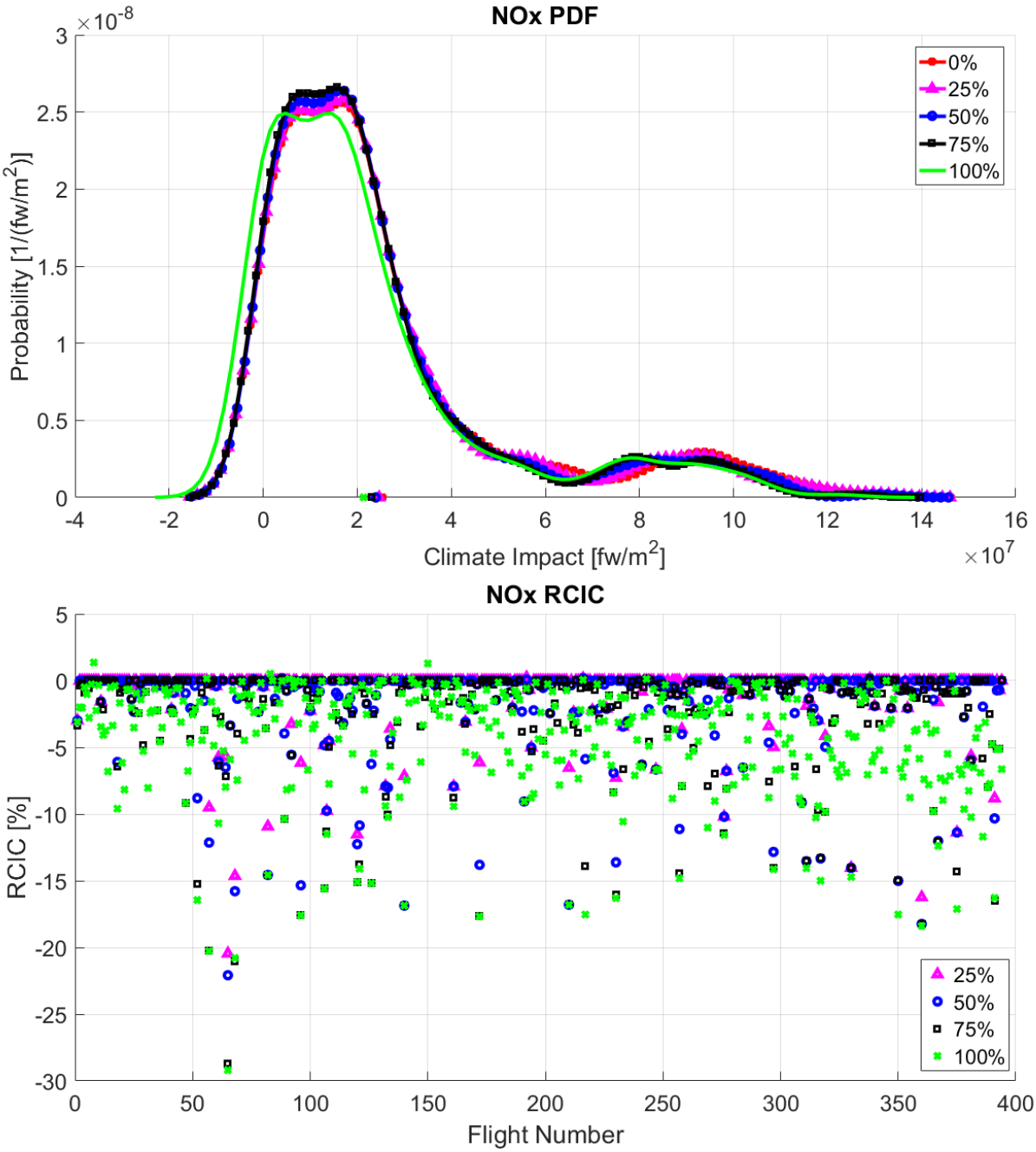

Figure 159. Probability Density Function and *RCIC* of NO_x for WP3-Westbound-AGWP100 case. The different curves and points represent the values for 0%, 25%, 50%, 75% and 100% of *NTCIC*.

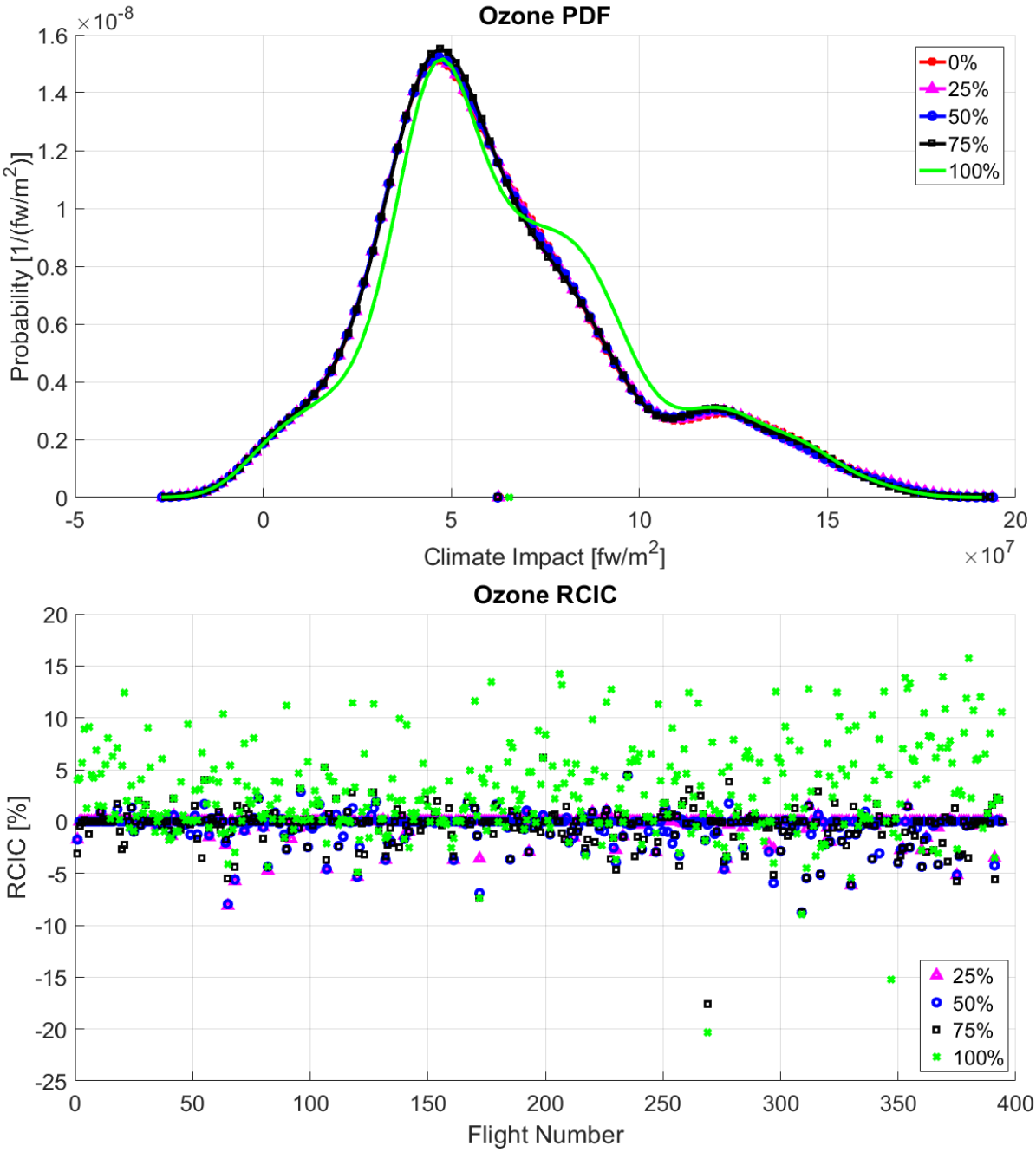

Figure 160. Probability Density Function and *RCIC* of ozone for WP3-Westbound-AGWP100 case. The different curves and points represent the values for 0%, 25%, 50%, 75% and 100% of *NTCIC*.

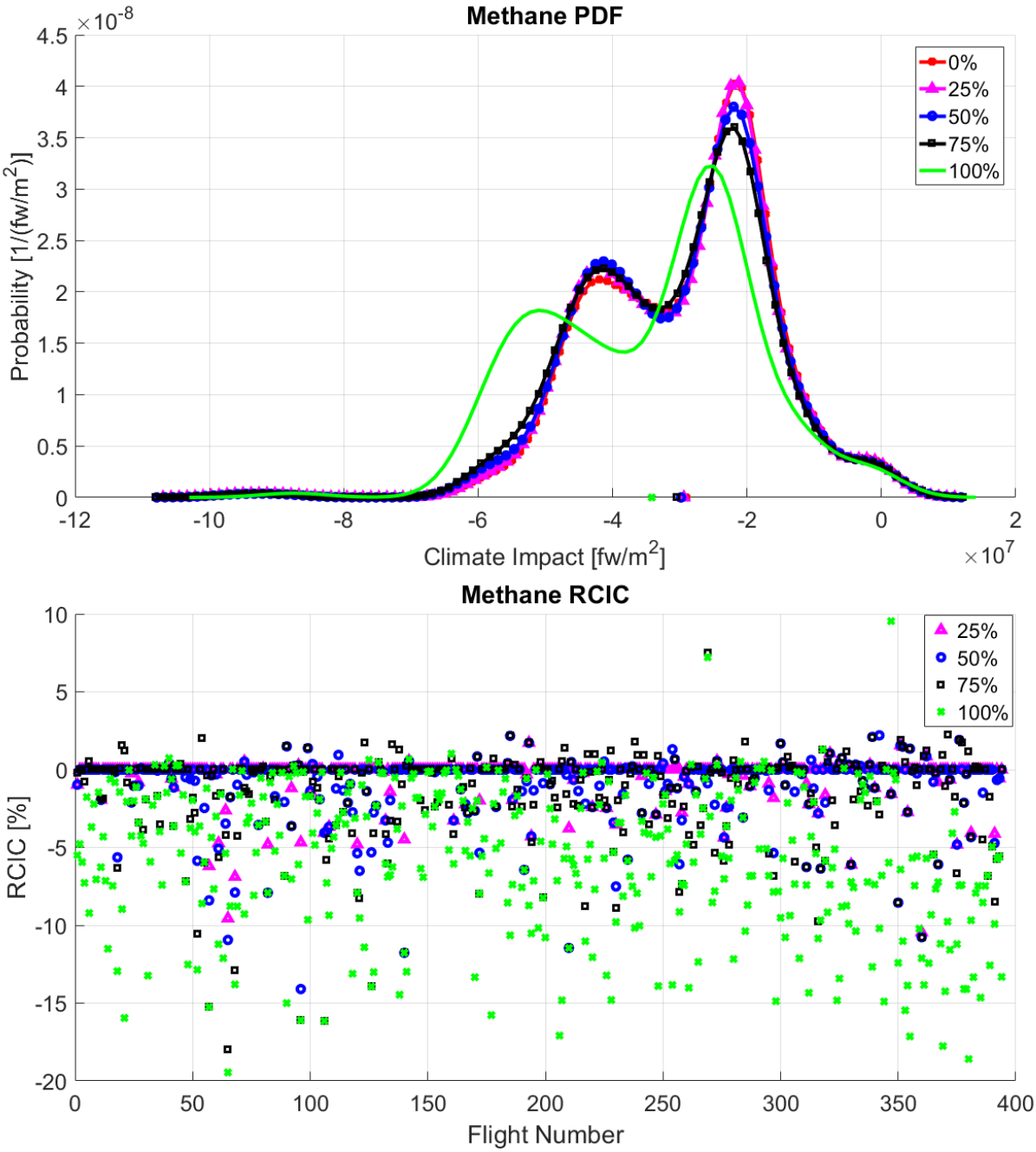

Figure 161. Probability Density Function and *RCIC* of methane for WP3-Westbound-AGWP100 case. The different curves and points represent the values for 0%, 25%, 50%, 75% and 100% of *NTCIC*.

C.13. Winter Pattern 4 – Eastbound

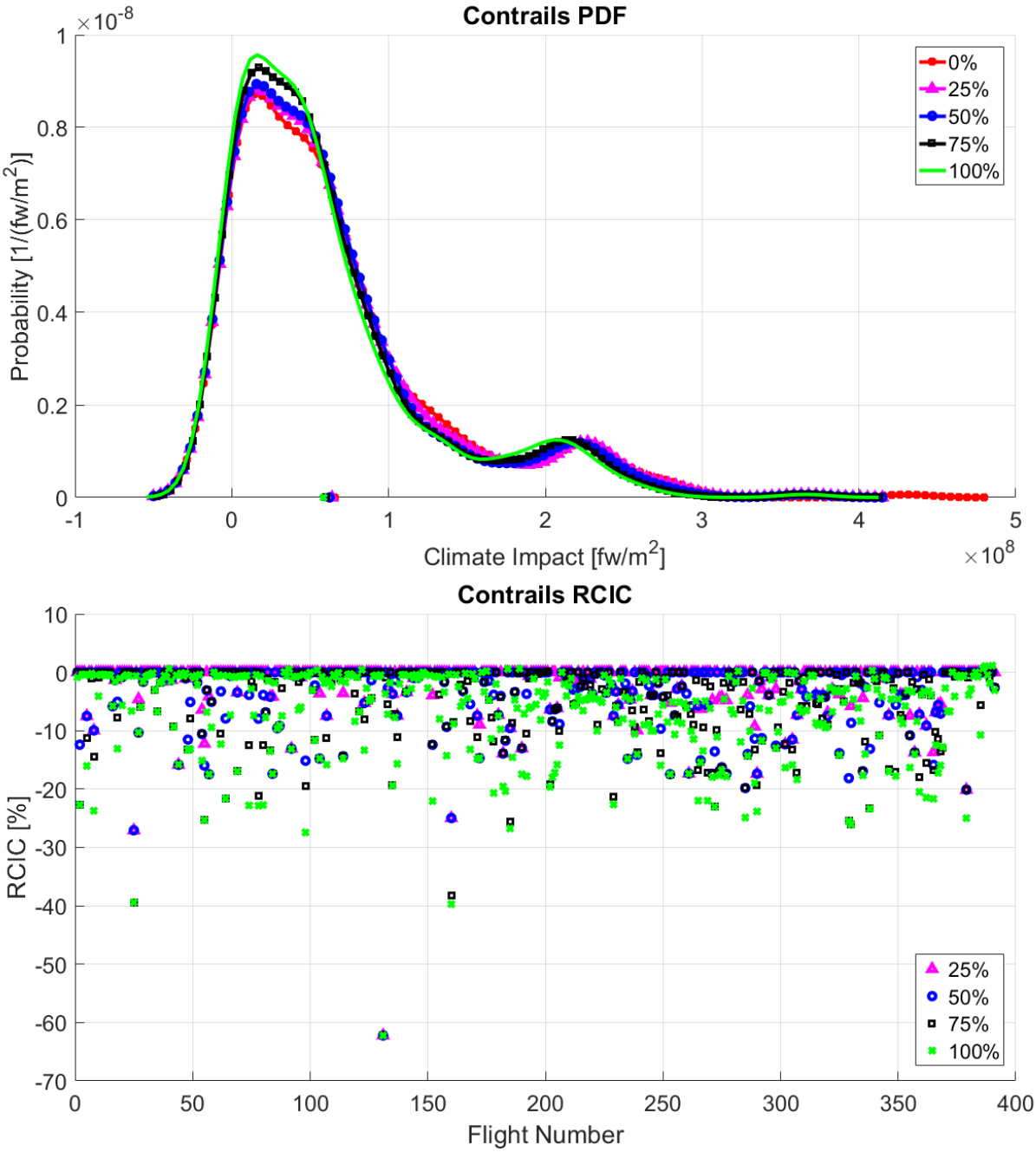

Figure 162. Probability Density Function and *RCIC* of contrails for WP4-Eastbound-AGWP100 case. The different curves and points represent the values for 0%, 25%, 50%, 75% and 100% of *NTCIC*.

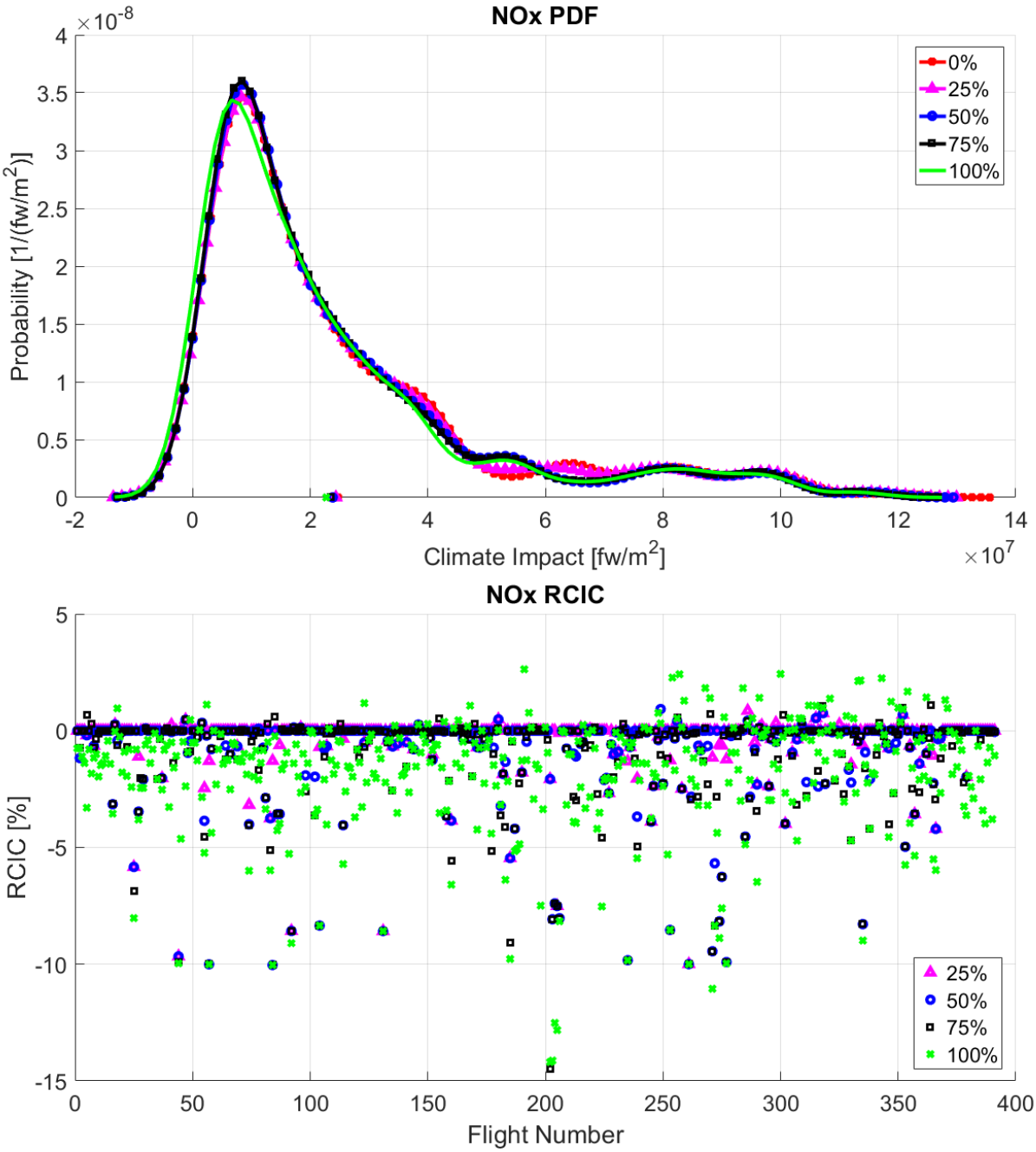

Figure 163. Probability Density Function and *RCIC* of NO_x for WP4-Eastbound-AGWP100 case. The different curves and points represent the values for 0%, 25%, 50%, 75% and 100% of *NTCIC*.

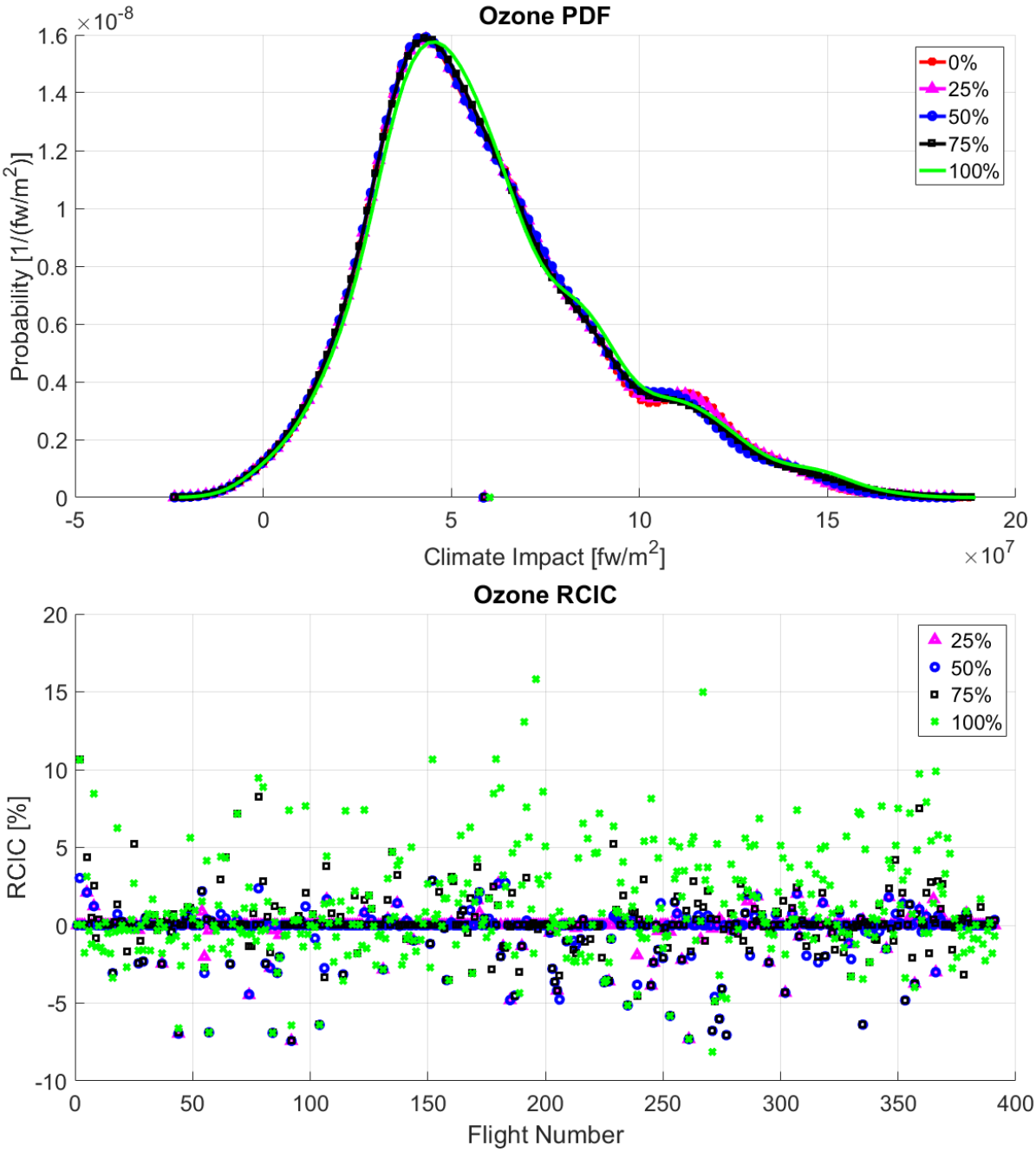

Figure 164. Probability Density Function and *RCIC* of ozone for WP4-Eastbound-AGWP100 case. The different curves and points represent the values for 0%, 25%, 50%, 75% and 100% of *NTCIC*.

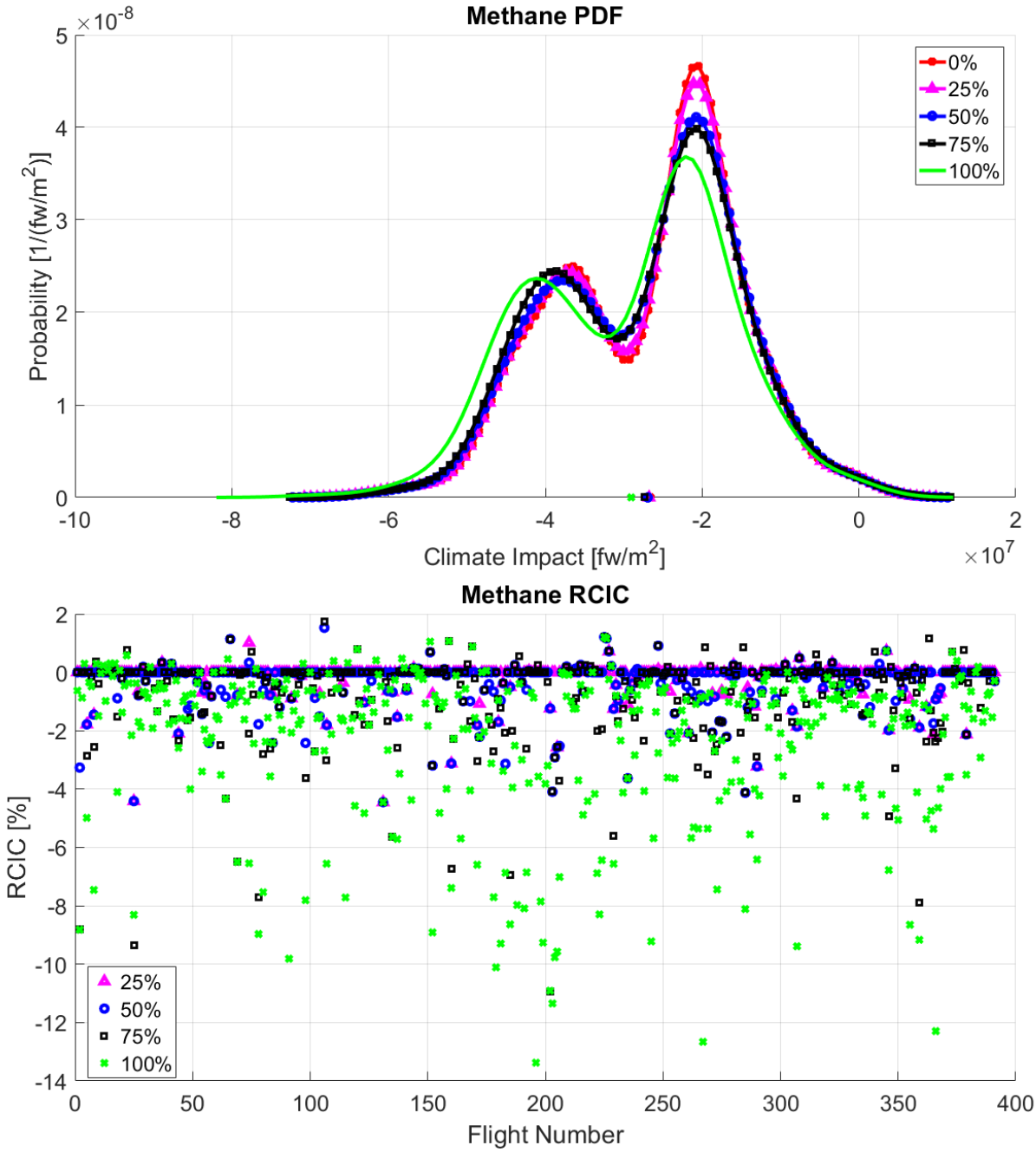

Figure 165. Probability Density Function and *RCIC* of methane for WP4-Eastbound-AGWP100 case. The different curves and points represent the values for 0%, 25%, 50%, 75% and 100% of *NTCIC*.

C.14. Winter Pattern 4 – Westbound

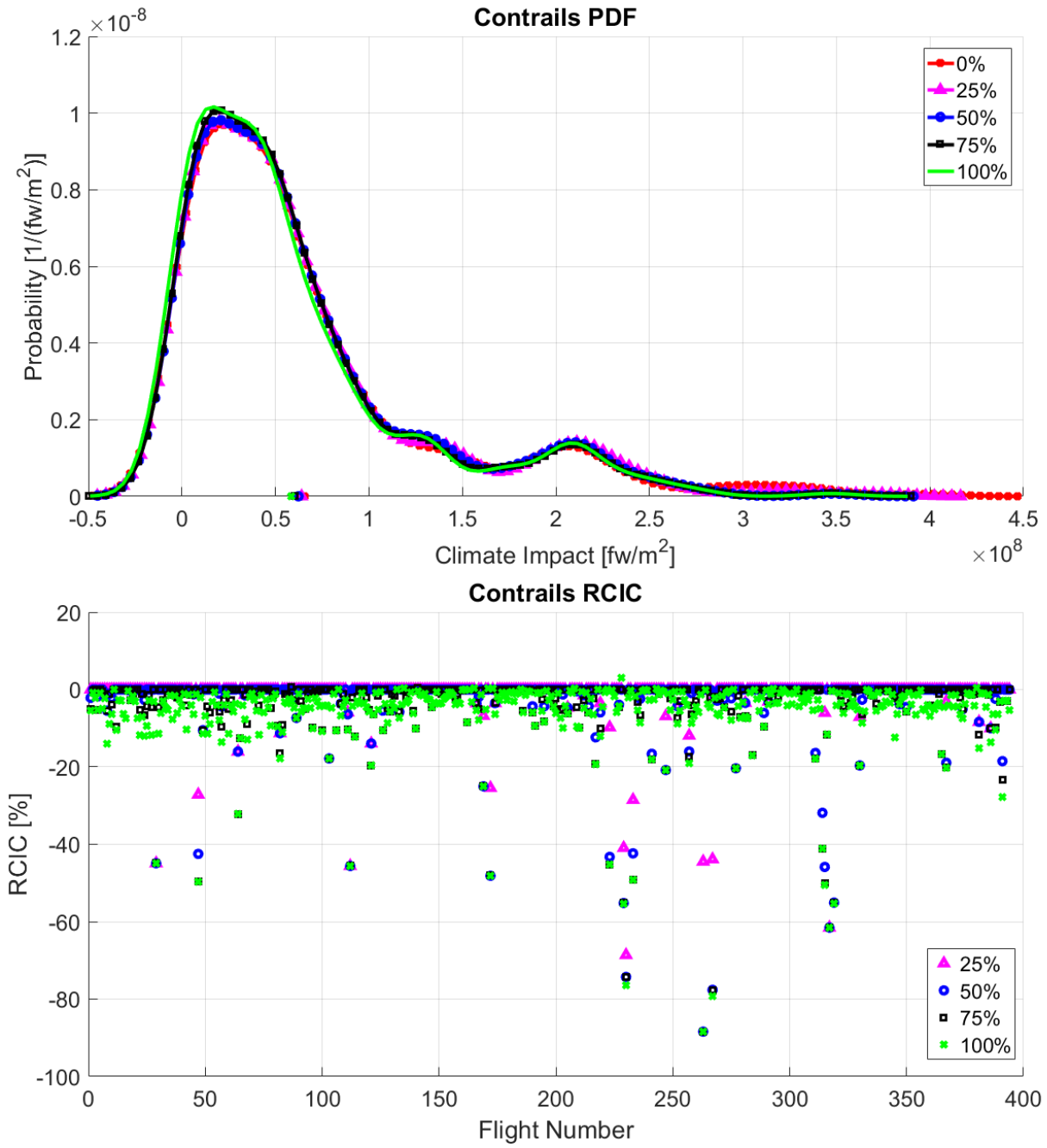

Figure 166. Probability Density Function and *RCIC* of contrails for WP4-Westbound-AGWP100 case. The different curves and points represent the values for 0%, 25%, 50%, 75% and 100% of *NTCIC*.

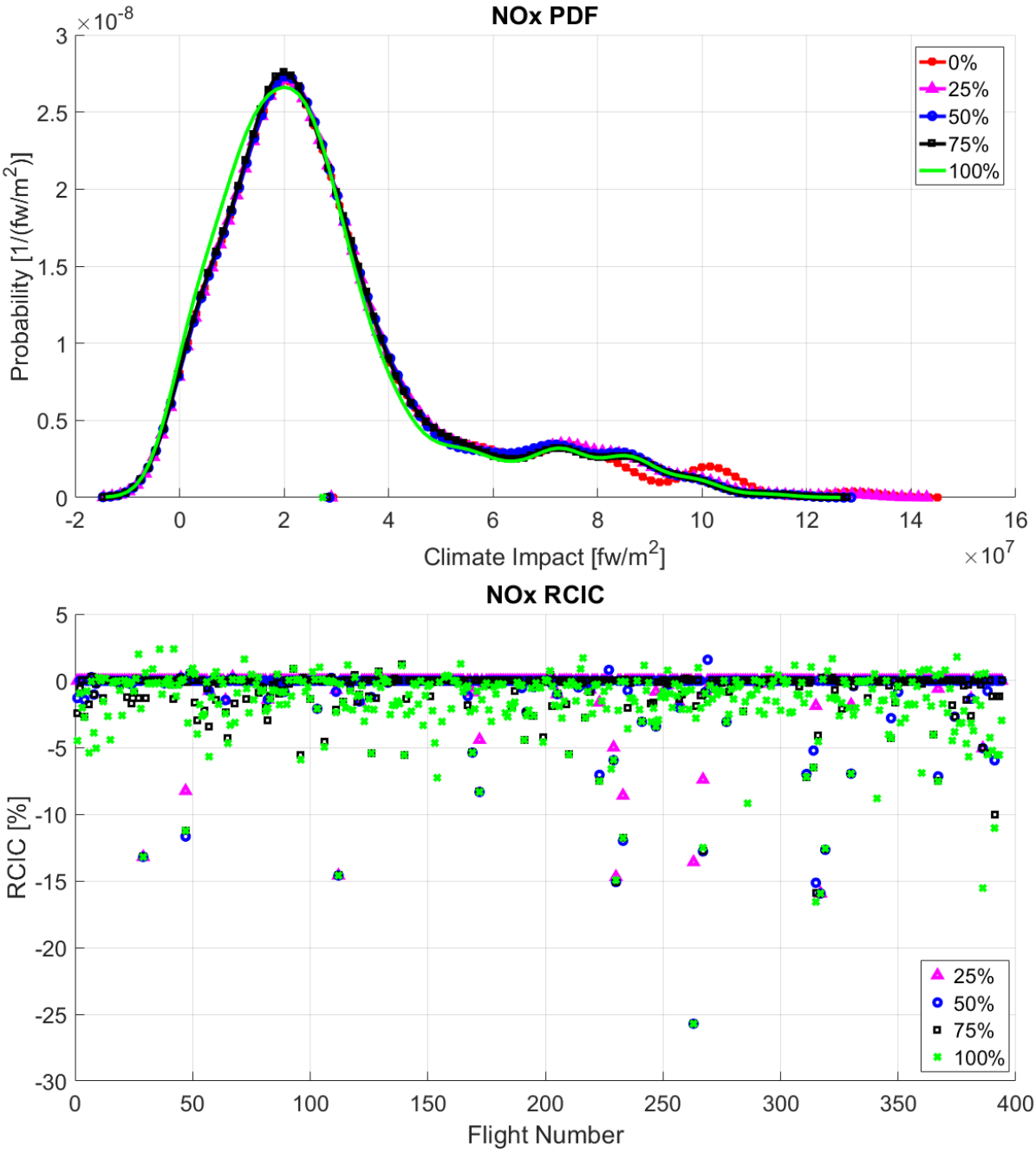

Figure 167. Probability Density Function and *RCIC* of NO_x for WP4-Westbound-AGWP100 case. The different curves and points represent the values for 0%, 25%, 50%, 75% and 100% of *NTCIC*.

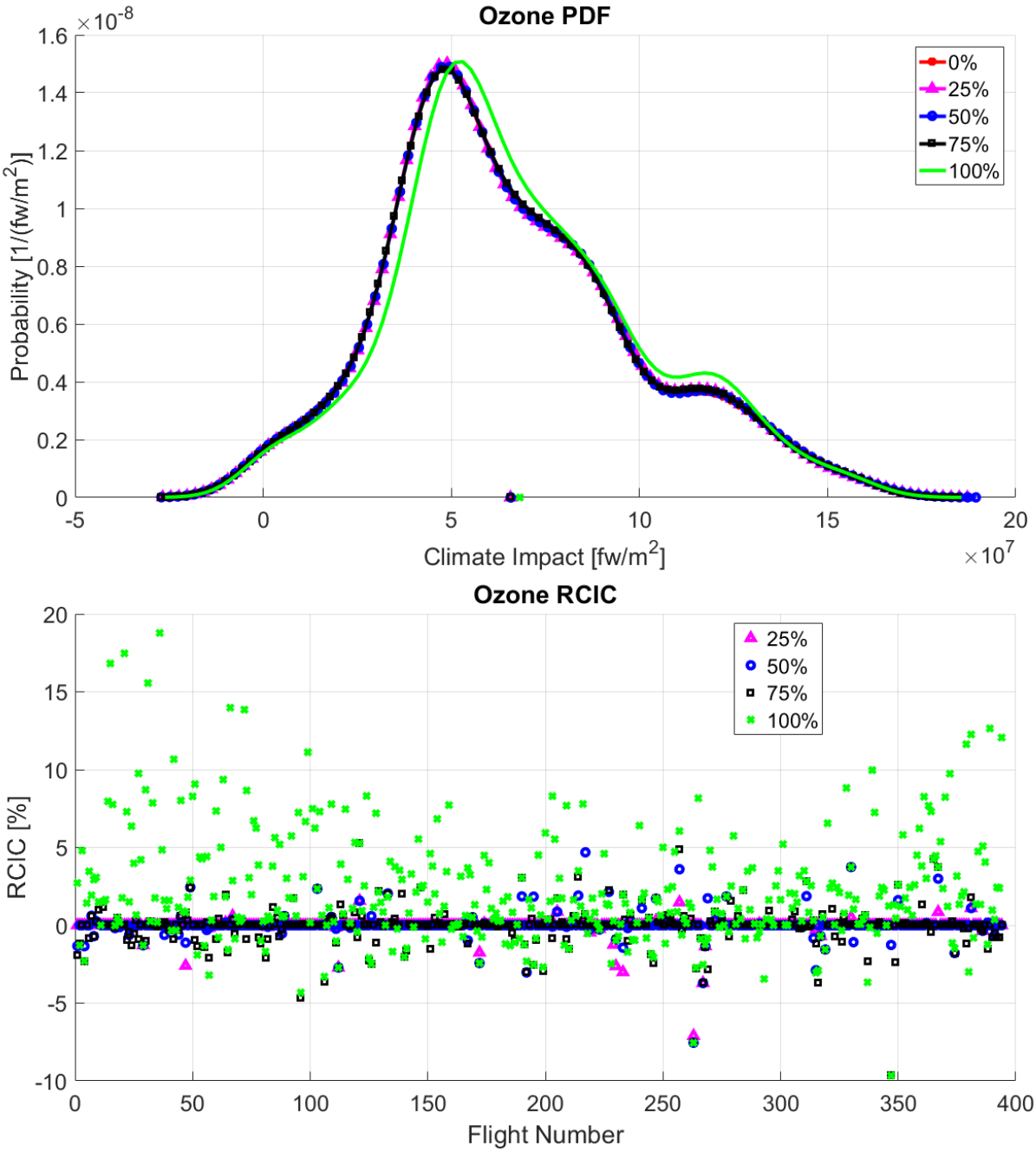

Figure 168. Probability Density Function and *RCIC* of ozone for WP4-Westbound-AGWP100 case. The different curves and points represent the values for 0%, 25%, 50%, 75% and 100% of *NTCIC*.

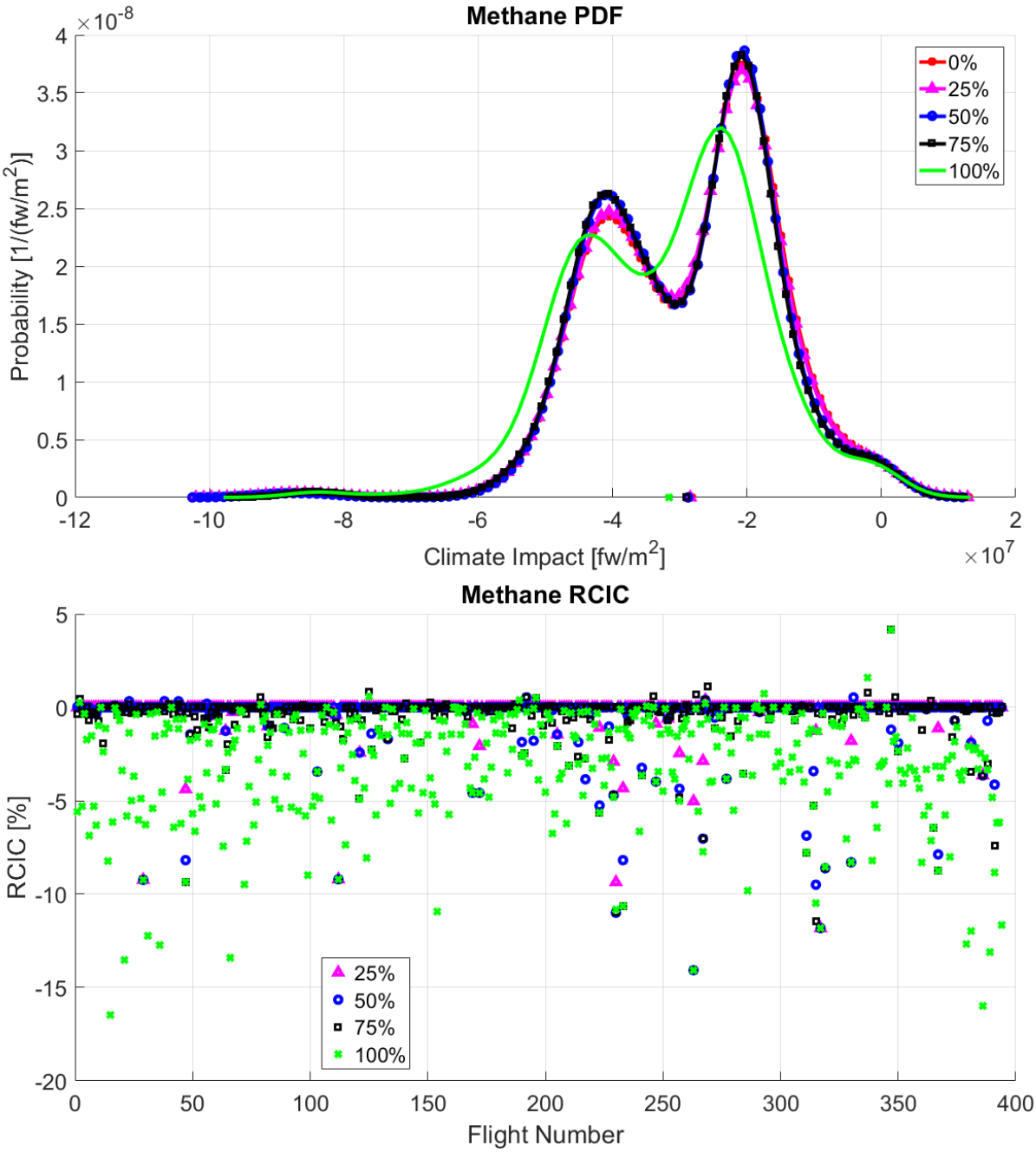

Figure 169. Probability Density Function and *RCIC* of methane for WP4-Westbound-AGWP100 case. The different curves and points represent the values for 0%, 25%, 50%, 75% and 100% of *NTCIC*.

C.15. Winter Pattern 5 – Eastbound

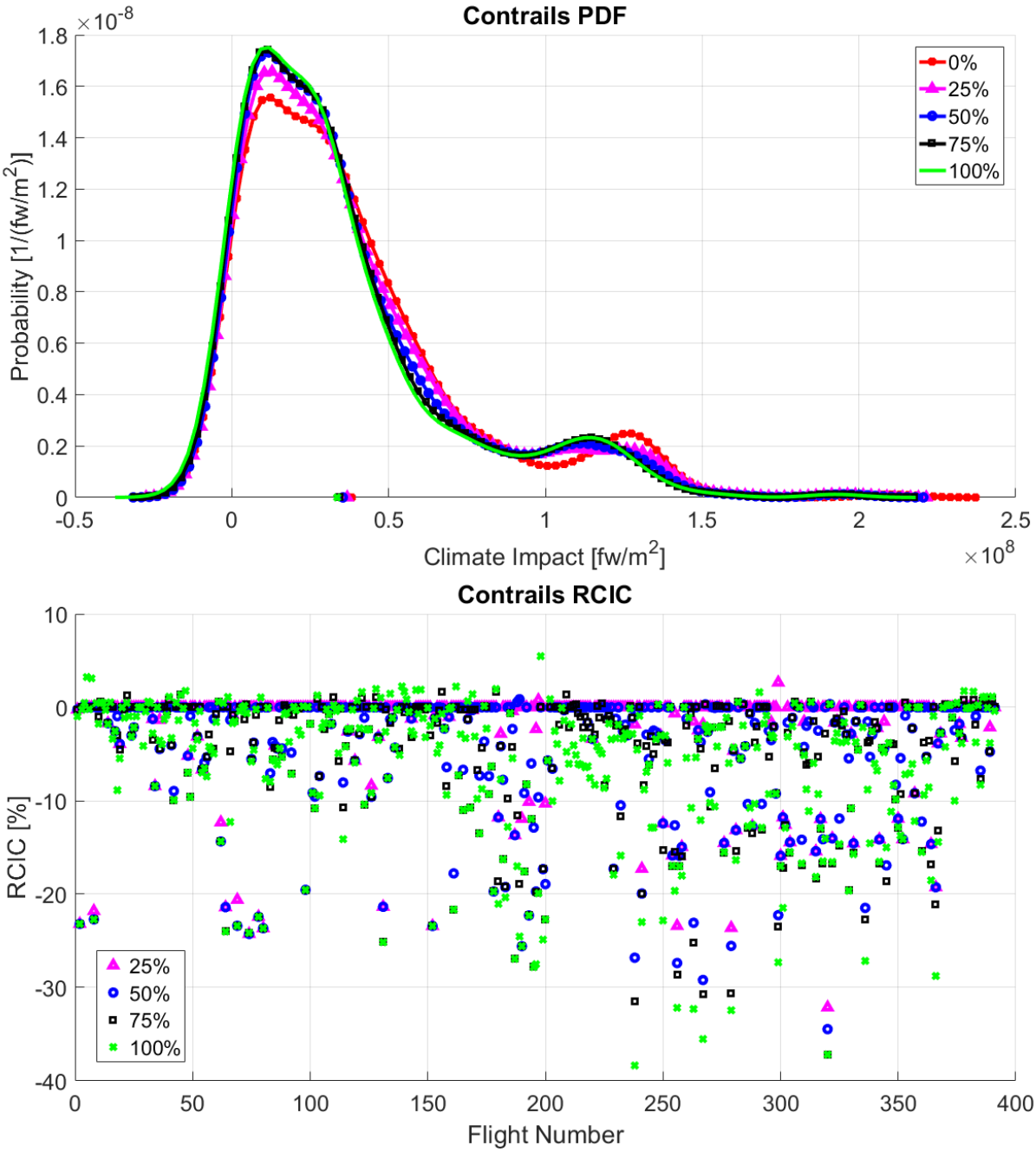

Figure 170. Probability Density Function and *RCIC* of contrails for WP5-Eastbound-AGWP100 case. The different curves and points represent the values for 0%, 25%, 50%, 75% and 100% of *NTCIC*.

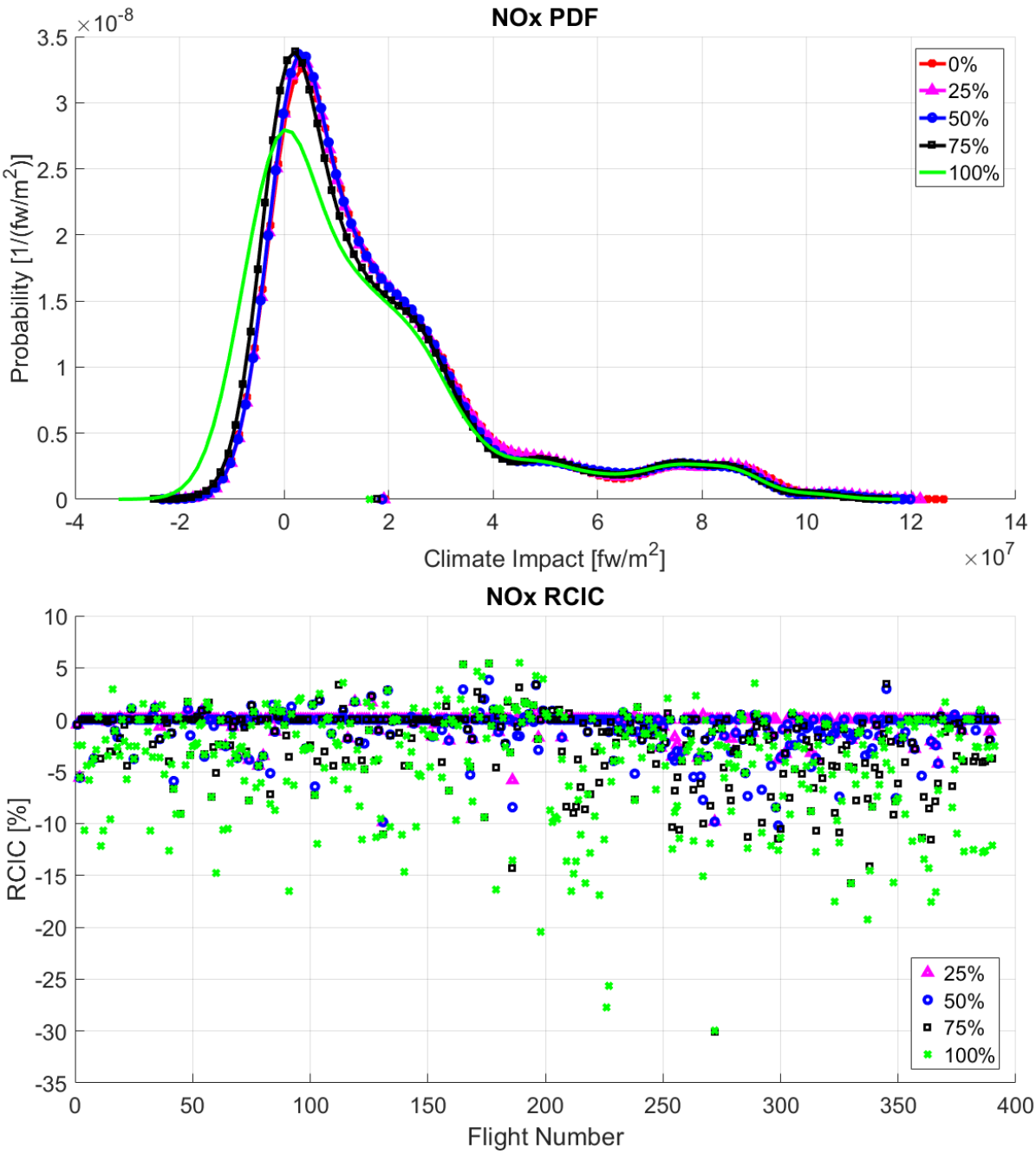

Figure 171. Probability Density Function and *RCIC* of NO_x for WP5-Eastbound-AGWP100 case. The different curves and points represent the values for 0%, 25%, 50%, 75% and 100% of *NTCIC*.

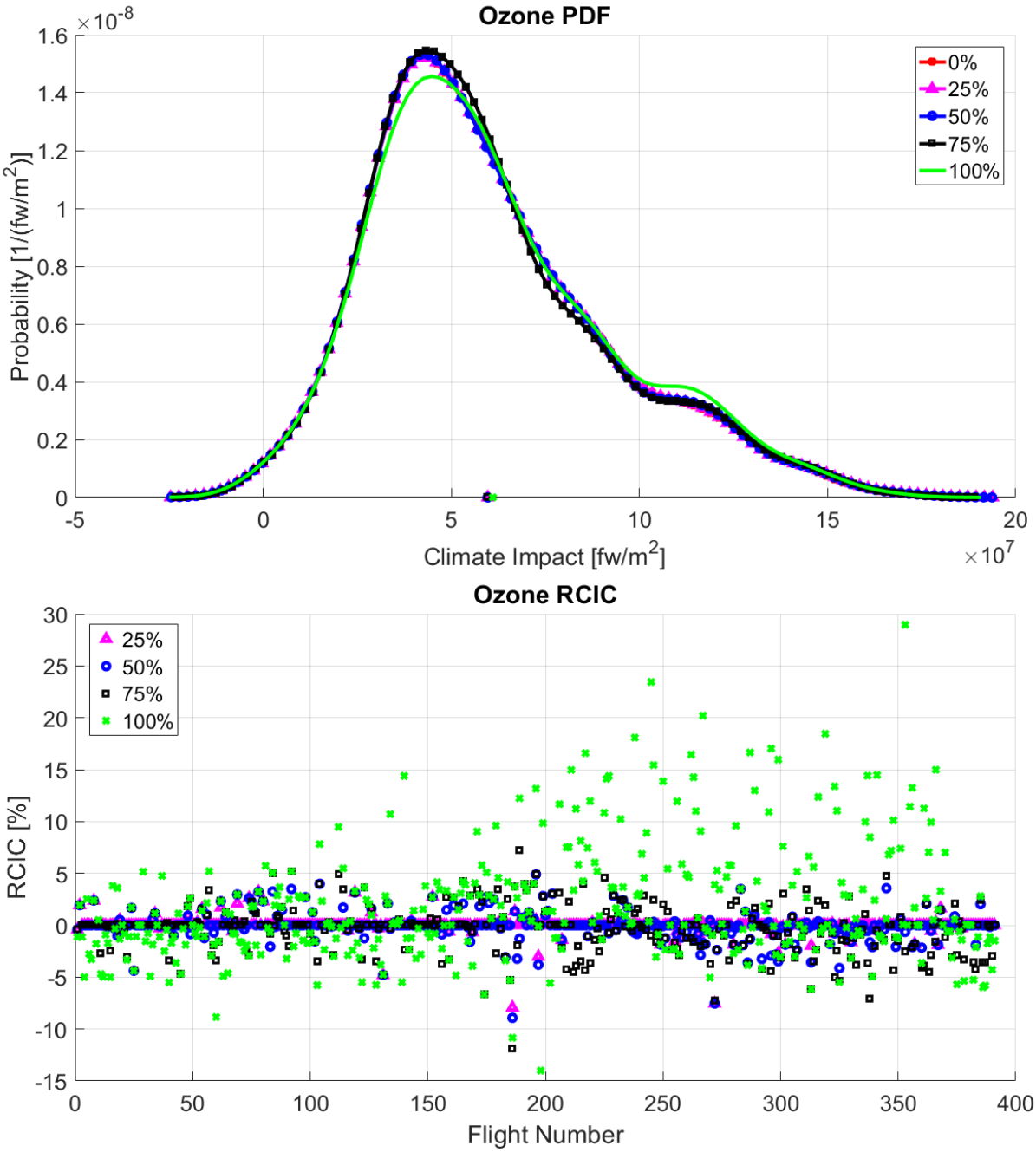

Figure 172. Probability Density Function and *RCIC* of ozone for WP5-Eastbound-AGWP100 case. The different curves and points represent the values for 0%, 25%, 50%, 75% and 100% of *NTCIC*.

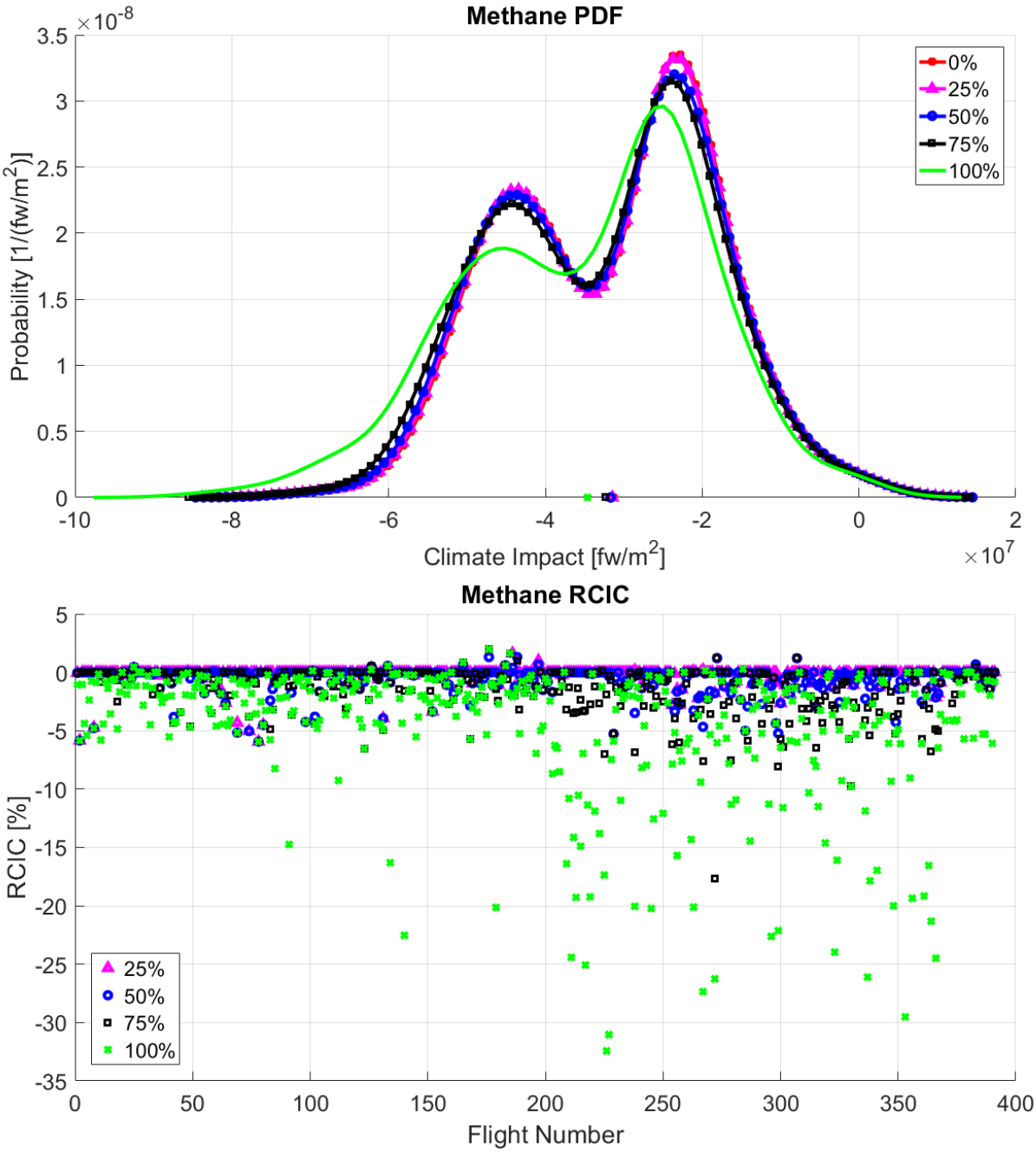

Figure 173. Probability Density Function and *RCIC* of methane for WP5-Eastbound-AGWP100 case. The different curves and points represent the values for 0%, 25%, 50%, 75% and 100% of *NTCIC*.

C.16. Winter Pattern 5 – Westbound

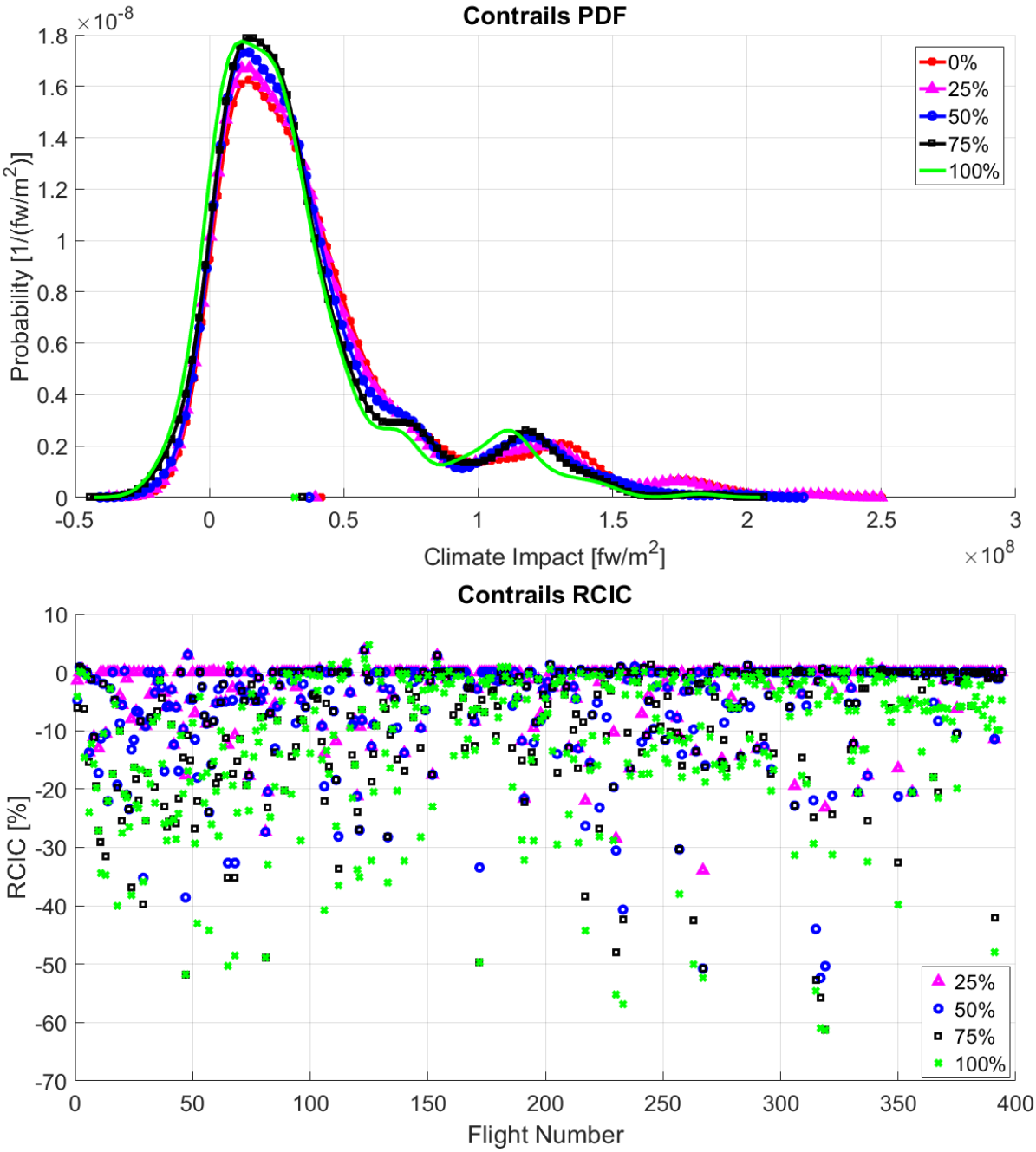

Figure 174. Probability Density Function and *RCIC* of contrails for WP5-Westbound-AGWP100 case. The different curves and points represent the values for 0%, 25%, 50%, 75% and 100% of *NTCIC*.

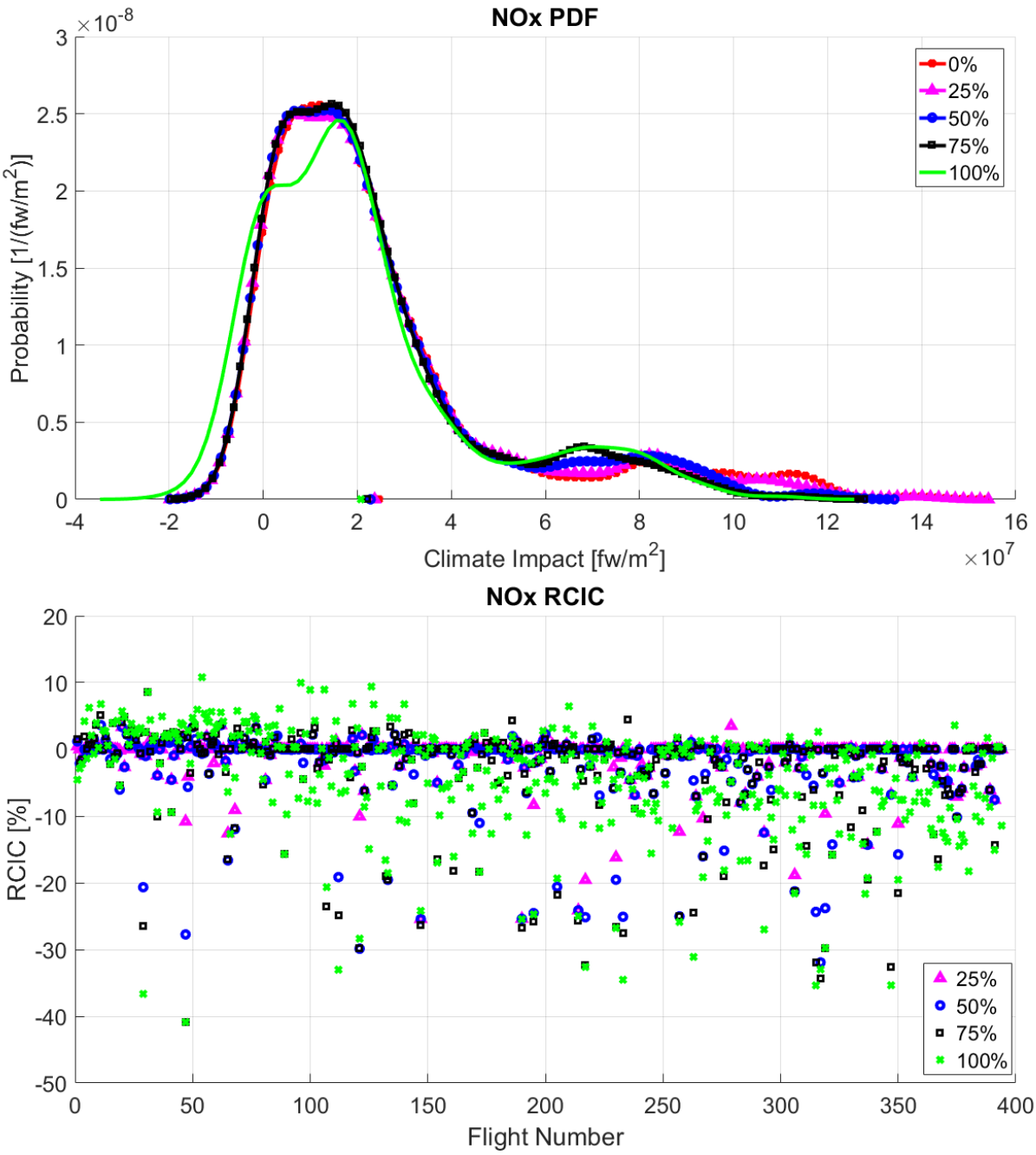

Figure 175. Probability Density Function and *RCIC* of NO_x for WP5-Westbound-AGWP100 case. The different curves and points represent the values for 0%, 25%, 50%, 75% and 100% of *NTCIC*.

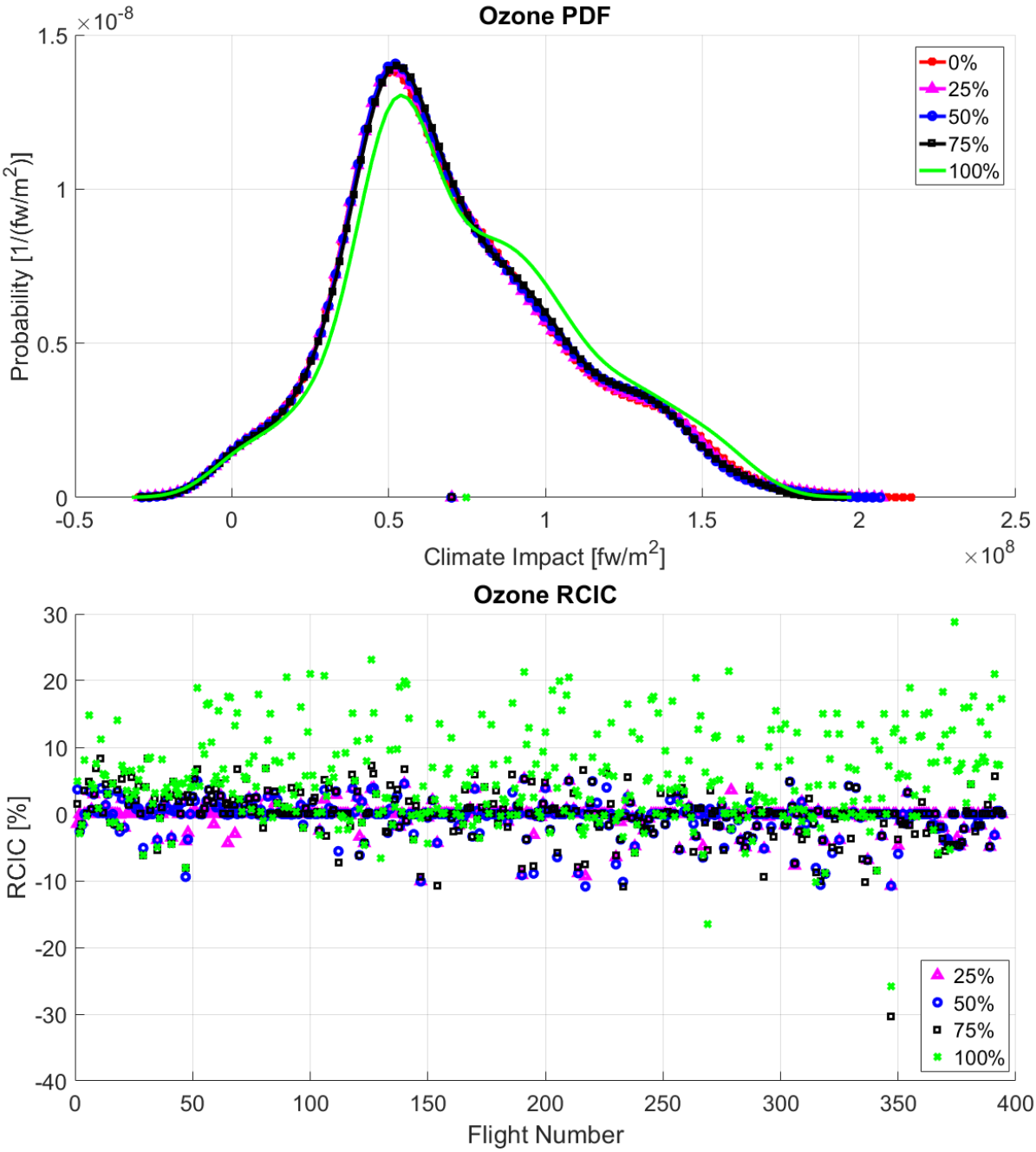

Figure 176. Probability Density Function and *RCIC* of ozone for WP5-Westbound-AGWP100 case. The different curves and points represent the values for 0%, 25%, 50%, 75% and 100% of *NTCIC*.

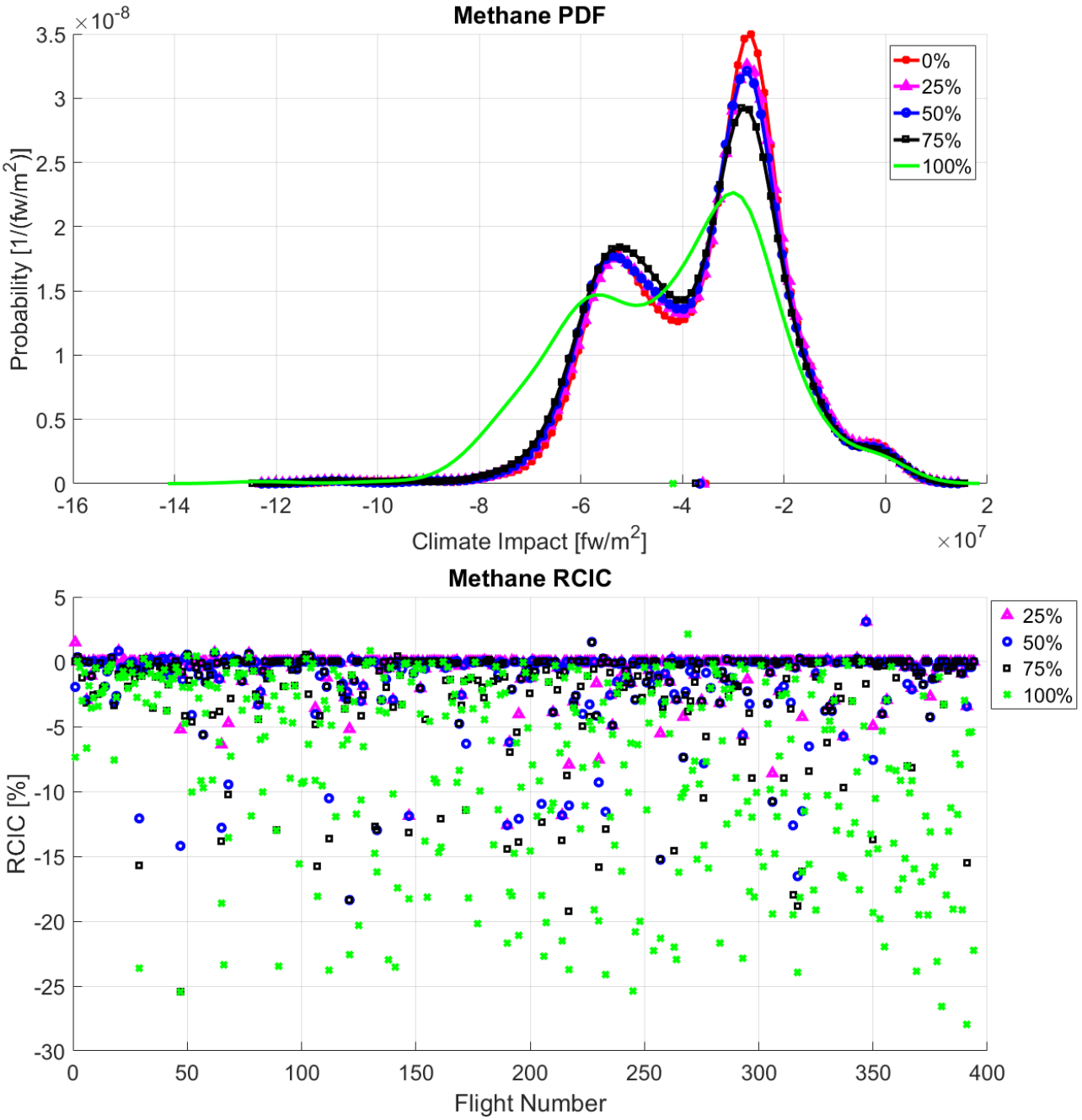

Figure 177. Probability Density Function and *RCIC* of methane for WP5-Westbound-AGWP100 case. The different curves and points represent the values for 0%, 25%, 50%, 75% and 100% of *NTCIC*.

D

Annex D

A list with the graphs showing the different *RCIC* values for the different combinations of weather pattern and flight direction is presented. The chosen climate metric is AGWP100. The shown *RCIC* values are the mean value (red), the 0.25 quantile (blue), the 0.5 quantile (black), and the 0.75 quantile (green). The climate metrics are contrails, NO_x, ozone, and methane. The *NTCIC* values presented are 25%, 50%, 75%, and 100%.

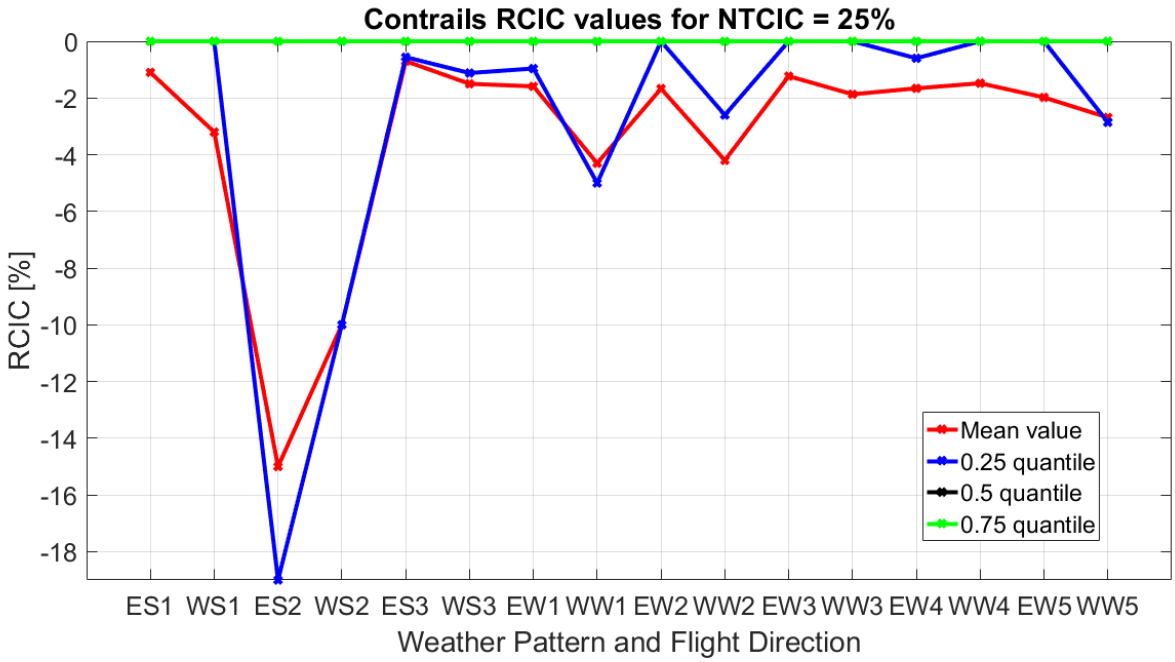

Figure 178. Comparison between mean value, 0.25 quantile, 0.5 quantile, and 0.75 quantile of *RCIC*. The climate parameter presented is contrails and *NTCIC* is equal to 25%. The climate metric is AGWP100.

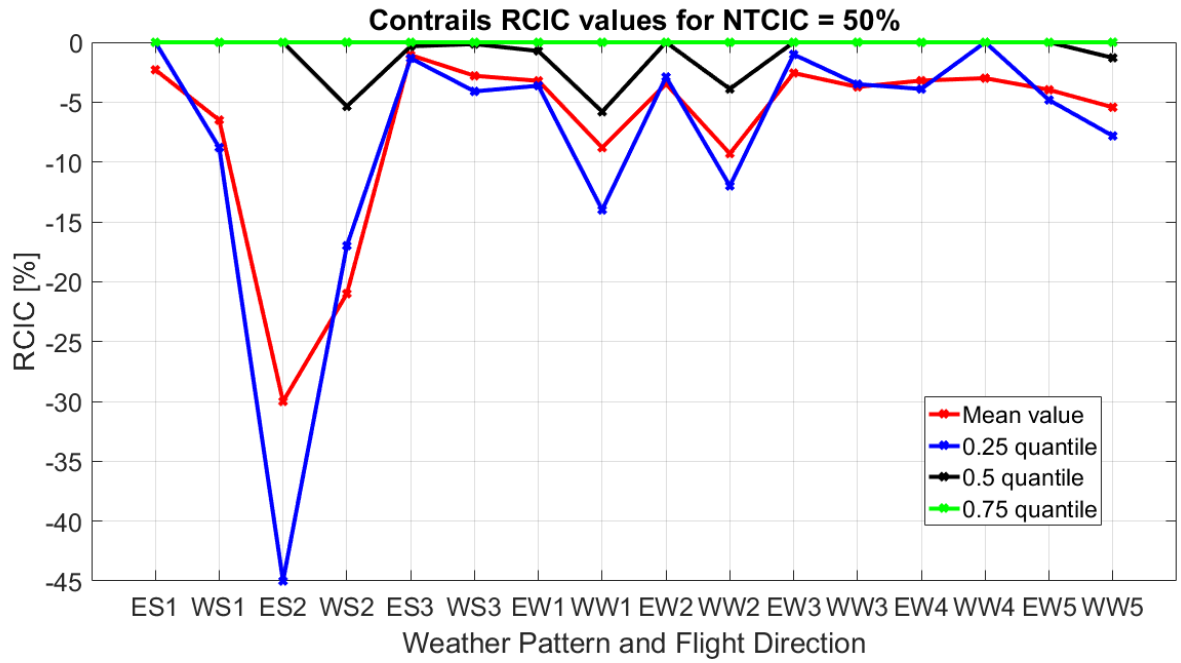

Figure 179. Comparison between mean value, 0.25 quantile, 0.5 quantile, and 0.75 quantile of *RCIC*. The climate parameter presented is contrails and *NTCIC* is equal to 50%. The climate metric is AGWP100.

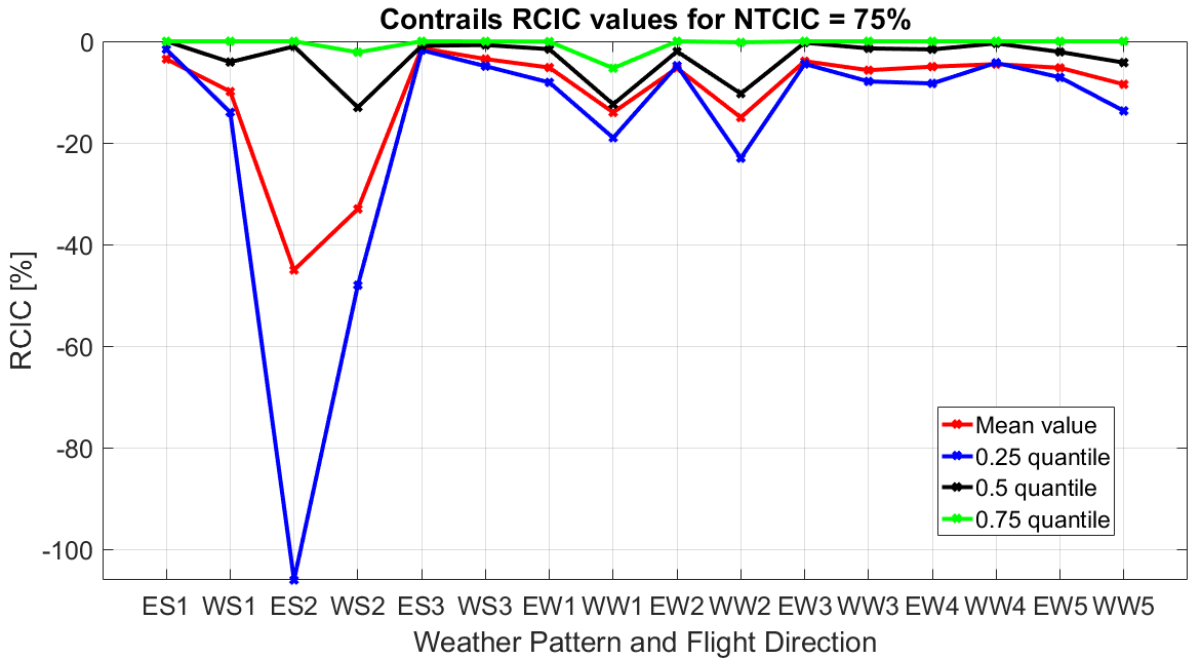

Figure 180. Comparison between mean value, 0.25 quantile, 0.5 quantile, and 0.75 quantile of *RCIC*. The climate parameter presented is contrails and *NTCIC* is equal to 75%. The climate metric is AGWP100.

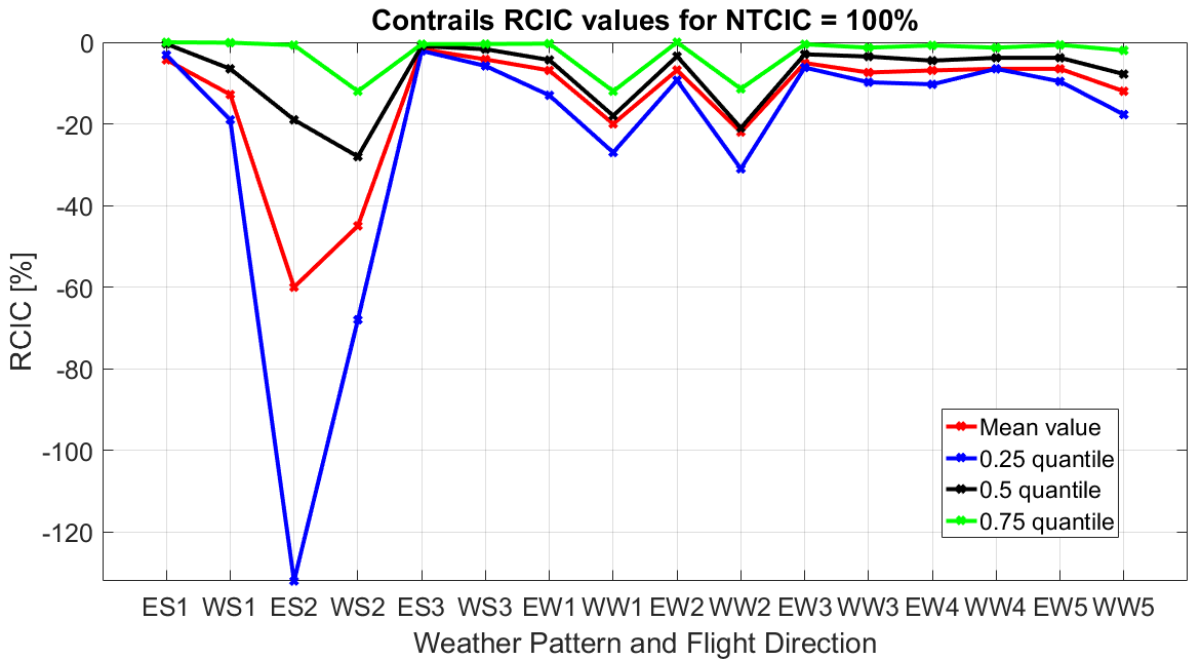

Figure 181. Comparison between mean value, 0.25 quantile, 0.5 quantile, and 0.75 quantile of *RCIC*. The climate parameter presented is contrails and *NTCIC* is equal to 100%. The climate metric is AGWP100.

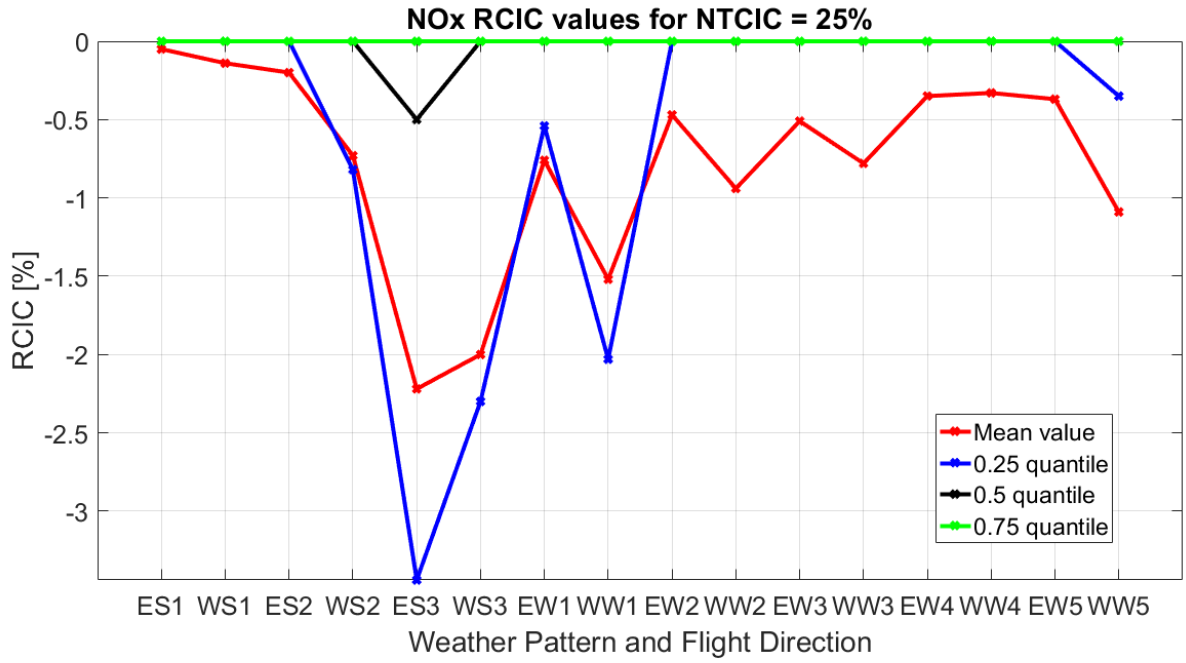

Figure 182. Comparison between mean value, 0.25 quantile, 0.5 quantile, and 0.75 quantile of *RCIC*. The climate parameter presented is NO_x and *NTCIC* is equal to 25%. The climate metric is AGWP100.

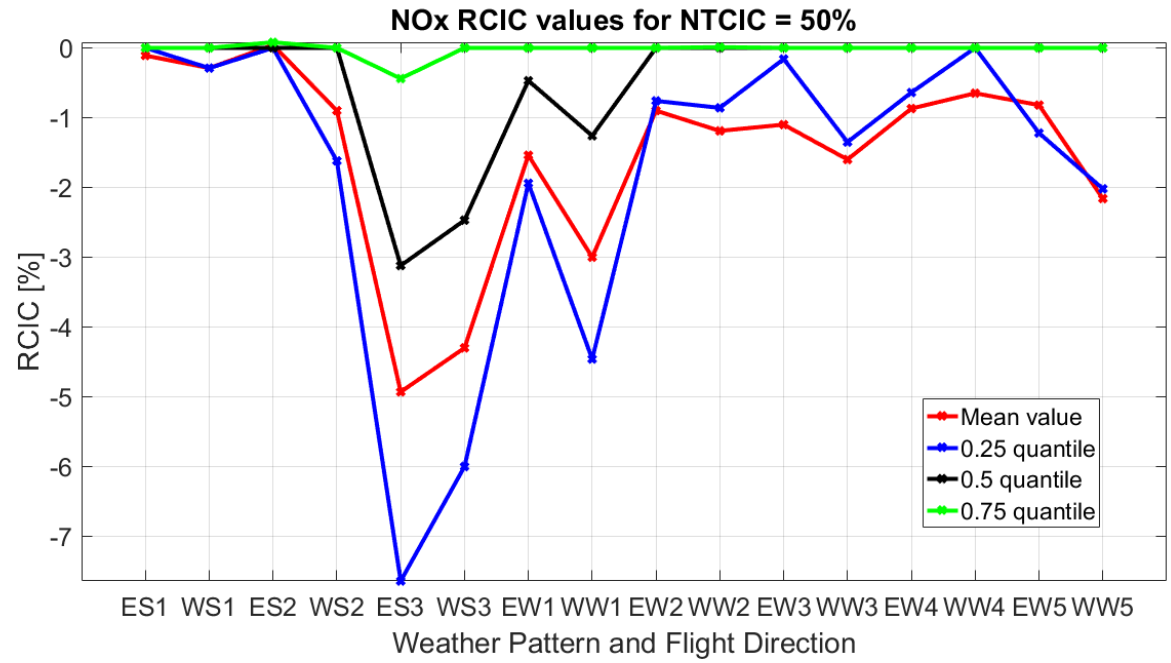

Figure 183. Comparison between mean value, 0.25 quantile, 0.5 quantile, and 0.75 quantile of *RCIC*. The climate parameter presented is NO_x and *NTCIC* is equal to 50%. The climate metric is AGWP100.

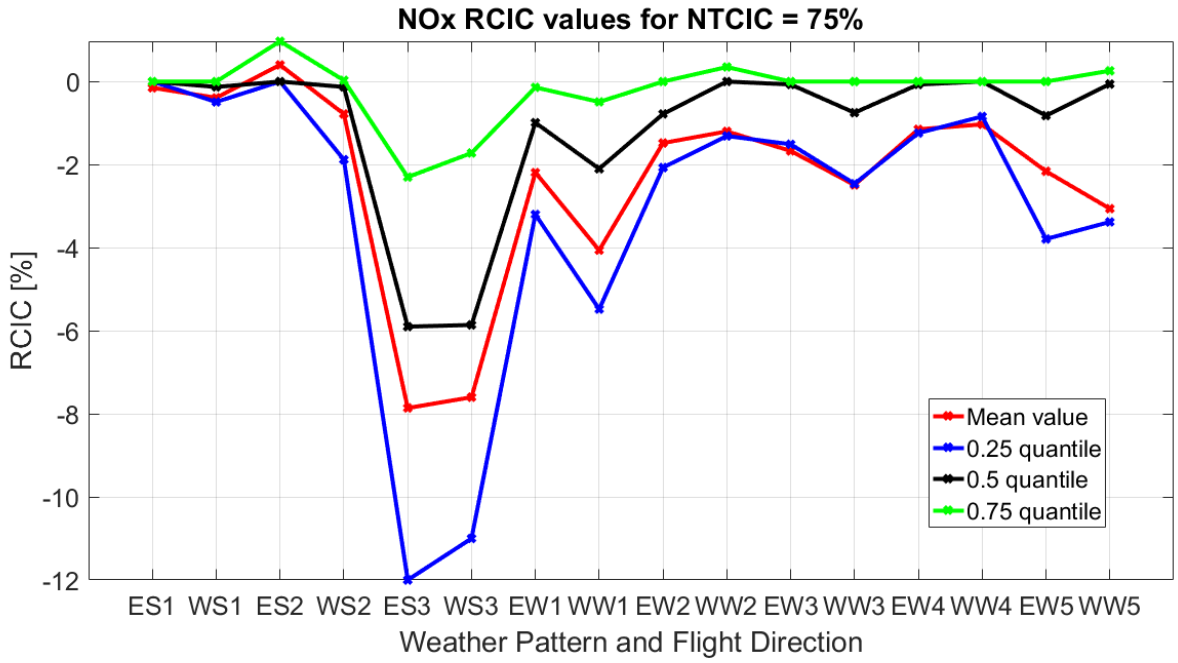

Figure 184. Comparison between mean value, 0.25 quantile, 0.5 quantile, and 0.75 quantile of *RCIC*. The climate parameter presented is NO_x and *NTCIC* is equal to 75%. The climate metric is AGWP100.

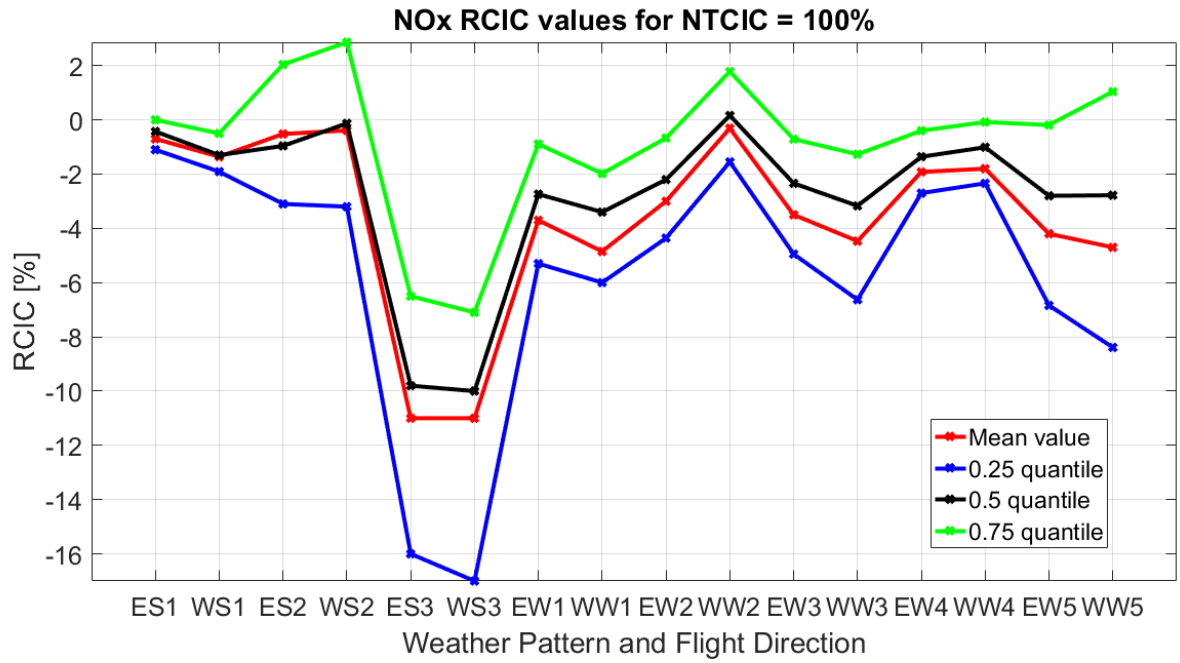

Figure 185. Comparison between mean value, 0.25 quantile, 0.5 quantile, and 0.75 quantile of *RCIC*. The climate parameter presented is NO_x and *NTCIC* is equal to 100%. The climate metric is AGWP100.

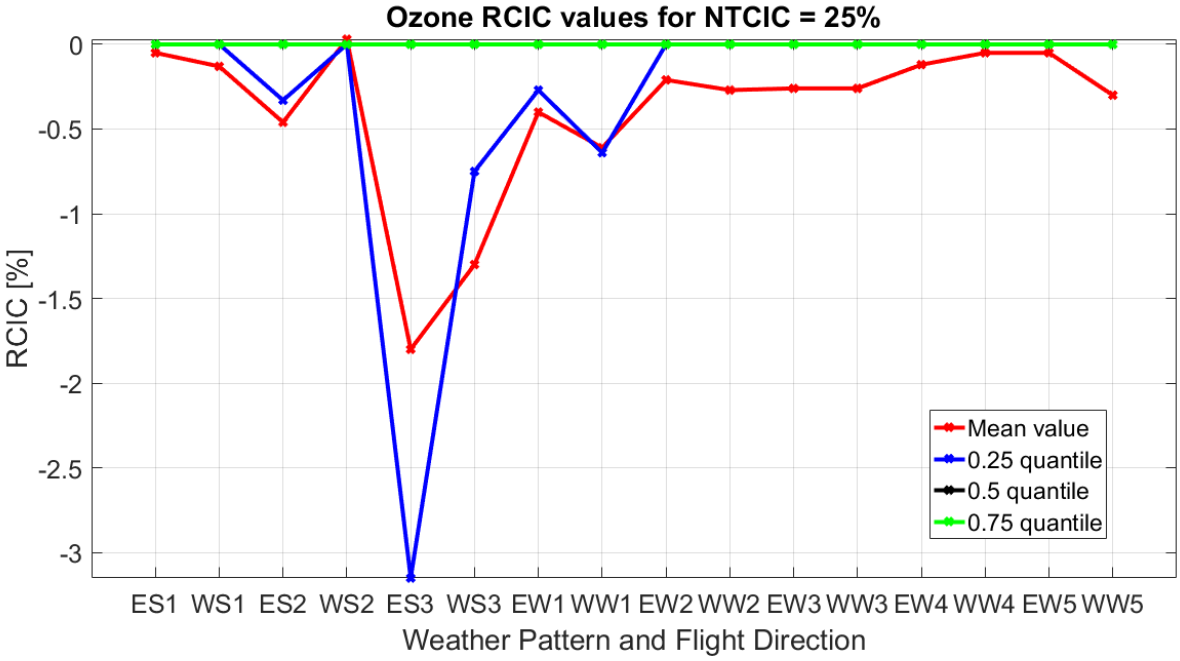

Figure 186. Comparison between mean value, 0.25 quantile, 0.5 quantile, and 0.75 quantile of *RCIC*. The climate parameter presented is ozone and *NTCIC* is equal to 25%. The climate metric is AGWP100.

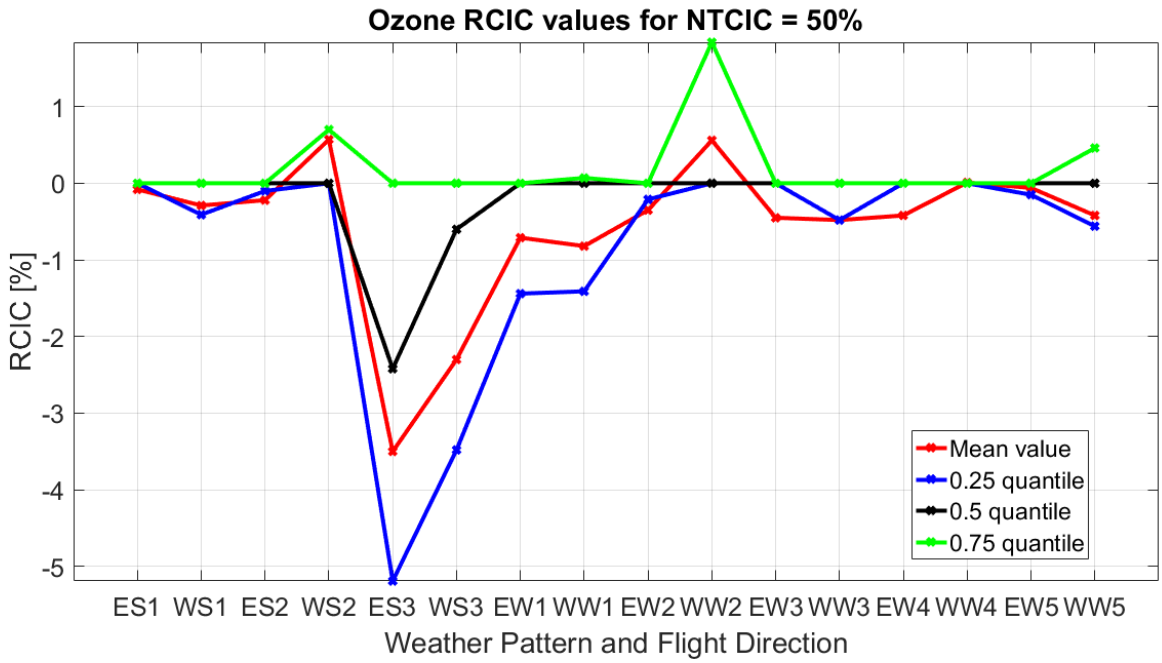

Figure 187. Comparison between mean value, 0.25 quantile, 0.5 quantile, and 0.75 quantile of *RCIC*. The climate parameter presented is ozone and *NTCIC* is equal to 50%. The climate metric is AGWP100.

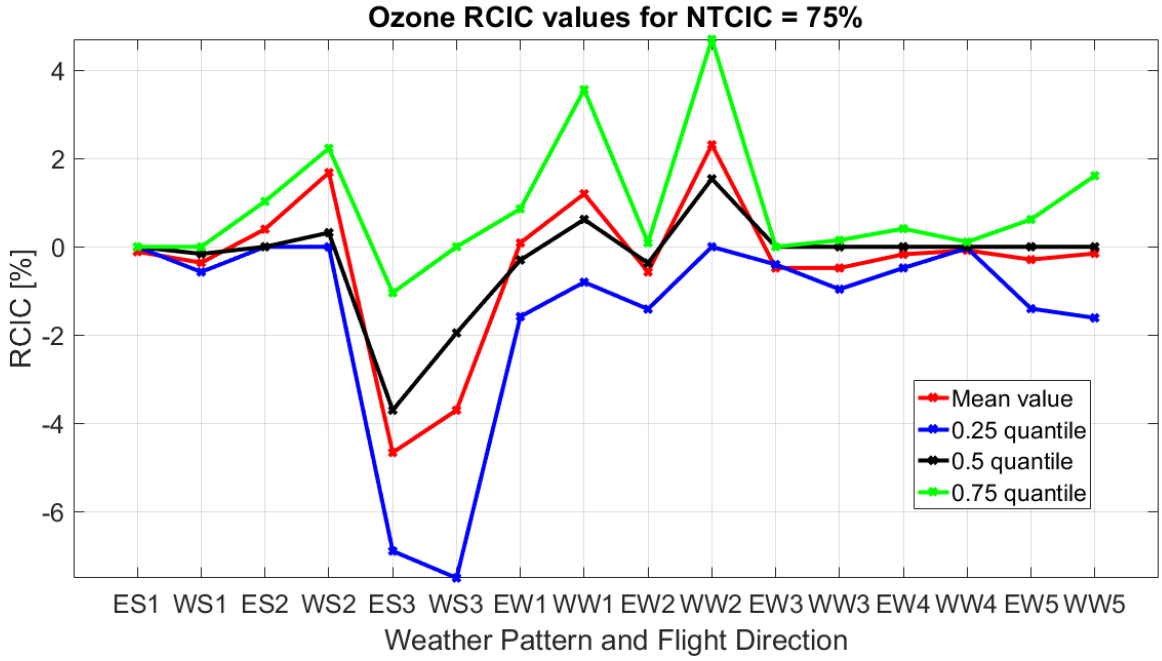

Figure 188. Comparison between mean value, 0.25 quantile, 0.5 quantile, and 0.75 quantile of *RCIC*. The climate parameter presented is ozone and *NTCIC* is equal to 75%. The climate metric is AGWP100.

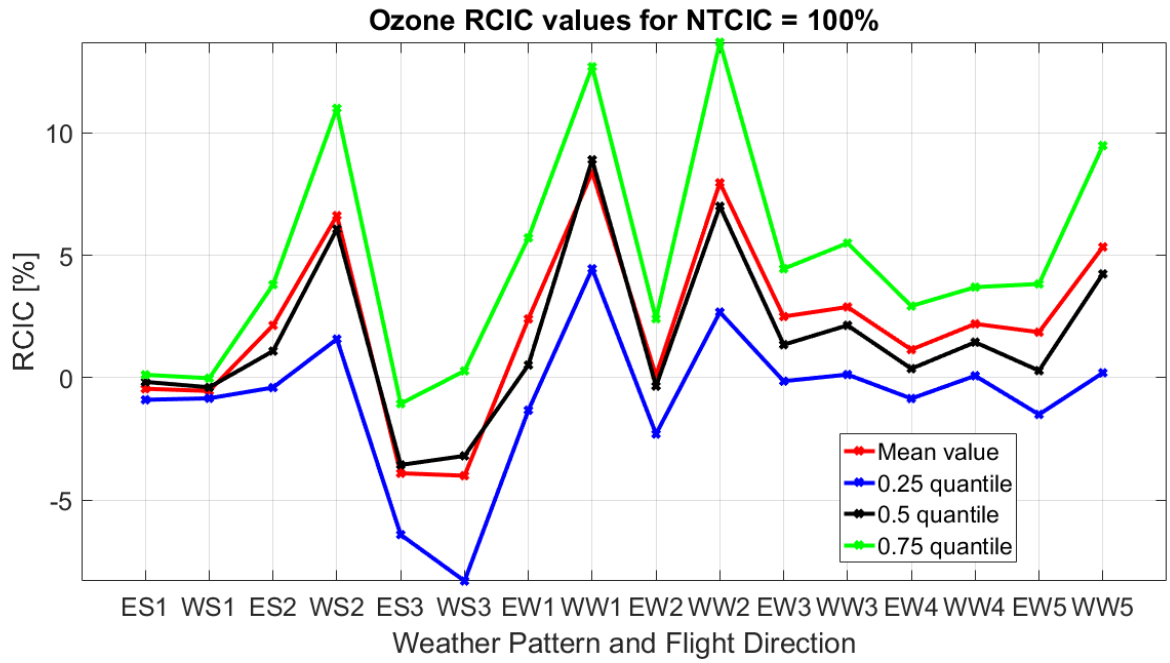

Figure 189. Comparison between mean value, 0.25 quantile, 0.5 quantile, and 0.75 quantile of *RCIC*. The climate parameter presented is ozone and *NTCIC* is equal to 100%. The climate metric is AGWP100.

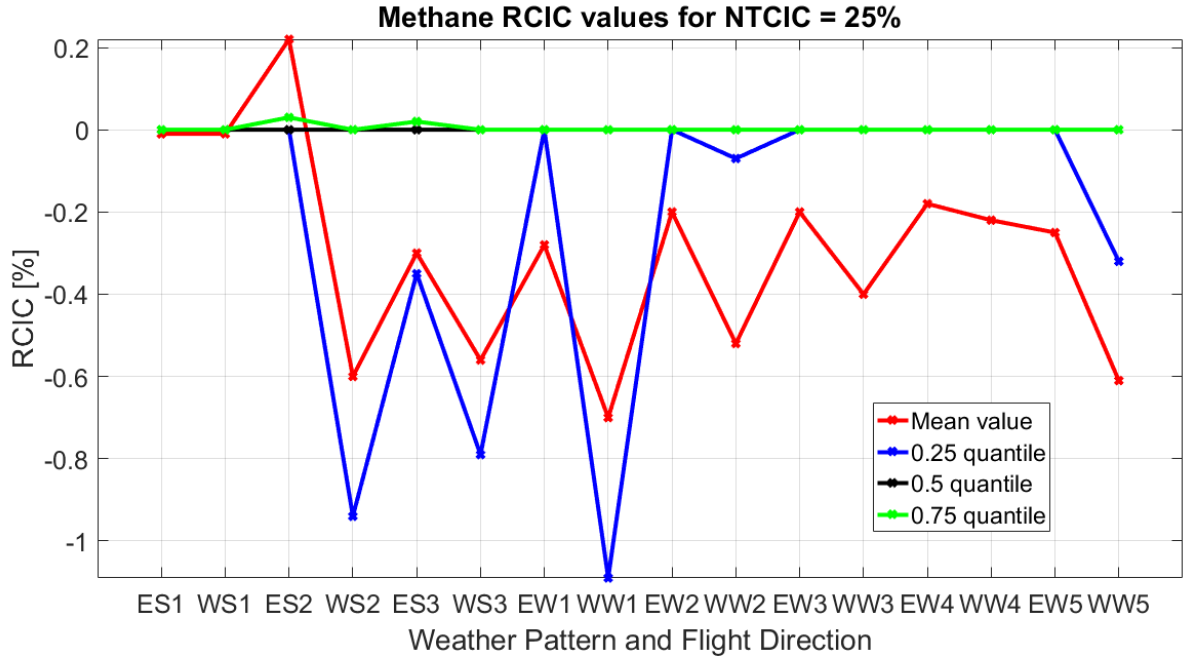

Figure 190. Comparison between mean value, 0.25 quantile, 0.5 quantile, and 0.75 quantile of *RCIC*. The climate parameter presented is methane and *NTCIC* is equal to 25%. The climate metric is AGWP100.

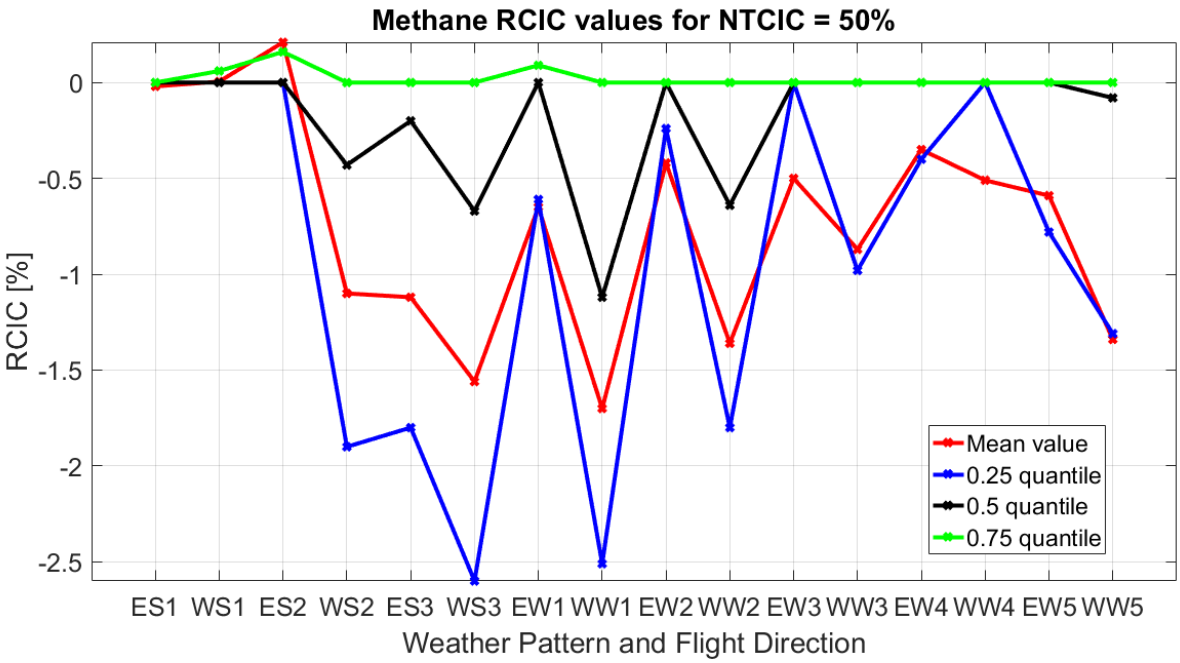

Figure 191. Comparison between mean value, 0.25 quantile, 0.5 quantile, and 0.75 quantile of *RCIC*. The climate parameter presented is methane and *NTCIC* is equal to 50%. The climate metric is AGWP100.

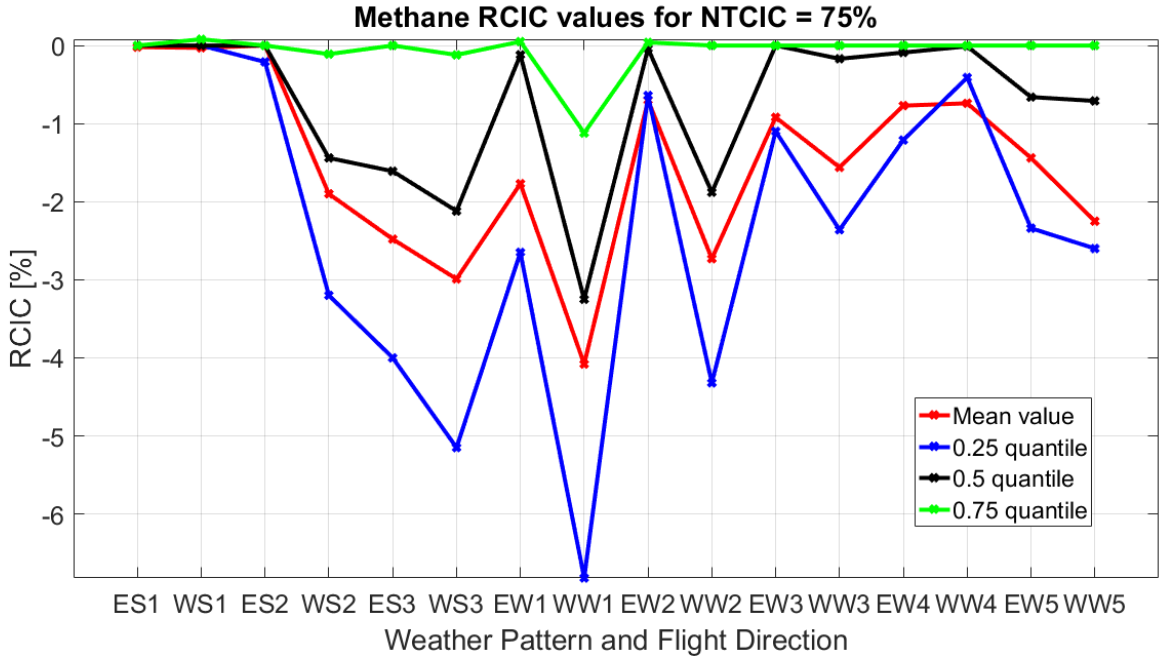

Figure 192. Comparison between mean value, 0.25 quantile, 0.5 quantile, and 0.75 quantile of *RCIC*. The climate parameter presented is methane and *NTCIC* is equal to 75%. The climate metric is AGWP100.

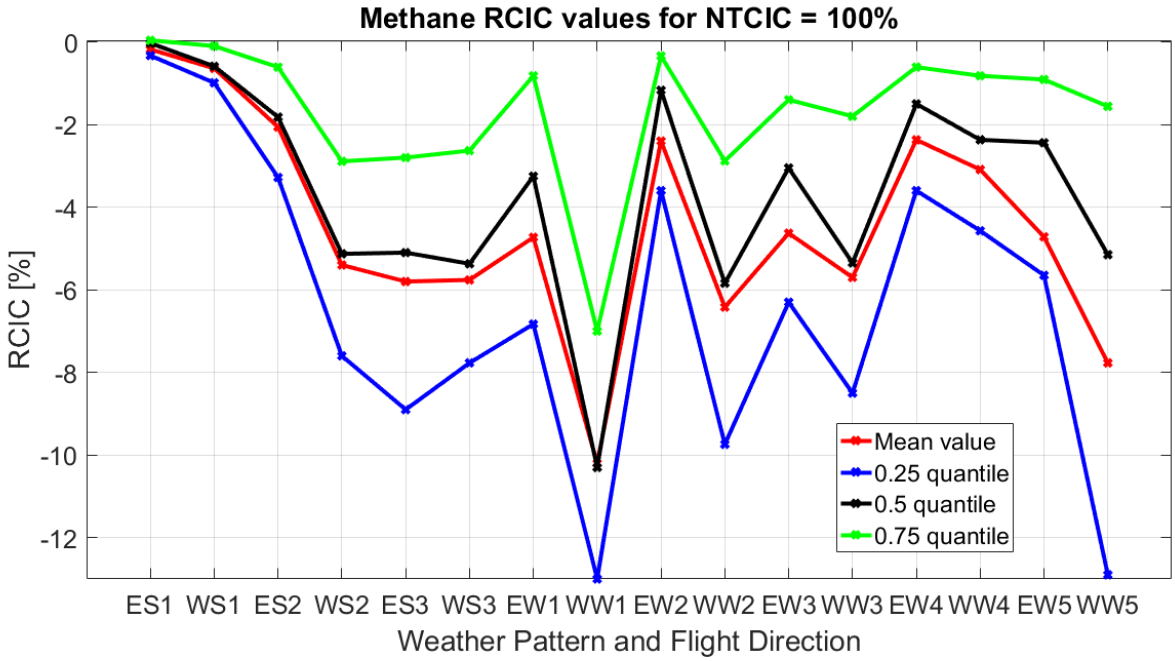

Figure 193. Comparison between mean value, 0.25 quantile, 0.5 quantile, and 0.75 quantile of *RCIC*. The climate parameter presented is methane and *NTCIC* is equal to 100%. The climate metric is AGWP100.

Bibliography

1 Grewe V. Aviation Emissions and Climate Impacts. Oberpfaffenhofen: -; 2015.

2 Lee DS, Fahey DW, Forster PM, Newton PJ, Wit RCN, Lim LL, Owen B, Sausen R. Aviation and global climate change in the 21st century. Atmospheric Environment. 2009;43:3520-3537.

3 Skeie RB, Fuglestvedt J, Berntsen T, Lund MT, Myhre G, Rypdal K. Global temperature change from the transport sectors: Historical development and future scenarios. Atmospherical Environment. 2009;43:6260-6270.

4 Wuebbles D, Gupta M, Ko M. Evaluating the Impacts of Aviation on Climate Change. EOS. 2007;88:157-168.

5 Lee DS, Pitari G, Grewe V, Gierens K, Penner JE, Petzold A, Prather MJ, Schumann U, Bais A, Berntsen T, et al. Transport impacts on atmosphere and climate: Aviation. Atmospheric Environment. 2010;44:4678-4734.

6 Schoeberl MR, Morris GA. A Lagrangian simulation of supersonic and subsonic aircraft exhaust emissions. Journal of Geophysical Research. 2000;105:11833-11839.

7 Land C, Feichter J, Sausen R. Impact of vertical resolution of the transport of passive tracers in the ECHAM4 model. TELLUS. 2002;54B:344-360.

8 Grewe V, Shindell DT, Eyring V. The impact of horizontal transport on the chemical composition in the tropopause region: lightning NOx and streamers. Atmospheric Environment. 2004;33:1058-1061.

9 Stevenson DS, Doherty RM, Sanderson MG, Collins WJ, Johnson CE, Derwent RG. Radiative forcing from NOx emissions: Mechanisms and seasonal dependence. Journal of Geophysical Research. 2004;109.

10 Prather MJ. Lifetimes and eigenstates in atmospheric chemistry. Geophysical Research Letters. 1994;21:801-804.

11 Prather MJ. Time scales in atmospheric chemistry: Theory, GWPs for CH4 and CO, and runaway growth. Geophysical Research Letters. 1996;23:2597-2600.

12 Schumann U. On condition for contrail formation from aircraft exhausts. Meteorologische Zeitschrift. 1996;5:4-23.

13 Meerkötter R, Schumann U, Doelling DR, Minnis P, Nakajima T, Tsushima Y. Radiative forcing by contrails. Annales Geophysicae. 1999;17:1080-1094.

14 Gierens K, Sausen R, Schumann U. A diagnostic study of the global distribution of contrails part II: Future air traffic scenarios. Theoretical and Applied Climatology. 1999;63:1-9.

15 Gettelman A, Fetzer EJ, Eldering A, Irion FW. The Global Distribution of Supersaturation in the Upper Troposphere from the Atmospheric Infrared Sounder. Journals of Climate. 2006;19:6089-6103.

16 Dahlman K, Grewe V, Frömming C, Burkhardt U. How ambiguous are climate metrics? And are we prepared to assess and compare the climate impact of new air traffic technologies? Atmospheric Environment. 2014;46:40-55.

17 Grewe V, Frömming C, Matthes S, Brinkop S, Ponater M, Dietmüller S, Jöckel P, Garny H, Tsati E, Dahmann K, et al. Aircraft routing with minimal climate impact: the REACT4C climate cost function modelling approach (V1.0). Geoscientific Model Development. 2014a;7:175-201.

18 Schumann U, Graf K, Mannstein H. Potential to reduce the climate impact of aviation by flight level changes. In: 3rd AIAA Atmospheric Space Environments Conference; 2011; Honolulu, Hawaii.

19 Jöckel P, Tost H, Pozzer A, Brühl C, Buchholz J, Ganzeveld L, Hoor P, Kerkweg A, Lawrence MG, Sander R, et al. The atmospheric chemistry general circulation model ECHAM5/MESSy1: consitent simulation of ozone from the surface to the mesosphere. Atmospheric Chemistry and Physics. 2006;6:5067-5104.

20 Jöckel P, Kerkweg A, Pozzer A, Sander R, Tost H, Riede H, Baumgaertner A, Gromov S, Kern B. Development cycle 2 of the Modular Earth Submodel System (MESSy2). Geoscientific Model Development. 2010;3:717-752.

21 Eurocontrol. SAAM Reference Manual 4.2.0 Beta, Version 21-12-2012. 2012.

22 Eurocontrol. User guide AEM-kernel, Internal Document V2.26. 2013.

23 Grewe V, Tsati E, Hoor P. On the attribution of contributions of atmospheric trace gases to emissions in atmospheric model applications. Geoscientific Model Development. 2010;3:487-499.

24 Grewe V, Dahlmann K, Matthes S, Steinbrecht W. Attributing ozone to NOx emissions: Implications for climate mitigation measures. Atmospheric Environement. 2012;59:102-107.

25 Schumann U. Influence of propulsion efficiency on contrail formation. Aerosp. Sci. Technol. 2000;4:391-401.

26 Burkhardt U, Kärcher B, Ponater M, Gierens K, Gettelman A. Contrail cirrus supporting areas in model and observations. Geophysical Research Letters. 2008;35.

27 Burkhardt U, Kärcher B. Process-based simulation of contrail cirrus in a global climate model. Journal of Geophysical Research. 2009;114.

28 Ponater M, Marqueart S, Sausen R. Contrails in a comprehensive global climate model: Parameterization and radiative forcing results. Journal of Geophysical Research. 2002;107:ACL 2-1 - ACL 2-15.

29 Heymsfield AJ, Donner LJ. A scheme for parameterizing ice cloud water content in general circulation models. Journals of the Atmospheric Sciences. 1990;47:1865-1877.

30 Grewe V, Stenke A. AirClim: an efficient tool for climate evaluation of aircraft technology. Atmospheric Chemistry and Physics. 2008;8:4621-4639.

31 Fuglestvedt JS, Shine KP, Berntsen T, Cook J, Lee DS, Stenke A, Skeie RB, Velders GJM, Waitz IA. Transport impacts on atmosphere and climate: Metrics. Atmospheric Environment. 2010;44:4648-4677.

32 Shine KP, Derwent RG, Wuebbles DJ, Morcrette JJ. Radiative forcing of climate. In: Houghton JT, Jenkins GJ, Ephraums JJ. IPCC. Cambridge University Press, Cambridge, Great Britain, New York, NY, USA and Melbourne, Australia: UNOG Library; 1990. p. 41-68.

33 Dahlmann K. Eine Methode zur effizienten Bewertung von Maßnahmen zur Klimaoptimierung des Luftverkehrs. 2012.

34 Grewe V, Champougny T, Matthes S, Frömming C, Brinkop S, Sovde OA, Irvine EA, Halscheidt L. Reduction of the air traffic´s contribution to climate change: A REACT4C case study. Atmospheric Environment. 2014b;94:616-525.

35 Irvine EA, Hoskins BJ, Shine KP, Lunnon RW, Froemming C. Characterizing North Atlantic weather patterns for climate-optimal aircraft routing. Meteorological Applications. 2013;20:80-93.